ABSTRACT

ASADUZZAMAN, FNU. Enzyme Functionalized Solution Blown Nonwovens. (Under the direction of Dr. Sonja Salmon).

This Ph. D. dissertation presents the innovation and development of a new category of functional materials that uses a solution blown spinning (SBS) process to produce novel, useful biocatalytic functionalized nonwovens. SBS is a rapid, mild nanofiber formation process that is not limited to thermal-plastic polymers or high dielectric constant solvent-soluble polymers. With the SBS technique, it was possible to achieve single-step enzyme immobilization into polymeric carriers from enzyme-compatible polymer solutions. The goals of this research were to explore techniques for preparing polymer-solvent-enzyme compatible triads, optimize solution spinning processes for producing enzyme functionalized solution blown nonwovens (EFSBN), and validate the anticipated application features of EFSBN.

Chapter 1 is a review of the literature to assess the potential for compatible polymer-solvent-enzyme triads for co-immobilization solution processing to increase immobilization yield and reduce immobilization complexity. The particular focus is to produce enzyme compatible polymer solutions in an organic solvent for solution blown spinning process where in-situ fiber formation and enzyme immobilization happen. In-situ co-immobilization is one of the promising methods in enzyme immobilization due to its high enzyme loading, versatility, and single-step fabrication processability. However, the stability and compatibility of enzymes in polymer solutions (especially organic solvent-soluble polymer solutions) are challenging. Enzymes may denature in the presence of organic solvents or at elevated temperatures, limiting how enzymes

can be combined with organic solvent-soluble polymers. This chapter discusses strategies for producing compatible polymer-solvent-enzyme triads that span aqueous and non-aqueous fabrication requirements.

Chapter 2 reports the novel production of unique enzyme functionalized solution blown nonwoven (EFBSN) webs from aqueous soluble polyethylene oxide (PEO) polymer solution by the solution blow spinning method. Protease co-immobilization via entrapment in PEO nanofibers by solution blowing was demonstrated as a simple and efficient process for loading a broad concentration range of enzymes. The rapidly water-soluble and non-dusting EFSBN solid materials preserve a high enzyme activity level over long periods of ambient storage without adding a stabilizer and are easy to handle, making EFSBNs a potential alternative format for delivering enzymes in products that require fast-dissolving solid formulations, like detergents.

Chapter 3 reveals an approach to produce an enzyme (CALB) compatible polycaprolactone (PCL)-chloroform solution for enzyme co-immobilization via entrapment in PCL nanofibers. CALB enzymes survived in the microemulsion (water-in-oil) of the PCL-chloroform-CALB compatible triad and retained around half of their initial activity after solution blow spinning. These novel CALB-loaded-EFSBN-PCL webs demonstrated stability under ambient environments while enabling facile enzymatic degradation (completely degraded within 15-60 mins) in buffer. The unique degradation properties of EFSBN-PCL can be exploited for degradable packaging material applications under ambient conditions and simple waste management after use.

Chapter 4 investigates enzyme post-immobilization on a durable polymer carrier. Polystyrene (PS) solution blown nonwoven (SBN) nanofibers were employed for CALB adsorption on the SBN-PS fiber surface from a CALB-buffer solution. The high surface area of nanofibers enables high-quantity enzyme adsorption and over two-thirds catalytic activity compared to free enzymes. The homogenously distributed immobilized CALB on the nanofiber surface had good storage and thermal stability. The durable (water-insoluble) EFSBN-PS were easy to separate from the reaction mixture and showed over 70% of the initial lipase activity after fifteen reuse cycles.

Chapter 5 summarizes recommendations for future research in applying and commercializing EFSBNs. EFSBN production using solution blow spinning for a range of enzymes and polymers and their related commercial applications, as well as some issues that must be addressed, are discussed in this chapter, along with the potential solutions.

Enzyme Functionalized Solution Blown Nonwovens

by
Fnu Asaduzzaman

A dissertation submitted to the Graduate Faculty of
North Carolina State University
in partial fulfillment of the
requirements for the degree of
Doctor of Philosophy

Fiber and Polymer Science

Raleigh, North Carolina
2022

APPROVED BY:

_____	_____
Dr. Sonja Salmon Committee Chair	Dr. Jan Genzer
_____	_____
Dr. Saad Khan	Dr. Benoit Maze

DEDICATION

To Farzana Khan Rony, my beloved beautiful wife and Riham Tahfeem Arya, our daughter, the heart of our life.

Thank you for making my world beautiful!

To my parents for all their support and sacrifices.

.

BIOGRAPHY

Mr. Asaduzzaman was born and raised in Gazipur, Dhaka, Bangladesh, a rural farming community. He is a first-generation college student who was the first person in his family to attend college and university. He graduated with his master's and bachelor's degrees from the Department of Applied Chemistry and Chemical Engineering, University of Dhaka, Bangladesh, in 2010 and 2012, respectively. In September 2012, Mr. Asaduzzaman started his career as a lecturer at the Department of Natural Sciences, Daffodil International University, Bangladesh. From February 2013 to April 2014, he worked as a scientist at the Bangladesh Council of Scientific and Industrial Research (BCSIR), Dhaka, Bangladesh. In April 2014, he joined as a young faculty at the Department of Applied Chemistry and Chemical Engineering, University of Dhaka, Bangladesh. In 2018 Fall, Asaduzzaman began his Ph.D. in Fiber and Polymer Science at NC State University, and next year June, he joined the lab of Professor Sonja Salmon, studying enzyme immobilization in polymer fiber. He also got a graduate certificate in nonwoven science and technology, where he learned nonwoven processes, products, and applications. His past research focused on modifying polymers and biopolymers, preparation, characterizations, and applying biocomposites. He is skilled in FTIR, UV-visible spectroscopy, TGA, DSC, UTM, ion chromatography, GC, SEM, OM, etc. In his Ph.D., he worked on enzyme-functionalized solution-blown nonwovens. Beyond Academics, his favorite things are spending time with Arya, Rony, and his friends and playing and watching cricket and soccer.

ACKNOWLEDGMENTS

The completion of my Ph.D. would never have been possible without the support of many people, and I wish to express my sincere appreciation to all of you who supported me over the last four and half years. A very special thanks to my thesis advisor, Professor Dr. Sonja Salmon, for allowing me to explore all the facets of this project and supporting my non-scientific interests throughout my years in the USA. I truly appreciate your endless support, encouragement, and guidance throughout my doctoral study. I never forgot your hand-on-teaching and lab practice. Thank you for being extremely patient with me for the past 3.5 years. Furthermore, I would like to thank my committee members for their contributions of time and expertise, which have led to the successful completion of this dissertation: Dr. Saad Khan (Department of Chemical Engineering), Dr. Jan Genzer (Department of Chemical Engineering), and Dr. Benoit Maze (Wilson College of Textiles). I appreciate Dr. Jan Genzer's constructive feedback on publishing my first paper. I want to thank Dr. Behnam Pourdeyhimi faith in us.

Special thanks to Dr. Joshua R. Uzarski for his in-depth suggestions on enzymes and for helping me get rid of the stuck position. I would like to thank Dr. Shae Brown for advising me from an industry perspective. I would like to thank Dr. Jialong Shen for all the genuine support you offered to me throughout the journey. Many works became simpler because of your incredible help. You are going to make an incredible professor, and I wish all the best for you. I appreciate the lab managers at Wilson College of Textiles (Mrs. Birgit Andersen), AIF (Dr. Chuck Mooney, Dr. Chuanzhen Zhou, Mr. Fred Stevie), and CMIF (Dr. Mariusz Zareba) for the resources and training in this research. I also appreciate the NWI family (Dr. Thomas Daugherty, Mr. Roman Braga, Mr.

Mike Haskins, and Mrs. Jimei Wang) successfully finishing my work. I am thankful for funding support from the Nonwovens Institute and the Department of Textile Engineering, Chemistry, and Science at NC State University.

Finally, I thank my wife and daughter for making my life beautiful. Special thanks to my father and mother for all the sacrifices you made.

TABLE OF CONTENTS

LIST OF TABLES

LIST OF FIGURES

Abbreviations

AOT	Sodium bis(2-ethylhexyl) sulfosuccinate
BCA	Bicinchoninic acid
BSA	Bovine serum albumin
CA	Carbonic anhydrase
CALB	*Candida antarctica* lipase B
CALB-EFSBN-PCL	*Candida antarctica* lipase B-Enzyme functionalized solution blown nonwoven-polycaprolactone
CALB-EFSBN-PS	*Candida antarctica* lipase B-Enzyme functionalized solution blown nonwoven-polystyrene
CLEAs	Cross-linked enzyme aggregates
CLECs	Cross-linked enzyme crystals
CO_2	Carbon dioxide
CTAB	Cetyltrimethylammonium bromide
DCM	Dichloromethane
DMAc	Dimethyl acetamide
DMF	Dimethylformamide
DMSO	Dimethyl sulfoxide
EDTA	Ethylenediaminetetraacetic acid
EFSBN	Enzyme functionalized solution blown nonwoven
EFSBN-PCL	Enzyme functionalized solution blown nonwoven-polycaprolactone
EFSBN-PEO	Enzyme functionalized solution blown nonwoven-polyethylene oxide
EFSBN-PS	Enzyme functionalized solution blown nonwoven-polystyrene
FITC	Fluorescein isothiocyanate
HFIP	Hexafluoroisopropanol
MEK	Methyl ethyl ketone
NMP	N-methyl pyrrolidone
PAN	Polyacrylonitrile
PANi	Polyaniline
PCL	Polycaprolactone
PE	Polyethylene
PEG	Polyethylene glycol
PET	Polyethylene terephthalate
PEO	Polyethylene oxide
PI	Polyimide
PLA	Polylactic acid
PLGA	Poly(lactic-co-glycolic acid)
PMA	Poly(methyl acrylate)
PMMA	Polymethyl methacrylate
p-NP	Para-nitrophenol
p-NPAc	Para-nitrophenyl acetate
PP	Polypropylene

PS	Polystyrene
PVA	Polyvinyl alcohol
PVAc	Polyvinyl acetate
PVC	Polyvinyl chloride
PVDF	Polyvinylidene fluoride
PVP	Polyvinylpyrrolidone
RM	Reverse micelle
SBS	Solution blow spinning
SBN	Solution blown nonwoven
SBN-PCL	Solution blown nonwoven-polycaprolactone
SBN-PEO	Solution blown nonwoven-polyethylene oxide
SBN-PS	Solution blown nonwoven-polystyrene
SDS	Sodium dodecyl sulfate
TCA	Trichloroacetic acid
THF	Tetrahydrofuran
TX-100	Triton-100
W-A	Wilbur-Anderson

Chapter 1: Literature Review on Enzyme Immobilization: Polymer-Solvent-Enzyme Compatibility

The content of this chapter was previously published with the following citation: Asaduzzaman, Fnu, and Sonja Salmon. "Enzyme immobilization: polymer-solvent-enzyme compatibility." ***Molecular Systems Design & Engineering*** (2022), 7, 1385-1414.

Abstract:

Immobilization improves enzyme stability, allows easy enzyme separation from reaction mixtures, and enables repeatable use over prolonged periods, especially in systems requiring continuous chemical reactions. Immobilization also delivers enzymes for controlled release or promotes triggered degradation of entrapping materials. Polymeric materials in different physical forms, such as films, beads, coatings, and fibers, are increasingly used as support matrices for enzyme immobilization because they are easily fabricated and offer excellent mechanical versatility. Enzymes are generally compatible with water environments and can be mixed with water-soluble polymers and dried to produce immobilized enzyme products. However, while important, the utility of such water-soluble materials is limited. Many durable polymers, especially synthetic polymers, are intrinsically hydrophobic and not water-soluble. They are processed into different shapes by melting or solubilizing them in organic solvents. However, enzymes may denature in the presence of organic solvents or at elevated temperatures, limiting how enzymes can be combined with hydrophobic polymers. Fortunately, research has revealed several approaches for successful enzyme incorporation into polymer matrices that rely on solution processing with organic solvents. This review discusses strategies for producing immobilized enzymes by solution processing methods. Compatible polymer-solvent-enzyme triads that span aqueous and non-aqueous fabrication requirements are

identified. Finally, based on the existing research on enzyme immobilization using enzyme compatible polymer solutions, prospects for future developments are summarized.

Keywords: Enzyme, immobilization, supporting materials, polymer, solvent, compatibility.

1.1. Introduction

Enzymes are protein-based natural biocatalysts. They are highly specific, selective, and have exceptional catalytic activity for chemical and biochemical reactions. Because enzymes function selectively and efficiently at mild conditions, such as at near-neutral pH, ambient temperatures, and pressures, enzymes are utilized in numerous commercial applications to replace conventional harsh chemicals and save energy.[1,2] Many commercial enzyme applications are operated as batch processes, where enzymes are delivered to the substrate as an aqueous solution, incubated for some time, often with mixing, and are disposed of afterward along with the effluent process water.[3] Economic feasibility of batch processes require that sufficiently low amounts of enzymes are used each time to "afford" single-use. Enzyme requirements for industrial applications and physical forms vary among crude enzymes, purified, or immobilized enzymes.[4] For example, while different industrial carbohydrate processes may require enzyme amounts in the form of 0.5 g pure enzyme, 2-5 g cell-free enzyme extract, or 10-60 g whole-cell wet weight per kilogram of product produced, immobilized enzyme processes (e.g., high fructose corn syrup production using glucose isomerase) can require only 0.05 g formulated biocatalyst/kg product.[5] For some applications, the consumption of biocatalyst is high (e.g., the enzymatic reduction of a prochiral ketone to a chiral alcohol required 9 g/L ketoreductase biocatalysts for 160 g/L substrate loading)[5], limiting the economic feasibility for industrial applications.[6]

Economically viable conversion levels for these types of applications could only be achieved by recycling enzymes. However, the separation and recovery of soluble (or "free") enzymes from a reaction medium after an enzymatic reaction is time-consuming and inefficient.[7] Therefore, the separation of enzymes is a crucial problem in real applications. Also, enzymes tend to function optimally within narrow reaction conditions. Partially this is due to chemical mechanisms that occur in the enzyme active site, e.g., reactions may require a specific pH for proper chemical group ionization. More generally, poor heat stability is caused by irreversible unfolding (denaturing or "melting") of the protein's three-dimensional (3D) structure, which physically disrupts the active sites or makes them inaccessible due to molecular agglomeration. The conditions for optimal catalytic activity and protein structural stability are not necessarily the same, resulting in poor longevity and often making soluble enzyme recycling impractical.[8,9]

Attaching ("immobilizing") enzymes on or into solid supporting materials can help improve enzyme pH[10], thermal[11], and storage[11] stability while overcoming recyclability issues that limit the broader use of enzymes. Enzyme embedded in solid carriers facilitates recycling and reuse in biocatalytic continuous processes that helps to increase biocatalyst utilization.[12] Immobilized enzymes overcome drawbacks of free enzymes by improving performance properties including activity, selectivity, specificity and purity.[13,14] In addition, immobilized enzymes are more resistant to inhibitors which may extend the operating longevity.[13] Immobilized enzymes also enhance product quality by avoiding protein contamination in the final product and improve process efficiency and control by allowing prolonged use or rapid termination of enzymatic catalysis.[15] Immobilized enzymes can be removed from process liquids by simple methods like

filtration[16] or centrifugation[17] or more sophisticated techniques like magnetic recovery.[18] Ultimately, these benefits must provide sufficient advantages to overcome immobilization costs. Sufficiently high productivity levels are needed to justify using immobilized enzymes, estimated at 2,000-10,000 kg product/kg immobilized enzyme for commodity applications and 50-100 kg product/kg immobilized enzyme for premium applications, like pharmaceutical products. By comparison, even higher productivity levels of 5,000-20,000 kg product for commodity applications and 100-250 kg product for premium applications are required when using non-immobilized enzymes.[19] Although immobilization processes incur some cost, in successful applications, the higher productivity levels achieved through recycling and other intrinsic benefits of making the biocatalyst easily separable from the reaction mixture accommodate this. Based on their advantages, immobilized enzymes have been widely applied in various fields like the pharmaceutical industry[20], food industry[21], animal feed[22], detergents[23], chemical industries[24], personal care, and cosmetics[24], biomedical applications[25], ultrafiltration[26], wastewater treatment[27,28], textile industry[29–31], biosensors[32], biofuel production[33], bioreactors[34,35], carbon capture[36] and others.

Enzyme immobilization is not a new concept. Numerous unique enzyme immobilization methods, characterizations, and applications have been investigated, published, and reviewed.[37,38,47–56,39,57–63,40–46] Certain reviews have discussed enzyme stability and catalysis in organic solvents[64–68] and explored enzyme engineering for *in situ* immobilization involving self-assembly into insoluble particles.[69] However, no prior reviews have focused on critically assessing enzyme-compatible polymer-solution triad systems as a fundamental material fabrication approach. The

co-immobilization of enzymes in polymers requires forming stable polymer-solvent-enzyme compatible triad solutions or dispersions that preserve native enzyme structure and activity. Forming compatible triads is straightforward when water-soluble enzymes are combined with aqueous solutions of water-soluble polymers. Incorporating water-soluble enzymes in polymer solutions made with organic solvents is more challenging. This literature review assesses compatible polymer-solvent-enzyme triads for co-immobilization solution processing to increase immobilization yield and reduce immobilization complexity.

1.2. Enzyme Immobilization Approaches

Ideally, immobilized enzymes are localized and confined on or inside a solid carrier while fully retaining their catalytic activity.[70] This ideal is difficult to achieve, not least because immobilized enzymes have a larger physical size than "free" dissolved enzymes, which can interfere with substrate accessibility to the active site. When an enzyme molecule is attached to other enzymes (self-immobilization) or to matrix materials by adsorption, entrapment or chemical bonding the total size of the enzyme plus matrix is larger than the enzyme molecule itself causing the immobilized enzyme to have different physical behavior than the enzyme molecule alone. Solid carriers can be selected from all types of different materials. Carrier properties dictate what mode of enzyme immobilization can be used. Enzyme immobilization with polymeric carriers is accomplished in two main ways: single-step co-immobilization or post-immobilization, as shown in **Figure 1.1**.

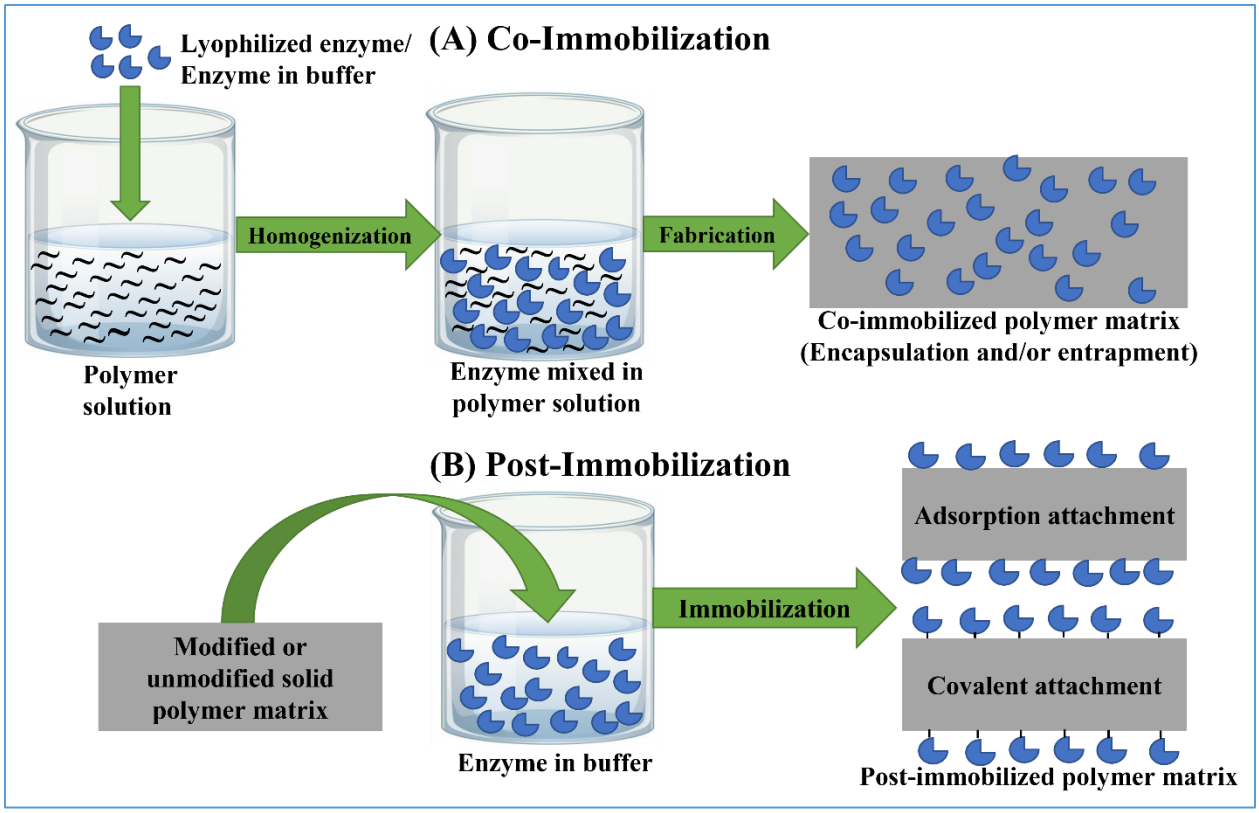

Figure 1.1: Schematic illustration of enzyme (A) co-immobilization and (B) post-immobilization modes, inside or on polymer matrices.

The interaction mechanisms of enzymes and supporting materials vary in co- and post-immobilization modes. Entrapment, encapsulation, and adsorption methods, where there is no covalent bond formation between enzymes and support carriers, are categorized as physical methods. Covalent attachment and cross-linking are classified as chemical methods.[71] **Figure 1.2** illustrates the main enzyme immobilization mechanisms where gray and blue represent carrier materials and enzyme, respectively. Immobilized enzymes that result from mixing enzymes together with dissolved carrier molecules (or sometimes carrier monomers) prior to the formation of the solid carrier matrix – herein referred to as "co-immobilized enzymes" – are confined mainly by physical encapsulation and entrapment mechanisms. Post-immobilized

enzymes are held on carrier surfaces via physical adsorption or by covalent chemical attachment between enzyme and carrier. “Self-immobilization” occurs when enzymes are chemically crosslinked to directly to each other, without added carrier material present, to form large insoluble molecular clusters.

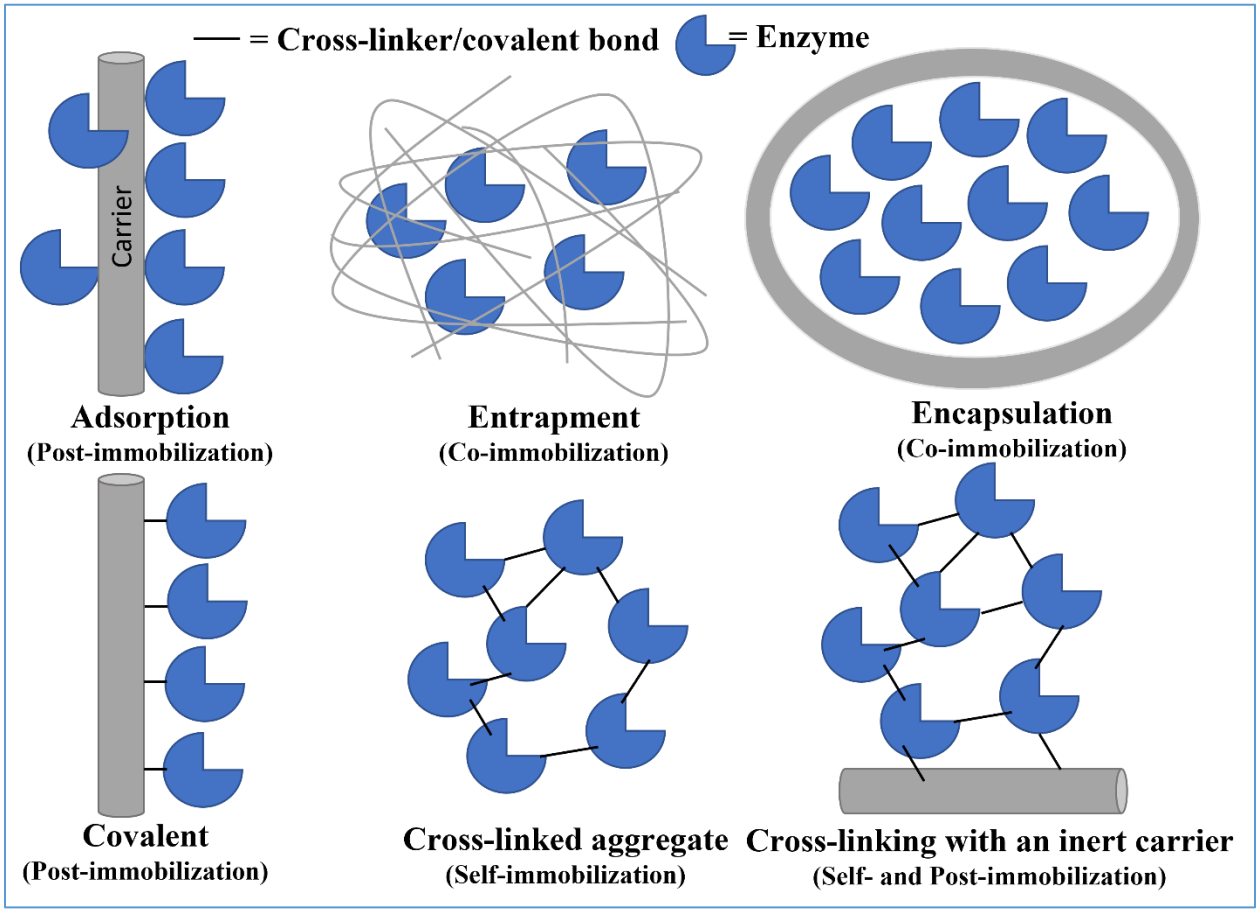

Figure 1.2: Schematic presentation of the main mechanisms of enzyme immobilization on or in polymeric supporting materials.

The choice of immobilization technique mainly depends on the properties of the solid matrix and the performance behavior required. Enzyme immobilization is generally accompanied by changes in apparent enzymatic activity and may involve changes in optimum pH, temperature, and stability. Characteristics of different enzyme immobilization methods are compared in **Table 1.1**.

Encapsulation and entrapment methods are desirable for achieving high enzyme loading (e.g. 76% immobilized yield was reported for maltase from *B. licheniformis* entrapped into agarose beads[72]) with minimal impact on enzyme structure, though the resulting catalytic activity is typically lower than post-immobilized enzymes because the presence of physical barriers slows down substrate diffusion to enzyme active sites. Performing co-immobilization can be as simple as a "single step" mixing of a water-soluble polymer with an enzyme solution and forming the mixture into the desired shape while drying to solidify it. Enzyme becomes surrounded by and is held inside the solid, which may nevertheless remain permeable to small substrate and product molecules. Immobilization in water-soluble polymers can be useful for applications that require organic solvents, or the materials can be made water-insoluble by treatment with cross-linking chemicals. When co-immobilizing enzymes with a non-aqueous polymer solution, more complex recipes involving additives may be needed to form enzyme-compatible polymer solutions. Enzymes that are post-immobilized by covalent chemical bonding or cross-linking are firmly attached to the outside surfaces of carriers, resulting in minimal leaching. Post-immobilized enzymes positioned on the carrier surface experience minimal substrate diffusion limitations and exhibit high catalytic activity.

Table 1.1: Comparison of various enzyme immobilization methods [modified from Thangaraj and Solomon[73]].

Characteristics	Encapsulation	Entrapment	Physical adsorption	Covalent attachment	Cross-linking
Immobilization mode	Co-immobilization	Co-immobilization	Post-immobilization	Post-immobilization	Self-immobilization
Preparation complexity	Varies	Varies	Low	Moderate to high	Low to moderate
Cost	Low	Low to moderate	Low	High	Low to moderate
Binding nature	Strong	Strong	Weak	Very strong	Strong
Stability	High	High	Low	High	High
Enzyme leaching	Very low	Low to moderate	High	Low	Low
Substrate diffusion limitations	High	High	Very low	Low	Low to moderate
Enzyme loading	Very high	High	Low to high	Low	High
Immobilization yield	Very high	High	Low to moderate	Low	High
Enzyme structure	Almost no impact	Minimal impact	Minimal impact	Potential changes	Potential changes
Enzyme activity	Low	Low	Intermediate	High	High
Chemical additives	Varies	Varies	Not required	Required	Required
Applicability	Very wide	Broad	Broad	Selective	Broad

1.2.1. Self-immobilization

Cross-linked enzyme aggregates (CLEAs) and cross-linked enzyme crystals (CLECs) are forms of enzyme self-immobilization, in which the formation of chemical bonds between enzyme molecules increases their molecular size to the extent that enzyme clusters precipitate from the solution. CLEAs are formed by physical aggregation of enzymes from an aqueous buffer using a precipitant (e.g., salts, water-miscible organic solvents, non-ionic polymers) and in situ chemical crosslinking using a bifunctional reagent (**Figure 1.2**).[74] A highly purified enzyme solution is not required for the preparation of CLEAs. CLECs are prepared by crystallizing enzymes from highly purified enzyme solutions and stabilizing them as water-insoluble solids by introducing covalent bonds using crosslinking reagents.[75] These carrier-free immobilization methods avoid costs associated with carriers, but may require additional enzyme purification, and while the range of physical size, shape, and properties of the aggregates alone could be limited, they can be attached to solid supporting materials.[76] Further elaboration on self-immobilization mechanisms is found in Sheldon *et al*.[77]

1.2.2. Post-immobilization

Post-immobilization is a two-step process, where the carrier material is fabricated first, and the enzyme is then attached to the prefabricated matrix (**Figure 1.1)**. There is no requirement for carrier materials to change between solid and liquid forms during the immobilization procedure, and carrier matrices can be prepared by any method without concern for whether enzymes can tolerate carrier fabrication conditions. However, the carrier matrix may require surface modification to create attachment points for the enzyme.[78] Immobilizing enzymes can then be

as simple as immersing suitably modified matrices in an enzyme solution for sufficient time to complete the immobilization process (for adsorption immobilization). More complex reagents and reactive sequences are also common (for covalent immobilization).

1.2.2.1. Covalent attachment

In covalent immobilization, a covalent bond is formed between enzymes and carriers (**Figure 1.2**). In this post-immobilization mode, carrier materials are synthesized separately, carrier surfaces are activated, and enzymes are covalently bonded to carrier surfaces using bifunctional or multifunctional coupling reagents. Functional groups on the polymer carrier such as amino, carboxylic acid, imidazole, indolyl, and phenolic hydroxyl groups form covalent bonds with one end of the coupling reagent, and the other end reacts with enzyme chain end functional groups or with side-chain amino acid (e.g., lysine, cysteine, aspartic acid, and glutamic acid) functional groups.[79,80] Dicyclohexyl carbodiimide,[81] 1,1'-carbonyldiimidazole,[82] hydrate-acyl azide,[83] diazonium salt,[84] bromide-cyanogen,[71] glutaraldehyde,[85,86] and dextran aldehyde[87] are common coupling agents. Ideally, the coupling of enzymes with support materials by covalent bonding is irreversible, preventing leakage of enzymes from the carrier even under inhospitable reaction conditions.[88] In practice, some low level of leaching is usually observed initially, as non-covalently bound adsorbed protein is washed off. After that, the level of leaching can be very low, depending on the durability of the covalent bonds. Since the carrier materials are prepared separately, and the immobilization steps are conducted in buffer solution, polymer-solvent-enzyme compatible triads are not essential here. Further elaboration on covalent immobilization mechanisms is found in Cen *et al*.[89]

1.2.2.2. Adsorption attachment

Physical adsorption of enzymes onto solid supporting materials is a convenient and straightforward method of immobilization. In post-immobilization adsorption attachment, a carrier material is initially fabricated or modified in one step, and then afterward, it is exposed to an enzyme buffer solution for a specific time for physical adsorption to occur.[90] Almost any solid supporting material, including natural and synthetic polymers, can be used as post-immobilized carriers. Numerous commercially available enzymes have been immobilized on various solid materials, including alumina, silica gel, porous glass, porous ceramics, activated carbon, ion exchange resins, biopolymers, and blended synthetic-natural polymers.[91,92] The level of enzyme loading depends on the accessible surface area of the carrier because enzymes are adsorbed on the surface or in the pores of supporting materials in spontaneous reversible processes by weak physical forces: hydrogen-bonding, electrostatic interactions, hydrophobic interactions, or van der Waals forces.[93] Efficient enzyme loading on supporting materials by electrostatic interactions is controlled by changing enzyme solution pH.[94] Because the surfaces of enzyme molecules carry net positive or net negative charges below and above the enzyme's isoelectric point (pI), respectively, enzymes can be immobilized by electrostatic binding onto carrier materials having the opposite charge at a particular solution pH. Optimal electrostatic interactions for maximum enzyme adsorption can occur when the immobilization solution pH is in between the enzyme pI and the support pI. For instance, the highest adsorbed β-glucosidase (pI ~4.5) on SBA-15 (pI ~2) was observed at pH 3.5.[95] Alternatively, the extent of enzyme loading by physical adsorption can depend primarily on the accessible surface of carrier materials, where enzymes penetrate to a certain depth into the carrier matrix depending on carrier porosity. **Figure 1.3 (A)** shows a

synchrotron infrared microscopic image of a cross-section of Novozym 435 beads.[96] Novozym 435 is a well-known commercially available immobilized acrylate-based polymer bead where *Candida antarctica* lipase B (CALB) enzymes are physically adsorbed (post-immobilization mode) on the mesoporous surface.[97] Loading CALB at the solid surface keeps the enzyme accessible to its substrate. After adsorption, enzymes must sufficiently retain their native structure to achieve the high remaining catalytic activity. Simplicity and high activity retention are the key advantages of adsorption attachment over other attachment modes. However, the relatively weak interactive forces often result in enzymes leaching out from the carriers upon changed conditions, such as pH, temperature, and solvent polarity. The leaching out of enzymes from carrier materials is the main drawback of physical adsorption.[98]

Occasionally, physical enzyme adsorption is reported as part of a co-immobilization mode.[99–102] For example, CALB was immobilized on magnetic poly(urea-urethane) nanoparticles (MNPs-PUU) by single-step mini-emulsion polymerization using diisocyanate and 1,6-hexanediol monomers.[103] Diisocyanate monomer and organic coated MNPs were in the dispersed phase (organic), and free enzyme and polyol monomer were in the continuous phase (aqueous). The MNPs encapsulated PUU nanoparticle was synthesized, and CALB adsorbed on the produced MNPs-PUU surface simultaneously. **Figure 1.3 (B)** presents the single-step co-immobilization process of CALB enzyme on magnetic poly(urea-urethane) (MNPs-PUU) nanoparticles by single-step interfacial mini-emulsion polymerization. As shown in the schematic, this strategy was used to keep the CALB enzyme accessible at the particle surface.

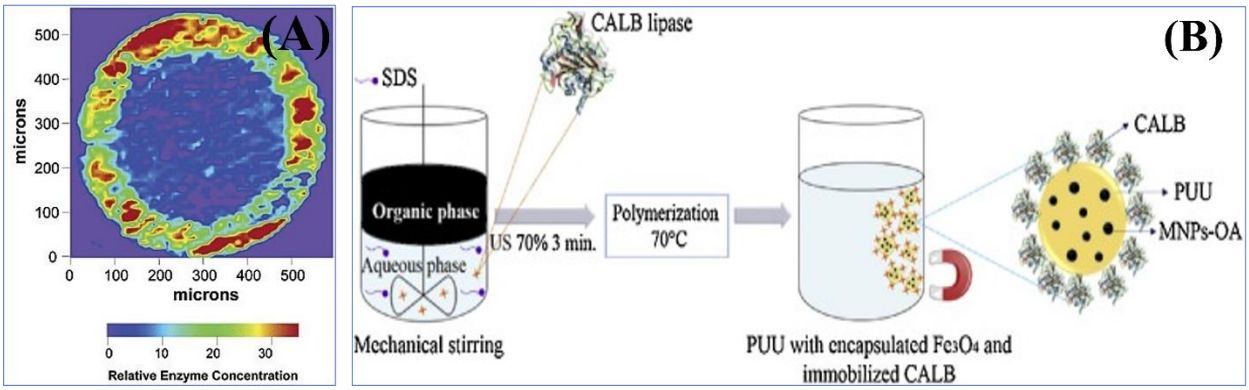

Figure 1.3: (A) infrared microscope image of Novozym 435 (immobilized CALB) showing CALB distribution on the Lewatit VP OC 1600 particle (Reprinted with permission from Mei et. al. [96]. Copyright (2003) American Chemical Society) and (B) Schematic representation of CALB enzyme immobilization on magnetic poly(urea-urethane) (MNPs-PUU) nanoparticles by single-step interfacial mini-emulsion polymerization (Reprinted with permission from Chiaradia et.al. [103]. Copyright (2016) Elsevier).

1.2.3. Co-immobilization

Co-immobilization is a process where the solid carrier support fabrication and enzyme immobilization are carried out simultaneously (in-situ process).[104] This approach requires the solid carrier to be processed in a liquid form, i.e., it needs to dissolve or melt. Since enzymes generally denature in hot polymer melts, a more feasible approach is to dissolve carrier polymers (or monomers) in solvents at moderate temperatures. Lyophilized powder or dissolved liquid enzymes are added to the monomer/polymer solution and homogenized. Then, the immobilization solution (or dispersion) is subjected to fabrication where polymerization occurs, or the polymer solution is solidified by removing the solvent (via drying or coagulation) with enzymes trapped inside the resulting polymer matrix (**Figure 1.1**). Various shapes can be produced, such as beads,[105] foams,[106] films,[107] membranes,[108] hydrogels,[109] nanoparticles,[105] and nanofibers.[110] The shapes are usually chosen to have a high surface area relative to their volume

on the principle that fewer enzymes will be hidden inside the matrix and more will be exposed to the surfaces. In some procedures, enzymes are added mid-way through the materials fabrication process while monomers are reacted to form polymers. For example, to produce lipase co-immobilized polystyrene (PS) particles, lipase enzymes are introduced into the emulsion polymerization reaction mixture approximately halfway through the reaction.[111] The term "co-immobilization" has alternatively been used to refer to the immobilization of multiple cooperating enzymes on the same support to impart stability and enhance cascade reaction kinetics by optimizing catalytic turnover.[112] For example, β-galactosidase, L-arabinose isomerase, and D-xylose isomerase were co-immobilized on Eupergit C 250 L and used for a mozzarella cheese whey lactolysis process. The multi-enzyme co-immobilization replaced multiple bioreactors with a single bioreactor and increased productivity by greater than 50% compared to single enzyme immobilizations.[113]

1.2.3.1. Entrapment immobilization

Entrapment immobilization is a type of co-immobilization in which enzymes are not directly attached to the carrier surface but entrapped and confined within a three-dimensional matrix (**Figure 1.2**). The network structure allows small substrates and products to pass through the matrix while physically retaining the larger-sized enzymes without covalent bonding to the solid. Entrapment preserves protein conformational structure, minimizes denaturation, and prevents leaching. Stabilized enzyme structures result in good storage stability with the potential for triggered enzyme release without compromising the biological catalytic activity of enzymes.[105,114] Entrapment immobilization relies on the enzyme's physical size being larger than the matrix pore

size formed around the enzymes during the entrapment process. Enzymes are large molecules with molecular weights ranging from around 12,000 to over 150,000 Da[115] and globular diameters in the range of approximately 3-7 nm[116] allowing them to be retained inside the solid matrix network while small substrates and products pass through during enzymatic reactions.[71] Entrapped enzymes could leak from the matrix if matrix pore sizes are too large, or enzyme activity could be limited if the pore size is too small. Therefore, pore size distribution is one factor that should be controlled to prevent enzymes from leaching into the liquid reaction medium while maximizing catalytic activity. Sometimes, water-soluble small-molecule porogen, like D-glucose, is used during immobilization to enhance porosity and increase substrate diffusion to enzyme active sites.[117]

Various matrices can be used for entrapment, such as chitosan, agar, gelatin, calcium alginate, collagen, cellulose triacetate, polyacrylamide, silicon rubber, polyvinyl alcohol, and polyurethane.[71] Some of the reported works on enzyme entrapment incorporate horseradish peroxidase in polyvinyl alcohol (PVA) hydrogels and graphene oxide doped PVA hydrogels[118], horseradish peroxidase in chitosan beads[119], protease in agar-agar beads[120], tyrosinase in gelatin gels[121], manganese peroxidase in calcium alginate beads[122], β-galactosidase in silica gel[123], protease in poly acrylamide beads[124], and manganese peroxidase in PVA-alginate beads[125].

1.2.3.2. Encapsulation immobilization

Encapsulation is the most common single-step co-immobilization method, wherein enzymes are enclosed/confined in a semipermeable membrane, usually a spherical-shaped matrix (**Figure 1.2**).[104,126] Macromolecule encapsulation is effective for preventing enzyme aggregation and denaturation.[61] The encapsulation method is widely used because of its simplicity, minimum leaching, and minimal impact on enzyme native structure. Theoretically, encapsulation can quantitatively immobilize all enzymes in a preparation, resulting in maximum immobilization yield. Like entrapment, encapsulation creates a physical barrier between enzyme and substrate. For reactions to occur with encapsulated enzyme, the substrate passes through the semi-permeable encapsulation membrane to reach enzyme active sites where biocatalytic reactions take place, and then the product migrates back out across the membrane, which meanwhile prevents enzyme leaching from the carrier.[57] Encapsulation can be performed under mild conditions to avoid impact on enzyme structure. The semi-permeable carrier retards enzyme structural deformation and helps preserve its native structure, resulting in benefits like triggered storage stability, enhanced thermal stability, and higher non-solvent stability (e.g., organic solvent).[104]

1.2.4. Polymer-enzyme combinations for post-immobilization

A wide variety of materials of both inorganic and organic origin have been used as stable and effective supports for enzyme immobilization. Microbial resistance, mesoporosity, mechanical and thermal strength are unique characteristics of inorganic supports. Limited biocompatibility, lower affinity to biomolecules, and fewer possible geometrical shapes are the main drawbacks

of inorganic carrier materials.[88] On the other hand, polymeric materials can be fabricated into various forms with strictly controlled porosity, but are usually sensitive to pressure or temperature. In principle, any combination of enzymes and polymeric materials can be used for post-immobilization, as long as sufficient affinity or covalent attachment is present. The presence of hydroxyl, carbonyl, and amine moieties in natural polymers (e.g., chitosan, alginate, agarose) endows these materials with an inherent good affinity for protein attachment on their surfaces. The two most prevalent structural polysaccharides, cellulose and chitin, are widely used for enzyme post-immobilization.[42,127–129] In comparison, strongly hydrophobic polymers, such as polyethylene (PE) and polystyrene (PS), must usually first be subjected to surface activation (e.g., plasma treatment), then modified with chemical cross-linkers to introduce functional groups for post-immobilization.[130–132] Synthetic polymers often require surface modification to achieve post immobilization.[133] Some commonly used synthetic polymers are PVA,[134] polyvinyl acetate (PVAc),[81] polyimide (PI),[91] polyacrylates (e.g., poly(methyl methacrylate) (PMMA), Eupergit®-C),[135,136] polyamide (e.g. nylon 6),[137] polyacrylonitrile (PAN),[138] polyaniline (PANi),[139] poly(ethylene glycol) (PEG),[140] and Poly(lactic-co-glycolic acid) (PLGA)[141].

Blending polymers or making copolymers is another way of enhancing enzyme affinity through the introduction of chemically functional side groups and polarity. Commonly used copolymer and polymer blends are cellulose acetate/PCL,[142] cellulose acetate/polyamide,[143] chitosan/PVA,[144] chitosan/PLA,[145] PMMA/PANi,[146] polyvinyl alcohol-polyvinyl acrylic acid (PVA-PAA),[82]PVA-PEG,[147] poly (glycidyl methacrylate-g-poly(ethylene terephthalate)),[85] poly (vinyl alcohol-co-ethylene),[33] and poly(N-isopropyl acrylamide-co-acrylic acid).[11]

Table 1.2 lists polymer-enzyme combinations that are immobilized through the post-immobilization process, where enzymes are attached to prefabricated carrier materials. In cases where carrier material fabrication involved solvent processing prior to enzyme immobilization, the solvent is listed. If modifiers were used, this is also indicated. The most common modifier is glutaraldehyde, a crosslinking agent. Enzyme loading, immobilization yield (relative to the amount of free enzyme used), activity retention (relative to free enzyme activity), and residual catalytic activity (after storage or reuse, relative to initial immobilized activity) are important immobilization metrics, yet individual reporting of these values is often incomplete. The relative parameters are defined as:

$$\text{Immobilization yield } (\%) = \frac{\text{Quantity of immobilized enzyme}}{\text{Total amount of enzyme used}} * 100 \quad \text{(1.1)}$$

$$\text{Activity retention } (\%) = \frac{\text{Immobilized enzyme activity}}{\text{Free enzyme activity}} * 100 \quad \text{(1.2)}$$

$$\text{Residual catalytic activity } (\%) = \frac{\text{Remaining activity after storgae/reuse}}{\text{Initial immobilized enzyme activity}} * 100 \quad \text{(1.3)}$$

Post-immobilization yield especially depends on the material surface area because a higher surface area gives more space for enzymes to attach. As a result, most of the listed supporting materials are nanostructure shapes (e.g., nanofibers, nanoparticles). Especially high enzyme loadings (> 10 wt %) were reported for polystyrene (PS) nanoparticles, which adsorbed 248 mg *Candida antarctica* lipase/g supports[148], polyvinyl alcohol (PVA)-polyacrylic acid (PAA) (4:1) electrospun nanofibers, which were covalently attached with 181 mg α-amylase/g support,[82] and poly(N-isopropylacrylamide-co-acrylic acid) (p(NIPAM-co-AA)) microspheres, which were covalently attached with 493 mg trypsin/g supports.[11] Post-immobilized support materials are

usually selected for their durability, and their insolubility in aqueous solutions enables repeatable applications. For example, covalently immobilized lactase (from *Agaricus bisporus*) on polyaniline nanofiber surface retained 98% of its initial activity after 10 reuse cycles[32], and trypsin immobilized on PVA-PAA nanofibers surface retained 82% of its initial activity after 15 cycles.[82]

Table 1.2: Compilation of typical enzyme post-immobilization on polymer carriers by surface modification/activation.

Carrier	Carrier form	Solvent	Enzyme	Enzyme origin	Immobilization medium	Modifier	Enzyme loading (mg/g supports)	Immobilization yield (%)	Activity retention (%)	Residual activity, (%/days/ °C)	Reuse cycle/ activity,%	Ref.
Adsorption method												
Cellulose	Nanofiber	-	Glutamate dehydrogenase		Phosphate buffer	-	1.8	-	32	64/56/25	9/83	[149]
Polycaprolactam	Nanofiber	Acetone	Protease	-	Phosphate buffer	-	-	-	60	-	5/48	[142]
Polycaprolactone (PCL)	Nanofiber	Formic acid	Protease	-	Phosphate buffer	-	-	-	65	-	5/30	[142]
PS	Particle	-	Lipase	*Pseudomonas fluorescens*	Phosphate buffer	Octyl silica	-	91	82		5/90	[150]
PS	Nanoparticles	-	CALB	*Candida antarctica*	PBS buffer	-	248	-	184	-	-	[148]
Cellulose monoacetate /polycaprolactone	Nanofibers	Acetone	Protease	-	Phosphate buffer	-	-	-	80	-	5/21	[142]
Cellulose monoacetate /chitosan	Nanofibers	Acetone	Protease	-	Phosphate buffer	-	-	-	66	-	32/5	[92]
PVA-co-PE	Membranes	70% isopropanol	Cellulase	-	Phosphate	sodium-3-sulfobenzoate	130	-	-	-	5/80	[33]
Covalent Attachment Method												
Cellulose	Nanofiber	-	Laccase	*Pleurotus florida*	sodium acetate buffer	Glutaraldehyde	0.4U/mg		88	-	5/85	[31]
Cellulose	Ultrafine	-	Lipase	*Candida rugosa*	Phosphate buffer	Glutaraldehyde	-		54	-	-	[34]

Table 1.2 Continued

Cellulose	Nanofiber	-	Glucanotransferage	*Bacillus macerans*	Phosphate buffer	1,2- dodecane diamine	10	62	45	-	10/60	[26]
Oxidized pulp	Fiber	-	Pectinase	Commercial	Phosphate buffer	Sodium periodate	8.7	-	-	-	7/60	[27]
Coconut fiber	-	-	Laccase	*Aspergillus*	Phosphate buffer	Oxidation	-	-	74	40/4/4	10/45	[30]
Gelatin	Bead	Water	Laccase	*Trametes versicolor*	Citrate phosphate buffer	Glutaraldehyde	-	31	50	45/6/60	-	[126]
Wool-g-polyethylacrylate	Fiber		Lipase	*Candida rugose*	Phosphate buffer	Hydrazine hydrate	81	95	80	-	6/89	[151]
Silk-g-PAN	Fiber	Methanol	β-galactosidase	*Escherichia coli*	Phosphate buffer	Hydrazine hydrate	76	98	71	-	6/92	[151]
Cellulose monoacetate /chitosan	Nanofibers	Acetone	Protease		Phosphate buffer	Glutaraldehyde	-	-	83	-	41/5	[92]
PET	Fabric	Dioxane	Trypsin	Porcine pancreas	Trizma buffer	N, N'-di-cyclo-hexyl-carbodiimide, and glutaraldehyde	60	-	-	45/20/4	15/18	[152]
Polyacrylonitrile	Hollow fibers		Urease	-	Aqueous	Glutaraldehyde	-	-	-	15/42/4	15/86	[138]
Polyaniline	Nanofibers	1 M HCl	Lactase	*Agaricus bisporus*	Phosphate buffer	Glutaraldehyde	-	73		95/96/25	10/98	[32]
PP	Film	-	Glucose oxidase	*Aspergillus niger*	-	Plasma treatment&Glutaraldehyde	-	-	74	-	-	[130]
PVDF	Membrane	-	Laccase		Phosphate buffer	Glutaraldehyde	-	-	97	85/7/4	5/75	[153]

Table 1.2 Continued

Polyamide	-	-	Protease	*Conidiobolus macro - sporus*	Phosphate buffer	Glutaraldehyde	-	-	58	-	-	[154]
Nylon 6	-	-	Lipase	*Bacillus coagulans*		Glutaraldehyde	0.2	70	88	-	8/85	[137]
PVA/PAA	Electro-spin NF	Water	α-Amylase	-	-	1,10-carbonyldiimidazole	181	-	78	83/30/30	15/82	[82]
Glycidyl methacrylate -g-poly (ethylene terephthalate)	Fibers	Acetone	Horseradish peroxidase	-	Phosphate buffer	1,6-diamino hexane and glutaraldehyde	-	-	-	-	5/70	[85]
Poly(N-isopropylacrylamide-co-acrylic acid)	Microspheres	Cyclohexane	Trypsin	-	Phosphate buffer	N-(3-dimethyl aminopropyl)-N'-ethyl carbodiimide hydrochloride	493	-	155	80/60/4	-	[11]

1.2.5. Polymer-solvent-enzyme combinations for co-immobilization

Co-immobilization processes require the polymer-solvent pairs, matrix properties, and the conditions used for immobilization to be compatible with enzymes. Many enzymes show maximum activity in aqueous media, and such enzymes can form compatible solutions for co-immobilization using aqueous polymer solutions. Certain natural polymers, like alginate, agarose and chitosan, are water-soluble, depending on pH, and can be mixed with enzymes to produce compatible solutions[155–157] that are then fabricated into different shapes, such as beads,[158] hydrogels,[159] capsules,[160] films,[161] particles,[162] nanoparticles,[163] and nanofibers.[164] Natural polymer derivatives (e.g., acetate, nitrate, carboxymethyl) having improved water and organic solvent solubility makes them available for co-immobilization,[165] and water-soluble synthetic polymers, like polyvinyl alcohol (PVA)[166] and polyethylene oxide (PEO),[167] can also be used, as well as natural-synthetic polymer blends that can facilitate single step co-immobilization.[168,169] A drawback is that water-soluble carriers generally cannot be repeatedly used in aqueous applications. However, these carriers can be converted to insoluble matrices using chemical modifiers (e.g., cross-linkers).[170]

Water-insoluble synthetic polymers broadens the application versatility of enzyme immobilization matrices with their excellent flexible mechanical properties and easy manipulation by melt- or solvent-processing into desired shapes. However, mixing enzymes with molten polymers is usually avoided due to enzyme thermal instability. Instead, enzymes are mixed with polymers dissolved in organic solvents or mixed in situ with monomers during polymer synthesis (by emulsion polymerization). Typical recipes for enzyme entrapment or encapsulation using aqueous solutions or by aqueous-organic emulsion polymerization are listed

in **Table 1.3**. The listed carriers were synthesized in four ways: solubilization in aqueous media and fabrication, solubilization in non-aqueous media (forming water/oil microemulsion) and fabrication, in-situ polymerization (aqueous media), and microemulsion polymerization (non-aqueous media). In solubilization in aqueous media and fabrication, enzymes were mixed in an aqueous polymer solution and formed enzyme-compatible aqueous polymer solutions (polymer-water-enzyme triad). The enzyme immobilized aqueous solution was then directly used to prepare the final form of the supporting materials. In encapsulation through water-oil micro-emulsions, polymers were dissolved in organic solvents, enzymes were placed in the aqueous phase, and a surfactant was used to form the water-oil microemulsion (polymer-solvent-enzyme compatible triad). The water/oil microemulsion compatible triads are then fabricated to the desired shapes. For in-situ polymerization, polymer matrices were synthesized in the presence of enzyme solution where enzymes are encapsulated or entrapped into synthesized matrixes. Finally, with microemulsion polymerization, enzymes, initiator and surfactant were added in the aqueous phase and monomers were dispersed in the aqueous phase. Enzymes were co-immobilized (entrapment or adsorption or encapsulation) into/on the produced polymers. Most of the reported co-immobilized enzymes were produced by entrapment and encapsulation in polymer matrices. For example, water-in-oil microemulsion encapsulation was performed using polycaprolactone (PCL) and its copolymers,[142] polylactic acid (PLA)[171], and poly(lactide-co-glycolide) (PLGA),[172] while entrapment was accomplished through in-situ polymerization of polyacrylamide with enzymes in the reaction mixture.[124] However, some physically adsorbed co-immobilized enzymes were also reported. In addition, single-step co-immobilizations are not reported as frequently as post-immobilization approaches.

Table 1.3: Compilation of typical cases of enzyme co-immobilization into polymer carriers.

Enzyme	Enzyme origin	Carriers	Reaction medium/ Solvent	Final form	Immobilization method	Enzyme loading (mg/g supports)	Immobilization yield (%)	Activity retention (%)	Residual activity, (%/days/ °C)	Ref.
Dissolved in aqueous media and fabrication										
Cellulase	*Trichoderma reesei*	Alginate	Aqueous $CaCl_2$	Bead	Encapsulation	3.4	-	-	60/21/37	[105]
Maltase	*B. lichenifo rmis*	Agarose	K phosphate buffer	Bead	Entrapment		76	-	80/180/4	[72]
Facin extract	Fig latex	Agarose	$NaCO_3$ solution	Bead	Entrapment	10	-	95	-	[161]
Maltase	*B. lichenifo rmis*	Agar-agar	K phosphate buffer	Bead	Entrapment	-	83		80/180/4	[72]
Bromelain	Pineapple stem	Cellulose triacetate	Acetone:DMF (85:15)	Electros pun NF	Encapsulation	-	92	47	-	[165]
β-D-glucosidase	*Aspergillus niger*	Chitosan	Na tripolyphosphate	Bead	Entrapment	5	35	30	100/91/16	[87]
Lipase	*Yarrowia lipolytica*	Chitosan-alginate blend	Aqueous $CaCl_2$	Bead	Encapsulation	-		79	35/75/25	[104]
Horseradish peroxidase	-	Chitosan-PEG blend	Acetic acid	Particle	Encapsulation	-	52	60.4	-	[101]
Maltase	*B. lichenifo rmis*	Polyacrylamide copolymer	water	Bead	Entrapment	-	71		5/180/4	[72]
Horseradish peroxidase	-	PVA	Water	Electros pun NF	Entrapment	3.5	98	-	-	[173]
Cellulase	-	PVA	Acetic acid buffer	Electros pun NF	Encapsulation	-	-	65	-	[108]
Monoamine oxidase	*Aspergillus niger*	PVA-PEG	water	Gels	Encapsulation	-	-	-	-	[147]

Table 1.3 Continued

Phytase	Cowpea seed	PVA-chitosan	Sodium acetate buffer	Electrospun NF	Entrapment	2.5	-	-	-	[164]
Dissolved in non-aqueous media (forming water/oil microemulsion) and fabrication										
CALB	*Candida antarctica*	PCL	PS,, enzyme, toluene, AOT	Film	Encapsulation	16 & 65	-	-	-	[107]
α-chymo-trypsin	-	PS	PS, enzyme, toluene, AOT	Electrospun NF	Encapsulation	13	-	35	-	[110]
Trypsin	-	PCL	PCL, chloroform/DMF, span 80, enzyme buffer	Electrospun NF	Encapsulation	23	-	66	57/15/4	[174]
Laccase	*Trametes versicolor*	PLA	PLA, methylene chloride, PEO-triblock copolymer, laccase solution	Electrospun NF	Encapsulation	-	-	67	50/14/4	[175]
Pyruvate de-hydrogenase	Porcine heart	PLGA	PLGA, acetone, enzyme buffer, SDS	Nanoparticles	Encapsulation	2.5	20	-	63/6/4	[172]
In-situ polymerization (aqueous media)										
CALB	*Candida antarctica*	Polyurethane	Polyol, isocyanate, enzyme solution (polymerization)	Foam	-	-	-	535	87/360/25	[106]
Protease	*Aspergillus niger*	Polyacrylamide	Acrylamide, methylene bisacrylamide, enzyme solution polymerization	Beads	Entrapment	-	76	-	33/30/4	[124]
Mini-emulsion polymerization (using surfactants)										
Cellulase	-	PMMA	Methyl methacrylate, SDS, water, enzyme, initiator	Nanoparticles	Adsorption	60	60	-	>90/7/4	[100]
CALB	*Candida antarctica*	PMMA	Methyl methacrylate, SDS, water, enzyme, initiator	Nanoparticles	Adsorption	50	75	-	-	[102]
Lipase	*Thermomyces lanuginosus*	PS	Styrene, PVA, span 80, enzyme buffer	Nanoparticles	Adsorption	-	60	57	-	[111]
CALB	*Candida antarctica*	PEGylated poly(urea-urethane)	Isophorone diisocyanate, PEG, PCL, cyclohexane, SDS	Nanoparticles	-	-	-	67	-	[99]
CALB	*Candida antarctica*	Magnetic poly(urea-urethane)	Diisocyanate, hexanediol, MNPs-OA, cyclohexane, water, SDS	Nanoparticles	Adsorption	-	-	85	-	[103]

1.3. Polymer-Solvent-Enzyme Compatible Triads

Non-membrane-bound enzymes are usually insoluble in organic solvents because their exterior surfaces are decorated with polar and ionic amino acids that interact with water.[66] When enzymes are exposed to non-aqueous media (e.g., organic solvents, synthetic polymer solutions), internal hydrophobic segments tend to interact with the media, causing enzymes to denature ("unfold") or aggregate, making them unavailable for biocatalytic reactions.[176,177] However, because organic-soluble synthetic polymers have desirable properties as immobilization supports, namely the potential for creating water-insoluble high surface area flexible materials, the possibility of enzyme co-immobilization in these systems warrants investigation. This requires selecting polymer-solvent-enzyme compatible triads for enzyme co-immobilization methods. The following discussion identifies compatible polymer-solvent combinations, compatible enzyme-solvent combinations and finally assesses which combinations could generate compatible polymer-solvent-enzyme triads. Strategies to enhance compatibility are also considered.

1.3.1. Polymer-solvent compatibility

Polymer solubility is not straightforward like small molecules because of the vastly different sizes of polymer and solvent molecules. The interaction of polymer and solvent depends on many factors, such as polymer type, copolymer type and composition, molecular weight, branching, crystalline form, degree of crystallinity, temperature, and solvent polarity.[178] Polymers have a high molecular weight, and crystalline polymers have well-ordered chains that often require extended time and heat to disrupt intermolecular forces for dissolution. Solubility decreases with

increasing polymer molecular weight, crystallinity, and degree of cross-linking, and other factors, like chain branching, can lead to unpredictable solubility behavior within a given polymer class.

Polymers exert attractive interactions between adjacent molecules, including van der Waals forces for simple hydrocarbon polymers (e.g., PE, PP, PS) and dipole/dipole interactions for polar side group polymers (e.g., PAN and PVC). Polyamide and polyurethane polymers have strong polar and hydrogen bonding interactions that lead to stiff structures. Solid polymers having polar interactions and hydrogen bonds holding the polymer chains together require highly polar solvents for dissolution because the dissolution process requires higher interactive forces between polymer and solvent than between polymer chains.[179] Suitable solvent selection depends on the polymer type. **Table 1.4** lists common polymers with their typical solvents according to four categories: polymers that dissolve in aqueous solvents; polymers that require strong acids to dissolve; polymers that dissolve in non-polar organic solvents; and polymers that dissolve in polar organic solvents. The table also ranks organic solvent polarity based on the dielectric constant at 20 °C. Polar-organic solvents with a higher dielectric constant are more effective at breaking electrostatic interactions between molecules and separating charges than nonpolar organic solvents and are thus able to dissolve polymers (e.g., PCL, PVP, PAN) comprising polar functional groups along their backbone. Thermoplastic polyamides (e.g. nylons) dissolve in strong mineral acids due to the presence of ionizable end groups and protonation of backbone amide group oxygens that disrupt the very strong intermolecular hydrogen bonds.[180] The solubility of non-polar hydrophobic polymers (e.g., PS, PP) is governed by dispersion forces, and non-polar organic solvents are required to dissolve them.[181]

Table 1.4: Compilation of common polymer-solvent systems and organic solvent polarity ranking.

Polymers	Common Solvents	Ref.
	Aqueous-soluble	
PEO, PEG, PVA, PVP	Water	[182–184]
Chitosan and derivatives	Dilute acids, e.g., formic acid, acetic acid, lactic acid; TCA	[185,186]
Cellulose ether derivatives	Aqueous alkali, NaOH/urea	[187,188]
Alginate and derivatives, Agarose	Aqueous and aqueous-organic media	[189,190]
	Strong Acid soluble	
Polyamide (nylon)	Strong inorganic acid, formic acid, acetic acid,	[180]
Polyacrylamide	Formic acid, strong inorganic acid	[191]
	Organic-soluble (non-polar organic)	
PE, PP	Above 80°C: xylene, benzene, toluene, halogenated hydrocarbons, higher aliphatic esters, and ketones	[188,192]
PS	Xylene, benzene, toluene, THF, MEK	[188,193]
	Organic-soluble (polar organic)	
Cellulose acetate derivatives	THF, DCM, ethylene carbonate	[188,194]
PEO, PEG, PVA, PVAc	Chloroform, THF, DMF, hexafluoro propanol, chloroform: acetone (3:1)	[182–184]
PLA, PLGA	Dioxane, chloroform, THF, DCM, hexafluoro propanol, THF: DMF (3:1), chloroform: acetone (4:1)	[195–198]
PVP	Chloroform, THF, pyridine, acetone, DMAc, DMF, acetone	[188,199]
PVDF	NMP, DMAc, DMF, DMSO, DMF-acetone (1:9), isopropanol-H_2O	[200–205]
PCL	Chloroform, THF, DCM, hexafluoro isopropanol, methanol, DMF:chloroform (1:2)	[206,207]
Polyacrylonitrile (PAN)	DMF, ethylene carbonate	[188,208]
Polyaniline (PANi)	DMF	[209]
Polyacrylamide	Phenol, morpholine	[188,191]
Polyacrylate (PMA, PMMA)	Benzene, toluene, chloroform, THF, DCM, acetone, DMF	[210,211]
Polyesters (PET)	THF, phenol, chlorophenol, DMSO, nitrobenzene	[188,212]
Polyamide (nylon)	m-cresol, THF, phenol, chlorophenol	[188,211,213]
Polyurethane	DMF, DMF-THF, Hexafluoro isopropanol	[188,214,215]
	Organic solvent polarity rank (Dielectric constant at 20 °C)	
Aprotic solvents	Hexane (1.88) <octane 1.96 <carbon tetrachloride (2.24) <1,4-dioxane (2.25) <p-xylene (2.27) <benzene (2.28) <toluene (2.38) <chloroform (4.81) <THF (7.52) <DCM	[216,217]

	(9.08) <pyridine (12.4) <MEK (18.51) <acetone (20.7) <NMP (32) <nitrobenzene (34.82) <acetonitrile (36.64) <DMAc (38) <DMF (38.25) < DMSO (46.7) <propylene carbonate (64.9)	
Protic solvents	TCA (4.5 at 15.6 °C**)** Acetic acid (6.20) <t-butyl alcohol (12.5) <HFIP (15.7) <iso-propanol (17.9) <ethanol (24.6) <methanol (32.7) <water (78.54)	[216,218]

DCM: dichloromethane, DMAc: dimethyl acetamide, DMF: Dimethylformamide, DMSO: dimethyl sulfoxide, HFIP: hexafluoroisopropanol, MEK: Methyl ethyl ketone, NMP: N-methyl pyrrolidone, TCA: Trichloroacetic acid, THF: Tetrahydrofuran, TMP: Trimethyl phosphate

The ability of certain natural and synthetic polymers or their derivatives to dissolve in aqueous solvents depends on the presence of hydrogen bond donor and acceptor groups (such as hydroxyl, amine, and carbonyl) along the polymer chain that participates in hydrogen bonds with water molecules and/or ionizes in aqueous solutions.[219] Similarly, electronegative oxygen atoms that form ether linkages in poly(ethylene oxide) act as hydrogen bond acceptors with water molecules to form high-weight percentage aqueous polymer solutions.[184] Using aqueous media to manipulate polymers during fabrication is convenient because water-soluble enzymes are generally compatible with these systems, provided that pH-dependent charge neutralization does not lead to flocculation. For example, enzymes can be directly mixed with viscous aqueous solutions of alginate and agarose salts.[114,158] Also, because chitosan amine groups become protonated at low pH values, making this polymer soluble in aqueous organic acids (e.g., acetic acid, formic acid, lactic acid) and organic acid buffers (e.g., acetate buffer),[220] enzymes capable of tolerating acidic pH conditions can be mixed directly with pH-buffered chitosan solutions.[157] Enzyme (e.g., lipase from *Candida rugosa*) can be immobilized in polyvinyl alcohol (PVA) matrix (e.g., electrospun fiber) from aqueous mixtures of enzyme and PVA solution.[221] However, the residual aqueous solubility of enzyme immobilized PVA matrices renders them impractical for

repeated use in water. To improve durability, PVA, with its multiple hydroxyl groups, can be converted to a water-insoluble matrix by applying chemical modification (e.g., cross-linking with glutaraldehyde).[222] Polyvinylpyrrolidone (PVP) has polar carbonyl moieties that promote its solubility in aqueous and high polarity organic solvents (e.g., acetone, ethanol, dimethylacetamide (DMAc), and in dimethylformamide (DMF)).[199,223] The aqueous solubility of PVP enables the production of enzyme compatible triad solutions by simply mixing PVP polymer solutions and aqueous enzyme solutions. The resulting miscible solution can be directly formed into fibers by solution spinning techniques, like electrospinning.[224] The chief limitation of using water-soluble polymers for enzyme immobilization is that their use as durable immobilization matrices is limited to non-aqueous environments, which nevertheless may be important for some applications such as esterification reaction in non-aqueous media.[225]

Some natural polymers, like cellulose, that have linear unbranched polymer chains capable of forming stiff intra-molecular hydrogen-bonded structures do not readily dissolve in aqueous or organic solvents. However, derivative forms, such as cellulose acetate, are soluble in organic solvents that can be used for enzyme co-immobilization.[187] For example, a solution of cellulose triacetate (in 85:15 acetone:DMF) and bromelain solution (using the same solvents mixture) was mixed to produce a compatible triad and subjected to electrospinning to produce bromelain encapsulated cellulose triacetate nanofibers.[165] Another water soluble cellulose derivative is carboxymethyl cellulose, which can be dissolved in water, mixed with enzyme (e.g., lipase) solution and fabricated into desired shapes (e.g., film) to make enzyme-embedded matrixes.[226]

Synthetic “plastic” polymers span a wide range of solubility behaviors. Similar to cellulose, polyamide polymers (e.g. nylon) strongly interact to form intermolecular hydrogen bonds between amide groups and only a few solvents, such as formic acid, cresol, 1:1 trifluoroacetic acid (TFA), and acetone, can dissolve nylon.[180] Simple hydrocarbon polymers, such as polyethylene (PE), polystyrene (PS), and polypropylene (PP), are highly hydrophobic and soluble in relatively low polarity organic solvents (e.g., cyclohexane, hexane, xylene, benzene, and toluene.[192,193] PVDF, PCL, PLA, and PLGA are insoluble in aqueous solvents yet are soluble in most polar organic solvents, such as DMF, DMSO, DMAc, NMP, DCM, THF, chloroform, and hexafluoroisopropanol.[183,205,206,227] These biodegradable and biocompatible polymers have been extensively studied as delivery vehicles for biologics.[53] Suitable polymer-solvent-enzyme compatible triads of these polymers could produce useful enzyme carrier matrices for co-immobilization. In addition, polyacrylates (e.g., PMA, PMMA), polyesters (e.g., PET), polyaniline, polyacrylonitrile, and polyurethane have polar moieties in the backbone and are soluble in polar organic solvents (e.g., DMF) that creates a potential for making enzyme compatible polymer solutions using solution modification.[208,209,211,212,214]

1.3.2. Solvent-enzyme compatibility

Most commercial enzymes are formulated as liquids or in granulated solid forms for industrial, consumer, and medical applications and are designed to disperse when exposed to a water environment.[228] The globular three-dimensional structure of a water-soluble enzyme is essential for carrying out its catalytic role,[229] usually having a hydrophobic inner core and hydrophilic outer surface.[230] The inner body of the tertiary structure is mainly composed of non-polar amino acids

(e.g., phenylalanine, leucine, isoleucine) that are stabilized through hydrophobic forces. The outer surface has ionic side group amino acids (e.g., glutamic acid, lysine) and polar amino acids (e.g., serine, glutamine) to create a hydrophilic environment outside the folded protein, making it water-soluble. Handling native enzymes in aqueous solvents preserves their three-dimensional folded structure. Water molecules are also an essential part of the protein structure, and even crystallized enzymes retain some water. These essential water molecules are located throughout the enzyme structure. A typical protein subunit contains around 200 water molecules. For example, the crystal structure of pyruvate decarboxylase (EC 4.1.1.1) from *Saccharomyces cerevisiae* has 1074 amino acid residues (two subunits) and 440 water molecules (220 per subunit).[231] This structural water acts as a 'molecular lubricant' to promote the conformational mobility required for optimal enzyme catalysis.[64] Therefore, if enzymes are to be incorporated into non-aqueous polymer solutions as part of an immobilization process, enzyme behavior in non-aqueous media needs to be understood.

Relative enzyme catalytic activities in organic solvents or aqueous-organic solvents compared to 100% activity in buffer solutions are listed in **Table 1.5**. Enzymes in this list have substantial catalytic activity in aqueous-organic co-solvents and in neat organic solvents. Thus, these enzyme-solvent pairs could be employed for developing polymer-solvent-enzyme compatible triads. Organic solvents act as non-solvents for the hydrophilic outer surface of enzymes, causing them to become rigid, phase-separate, denature or lose catalytic activity.[66] These behaviors are most often observed for aqueous-organic solvent mixtures. A major factor in enzyme destabilization in pure organic solvents is the interaction between solvents and enzyme-bound

water. Somewhat counterintuitively, results show that enzymes tend to be more tolerant of neat hydrophobic (non-polar) organic solvents than neat polar solvents. Polar organic solvents can penetrate enzyme active sites, remove tightly bound water from enzyme molecules through electrostatic interactions, and induce secondary and tertiary structural changes in proteins that lead to destabilization.[232] Even small conformational changes, especially in the active site pocket, can cause enzyme deactivation. For example, consider octane, tetrahydrofuran (THF), and acetonitrile organic solvents, with dielectric constants at 20 °C of approximately 2, 7.5 and 37, respectively (**Table 1.4**). As solvent polarity increases (octane < THF < acetonitrile), enzymatic activity drops drastically because solvents with higher polarity are more efficient at extracting essential water from the protein structure[233] and surface.[234] In addition, small, highly polar THF and acetonitrile molecules can penetrate into crevices in the enzyme structure, especially into the active site, and remove mobile or weakly bound water molecules, only leaving tightly bound water in those regions. Conversely, non-polar hydrophobic solvents, like octane, do not strip essential water. Molecular dynamics simulations that predict the location of mobile and bound water and protein flexibility in different solvents, for example in the structure of CALB exposed to water or different organic solvents, imply that the reduced flexibility of CALB in organic solvent is caused by a spanning water network resulting from less mobile and slowly exchanging water molecules at the protein-surface.[235] The number of surface bound water molecules and size of the spanning network increases with decreasing dielectric constant of solvents. This allows the enzyme structure and active site to remain hydrated with essential water molecules. Therefore, when choosing among organic solvents to prepare polymer-solvent-enzyme compatible triads, solvents with lower dielectric constant values are more likely to be compatible with enzymes.

Along with solvent polarity, solvent molecule size also plays a vital role. Smaller-sized polar solvents can more deeply penetrate the essential water sites of proteins than larger polar solvents. As a result, small-sized polar solvents strip more bound water from proteins and facilitate protein denaturation. For instance, smaller acrylonitrile (ACN) solvent could cause more penetration to the protein structure's crevices and strip more water molecules than octane.[234] Enzyme hydrophilicity and hydrophobicity also impact structural stability in neat organic solvents. For example, the surface of *Candida rugosa* lipase has more hydrophobic amino acids than chymotrypsin protease, enabling the lipase to remain more stable in non-polar organic solvents than protease.[236]

Notably, incorporating a few water molecules in an organic solvent promotes enzyme conformational mobility and increases catalytic activity, whereas increasing the water content of an organic solvent beyond an "optimum water activity" can lead to enzyme denaturing because of excessive conformational mobility. The absolute amount of water required for optimal catalysis varies greatly from non-polar to polar solvents. For instance, the enzymatic activity of alcohol oxidase from *Pichia pastoris* in the presence of 0.6% water in hydrophobic ethyl ether was more than 1000 times greater than in polar 2-butanol with the same water concentration.[237] When excess water is present, high conformational mobility increases the likelihood of interaction between an enzyme's hydrophobic core and organic solvents that ultimately disrupt enzyme 3D structure. Thus, increasing the water content beyond a specific limit in a water-miscible organic co-solvent generally decreases enzyme activity.[238] Moreover, enzymes are more thermally stable in anhydrous organic solvents than in water because of their conformational rigidity in the dehydrated state. Enhanced enzyme thermal stability facilitates their use in higher

temperature polymer processing.[64] For instance, evaporating solvent from a solution-cast film while preserving the activity of enzymes inside could be accomplished at a comparatively higher temperature with anhydrous organic solvents.

In addition to careful solvent selection, a number of strategies (e.g., solvent engineering, protein engineering, using lyoprotectants) are now available that allow enzyme use in organic solvents under nearly non-aqueous conditions.[67,239–241] Some are very sophisticated (e.g., genetic modification) and time-consuming (e.g., isolation of novel enzymes functioning under extreme conditions). Solvent engineering with additives or surfactants to modify the solvent environment is a relatively straightforward way to enhance enzyme stability in organic solvents.[242] Another way is to incorporate crystalline or dry enzymes. Since native enzymes are typically insoluble in organic solvents, lyophilized powder suspensions must be stirred vigorously to homogenize the mixture.[64] Note that precautions are needed when handling dusty enzyme protein powders to avoid inhalation that could provoke an allergic response. The resulting liquid mixtures with crystalline or lyophilized enzymes show more stability and activity in non-aqueous solvents than their aqueous enzyme counterparts.

Factors contributing to enzyme stability in organic solvents are summarized in **Figure 1.4**. Overall, anhydrous non-polar "hydrophobic" organic solvents are more favorable than polar and hydrated "hydrophilic" organic solvents. Optimal amounts of essential water greatly enhance enzyme activity in organic solvents. Lyophilized and crystalline enzyme preparations are more accessible to combine with non-aqueous solvents than aqueous liquid enzyme formulations.

Finally, solvent engineering using surfactants and additives effectively improve enzyme stability in organic solvents.

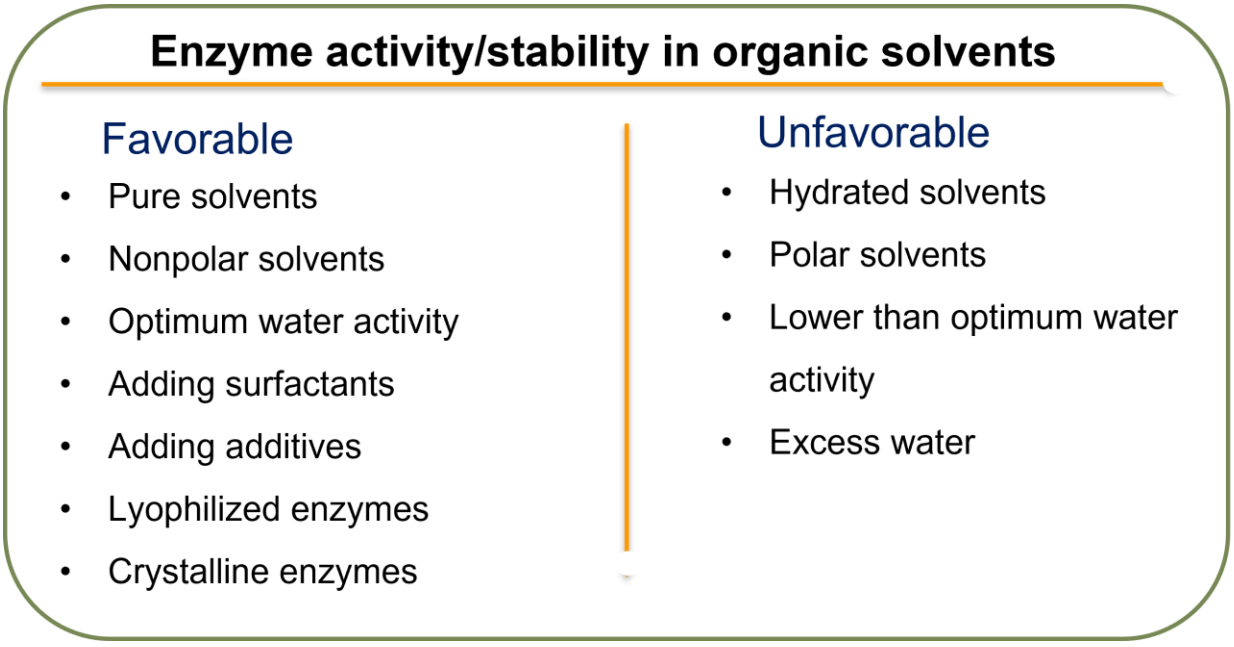

Figure 1.4: Summary of favorable and unfavorable enzyme stability factors in non-aqueous solvents.

Table 1.5: Compilation of enzyme activities in non-aqueous solvents (solvents are listed as hydrophobic to hydrophilic).

Enzyme	*Origin*			Enzyme relative catalytic activity in organic solvents (%)														Ref.
		Solvent, %	Time, hrs	Hexane	p-xylene	Benzene	Toluene	THF	Chloroform	DCM	Acetone	DMAc	DMF	DMSO	Isopropanol	Ethanol	Methanol	
α-amylase	*Bacillus licheniformis*	20	0.5	98	-	-	-	-	98	-	85	-	-	-	-	99	96	[243]
α-amylase	*Nesterenkonia sp.*	20	2			115	114		102		111	-	-	-	-	108		[244]
α-amylase	*Aspergillus agaradhaerens*	30	-	61	-	-	-	-	-	-	-	-	-	-	-	-	47	[238]
Catalase	*Bovine*	30	-	-	-	-	-	-	-	-	-	-	85	120	-	-	-	[245]
Cellulase	*Mahella australiensis 50-1 BON*	10	-	-	-	-	-	-	-	-	80	-	-	-	90	84	90	[246]
Cellulase	*Bacillus vallismortis RG-07*	30	24	143	112	112	180	-	-	-	116	-	-	-	104	107	125	[247]
Cellulase	*Bicillus amyliliquefaciens AK9*	30	24	117	98	102	113	-	-	-	98	-	-	-	99	103	109	[248]
β-Glucosidase	*Aspergillus niger NL-1*	20	0.5	-	-	-	-	-	-	-	74	-	-	-	-	92	109	[249]
β-Glucosidase	*Aspergillus niger NL-1*	30	1	-	-	-	-	-	-	-	-	-	-	90	-	90	80	[250]

Table 1.5 Continued

β-Glucosidase	*Aspergillus niger*	30	0.5	-	-	-	-	-	-	-	-	-	-	-	-	130	180	[251]
Laccase	*Rhus vernicifera*	10	-	-	-	-	-	-	-	-	95	-	-	-	-	75	76	[252]
Laccase	*Bicillus* licheniformis LS04	30	-	-	-	-	-	-	-	-	-	-	-	86	60	122		[253]
Lipase	*Pseudomonas aeruginosa*	50	0.5	57	-	19	46	-	35	-	-	92	10	99	28	21	25	[254]
Lipase	*Rhizopus oryzae*	100	24	98					38	-	88	-	-	-	-	-		[255]
Lipase	*Aspergillus niger MYA 135*	50	1	75	-	-	-	-	-	-	99	-	-	-	-	95	95	[256]
Lipase	*Geobacillus thermocatenulatus*	100	-	118	-	72	-	-	-	-	-	-	-	-	47	107	72	[257]
Lipase	*Candida rugosa*	100	1	90	-	-	-	-	57	55	-	-	-	-	-	-	-	[258]
Peroxidase	*Horseradish*	10	-	-	-	-	-	-	-	-	-	-	-		84	-	-	[259]
Peroxidase	*Horseradish*	10	1	55	-	-	-	45	80	60	-	-	-	50	-	60	-	[260]
Peroxidase	*Horseradish*	10	1	-	-	-	-	-	-	-	-	-		90	-	-	-	[261]
Protease	*Virgibacillus sp.*	25	4	-	-	-	-	-	114		72	-	-	85	92	76	144	[262]
Protease	*Bacillus subtilis*	50	12	-	-	98	-	-	-	-	-	-	-	-	54	68	59	[263]
Alkaline Protease	*Citricoccus sp.*	25	1	-	92	40	38	-	18	-	15	-	-	95	-	-	-	[264]

Table 1.5 Continued

Trypsin	Porcine pancreas	10	0.5	-	-	-	-	45	-	-	-	-	58	75	-	-	-	[265]
Xylanase	*Streptomyces sp. CS428*	10	2	-	-	-	-	-	-	-	-	-	-	-	11 1	110	12 1	[266]

Table 1.6: Relative catalytic activity of enzymes in different surfactant solutions and with ions.

Enzyme	Origin	Optimum temperature °C/pH	Relative activity in the presence of surfactants							Relative activity in the presence of metal ions					Ref.
			Conc%/ time, hr	SDS	CTAB	TX-100	Tween 20	Tween 80	AOT	Conc, mM%/tim.	Na^+	Ca^{2+}	Mg^{2+}	EDTA	
α-amylase	*Bacillus licheniformis*	100/5.0	5-10/0.5	55	-	88	110	96	-	-	-	-	-	-	[243]
α-amylase	*Aspergillus niger*	30/7.0	2/-	80	-	90	-	-	-	2/-	65	75	100	-	[267]
Cellulase	*Bacillus amyliliquefaciens AK9*	60/5.0	0.5/0.5	18	-	88	90	92	-	10/0.5	-	79	-	25	[248]
Cellulase	*Bacillus vallismortis RG-07*	65/7.0	0.1/1	130	-	105	-	116	-	10/1	141	156	146	-	[247]
Dextranase	*Talaromyces pinophilus*	45/6.0	1mM/-	102	-	-	-	-	-	5/-	-	98	91	77	[268]
β-Glucosidase	*Aspergillus niger*	50/5.0	1/0.5	97		239	211	-	-	1/0.5	-	-	100	100	[251]
β-Glucosidase	*Aspergillus niger NL-1*	60/4.0	-	-	-	-	-	-	-	1/0.5	-	98	95	98	[249]
Laccase	*Bacillus licheniformis* LS04	60/-	1/-	70	-	-	-	-	-	100/-	103	-	-	88	[253]
Lipase	*Geobacillus thermocatenulatus*	60/7.0	10/-	10	-	156	5	17		-	-	-	-	-	[257]
Peroxidase	Horseradish	30/5.5	5/-	-	-	90	-	-	-	2/0.25	-	44	-	-	[259]
Protease	*Virgibacillus sp.*	60/7.0	1/1	78	-	85	106	87	-	-	-	-	-	-	[262]
Protease	*Citricoccus sp.*	40/10.0	5/1	196	-	162	97		-	-	-	-	-	-	[264]

Table 1.6 Continued

Protease	*Bacillus circulans*	60/10.0	1/1	93	-	107	-	98	-	-	-	-	-	-	[269]
Protease	Metagenomic	55/11.0	1/0.5	100	55	95	-	95	-	-	-	-	-	-	[270]
			5/0.5	93	44	79	-	83	-	-	-	-	-	-	
Protease	*Bacillus subtilis*	50/11.0	1/1	100	-	102	-	97	-	-	-	-	-	-	[263]
Protease	*Nocardiopsis sp.*	-/4.0	200 mM/-	-	-	-	-	-	95	-	-	-	-	-	[271]
Xylanase	*Streptomyces sp. CS428*	80/7.0	0.25/-	36	-	124	111	114	-	1/-	104	133	55	-	[266]
Endo-1,4-β-xylanase	*Trichoderma longibrachiatum*	-	0.25/-	76	-	179	185	180	-	1/-	119	154	53	-	[266]

SDS: Sodium dodecyl sulfate; CTAB: Cetrimethylammonium bromide, TX-100: Triton X-100, AOT: Sodium bis(2-ethylhexyl)sulfosuccinate, EDTA: Ethylenediaminetetraacetic acid

1.3.3. Polymer-solvent-enzyme compatibility

The primary barrier to enzyme co-immobilization with synthetic polymers is the physical incompatibility of hydrophilic enzymes with hydrophobic organic solvents. Native hydrated enzymes are insoluble in most organic solvents and will phase-separate from organic solvents and organic solvent-polymer solutions.[272] Attempts to co-immobilize enzymes that experience this physical incompatibility with organic solutions result in low immobilization yield and low catalytic activity. **Figure 1.5** illustrates enzyme behavior in non-aqueous polymer solutions. When enzymes are compatible with non-aqueous media, they maintain their native three-dimensional structure, are uniformly distributed throughout the media, and exhibit catalytic activity when provided with the chemically required substrates. To overcome phase separation, one way that enzymes can maintain their native structure in a hydrophobic environment is by forming microemulsions together with surfactants. In comparison, enzymes in incompatible media lose their native structure and do not exhibit catalytic activity. Therefore, successful co-immobilization with hydrophobic polymer media requires careful selection of polymer-solvent-enzyme compatible triads. The same strategies that enhance enzyme stability in organic solvents can be applied to producing hydrophobic polymer-solvent-enzyme compatible triads (**Figure 1.6)**, namely: (i) solvent selection and polymer solution engineering, (ii) enzyme selection, formulation and modification, and (iii) selection and modification of polymer matrices.

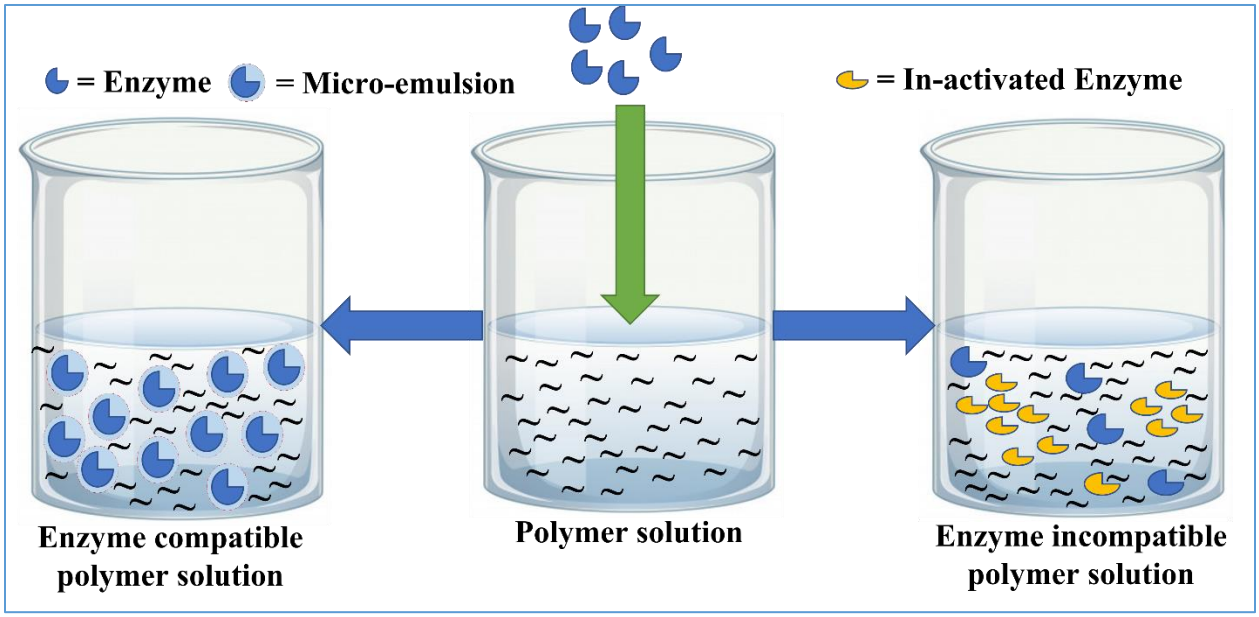

Figure 1.5: Illustration of enzyme compatibility (active enzyme) and incompatibility (in-activated enzyme) in polymer solutions.

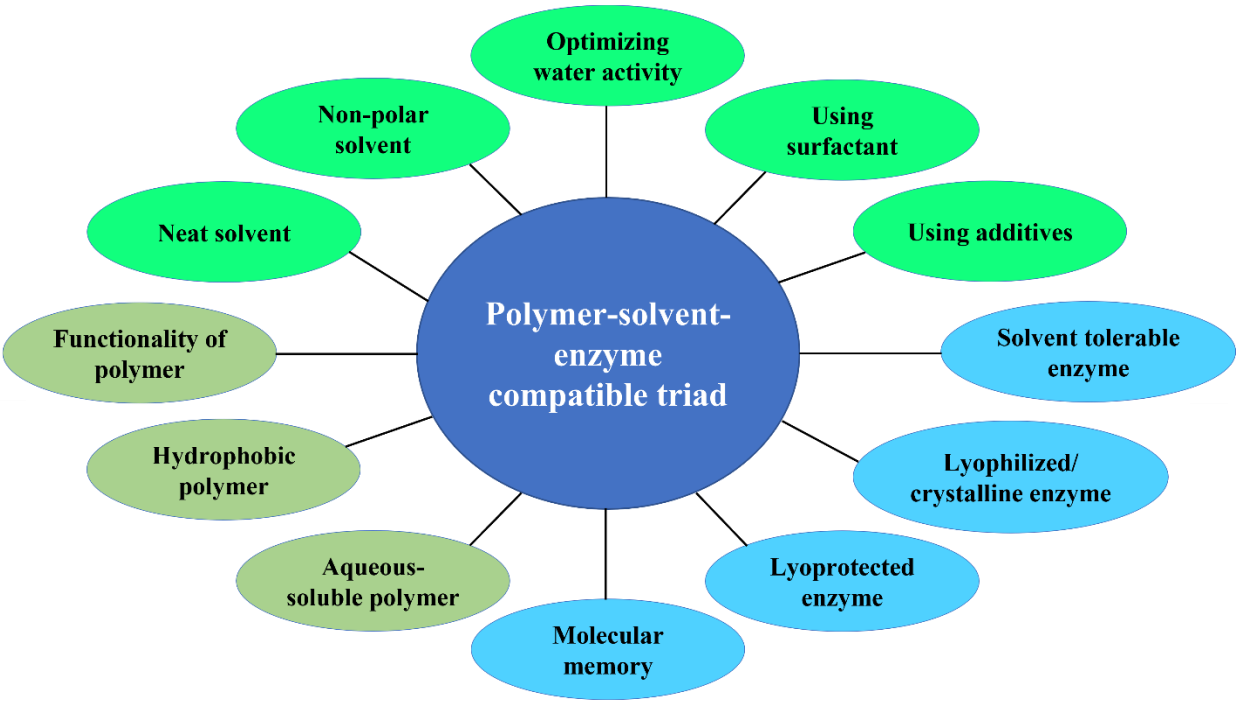

Figure 1.6: : Strategies for achieving polymer-solvent-enzyme compatible triads.

1.3.3.1. Solvent selection and solution engineering

The goal of solvent selection and solution engineering is to decrease solvent denaturing effects on enzymes. The activity (or solubilizing power) of solvents in polymer solutions is lower than for free solvents because solvent molecules are occupied in interactions with polymer molecules.[273] As a result, a more pronounced non-solvent effect of hydrophobic polymer solutions on enzyme structure is expected compared to the pure solvent. This can lead to pronounced phase separation. However, non-aqueous polymer solutions are also less likely to strip water from enzyme structures. Also, because polymer molecules are much larger in size compared to solvent molecules, polymer molecules cannot penetrate crevices on the enzyme surface. Therefore, hydrophobic polymer solutions do not strip water from enzymes and instead preserve the hydration of enzyme active sites by mobile and weakly bound water.[234]

Non-polar solvent: Enzymes are less denaturated by non-polar solvents than polar solvents. Non-polar solvents have less tendency to strip essential structural water from enzymes and have minimal interaction with the protein structure.[274,275] This implies that polymer solutions mixed with enzymes should be prepared using solvents with the lowest polarity available that still give adequate polymer solution properties. For example, PCL is soluble in THF, DCM, and hexafluoroisopropanol (HFIP). According to their dielectric values (**Table 1.4**), the polarity ranking of these solvents is THF < DCM < HFIP. Therefore, THF is expected to be the best choice for making enzyme-compatible polymer solutions with PCL. This principle can also be applied to solvent mixtures. For example, PCL dissolved in the mixed solvent DMF/chloroform (2:3) and lipase from *Burkholderia cepacia* were mixed to produce a polymer-solvents-enzyme compatible triad. The resulting compatible triad solution was processed by electrospinning to co-immobilize

(encapsulate) the enzymes inside the fibers.[275] In this example, DMF, which is likely to be damaging to enzymes because of its high dielectric value (~38), was combined with low dielectric chloroform (~4.8) to provide better spinnability by reducing the solution viscosity while preserving a sufficiently non-polar environment for enzyme compatibility. Highly hydrophobic non-polar solvents, such as hexane, xylene, and toluene, are good solvents for hydrophobic polymers (e.g., PS, PP) and are compatible with enzymes, but phase-separation occurs because of immiscibility between these solvents and hydrated enzymes. Using lyophilized enzymes instead of liquid enzyme minimizes the phase-separation issue. However, since, enzymes are insoluble in organic solvent, the lyophilized enzyme particles should be sufficiently small and the polymer-solvent-enzyme suspension should be vigorously mixed to achieve a stable triad.[276]

Neat solvent: Enzymes are usually believed to become denatured in organic solvents. This notion mainly comes from examining enzymes in aqueous-organic mixtures rather than in pure organic solvents.[64] When water is not present to lubricate the structure, enzyme molecules become rigid and resist denaturing. Therefore, dry enzymes dispersed in polymer solutions made with neat organic solvents can form polymer-solvent-enzyme compatible triads. Absent water, protein molecular rigidity also makes it possible to apply higher heat during fabrication processes, such as solution casting or solution spinning, than is tolerated by enzymes in aqueous environments. Once immobilized materials made in this way are exposed to water, enzymes become rehydrated, relax their rigid structure and exhibit catalytic activity.

Optimizing water activity: Water activity characterizes the availability of water in a system and plays a crucial role when enzymes are used in primarily non-aqueous media.[277] Water activity is defined as the ratio of the partial vapor pressure of water in the solution to the partial vapor pressure of free water at the standard state (equation iv).[278] In other words, high water activity means that water molecules are freely available. In proteins, water acts as a lubricant, promoting conformational mobility. Higher water content (and corresponding higher water activity) in organic solvents leads to increased enzyme mobility and activity.[66] For example, the catalytic activity of alcohol oxidase was more than 1000-fold higher in ethyl acetate solvents when the water concentration in the solvent was changed from 0.5 to 1.1%.[237] However, enzyme catalytic activity, and structural stability reach a maximum at a specific amount of water (optimal water activity). Once the water content exceeds that limit, the enzyme denatures tendency also increases because of higher conformational mobility. The optimal water activity value varies for different enzymes. For instance, *Candida antarctica* lipase B showed optimum catalytic activity at less than 0.06 water activity, while *Rhizomucor miehei* lipase required 0.5 water activity for the highest activity.[279] On the other hand, glycoside hydrolases require relatively high water activity. For example, *Pyrococcus furiosus* β-glucosidase needed at least 0.29 water activity for the synthesis of pentyl- β-glucoside and optimal catalytic activity was observed at water activity as high as 0.92.[280] A similar level of water activity was needed for the protease α-chymotrypsin from bovine pancreas, which exhibited optimal alcoholysis of N-acetyl-L-phenyl-alanine ethyl ester at 0.94 water activity.[281] On the other hand, water activity largely depends on solvent polarity, meaning that at the same quantity of water loading, non-polar solvents have higher water activity than polar solvents. For instance, for a 0.2 mole fraction water content, ethyl

acetate and ethanol exhibit ~0.99 and 0.4 water activity, and toluene need less than 0.01 mole fraction water to achieve ~1.0 water activity.[282] The amount of water in organic solvent required for optimum enzyme catalytic activity can be calculated from these two values: water activity for optimal enzyme catalytic activity and water mole fraction for highest water activity (equation v).

$$\text{Water activity} = \frac{\text{Partial vapor pressure of water in solution}}{\text{Partial vapor pressure of free water at standard state}} \quad \text{.....(1.4)}$$

Amount of water for optimum enzyme activity (mole fraction) =

water activity for optimal catalytic activity * mole fraction of water for solvent saturation ……(1.5)

For instance, CALB has optimum catalytic properties at less than 0.06 water activity and toluene solvent becomes saturated with less than 0.01 mole fraction water. Thus, for a PS-toluene-CALB triad, the mole fraction of water should not exceed 0.0006 (=0.06*0.01). Similarly, for a PS-toluene-β-glucosidase (*Pyrococcus furiosus*) compatible triad, the optimum mole fraction of water in the polymer solution would be 0.092 (=0.92*0.01). By similar calculations (equation v), using the water activity and water mole fraction values mentioned above, the optimum water quantity for PS-toluene-lipase (*Rhizomucor miehei*), PS-ethyl acetate-CALB, PS-ethyl acetate-β-glucosidase (*Pyrococcus furiosus*) and PMMA-toluene-α-chymotrypsin can be estimated as 0.005, 0.002, 0.184 and 0.0094 respectively. The mole fraction of water should be near these values for optimal enzyme stability in “neat” solvent. If the value is too low, solvent can penetrate the enzyme and if the value is too high, enzyme has excessive destabilizing mobility.

Surfactants and additives: Addition of surfactants or other additives as part of solution engineering can overcome water mole fraction limitations and phase-separation issues and thereby help water soluble enzymes disperse more readily in organic solvents. Surfactants reduce the surface tension between organic solvents and proteins. However, this comes at the risk of denaturing enzyme proteins. Therefore, preferred surfactants are those that improve enzyme dispersion while retaining the native protein structure. Likewise, the addition of ions can help stabilize enzyme protein structure in stressed environments by forming and stabilizing ionic bonds within the protein structure. Conversely, ions may also promote agglomeration between protein molecules that could exaggerate phase separation by causing protein precipitation. These phenomena depend on the specific protein structures, and testing is usually needed to assess the true impact of specific additives. The relative activity of enzymes in the presence of surfactants and ions compared to their activity without additives is shown in **Table 1.6**. These tabulated activity values are based on studies where enzymes were exposed to the indicated surfactant/ion concentrations for the specified time. Overall, enzymes showed higher activity in non-ionic surfactants than in cationic or anionic surfactants. In 40% of the consolidated cases, the reported catalytic activities either increased or remained unchanged with the addition of surfactants and ions. In 72% of the cases, enzymes exhibited at least 80% of their initial activity, a level that is commonly considered to represent "retention" of activity. For example, the cellulase from *Bacillus vallismortis* RG-07 showed relative activities of 130, 105, and 116% in 0.1 wt% sodium dodecyl sulfate (SDS), Triton X-100 (TX-100), and Tween 80, respectively. The relative activity of this same enzyme was 141, 156, and 156% in Na^{+}, $Ca^{2+,}$ and Mg^{2+}, respectively.[247] In another example, protease from *Virgibacillus sp*. showed relative activities of

78, 85, 106 and 87% in 1% SDS, Triton X-100, Tween 20 and Tween 80, respectively.[262] Reduced activity in SDS was attributed to enzyme conformation changes. In fact, SDS is commonly used as a denaturant during the preparation of enzyme samples for gel electrophoresis. The presence of non-ionic surfactants decreased surface tension of the medium with minimal effect on protease catalytic activity. Other additives, like chelating agents such as EDTA, can dramatically negatively affect enzymes that use ions to stabilize their structures.

The special importance of surfactants for enzyme immobilization is that their amphiphilic properties promote the formation of water-in-oil microemulsions. Hydrophilic enzymes can be encapsulated within such reverse micelles and retain their native structure because enzymes will partition into the aqueous phase.[283] Thermodynamically stable microemulsions can be used for co-immobilization material fabrication. Two approaches (single solvent-surfactant and double solvent-surfactant solution engineering) have been used to produce surfactant stabilized polymer-solvent-enzyme compatible triads (**Figure 1.7**).

Single solvent-surfactant microemulsion: In single solvent-surfactant systems (**Figure 1.7 A**), an enzyme solution is dispersed in an organic solvent-surfactant solution to form a reverse micelle (RM) water-in-oil microemulsion. In reverse micelles, surfactant molecules are positioned with their hydrophilic polar 'heads' facing water inside the micelles and their hydrophobic nonpolar 'tails' oriented toward the surrounding non-polar organic medium. Enzymes, such as tyrosinase and glucose oxidase, residing in the aqueous environment inside the micelle maintain their native structure and exhibit catalytic activities comparable to those in the aqueous state.[283] Other enzymes, such as α-chymotrypsin, laccase, peroxidase, and aldehyde oxidoreductase, are also

reported to be well-stabilized and have excellent catalytic activity in RM.[284–287] After forming RM, a separate polymer solution is added, or a solid polymer is dissolved in the continuous organic phase of the microemulsion, to produce a polymer-solvent-enzyme mixture. The total volume of aqueous enzyme solution dispersed in the microemulsion is minimal compared to the total organic solvent volume. For example, Shipovskov *et al*. prepared enzyme microemulsions by adding 10 µl of an aqueous phase containing 30 µM solution of glucose oxidase (from *Aspergillus niger*) in an acetate-phosphate buffer solution to 2 ml of an organic phase containing 0.1 M AOT in anhydrous octane to produce a microemulsion where the amount of organic phase was 200 times larger than the aqueous phase.[283] In this work, a polymer-solvent-enzyme compatible triad was produced by subsequently combining a caoutchouc (1,4-polyisoprene) polymer solution with the microemulsion and using the mixture to immobilize glucose oxidase on an electrode by spraying. In principle, this single solvent RM approach could be used with any kind of enzyme to form polymer-solvent-enzyme compatible triads.

Double solvent-surfactant microemulsion: The double solvent-surfactant (**Figure 1.7 B**) approach uses two solvents and one surfactant. A surfactant stabilized enzyme (surfactant-enzyme complex) is prepared using a highly volatile non-polar solvent. A second solvent is used to redissolve the enzyme-surfactant complex and dissolve the polymer to produce a uniform enzyme-containing polymer solution. In this method, buffer solution containing enzyme is mixed thoroughly with a surfactant-loaded non-polar dry organic solvent and allowed to phase-separate. The hydrophilic surfactant head binds to the enzyme and the hydrophobic tail interacts with the organic solvent, causing the enzyme-surfactant complex to be drawn into the organic phase and separated along with the organic layer. After separating the organic from the aqueous

layer and evaporating the organic solvent from the separated layer, a stabilized surfactant-enzyme complex is formed that can be homogeneously combined with other suitable organic solvent-polymer systems.

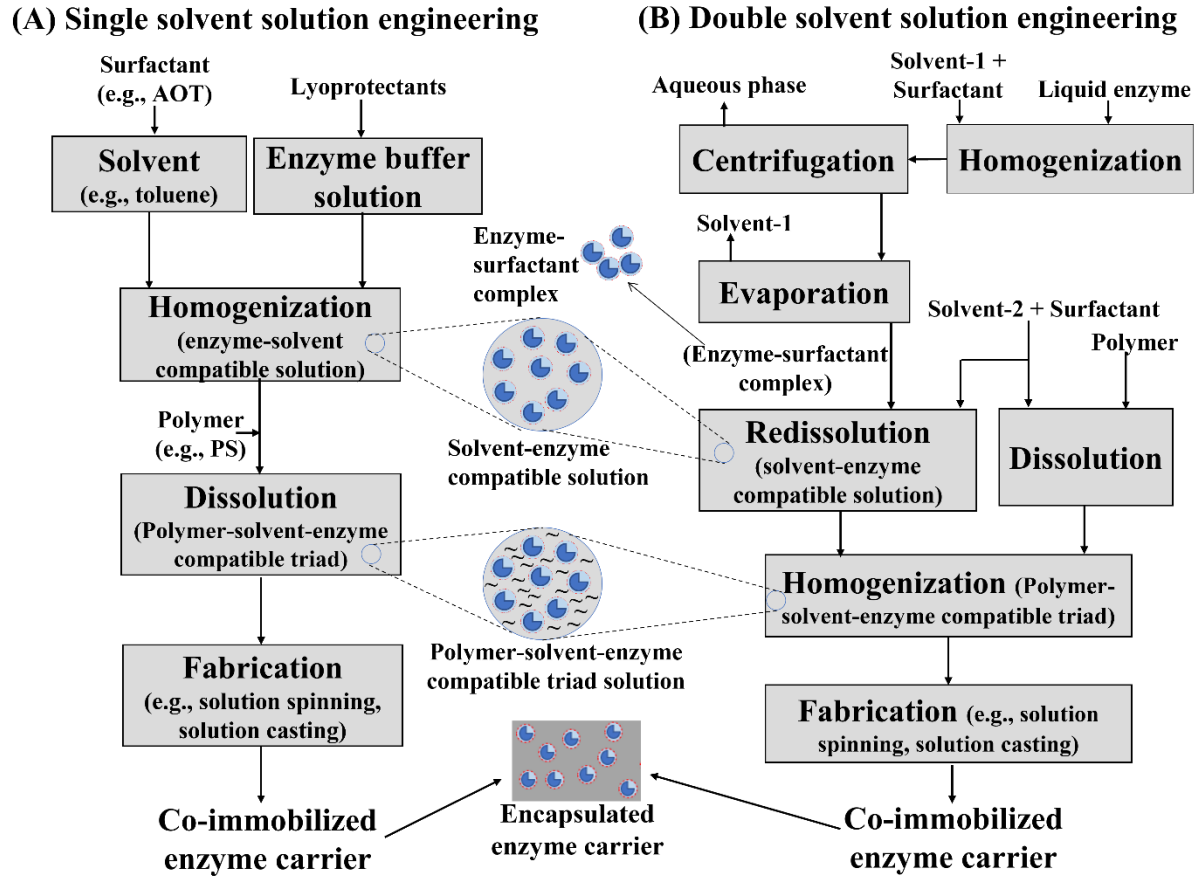

Figure 1.7: Polymer solution engineering approaches using a surfactant to produce a polymer-solvent-enzyme compatible triad.

Numerous works utilizing this strategy have been reported.[110,288,289] For example, Herricks *et al*. produced a polystyrene-toluene-α-chymotrypsin compatible triad polymer-enzyme solution.[110] The α-chymotrypsin (CT) enzyme was first dissolved in a Bis-Tris propane buffer solution and mixed with hexane containing (2 mM) dioctyl sulfosuccinate (AOT) surfactant. The solution was homogenized by rapid stirring and then centrifuged. The resultant top layer of hexane was

separated from the aqueous phase, and the hexane was evaporated under a nitrogen stream to leave behind the AOT-CT complex. Since polystyrene is not soluble in hexane, the dried CT-AOT complex was added to toluene, which is a good solvent for PS. A separate PS solution was prepared by dissolving PS into an AOT-toluene solution (0.1 g/ml for AOT). Then the two solutions were mixed thoroughly by vortexing. The enzyme was stable in the new solvent system because a hydrated layer formed within AOT stabilized enzymes through the hydrophilic sulfosuccinate surfactant "head", while the dioctyl "tail" was sufficiently hydrophobic to interact well with toluene and suspend the enzyme-surfactant complex in the organic solvent. Different recipes of the final solutions were used to produce nanofibers by electrospinning, where CT was entrapped in the nanofibers as the polymer solutions rapidly solidified during extrusion by evaporation of toluene solvent. Immobilized CT nanofibers made in this way without surfactant lost activity very rapidly (complete activity loss within a few hours), while immobilized CT with AOT stabilization retained at least 30% relative activity after one-week storage in buffer, confirming that polymer-solvent-enzyme compatible triads were produced. Another example of the two solvents approach was reported by Ganesh *et al*.[288]. In this work, *Candida antarctica* lipase (CALB) was extracted from an aqueous phase to an organic phase by using 2 mM AOT/anhydrous isooctane. The aqueous media contained CALB (0.5 mg/ml), calcium chloride (9 mM), isopropyl alcohol (0.25% v/v) and sodium acetate buffer (20 mM, pH: 4.5). Equal volumes of aqueous and organic phases were mixed using a bench top shaker at 30 °C for 15 min at 100 rpm. The organic layer was separated using a centrifuge and solvent was evaporated to form an ion-paired CALB-surfactant complex. The ion-paired CALB complex dissolved in anhydrous toluene solvent, was mixed with 10% w/v PCL-anhydrous toluene solution to form a polymer-solvent-enzyme

compatible triad. Several prospective hydrophobic polymer-solvent compatible systems (from **Table 1.4**) and enzyme-solvent compatible systems (from **Table 1.5**) that could form triads are: PS-benzene-(lipase-AOT complex), PS-xylene-(lipase-AOT complex), PS-benzene-(chymotrypsin-AOT complex), PS-xylene-(chymotrypsin-AOT complex), PCL-toluene-(lipase-AOT complex), and PCL-DMF-(lipase-AOT complex).

1.3.3.2. Enzyme selection, formulation and modification

Organic solvent tolerant enzymes: Appropriate enzyme selection (isolation of novel enzymes functioning under extreme conditions) or modification of enzyme structures (protein engineering) to increase their resistance toward organic solvent is important for developing polymer-solvent-enzyme compatible triads. Strategies used to select and adapt enzymes to synthetic chemistry reaction environments in organic solvents are relevant, including protein engineering to stabilize enzymes in the presence of organic solvents and selecting natural enzymes which are organic solvent-stable.[290] Although natural enzymes generally display lower catalytic activity in organic solvents, certain types of enzymes nevertheless exhibit substantial catalytic activity and stability in organic solvents.[66] In particular, interfacial active lipases that evolved naturally to act at water/lipid interfaces[291] or enzymes isolated from extremophiles[292] (e.g., organic solvent tolerant bacteria, halophilic, and alkaliphilic organisms) show good stability in organic solvents. The isolated protease and lipase from *Pseudomonas aeruginoa* PseA, α-amylase from *Halocarcula sp*. strain S-1, and alkaline phosphatase from *Streptomyces clavuligerus* strain Mit-1 demonstrate organic solvent tolerance.[293–296]

Lyoprotected lyophilized and crystalline enzymes: A general strategy for preserving enzyme activity is lyophilizing enzymes in the presence of lyoprotectants, such as sugars, poly(ethylene glycol), inorganic salts (notably KCl), substrate-resembling ligands, and crown ethers.[64,241] Lyoprotectants maintain enzyme structure during freeze-drying. Enzymes lyophilized in the presence of lyoprotectants remain catalytically active and stable in non-aqueous media because the drying environment is presumed to lock enzyme molecules into their kinetically optimal conformations. For instance, sorbitol-protected subtilisin Carlsberg protease was 25 times more reactive in transesterification reactions than its non-protected counterpart.[240] Similar phenomena have been observed with crystalline enzymes. Protected lyophilized and crystalline enzymes exhibit excellent resistance to dehydration-induced denaturation in various, mainly nonpolar, organic solvents. For example, lyophilized subtilisin Carlsberg protease from *Bacillus subtilis* showed robust catalytic activity in dry hexadecane, octane, and tert-amyl alcohol.[239] The same study reported that crystalline α-chymotrypsin from bovine pancreas had excellent catalytic activity in the presence of hexadecane and octane solvents. Both crystalline and lyophilized enzymes have excellent physical stability in hydrophobic solvents because in the absence of water, the kinetic energy required to change their native molecular conformation increases.[66] Crystalline and lyophilized enzymes are expected to show a similar structural stability mechanism in polymer solutions made with dry organic solvents, especially solutions of hydrophobic polymers in non-polar solvents, such as PS-toluene or PS-hexane. Vigorous mixing must be applied to disperse enzymes into the polymer solution to achieve a stable polymer suspension.

'Molecular memory' effect: 'Molecular memory' is a fascinating property of enzymes in organic solvents.[297,298] In this phenomenon, enzyme properties in organic solvents depend on their prior processing history; they carry over properties that were adopted in their previous solution environment. This happens because high conformational rigidity imposed by anhydrous environments preserves prior enzyme structure. Since pH is one of the most influential parameters affecting enzymatic activity in an aqueous solution, enzymes lyophilized from their optimum buffer solution retain their optimal catalytic structure (pH memory). This optimal ionization structure can be retained in the organic solvents. The 'pH adjusted' lyophilized enzymes show great physical and catalytic stability in organic solvents. For instance, the rate of transesterification of N-acetyl-L-phenylalanine ethyl ester substrate in octane solvent catalyzed by a "pH adjusted" sample of subtilisin Carlsberg from *Bacillus subtilis* is 75 times greater than that of the enzyme "straight from the Sigma bottle".[237] Enzyme lyophilization in the presence of lyoprotectants can provide a beneficial "Ligand memory" effect[299] that results in higher catalytic activity in organic solvents. For example, α-chymotrypsin lyophilized from an aqueous solution with N-acetyl-L-phenylalanine ligands showed 35-times higher catalytic activity during transesterification reactions in octane solvent than without lyophilizing counterparts.[239] Such lyophilized protected enzymes could keep their memory effect in the dry organic solvent to produce compatible enzyme-polymer solutions. Importantly, enzymes lose their molecular memory effect in the presence of small amounts of water in organic solvents.[298] Therefore, neat solvent polymer solutions have greater potential for forming enzyme compatible triads than aqueous-organic mixed solvents.

1.3.3.3. Selection and modification of polymer matrices

Fundamentally, the selection of polymer for the immobilization matrix depends on the chemo-physical behavior required by the fabrication method and on the performance required by the immobilized enzyme application. Polymer-solvent-enzyme compatible triads can be prepared by selecting aqueous soluble polymers, changing the functionality of polymers, or by in-situ mini-emulsion polymerization of hydrophobic polymers with aqueous enzyme solutions. Careful polymer selection can minimize the extent of solution engineering, enzyme selection and protein engineering needed to produce enzyme compatible polymer solutions.

Aqueous-soluble polymers: Aqueous-soluble polymer solutions are generally compatible with aqueous-soluble native enzymes. Therefore, using aqueous-soluble polymers is the simplest way to produce polymer-solvent-enzyme compatible solutions. Advantages of these systems are their simple and environmentally friendly fabrication methods (e.g., adding $CaCl_2$ salt for alginate precipitation, or water vapor evaporation during spinning processes) and the diverse end applications they enable, including enzyme stability and reaction in non-aqueous media, controlled release of enzymes, and rapid aqueous dissolution of solid-product enzyme formulations that have been made in convenient shapes, like granules, films and fibers. Commonly used aqueous-soluble natural polymers include chitosan, alginate salts, and agarose salts. Common synthetic polymers include PVA, PEO, and PEG. Aqueous solutions made with these polymers are directly mixed with aqueous enzyme preparations, usually in the presence of a buffer to control the pH, followed by a solidification step to achieve enzyme co-immobilization. **Table 1.3** lists several aqueous soluble polymer-enzyme combinations, such as *Trichoderma*

reesei cellulase encapsulated in alginate beads,[105] *Bacillus licheniformis* maltase encapsulated in agarose beads,[72] *Aspergillus niger* β-D-glucosidase entrapped in chitosan beads,[87] and horseradish peroxidase entrapped in PVA electrospun fibers.[173] Others enzymes can also be mixed with these water-soluble polymers to form polymer-solvent-enzyme compatible triads for enzyme co-immobilization.

Hydrophobic polymers: From a reaction process perspective, main advantages of hydrophobic polymers as enzyme immobilization matrices are their durability and insolubility in aqueous solutions, making repeated use in aqueous applications possible. Selecting polymers that can be formed by emulsion polymerization is a mild and efficient way to immobilize hydrophilic enzymes that do not readily combine with hydrophobic polymers. During mini-emulsion polymerization, polymer synthesis from monomers and enzyme immobilization take place simultaneously during the polymerization reaction. Typically, monomers and initiators are dissolved in the organic solvent phase, while the aqueous phase consists of water, enzyme, surfactants, and additives. Enzymes are co-immobilized in/on the synthesized polymer by single-step mini-emulsion polymerization.[99–103,300] For instance, *Candida antarctica* lipase B (CALB) was immobilized using PMMA nanoparticles by mini-emulsion polymerization.[102] The organic phase comprised methyl methacrylate monomers, Crodamol (a fully saturated triglyceride), and an soluble initiator (2,2'-azobisisobutyronitrile (AIBN)). The aqueous phase contained water, SDS as a surfactant, CALB enzyme, and a water soluble initiator (potassium persulfate). The organic phase was added to the aqueous phase to form a dispersion that was stirred for 10 minutes, followed by two minutes of sonication. Finally, the polymerization reaction was completed at a constant temperature (70

°C), resulting in PMMA nanoparticles with co-immobilized CALB enzyme that exhibited increased relative enzyme activity with increased enzyme loading. In other work, glucose oxidase was encapsulated in poly *tert*-butyl methacrylate nanocapsules via inverse mini-emulsion periphery reversible addition-fragmentation chain-transfer (RAFT) polymerization.[301] In inverse mini-emulsion polymerization, the continuous phase (95% of total volume) contains monomers, crosslinkers, initiators, and RAFT agent in toluene solvent, and the dispersed aqueous phase (5% of total volume) comprises enzyme (e.g. glucose oxidase) in PBS buffer. Photoinitiated polymerization is carried out for 1 hr under blue LED light with constant stirring whereupon enzymes become encapsulated in the polymeric nanocapsules (~200 nm). By this method, encapsulated glucose oxidase showed 71-100% relative activity compared to free glucose oxidase. In addition, nanocapsules protected the enzymes, as evidenced by almost full retention of encapsulated enzyme activity in an organic solvent environment, whereas free glucose oxidase lost all activity through denaturation. Similar mini-emulsion approaches can be employed for other enzyme polymer systems like CALB-PS and amylase-PMMA.

Improving functionality of polymers: Polymer blends and copolymers often increase polymer functionality and enzyme compatibility. Increased polymer functionality can improve polymer-enzyme interactions to achieve higher immobilization yield and triggered stability. In addition to enhancing enzyme compatibility, polymer blending can improve mechanical stability, thermal properties, chemical functionality, hydrophilicity, and improve fabrication properties such as spinnability, such as for electrospinning processes. For example, blending PVA with chitosan improves the poor mechanical stability and film-forming ability of chitosan while the presence of

added functional groups (amino) from chitosan increases polymer-enzyme interactions in the blend compared to neat PVA.[144,171,302] The imparted properties of the PVA-chitosan blend facilitate enzyme co-immobilization in fabrication processes such as solution casting and solution spinning. For instance, phytase from cowpea seed is added to PVA-chitosan (90:10) acetate buffer solution to produce an enzyme-polymers-solvent compatible triad that entrapped enzymes in PVA-chitosan nanofibers by electrospinning.[164] **Table 1.3** reports additional polymer blends, copolymers, and enzyme pairs prepared by co-immobilization from enzyme-compatible polymer solutions such as horseradish peroxidase encapsulated in chitosan-PEG particles[101], *Candida antarctica* lipase adsorbed on poly(urea-urethane) nanoparticles[103], *Yarrowia lipolytica* lipase entrapped in chitosan-alginate beads[104], *Aspergillus niger* monoamine oxidase encapsulated in PVA-PEG gels[147] and *Bacillus licheniformis* maltase entrapped in polyacrylamide (acrylamide and bisacrylamide copolymer) beads.[72] Examples of post-immobilization functionality achieved by manipulation of physical and chemical properties of copolymers and polymer blends include creation of reversibly soluble immobilized enzymes[303], creation of nanoporous immobilization matrices with well-defined architecture using self-assembled sacrificial copolymer blocks[304], and creation of open pore immobilization microstructures using one polymer in the blend as a sacrificial porogen.[305]

1.3.4. Evaluation of immobilized enzyme activity

Many different enzyme activity assays exist and continue being developed, so there is no attempt to detail them here. However, there are some general principles to consider when developing assays to evaluate immobilized enzyme activity. Most importantly, immobilized enzyme activity

assays often require modified approaches compared to free enzyme activity assays because solid carriers create a heterogeneous phase in the enzyme assay which can interfere with reaction kinetics and interfere with spectrophotometric detection that is commonly used in enzyme assay measurements. The changed physical size of immobilized enzymes compared to free enzymes, and the enzyme location in or on the carrier matrix and exposure of enzyme active sites to dissolved substrates impact apparent enzyme reaction kinetics. Likewise, the presence of carrier materials can physically block the path of light sources used by spectrophotometric methods to detect changes in the reaction media that allow quantification of enzyme activity. Sometimes assay reagents can interact with the carrier, causing additional interference. Therefore, adaptation of enzyme assays, adjusting the selection of reagents, or changing the handling of samples during the assay (such as implementing solid-liquid filtration steps), is often required to enable analytical comparison between free and immobilized enzymes, as well as to evaluate immobilized biocatalyst robustness for material optimization. These considerations are especially important when enzyme reaction kinetics are “diffusion limited” meaning that the rate-limiting step is the physical transport of substrate to the enzyme active site, rather than the rate of the catalytic reaction itself. Diffusion limitations can sometimes be overcome by improving the reaction mixing efficiency. Adequate mixing may be identified by increasing mixing speeds until no further increase in reaction rates is observed, although this may still leave a gap between the activity expected for the heterogeneous immobilized system and what would be expected based on the enzyme loading when compared to a comparable amount of homogenous free enzyme.

To overcome reaction kinetics interference by the carrier itself, it can be important to "slow down" the overall enzyme reaction. In certain cases, the activity assay can be slowed down by using an alternative enzyme substrate. For example, Shen et al. reported using the slower ester hydrolysis activity of carbonic anhydrase (CA) to carry out a colorimetric hydrolysis reaction of p-nitrophenyl acetate (p-NPAc) in measuring the apparent activity of CA immobilized on cotton fiber textiles by entrapment with chitosan.[36] The conventional Wilbur-Anderson (W-A) type assay, which measures fast CO_2 hydration using dissolved CO_2 as the substrate, was found unsuitable for measuring the immobilized CA activity because the rate of the control reaction, detected by colorimetric indicator of pH change, was faster than the diffusion of adequate substrate to immobilized enzyme active sites. In addition to substrate selection, taking advantage of the immobilized enzyme carrier shape can overcome assay obstacles. For example, in the same work by Shen et al, the CA immobilized textile samples were either coiled at the perimeter of each well in a spectrophotometer multi-well assay plate or were cut into doughnut shapes that allowed the signal light to pass unhindered through the assay solution.[36]

For enzymes immobilized on small-sized carriers, sufficient continuous mixing is a practical way to overcome assay obstacles. Mixing works well for enzymes immobilized on particles, nanoparticles, beads or nanofibers that can be dispersed as suspensions and behave like dissolved enzymes when incubated with dissolved substrates.[23] After incubation, the reaction is stopped by a suitable reagent and/or the supernatant is separated from the solids by centrifugation or filtration to stop the reaction and produce a clarified liquid that can be measured for absorbance to quantify enzyme activity. Immobilized enzyme carriers that do not

form stable suspensions require constant shaking or stirring while incubating with the dissolved substrate.[26,85,103] However, it may not be possible to apply the above approaches to enzymes that are deliberately encapsulated in durable carriers (e.g. for controlled release) because durable carriers can block enzyme active sites from the assay substrate. In these cases, the active sites first need to be unblocked (e.g. by dissolving, cutting or otherwise disrupting the carrier) and then subjected to the enzyme assay.

Finally, depending on the situation, enzyme analytical activity alone may not be sufficient to accurately quantify immobilized enzyme performance in a particular application. In this case, application-relevant test methods are needed that position the immobilized enzyme in contact with the (usually flowing) reaction media together with suitable detection methods to monitor for the desired conversions of substrates to products. This remains an active area of research, discovery and development as the use of enzymes expands to new areas.

1.4. Conclusion

This review has aimed to create a guide for selecting polymer-solvent pairs (polymer solutions) in which enzymes can survive with substantial catalytic activity and that are useful for enzyme immobilization, preferably by single-step fabrication methods. Compatible polymer-solvent-enzyme triads facilitate the use of solvent-based approaches to fabricate immobilized enzyme structures in versatile shapes, like fibers, films, and beads, with high immobilization yield, high activity retention, longevity, and repeatable application. Solution processing is advantageous because it can be used with a broad range of polymers, even with polymers that do not melt.

Under sufficiently mild conditions, enzymes can be included in numerous different polymer solutions when proper attention is paid to component interactions.

The strategic approaches for producing enzyme compatible polymer solutions are different for water-soluble and hydrophobic polymers. Enzymes simply mixed with water-soluble polymers form polymer-water-enzyme compatible triads that can be directly subjected to fabrication and then solidified by removing water. However, water-soluble polymer-carriers require modification, such as cross-linking, to achieve repeatable use in aqueous environments. Preparing polymer-solvent-enzyme compatible triads using water-insoluble hydrophobic polymers includes selecting lyoprotected or crystalline enzymes, extremozymes, non-polar solvents, emulsion polymerization, and solution engineering. Extremozymes and lyophilized enzymes with inherent stability in dry non-polar solvents can produce polymer-solvent-enzyme compatible triads simply by dispersing dry enzyme powders in the polymer solution with vigorous mixing. The addition of lyoprotectants (e.g., PEG, sugar, inorganic salts) that prevent enzyme deformation during lyophilization, should impart similar stabilizing effects during rapid drying fabrication processes, like fiber spinning, which expands the fabrication and use the versatility of these materials. When the polymer synthesis mechanism allows, in situ emulsion polymerization is a mild way to entrap enzymes, and further exploration of this field can lead to novel fabrication approaches. Solution engineering using surfactants is convenient for altering solution properties and may ultimately be the most effective strategy for producing a broad range of enzyme-compatible polymer solutions, especially when using synthetic polymers. A lingering challenge is that hydrophobic polymer matrices can block enzyme active sites during material fabrication,

and more research is needed to overcome this issue. Imparting matrix porosity and increasing surface area are two approaches that can help. These can be achieved by fabricating nanoscale structures or incorporating volatile or water-soluble small molecules ('porogens') during immobilization matrix synthesis. Depending on the fabrication method, a sufficiently volatile solvent itself may participate in helping increase the co-immobilization matrix surface area to force enzymes toward the surface so that more active sites are accessible to substrates.

Enzyme co-immobilization in polymers with diverse properties and versatile matrix fabrication methods that expand the creation of various shapes and levels of durability will improve performance and lead to new applications, such as controlled degradation packaging, sensors, responsive medical textiles, controlled release biocatalysts, durable functional filters, and bio-catalytically active cleaning materials. Appropriate selection of polymer-solvent-enzyme combinations will improve the chances of success in these endeavors and help extend the utility of immobilized enzyme catalysts.

1.5. Motivation and Objectives

The potential to use enzymes in new ways can be expanded by controlling their placement in the desired reaction zone, ideally in a way that extends enzyme longevity and improves enzyme robustness to broad temperature and pH conditions. Enzyme immobilization in a solid carrier is a prospective solution for enzyme placement. The structure of supporting materials strongly affects the performance of an immobilized enzyme. Nanomaterials such as nanofibers and nanoparticles have a high surface-to-volume ratio of nanomaterials, provide a high enzyme loading, and often the associated high porosity of nanomaterials provides accessibility to enzyme active sites resulting in the low diffusion resistance necessary for a high reaction rate. Electrospinning and solution blown spinning techniques are perfect tools for producing nanofibers. Electrospun nanofibers are highly uniform but have low fiber production efficiency; e.g., at a lab scale with a single needle system, only 0.2 gm/hr fiber yield from 20% polystyrene (PS) solution with a 15 kV driving force was reported.[306] In contrast, solution blown techniques can produce much higher yield fibers, e.g., 1.4 gm/hr fiber yield was produced in a single needle system from the same PS concentration (20%) with 138 kPa air pressure driving force.[193] This suggests that, at least for some polymer-solvent systems, solution blowing could have seven times higher production efficiency than electrospinning.

Numerous prior works report enzyme entrapment and encapsulation on/into electrospinning nanofibers. However, enzyme immobilization with solution blown fibers is new. The attachment of enzymes in solution blown nonwoven fibers will generate new knowledge on the extent to which enzymes combine with solvents and polymers that are amenable to solution blowing and

enable evaluation of the characteristics and utility of these new materials. It would explore a more polymer-solvent-enzyme compatible triad that solvent is not limited only to high dielectric properties. Enzyme immobilization in advanced textile fibers is a boundary-spanning concept. Enzyme researchers do not typically have access to advanced fiber-forming processes, nor do they have the knowledge base to successfully combine enzyme, polymer solution, and solution blowing process technologies. Fiber extrusion experts do not typically have backgrounds in biocatalysts. This proposed work will connect these two concepts to fill the gap. The proposed work will utilize extraordinary nonwoven fibrous properties together with enzyme biocatalysts to produce new functional materials. This work applies solution-blown methods to produce nonwoven supporting materials for enzyme immobilization.

This proposed work aims to produce enzyme-functionalized solution-blown nonwovens and characterize catalytic properties. The three broad objectives of the proposed work are:

Objective 1: Develop a solution blowing process for producing Enzyme Functionalized Solution Blown Nonwovens (EFSBN) with high enzyme activity and desirable physical properties of the nonwoven webs for targeted model applications.

Objective 2: Characterize the chemical, physical and biocatalytic properties of the EFSBN, including stability, distribution, and position of the entrapped enzymes.

Objective 3: Validate the anticipated application features of EFSBNs, including enhanced storage and thermal stability, controlled release, and durable reactivity.

Chapter 2: Protease immobilization in solution blown polyethylene oxide nanofibrous nonwoven webs

The content of this chapter was previously published with the following citation: Asaduzzaman, Fnu; Salmon, Sonja. "Protease immobilization in solution blown polyethylene oxide nanofibrous nonwoven webs." ***ACS Applied Engineering Materials*** (2022) Accepted on November 7, 2022. doi.org/10.1021/acsaenm.2c00111

Abstract:

Unique enzyme functionalized solution blown nonwoven (EFSBN) fibers were produced by a single-step solution blow spinning (SBS) method that utilizes high velocity gas to simultaneously extrude the co-dissolved polymer-solvent-enzyme spinning solution and evaporate solvent at mild conditions to form a nanofibrous web with preserved enzyme activity. This is the first report of direct enzyme immobilization by solution blow spinning with the first physicochemical characterization of the novel fibers produced. A broad concentration range of (0.6-7.4 wt% protein) of subtilisin A protease from *Bacillus licheniformis* was successfully entrapped by polyethylene (PEO) during solution blow spinning nonwoven web production. The presence of enzyme protein in the solid nanofibers was detected by Fourier Transform Infrared Spectroscopy (FTIR) and X-ray photoelectron spectroscopy. Time of flight-secondary ions mass spectroscopy (ToF-SIMS) and laser confocal microscopy revealed the immobilized enzymes were mainly positioned inside the fibers and homogeneously distributed throughout the webs. Scanning electron microscopy (SEM) showed that fiber shape and diameter of PEO nanofibers containing enzymes were irregular compared to PEO-only nanofibers. Residual enzyme activity in the webs was measured by redissolving fibers in buffer and comparing the released enzyme activity to non-immobilized free enzyme using a casein substrate-based assay. Immobilized protease (1.3%

(w/w) protein in solid dry nanofiber webs) retained more than 90% of the free enzyme activity. Protease immobilized in solid nanofiber webs exhibited long storage stability at ambient (~22 °C) and 4 °C temperature storage conditions, with more than 60% remaining catalytic activity after 300 days compared to the initial activity. Immobilized protease had equally good thermal stability as a stabilized liquid commercial protease, both retaining above 95% of their initial activity after treatment for 12 hrs at 65 °C. In contrast, the same liquid protease diluted in buffer lost activity within 2 hrs at that temperature. The non-dusting, readily aqueous-soluble EFSBN solid materials are easy to handle and have good storage stability compared to liquid products.

Keywords: Immobilization, nonwoven, protease, polyethylene oxide, solution blow spinning, storage stability.

2.1. Introduction

Enzymes are protein-based biocatalysts with highly specific, selective, and excellent catalytic activity in chemical and biochemical reactions. Their ability to operate at mild pH, temperature, and pressure conditions allow enzymes to be used as benign catalysts in textile processing, food processing, and pharmaceutical synthesis to replace current harsh chemicals and, consequently, save energy.[79] Enzyme proteins can be dissolved or mixed directly into many types of batch processes or as ingredients or process aids in products.[19] Enzymes can be immobilized by entrapping them in microspheres[307] or attaching them to inert, insoluble supporting materials.[36] Immobilized enzymes offer many advantages over their free forms, including easy recovery and possible reuse, improved stability, rapid termination of enzyme-catalyzed reactions, and avoiding

protein contamination of the final product.[32] Some immobilization systems are primarily for product formulation, where they perform stabilization, packaging, and delivery roles.[66,301]

Proteases (E.C.3.4), representing 25-30% of the global enzyme market,[308] are an important category of enzymes. Proteases catalyze the hydrolysis of peptide bonds, causing proteins to break down into smaller polypeptides or single amino acids. Such proteolytic reactions are useful across a broad range of consumer, medical and industrial applications, such as laundry,[262] pharmaceutical,[309] food,[310] beverage,[311] textile,[312] leather processing,[313] and industrial waste treatment.[314] However, protease enzymes suffer from self-hydrolysis of peptide bonds in neighboring protease enzyme molecules, leading to poor storage stability, unless stabilizers are added that minimize water activity in liquid enzyme products, or unless the enzymes can be stored in lyophilized form. Protease attachment to inert materials (enzyme immobilization) increases enzyme stability, including storage[120] and thermal stability.[124] Immobilization techniques and the supporting material properties play a vital role in enzyme loading and activity retention. Nanomaterials are viewed as favorable immobilization matrices because they have high surface area that provide high enzyme immobilization yields.[92,164,315] Such high surface area materials could offer additional benefits as a delivery system for entrapped enzymes. Mild, single-step co-immobilization techniques such as solution blow spinning, spray drying and electrospinning that form nanoscale solid products from enzyme-compatible polymer solutions by versatile continuous processes would be an excellent approach for creating certain types of immobilized enzyme products by encapsulation or entrapment.[316]

Solution blow spinning (SBS) is a fiber processing method that produces micro-, submicron- and nanofibers in a continuous process from polymers dissolved in volatile solvents. The resulting fibers have different properties depending on the polymers used. Electrospinning is also capable of producing nanofibers, however, whereas electrospinning requires high electric voltage and a specific target to attenuate fibers, solution blowing uses high-pressure gas to extrude fibers from a concentric nozzle onto an arbitrary target with relatively high throughput. A solution blow spinning unit with a single annular die, including a spinning nozzle with an annular gas cavity surrounding it, is illustrated in **Figure 2.1**. A polymer solution is injected from a syringe pump to the core nozzle, and high pressure (speed) air or gas is delivered through the concentric nozzle. The polymer solution throughput is controlled by a peristaltic pump and a pressure regulator controls air pressure. The pressurized air generates a driving force that stretches the central polymer jet. After a short straight path, the polymer solution jet is subjected to both stretching and bending instability. These two instabilities result from the attenuation of the polymer solution jet and accelerate solvent evaporation. As the solvent evaporates, polymers solidify into nanofibers that can be collected on any type of collector placed in the path of the blowing jet.[317,318]

SBS fibers have a similar fiber morphology compared to electrospun fibers, but SBS is capable of higher polymer throughput leading to higher fiber yields, which reduces the cost of fiber production.[317,319] Moreover, solution blowing enables rapid fiber formation from polymeric materials that cannot be processed by melt blowing, such as polymers that degrade or decompose before melting. SBS is scalable to large manufacturing configurations, making it

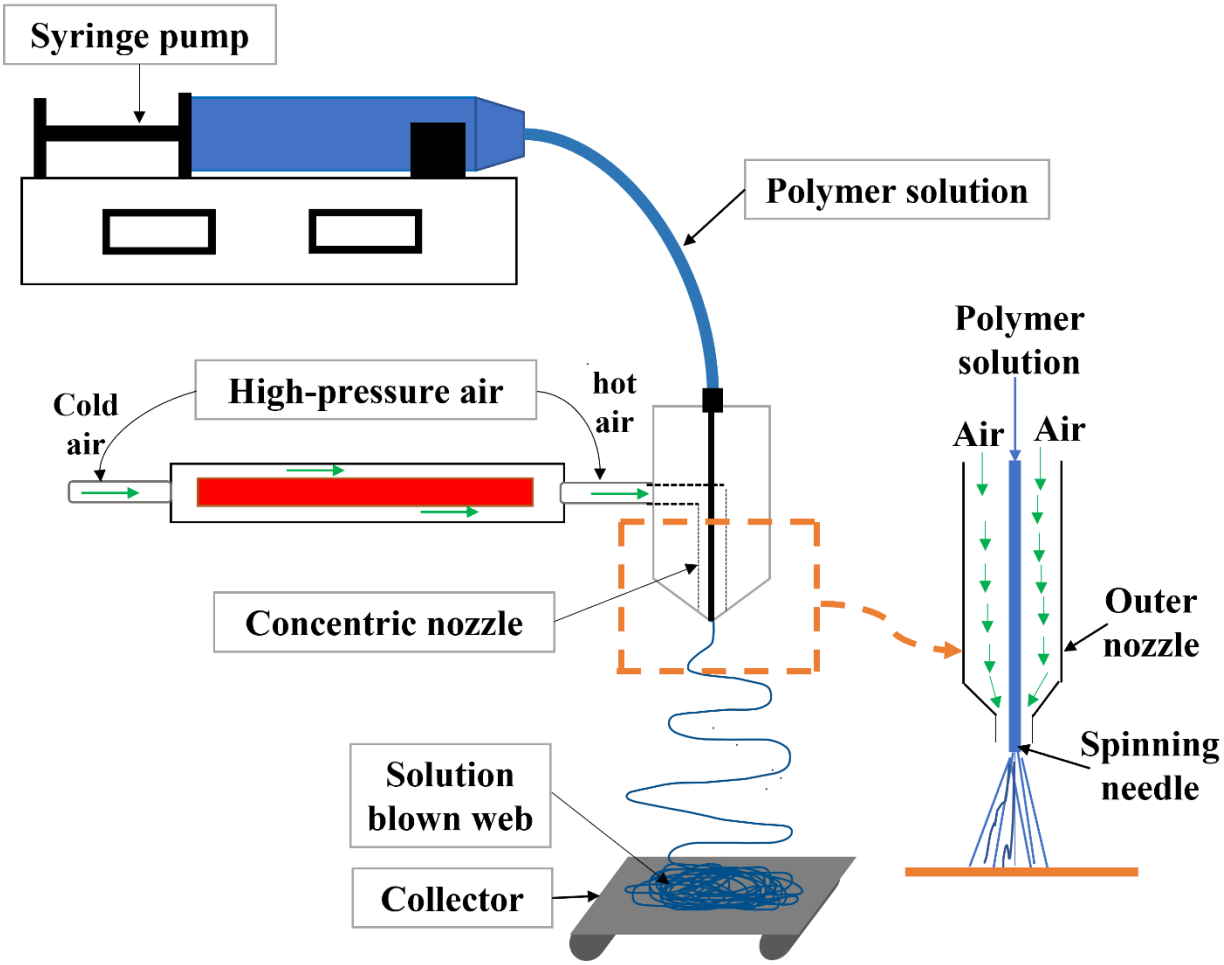

Figure 2.1: Schematic diagram of a single-needle solution blowing process.

commercially relevant across numerous applications.[317] Furthermore, solution blowing is not limited to thermal-sensitive polymers or high dielectric constant solvent-soluble polymers. This robust process can equally be used with petroleum-derived thermoplastic polymers solutions or biopolymer solutions to produce nanofiber webs. In view of this, SBS nonwoven fiber webs have been explored for biomedical applications,[198] filtration,[213,320] wound dressings,[321,322] electrical stimulation,[323] high-temperature fuel cells,[324,325] adsorbents,[183,209,326] periodontitis,[182] protective clothing,[327,328] and control release pesticides.[329] In this work, we explore for the first time SBS

fabrication as a way to achieve single-step enzyme co-immobilization with high enzyme loading from a polymer-solvent-enzyme compatible triad. Our hypothesis was that enzymes would well tolerate being incorporated in the mild SBS processing conditions, however, there were no previous reports of this approach in the literature. Our investigation was conducted using polyethylene oxide, water, and protease.

Polyethylene oxide (PEO) is an aqueous soluble polymer that forms fibers by solution spinning.[184] PEO is a nontoxic and biologically compatible polymer.[330] The PEO polymer is known to preserve protein native structure[167] making it a good candidate for the proof-of-concept work. Water-soluble proteases are known to be compatible with PEO/water solutions and form polymer-solvent-enzyme compatible trios.[331] Moreover, polyethylene glycol (PEG; same chemical composition but a lower degree of polymerization compared to PEO) has been used as a lyoprotectant to preserve or prevent enzyme deformation under harsh conditions.[64] Therefore, PEO was predicted to be an excellent matrix for exploring the fabrication and features of novel SBS fibrous webs produced in a single step with entrapped enzymes. Subtilisin A protease was selected as an example enzyme for the study to demonstrate the relevance of the SBS immobilization technique for a commercially important enzyme class.

The process described in this work is a single-step approach to fabricating unique enzyme-functionalized PEO nonwoven webs using a solution blow spinning process. Herein, we report entrapment immobilization of subtilisin A protease in PEO solution blown nano- and micro-fibrous nonwoven webs for the first time. Required operating conditions for SBN-PEO and EFSBN-

PEO fiber formation were determined, and detailed physiochemical characterizations of the products were performed, including enzyme activity, thermal stability, storage stability, and analysis of the position and distribution of enzymes in the SBS fibers.

2.2. Experimental Section

2.2.1. Materials

Protease (subtilisin A) from *Bacillus licheniformis* was purchased from Sigma-Aldrich as a liquid enzyme product (P4860, containing protease and ~50-70% glycerol according to the Safety Data Sheet) and used as supplied. Polyethylene oxide (M_v=300000 Da), N,N-dimethylated casein from bovine milk, tris-HCl, trichloroacetic acid, and L-tyrosine were purchased from Sigma-Millipore (Hampton, NH, USA). Pierce Rapid Gold BCA Protein Assay Kit (Catalog Numbers A53225, A53226, and A53227) (ThermoFisher Scientific, Waltham, MA, USA) was used to determine the protein concentration in the produced EFSBN using the bovine serum albumin (BSA) standard provided in the kit.

2.2.2. SBN-PEO and EFSBN-PEO webs production

Solution-blown nonwoven webs were produced using the modified apparatus of Kolvasob *et al*. [317] The production process had two main steps: 1) spinning solution preparation and 2) solution blow spinning. The polyethylene oxide (PEO) (M_v = 300000 Da) spinning solutions were prepared by dissolving PEO powder (1.2 g) in deionized water (10 ml) with continuous overnight stirring (100 rpm). The liquid protease from (subtilisin A) *Bacillus licheniformis* (60 µl-1200 µl) was added to the PEO solution and homogenized through stirring. These solutions comprising PEO, water,

and protease were then subjected to solution blowing. A solution-blown apparatus consisting of a single annular die with an annular gas cavity surrounding a spinning nozzle, as illustrated in **Figure 2.1**, was used. The PEO solution (5 ml, 12 w/v%) was supplied to the inner needle and feed rate was controlled with a fixed pump from 0.05-0.2 ml/min. A pressure regulator controlled the pressurized air, which varied according to the experiment. The produced SBN and EFSBN fibers were collected on flat polypropylene spun-bond material. The prepared solution blown webs were stored at room temperature (~22 ℃) or 4 ℃ until further analysis. The collector was positioned at a fixed working distance from the nozzle of 100 mm. To achieve optimal solution blowing conditions for producing PEO SBN without enzyme, the nozzle was operated with varying solution throughput (0.05, 0.10 & 0.20 ml/min), air pressure (138 & 207 kPa) (20&30 psi) and air temperature (~22, 50 & 60 ℃). Visual observation of fiber formation behavior was used to determine the optimum solution blowing parameters. After optimizing process parameters for PEO SBN webs, the EFSBN webs containing protease were produced using those same optimum solution blowing conditions. The schematic flow diagram of enzyme functionalized PEO solution-blown nonwoven webs is presented in **Figure 2.2**.

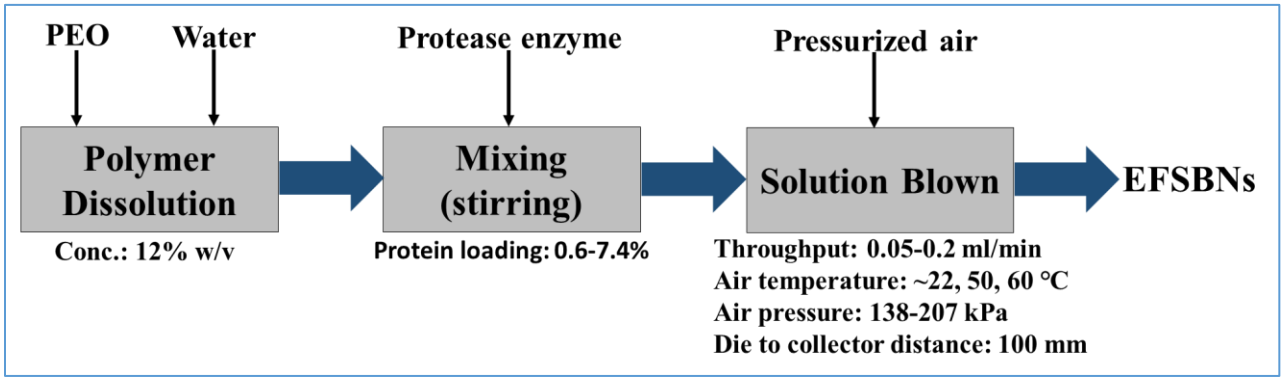

Figure 2.2: Schematic presentation of protease functionalized polyethylene oxide solution blown nonwoven webs.

2.2.3. Protease assay of immobilized enzymes

The protease activity of immobilized protease was measured using a casein-based assay method, with N, N-dimethylated casein from bovine milk (C9801 Sigma) as the substrate, as is described in the determination of general proteolytic activity reported by Kapperler *et al*.[332] This procedure was modified to include an initial step where the solid EFSBN webs were first pre-dissolved in assay buffer and then the dissolved webs were incubated with protease assay reagents. The amounts of reagents used in the activity assay are listed in **Table 2.1.** In the EFSBN web dissolution step, a suitable amount (approximately 10-15 mg, exactly weighed) of EFSBN web was placed into a 2.0 ml vial and dissolved in 1.50 ml Tris HCl buffer (100 mM, pH 8.0) to produce a stock solution by vortex mixing at 2000 rpm for 10 mins. In the incubation step, 0.35 ml of stock solution and 0.15 ml Tris HCl buffer (100 mM, pH 8.0) were mixed and preincubated for 5 mins. Then, 0.5 ml preincubated N, N-dimethylated casein (1.30 w/v%) substrate was added to the solution and mixed thoroughly by vortexing for 10 seconds. The final solution (total volume 1 ml) was incubated for 10 minutes at 40 ℃. After incubation, the reaction was stopped by adding 0.30 ml (39 w/v%) trichloroacetic acid (TCA). The final solution (total volume 1.3 ml) was cooled to room temperature (kept for 30 minutes at room temperature), and the precipitated proteins (non-digested) were removed by centrifugation at 10000 rpm for 10 minutes. The absorbance of the resulting supernatant was measured at 274 nm against a blank control. The absorbance determines the concentration of L-tyrosine, an amino acid released during casein degradation, with an absorbance maximum of 274 nm.[333] The blank control was made by maintaining the same procedure except adding an equivalent amount of SBN (neat PEO web) instead of EFSBN. All solutions were handled the same throughout the assay process. An L-tyrosine standard curve

was created by plotting absorbance versus known concentrations of L-tyrosine. The micromoles of tyrosine equivalents liberated by a test sample were determined from the absorbance reading for that sample by using the standard curve (**Figure 2.3**). One international unit (IU) of protease activity produces the amino acid equivalent of 1.0 µmole of tyrosine per minute at 40 ℃ in the presence of 100 mM pH 8.0 Tris-HCl buffer. Calculations are shown in the following calculation section.

Table 2.1: Protease assay of free protease, functionalized PEO webs (3.0 % subtilisin A-EFSBN-PEO webs).

Reagents	Blank, SB	Sample, SS-1	Sample, SS-2	Sample, SS-3
Step 1: Enzyme solution preparation				
Native PEO web, mg	10-20	-	-	-
Functionalized PEO web, mg	-	10-20	10-20	10-20
Tris buffer (100 mM, pH 8.0), ml	1.5	1.5	1.5	1.5
Prepared homogenous solution by vortex mixing for 10 mins with steel balls				
Step 2: Incubation				
Step 1 solution, ml	0.25	0.25	0.25	0.25
Tris buffer (100 mM, pH 8.0), ml	0.25	0.25	0.25	0.25
1.3 wt% Casein, N,N-dimethylated form, ml	0.50	0.50	0.50	0.50
Incubated at 40 ℃ for 10 mins				
39% TCA, ml	0.30	0.30	0.30	0.30
Total volume, ml	1.30	1.30	1.30	1.30

Table 2.2: L-tyrosine standard curve preparation.

Reagents	Blank, TB	TS-1	TS-2	TS-3	TS-4	TS-5
L-Tyrosine solution (200 µg/ml), ml	0	0.2	0.4	0.6	0.8	1.0
Buffer, ml	1.0	0.8	0.6	0.4	0.2	0
Total volume, ml	1.0	1.0	1.0	1.0	1.0	1.0

Calculations:

After incubating 10 mins, the reaction was stopped by 39% (w/v) tri acetic acid and kept for 10 mins to reach room temperature. Then, the solution was centrifuged for 5 mins at 10000 rpm and took 0.2 ml supernatant. The absorbance of the supernatant was measured at 274 nm.

L-tyrosine standard curve:

$$\Delta A_{Standard} = A_{Standard} - A_{Blank}$$

Then, plot $\Delta A_{Standard}$ vs. µmoles of tyrosine to get the standard curve (**Figure 2.3**).

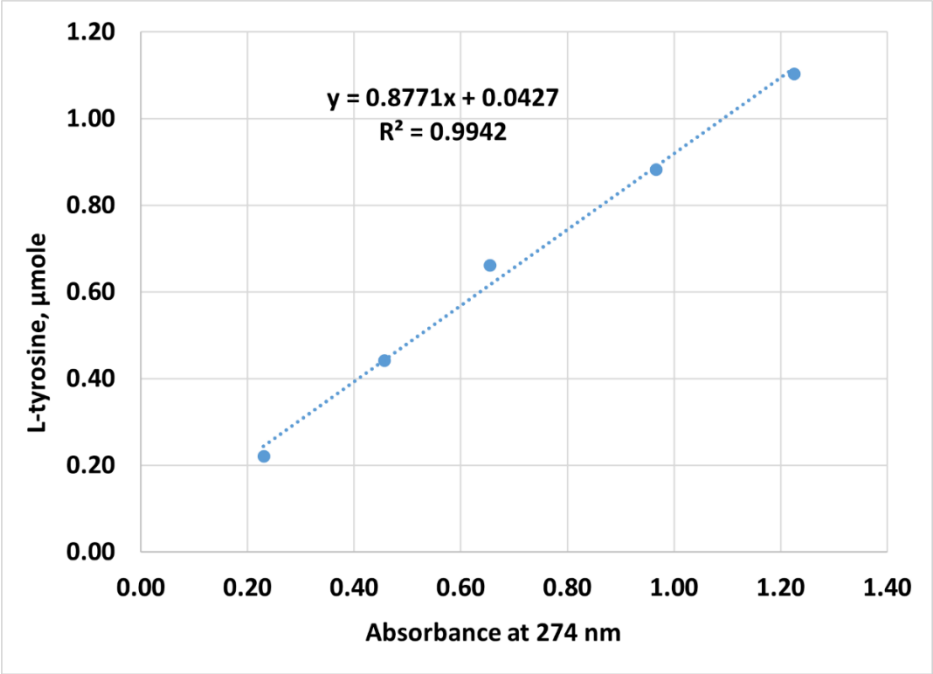

Figure 2.3: L-tyrosine standard curve at 274 nm absorbance maxima.

The micromole of tyrosine released from the casein substrate was calculated from the L-tyrosine standard curve equation and supernatant absorbance. The protease assay of the liquid-free enzyme upon dilution was calculated based on the following equations:

$$U/ml = \frac{\mu mole\ tyrosine\ equivalent\ release * volume\ of\ total\ assay,ml}{Time_{,min} * volume\ of\ enzyme\ used,ml} * dilution \quad \ldots\ldots\ldots\ldots\ldots\ldots\ldots\ldots\ldots\ldots (2.1)$$

$$\text{U/mg}_{\text{protein}} = \frac{\text{U/ml}}{\text{mg of}\frac{\text{protein}}{\text{ml}}\text{of liquid protease}} \ldots\ldots\ldots\ldots\ldots\ldots\ldots\ldots\ldots\ldots\ldots\ldots\ldots\ldots\ldots\ldots\ldots\ldots\ldots\ldots\ldots\ldots (2.2)$$

The protease assay of immobilized protease per mg of the EFSBN-PEO webs protein,

$$\text{U/mg}_{\text{ EFSBNs protein}} = \frac{\text{µmole tyrosine equivalent release} * \text{volume of total assay,ml}}{\text{Time,min} * \text{mg of}\frac{\text{protein}}{\text{ml}}\text{ in EFSBNs redissolved solution}} \ldots\ldots\ldots\ldots\ldots\ldots\ldots\ldots\ldots\ldots . (2.3)$$

The relative activity of immobilized protease was calculated as the percentage of the free protease activity and calculated as follows:

$$\text{Relative activity } (\%) = \frac{\text{Activity of immobilized protease}}{\text{Activity of free protease}} * 100 \ldots\ldots\ldots\ldots\ldots\ldots\ldots\ldots (2.4)$$

2.2.4. Protein content and immobilization yield of EFSBN-PEO

The protein (enzyme) content in EFSBNs was determined by the Lowry assay method,[334] using bovine serum albumin (BSA) as the standard. The method was performed using a Thermo scientific Pierce™ Rapid Gold Bicinchoninic Acid (BCA) Protein Assay Kit which develops an orange-gold color in the presence of two molecules of BCA and one cuprous ion. Solid EFSBN-PEO webs were first redissolved in tris buffer (pH 8.0, 0.5 M). These sample solutions were referred to as “unknown protein stock solution” in the test protocol. A series of dilutions of known concentration (50-1500 µg/ml) were prepared from BSA protein and assayed alongside the unknown protein stock solution**.** Absorbance was measured at 480 nm, and protein content for the unknown was determined based on the BSA standard curve. The percent protein content in an EFSBN sample was calculated according to the following formula:

$$\text{Protein content } (\%) = \frac{\text{measured protein,}\frac{\text{mg}}{\text{ml}} * \text{redissolved volume,ml} * 100}{\text{weight of redissolved EFSBN,mg}} \ldots\ldots\ldots\ldots\ldots\ldots (2.5)$$

The immobilization yield of EFSBN-PEO webs was calculated from the ratio of the measured amount of protein content (amount of protein detected in the final webs) in the EFSBN-PEO to the theoretical protein loading (amount of protein added to the spinning solution) in the web.

The immobilization yield percentage is calculated using the following formula:

$$\text{Immobilization yield } (\%) = \frac{\text{Measured protein content in EFSBN}}{\text{Theoretical protein in the spinning solution}} * 100. \ldots \ldots \ldots (2.6)$$

2.2.5. FTIR spectroscopy analysis of EFSBN-PEO

The presence of enzymes in the EFSBN-PEO was characterized by FTIR Spectroscopy (iS50, ThermoFisher Scientific, USA), with a build-in diamond crystal Attenuated Total Reflection sampling head. Spectra were collected for dried SBN-PEO fiber and EFSBN-PEO webs at room temperature from 500 to 4000 cm^{-1} with 64 scans and 4 cm^{-1} resolution. All specimens were stored in a desiccator for seven days before measurement to minimize moisture in the samples.

2.2.6. Morphological analysis using SEM

Morphologies of SBN-PEO and EFSBN-PEO samples were investigated using field-emission scanning electron microscopy (FESEM) (FEI Verios 460L, USA) with an accelerating voltage of 500 V and current of 2 pA. Images were analyzed using ImageJ software (NIH, USA), measuring the diameter of fibers in at least 100 places on each SEM micrograph.

2.2.7. Surface composition analysis using XPS

The surface composition of EFSBN-PEO and SBN-PEO webs was characterized by X-ray photoelectron spectroscopy (XPS) using an XPS/UVS-SPECS system with PHOIBOS 150 analyzer under a pressure of about 3 x 10^{-10} mbar. The instrument was equipped with a MgKα X-ray (hν = 1253.6 eV) and AlKα X-ray (hν = 1486.7 eV) sources. The data were acquired using the MgKα X-ray source operating at 10 kV and 30 mA (300 W) and analyzed with the CasaXPS software. XPS spectra of survey scan were recorded with a pass energy of 24 eV in a 0.5 eV step, and high-resolution scans were recorded with a pass energy of 20 eV in a 0.1 eV step. The C1s peak was used as an internal reference with a binding energy of 285 eV.

2.2.8. Surface analysis using ToF-SIMS

TOF-SIMS analyses were performed using a TOF SIMS V (ION TOF, Inc. Chestnut Ridge, NY) instrument equipped with a Bi_n^{m+} (n = 1-5, m = 1, 2) liquid metal ion gun, Cs^+ sputtering gun, and electron flood gun for charge compensation. Both the Bi and Cs ion columns were oriented at 45° with respect to the sample surface normal. The analysis chamber pressure was maintained below 5.0 x 10^{-9} mbar to avoid contamination of the surfaces to be analyzed. Positive and negative ions were collected across a 200 µm by 200 µm area for each sample. This study used a pulsed Bi^{3+} primary ion beam at 25 keV impact energy with less than 1 ns pulse width for high mass resolution spectra. An electron gun was used to prevent charge buildup on the insulting sample surfaces. The total ion dose for data acquisition was maintained well below the static limit of 1 x 10^{13} primary ions/cm^2. The mass resolution on the Si wafer was about ~8000m/Δm at 29AMU. For the high lateral resolution mass spectral images acquired in this study, a Burst Alignment setting of

25 keV Bi^{3+} ion beam was used to raster in a pixel region of 256 by 256 pixels. The negative secondary ion mass spectra obtained were calibrated using C^-, O^- , OH^- , CN^-, respectively. The positive secondary ion mass spectra were calibrated using C^+, $C_2H_3^+$, $C_3H_5^+$, $C_4H_7^+$.

2.2.9. Enzyme distribution in EFSBN by confocal microscopy

Protease was conjugated to fluorescein isothiocyanate (FITC) following the "large scale conjugation" procedure described in the Sigma Fluoro-tag-FITC conjugation kit. The FITC-tag-protease has two absorbances, at 280 nm and 495 nm. The eluent fractions containing these two absorbances (Sephadex G-25M column and phosphate buffered saline solution was used as the elution solvent) were collected. The average molar ratio of FITC to protease in the FITC-tag-protease, determined by the absorbance of FITC-tag-protease at 280 and 495 nm, was 0.46:1.0. The FITC-tag-protease was mixed with a polymer solution and subjected to the same solution blowing conditions as EFSBN-PEO webs. The EFSBN-PEO webs with embedded FITC-protease were placed on a glass slide and mounted under a No. 1.5 cover glass held up by modeling clay spacers to prevent sample compression. The 1.17 % (w/w) FITC tag protease-EFSBN-PEO webs were imaged by a Zeiss LSM 880 laser scanning confocal microscope using a 488 nm excitation laser to detect the FITC signal. The z-series images were collected using a 20x dry objective with NA=0.8 and 2 µm intervals. The z-series were further processed using Imaris 9.9 software (Bitplane, Zurich, Switzerland) to remove the background signal. Results show the location of protease in EFSBN-PEO webs.

2.2.10. Storage stability of free and immobilized protease

The storage stability of immobilized protease and commercial liquid protease (Sigma) was evaluated by the modified method of Awad *et al*.[335]. The EFSBN-PEO webs were kept in a zip bag and stored at room temperature (~22 °C) or 4 ℃. The protease assay was used to measure the residual activity of stored immobilized protease over time, up to 300 days. The as-supplied free liquid protease and free protease diluted (1µl/ml) in tris buffer (0.1 M, pH 8.0) were also stored at room temperature (~22 °C) and residual activity was measured using the protease assay over time. Residual activity was the ratio of measured activity at a time point to the initial activity at time zero, expressed as a percentage (Eqn. 2.7).

$$\text{Residual activity } (\%) = \frac{\text{Measured activity of stored sample}}{\text{Initial sample activity}} * 100\% \ldots\ldots\ldots\ldots\ldots\ldots\ldots\ldots (2.7)$$

2.2.11. Thermal stability of free and immobilized protease

Thermal stability tests were performed by incubating solid EFSBN-PEO webs, liquid commercial protease, and tris buffer (0.1 M, pH 8.0) diluted commercial protease (1µl/ml) at 65 ℃ for different times (0-240 mins) in a convection oven. After thermal treatment, the solid EFSBN-PEO webs were redissolved in buffer, and subjected to the protease assay, along with the liquid commercial protease and diluted commercial protease. The thermal stability of the liquid and immobilized solid forms of the enzyme was expressed as the residual activity after thermal treatment (Eqn. 2.8).

$$\text{Residual activity, } (\%) = \frac{\text{Sample activity after thermal treatment}}{\text{Initial sample activity}} * 100\% \ldots\ldots\ldots\ldots\ldots\ldots (2.8)$$

2.3. Results and Discussion

2.3.1. Solution blowing process parameter selection for SBN-PEO and EFSBN-PEO preparation

The first step in selecting solution blowing process parameters for producing EFSBN-PEO webs was to investigate the effects of key spinning parameters on PEO-only web formation. The polymer solution concentration (12 w/v%) and die-to-collector distance (DCD) (100 mm) were kept constant while the solution blowing process was operated with varying solution throughput (0.05, 0.10 & 0.20 ml/min), air pressure (69, 138 & 207 kPa)/(10,20&30 psi) and air temperatures (~22, 50 & 60 ℃). **Table 2.3** presents solution-blowing process parameters and fiber production observations for protease functionalized PEO solution-blown webs and PEO-only solution-blown webs. Solution throughput and air pressure (driving force) were the most crucial parameters for fiber formation. Solution throughput of 0.2 ml/ml or higher did not form fine fibers. The lower air pressure setting (138 kPa) also did not form fibers because it created an insufficient driving force to attenuate the polymer solution and evaporate the solvent. A viscous mass with very few fibers were observed at higher solution throughput and lower air pressure (**Figure 2.4 A**). Based on this parametric testing, the optimum conditions for PEO-only solution blown webs were determined to be 0.05 ml/min solution throughput, 207 kPa air pressure, and 50 ℃ air temperature. These conditions were then used to produce EFSBN webs across a wide range (0.6-7.4 % (w/w)) of protease-loading. **Figure 2.4 B** is present the EFSBN on collector that prepared using optimum conditions.

Table 2.3: Solution blown spinning process optimum condition for SBN-PEO and protease-EFSBN-PEO webs.

Trial	Solution throughput, ml/min	Air pressure, kPa	Air temperature, ℃	Visual observation
1	0.2	69, 138, 207	~22, 50, 60	No fiber formation at 0.2 ml/min solution throughput
2	0.1	69, 138	~22, 50, 60	No fiber formation at 0.2 ml/min solution throughput
3	0.1	207	~22	No fiber formation
4.	0.1	207	50, 60	Less fiber formation with central viscous mass
5.	0.05	69	~22	No fiber formation
6.	0.05	138, 207	~22	Less fiber formation with central viscous mass
7.	0.05	69	50, 60	Fiber formation with central viscous mass
8.	0.05	138, 207	50, 60	Good fiber formed

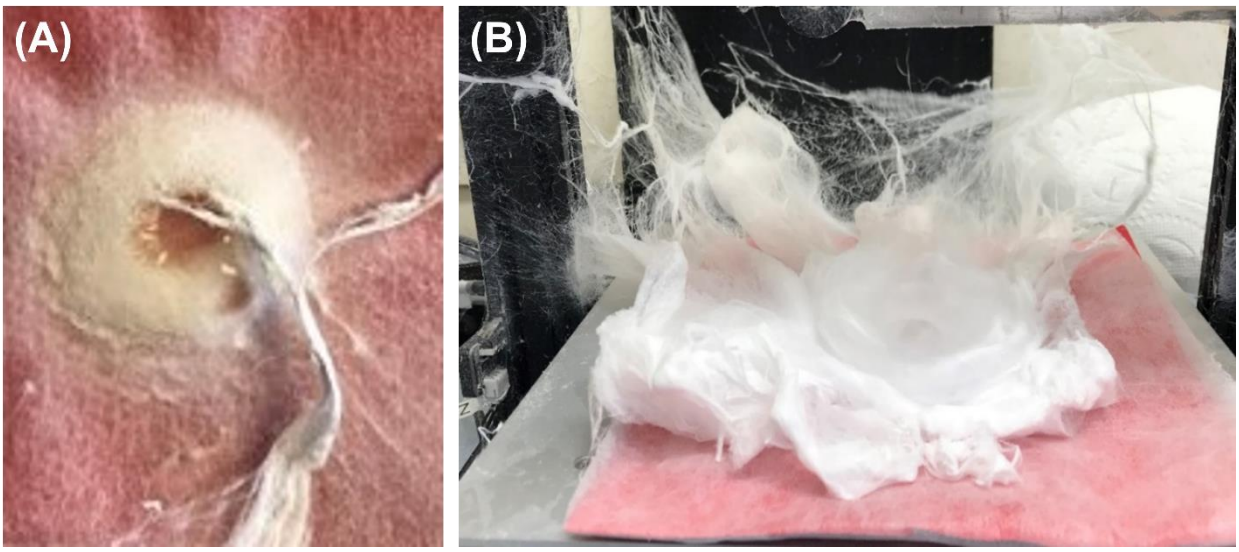

Figure 2.4: Enzyme functionalized solution blown nonwovens (EFSBN) on the collector at 12 w/v% polymer concentration, 50 ℃ air temperature, and 0.05 ml/min throughput (A) 69 kPa air pressure and (B) 207 kPa air pressure (picture captured while trial running).

2.3.2. FTIR analysis of SBN-PEO and EFSBN-PEO

The characteristic infrared absorption peaks of SBN-PEO and EFSBN-PEO webs are presented in **Figure 2.5**. PEO alone exhibits strong peaks at 2700-3000 cm^{-1} for symmetric and asymmetric stretching of -CH_2 groups; two strong splitting peaks at 1466 cm^{-1} and 1413 cm^{-1} for CH_2 scissoring (bending mode); two strong splitting peaks at 1359 cm^{-1} and 1341 cm^{-1} for CH_2 wagging; two splitting peaks at 1279 cm^{-1} and 1241 cm^{-1} for CH_2 twisting; three peaks around 1100 cm^{-1} for the results of the combination of ether group and methylene group stretching; and peaks at 961 cm^{-1}, 946 cm^{-1} and 841 cm^{-1} related to chain conformation of the PEO molecules.[336–338] Additionally, the double peaks at 1359 cm^{-1} and 1341 cm^{-1} are an indication of crystallinity (100% amorphous PEO shows only one peak at 1350 cm^{-1}).[336] The complex peaks for -C-O-C- stretching appearing at three wavenumbers 1145 cm^{-1} (medium intensity), 1096 cm^{-1} (strong intensity), and 1059 cm^{-1} (medium intensity) were present in all samples, indicating, as expected, no degradation of PEO chains during solution spinning.

The characteristic peaks of amide I and amide II bonds of protein are observed at 1650 cm^{-1} and 1550 cm^{-1}, respectively.[339] The N-H stretching peak of amide A overlaps with OH stretching at 3100-3500 cm^{-1} where the OH stretching peak could come from bound water in an enzyme.[231,340] The considerable amount of glycerol in liquid enzyme could also contribute to the OH stretching peak. Dry enzyme-free webs do not show peaks in this region. These peaks are absent in PEO-only webs and appear with increasing intensity as protease content in protease functionalized PEO solution blown webs increases. Likewise, the amides I and II show very small peaks at low

protease content (1.3% (w/w) and increase in intensity as the enzyme content increases to 7.4% (w/w) protease in EFSBN-PEO webs.

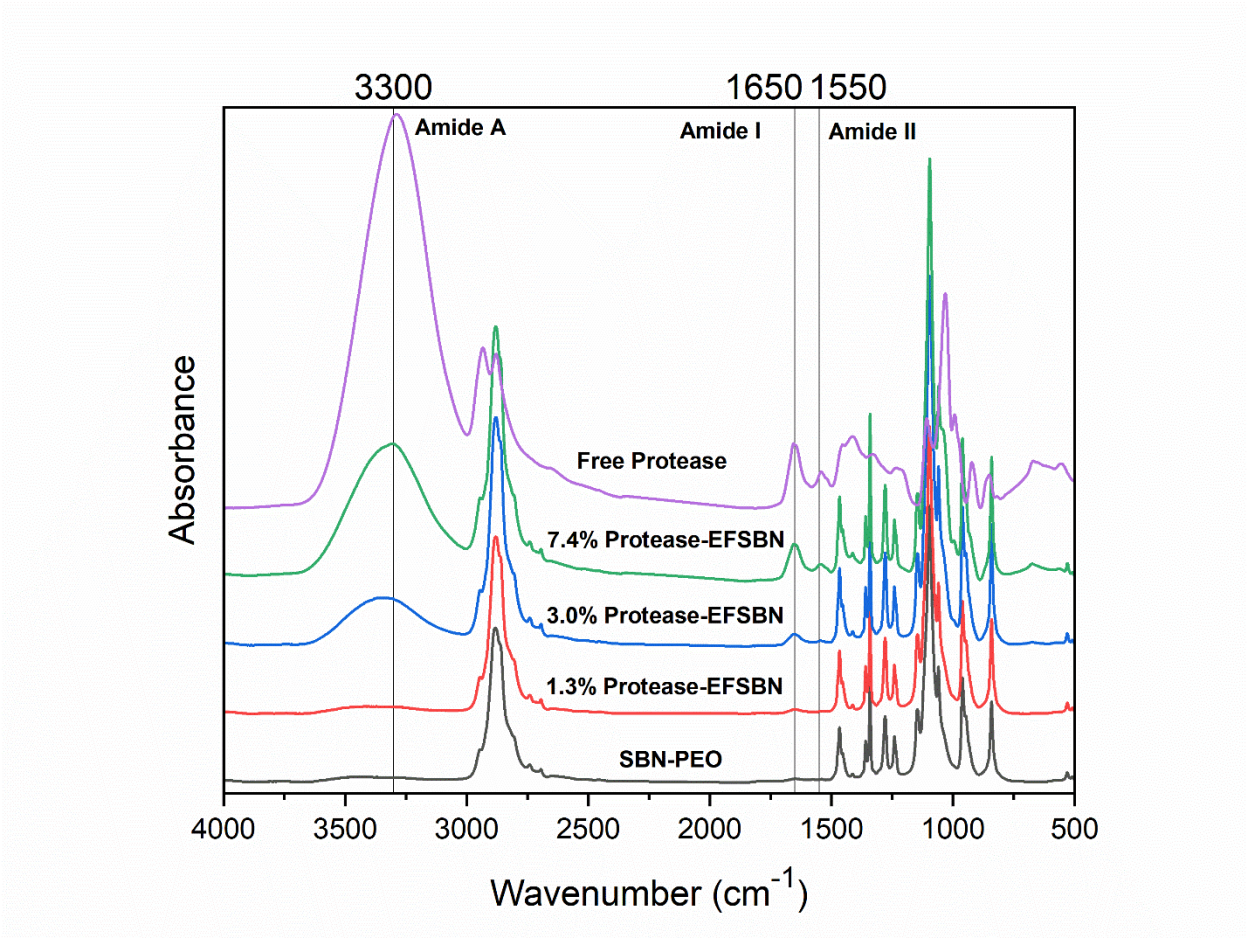

Figure 2.5: FTIR spectrum of pure PEO webs and protease functionalized PEO solution blown webs with varying protease content.

2.3.3. Enzyme loading and immobilization yield of EFSBN-PEO

The amount of enzyme loading accommodated by a carrier material is an important parameter for distinguishing the material as a "good" carrier. A wide range of protease (0.62 to 7.43 % (w/w)) loaded EFSBN-PEO webs were prepared, which indicates PEO is a good carrier for enzyme immobilization by physical entrapment. Measurements of immobilization yield reveal how much

enzyme added to the polymer solution is retained after solution blowing. Immobilization yields at different levels of enzyme loading in the polymer spinning solutions and corresponding retained protein content in the solid webs are presented in **Figure 2.6**. Protein content means the amount of protein detected in the final webs and protein loading means the amount of protein initially added to the spinning solution before solution blowing. At low enzyme loading, immobilization yields were greater than 90% indicating that more than 90% of supplied enzymes were entrapped in the PEO nanofibers. Rodriguez-deLuna *et al*. encapsulated horseradish peroxidase in PVA electrospun nanofibers and observed a similar pattern that greater than 90% protein retention was achieved at lower enzyme loading, but the relative enzyme loading decreased (to less than 10%) with increasing enzyme concentration in the spinning solution.[173] The cause for this repeatedly observed decrease in immobilization yield as enzyme loading increases has not yet been determined. The Rapid BCA technique detects across a broad protein concentration range (20-2000 μg BSA/ml), which encompassed all the sample concentrations evaluated, therefore errors in protein measurement are not suspected. The decrease is puzzling because the full inventory of homogeneous polymer-enzyme solution is pumped through the solution blowing nozzle. One explanation for the less than 100% immobilization yields may be that a certain portion of enzyme is aerosolized and blown away with the high-pressure air. High enzyme loading might lead to less interaction between polymer and enzymes or a decrease in the space available for entrapment, leading to increased enzyme loss to the pressurized air flow.

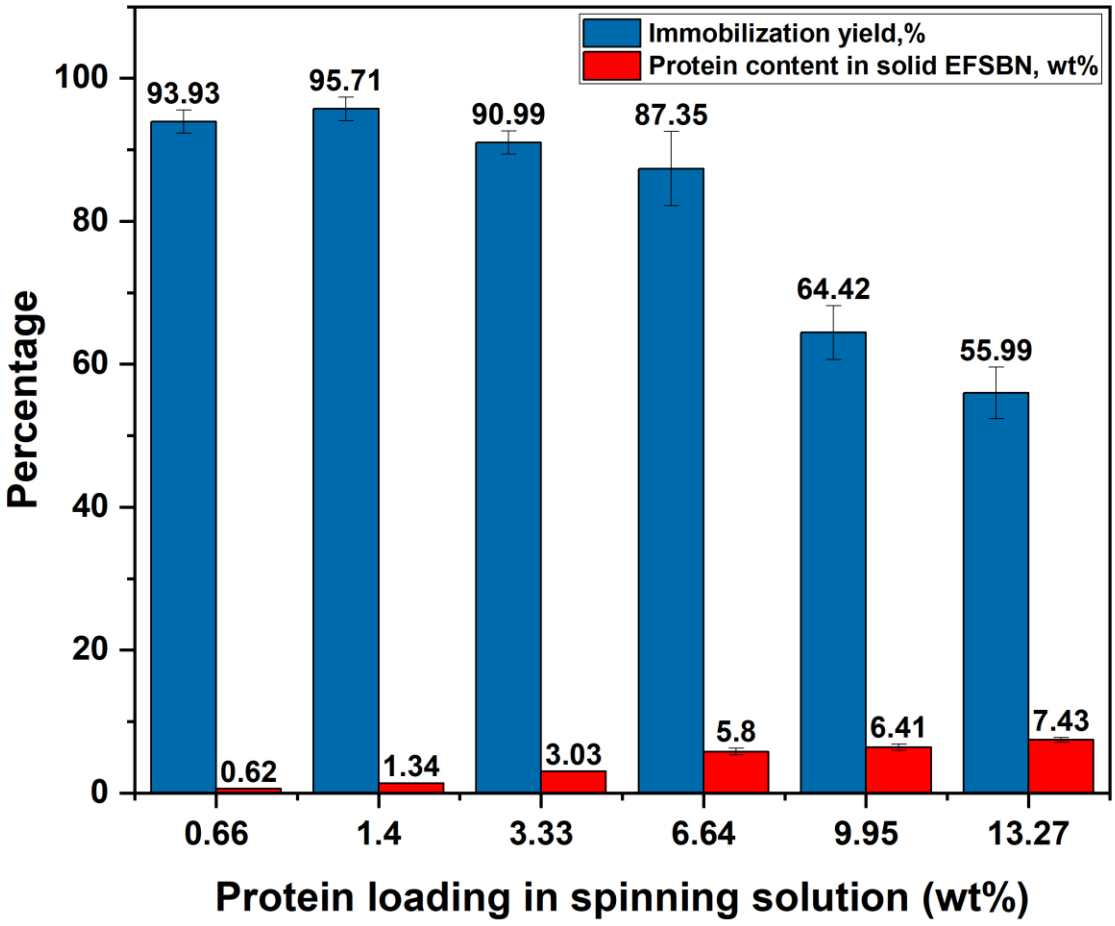

Figure 2.6: Immobilization yield of EFSBN and retaining protein in the solid EFSBN webs with different enzyme loading.

2.3.4. Protease-EFSBN-PEO catalytic activity

Immobilization methods and carrier materials affect the enzyme catalytic activity. The catalytic activity also changes with enzyme loading, immobilization processing conditions, and the final form of the supporting material. Nanofibrous EFSBN-PEO webs redissolved rapidly in the buffer because the high nanofiber surface area provided high contact between water and water-soluble PEO polymer that enhanced dissolution and released enzyme into the buffer as a free enzyme. Since PEO polymer is soluble in an aqueous assay buffer, the released enzyme behaved like a free

enzyme in responding to protease activity analysis. The activity of the redissolved webs was calculated based on the protein content detected in the solid webs. Then, the relative activity of enzyme-functionalized webs was measured as the activity of redissolved functionalized webs compared to the activity of an equivalent amount of free enzyme content, expressed as a percentage. The enzyme activities of protease EFSBN-PEO webs relative to their measured protein content are presented in **Figure 2.7**. The EFSBN showed substantial catalytic activity, indicating that most enzyme delivered through the solution blowing nozzle was still present in the final solid web products. The retained activity for EFSBN was comparatively higher than reported for electrospun immobilized protease activities. One study with immobilized bromelain protease in cellulose triacetate electrospun nanofibers reported retaining 47% activity.[228] Another study reported 65% retained activity for protease immobilized by adsorption on polycaprolactone (PCL) electrospun nanofibers.[142] Adsorption immobilization is considered to be mild method that has limited impact on enzyme structure, therefore the high level of enzyme activity detected in EFSBN (> 80%) implies that SBS is a benign process and that PEO is good carrier for protease immobilization. The high catalytic activity also indicated that immobilized protease retained or was able to recover its native functional structure after redissolving in a buffer. In contrast to the immobilization yield results (**Figure 2.6**), the relative activity results (**Figure 2.7**) reveals enzyme preserved their functional structure for a wide range of enzyme content in the solid EFSBN-PEO webs. The finding of the immobilization yield, protein content, and relative activity is revealed that PEO webs are an excellent carrier for protease entrapment with a wide range of enzyme carriers and quick delivery enzyme to the reaction zone.

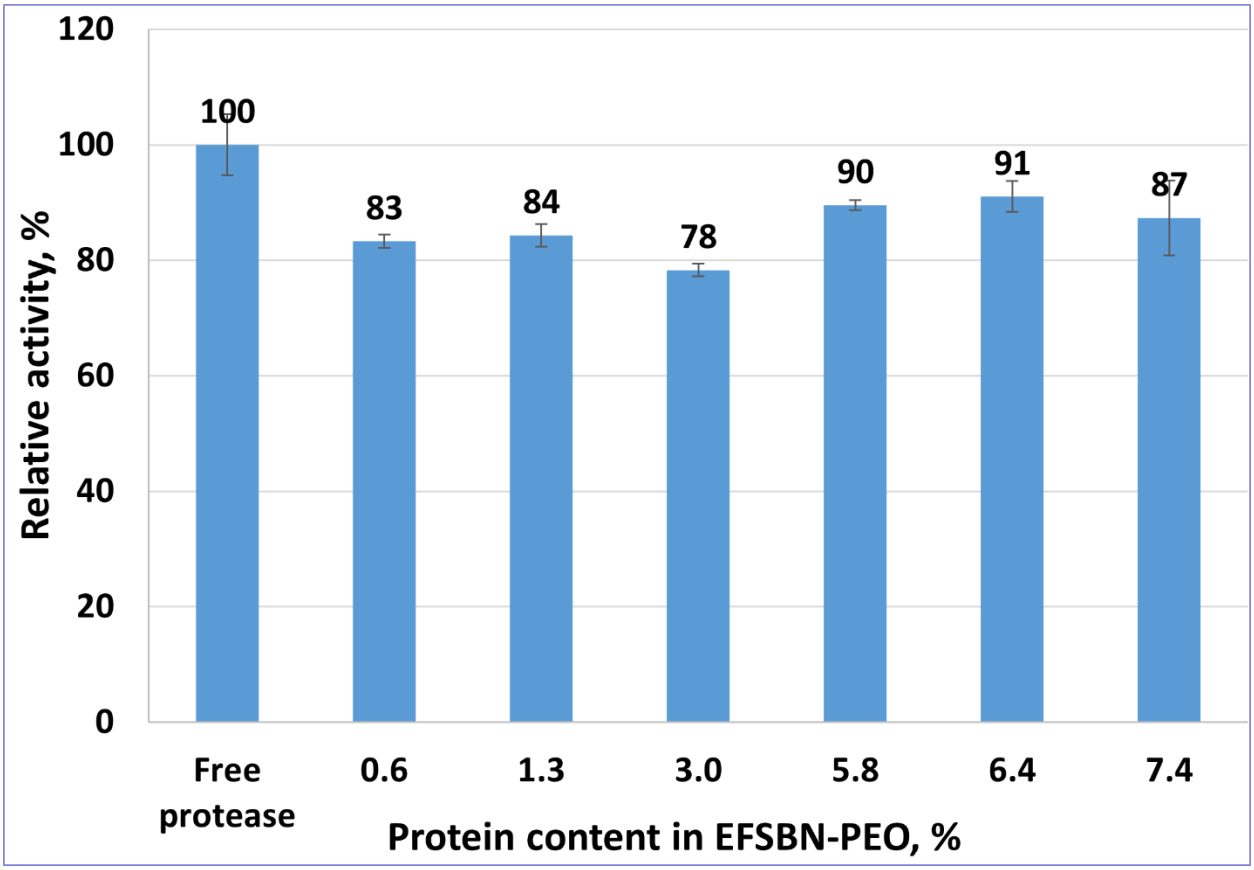

Figure 2.7: Relative protease activity of EFSBN-PEO webs with varying protein content in the solid webs.

2.3.5. Appearance and diameter of SBN-PEO and EFSBN-PEO by scanning electron microscopy

The morphology of SBN-PEO webs and EFSBN-PEO webs prepared with various protease loading were characterized by scanning electron microscopy EFSBN (**Figure 2.8**). The morphology is characteristic of a nonwoven structure with a distribution of micro- and nanofibers forming the web. The surface diameter and fiber surface appearance changed as enzyme loading increased. SBN-PEO webs had an average fiber diameter of 406±295 nm which is lower than a reported SBS-PEO average fiber diameter of 700±226 nm.[184] In addition to achieving a lower fiber diameter, the solution flow rate of the current work is at least three times higher than the prior reported

work. However, loading enzyme in the webs increased the average fiber diameter. For example, EFSBN-PEO webs loaded with 1.3 % (w/w) protease had a higher average diameter of 566±345 nm compared to fibers in the no-enzyme SBN-PEO webs. Higher enzyme-loaded webs had comparatively higher diameter and larger standard deviation, revealing that enzyme-free PEO web fibers were more uniform than enzyme-loaded PEO webs. The increases in fiber diameter and standard deviation probably resulted from concentrated poly(electrolyte) solution effects[341,342] and increasing viscosity (liquid protease had 50-70% glycerol that increased viscosity) [343,344] of more concentrated polymer solutions that would increase the solution resistance to being stretched. Similar, fiber roughness and diameter variability findings were reported by Moreno-Cortez et al. who studied papain encapsulation in polyvinyl alcohol (PVA) electrospun nanofibrous membranes.[170] The presence of enzymes in EFSBNs also causes surface irregularities and roughness. The highest protease loaded (7.4 % w/w) EFSBN web fibers exhibited the highest standard deviation in fiber diameter due to beadlike structures of thick and thin zones (marked by arrows). Since beading is not observed in PEO-only fibers, the thick bead zones in EFSBN webs are probably caused by enzyme proteins clustering in those regions and resisting uniform distribution during the blowing process.

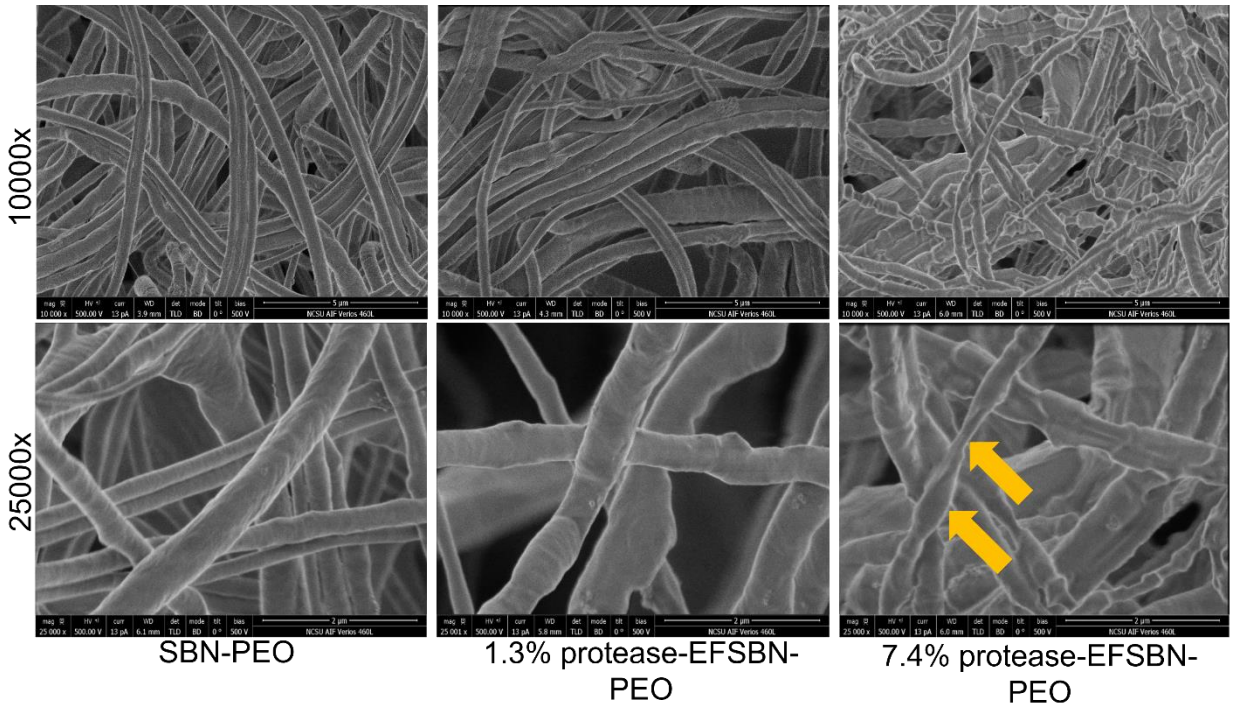

Figure 2.8: SEM micrograph of SBN-PEO webs and protease EFSBN-PEO webs with varying enzyme loading.

2.3.6. Surface composition analysis of EFSBN-PEO by XPS

The surface composition of EFSBN-PEO and SBN-PEO webs was characterized by X-ray photoelectron spectroscopy (XPS), as shown in **Figure 2.9**. The two main peaks of C_{1s} and O_{1s} are found in all spectra, while the peak of N_{1s} was only found in the spectra of EFSBN-PEO webs. Since SBN-PEO contains only C_{1s}, O_{1s}, and H elements and the N_{1s} signal comes from the presence of protein,[345] XPS further confirms that protease was successfully immobilized into PEO webs. The presence of the N_{1s} signal in XPS spectra again validates the FTIR results of the presence of protease in the EFSBN-PEO webs.

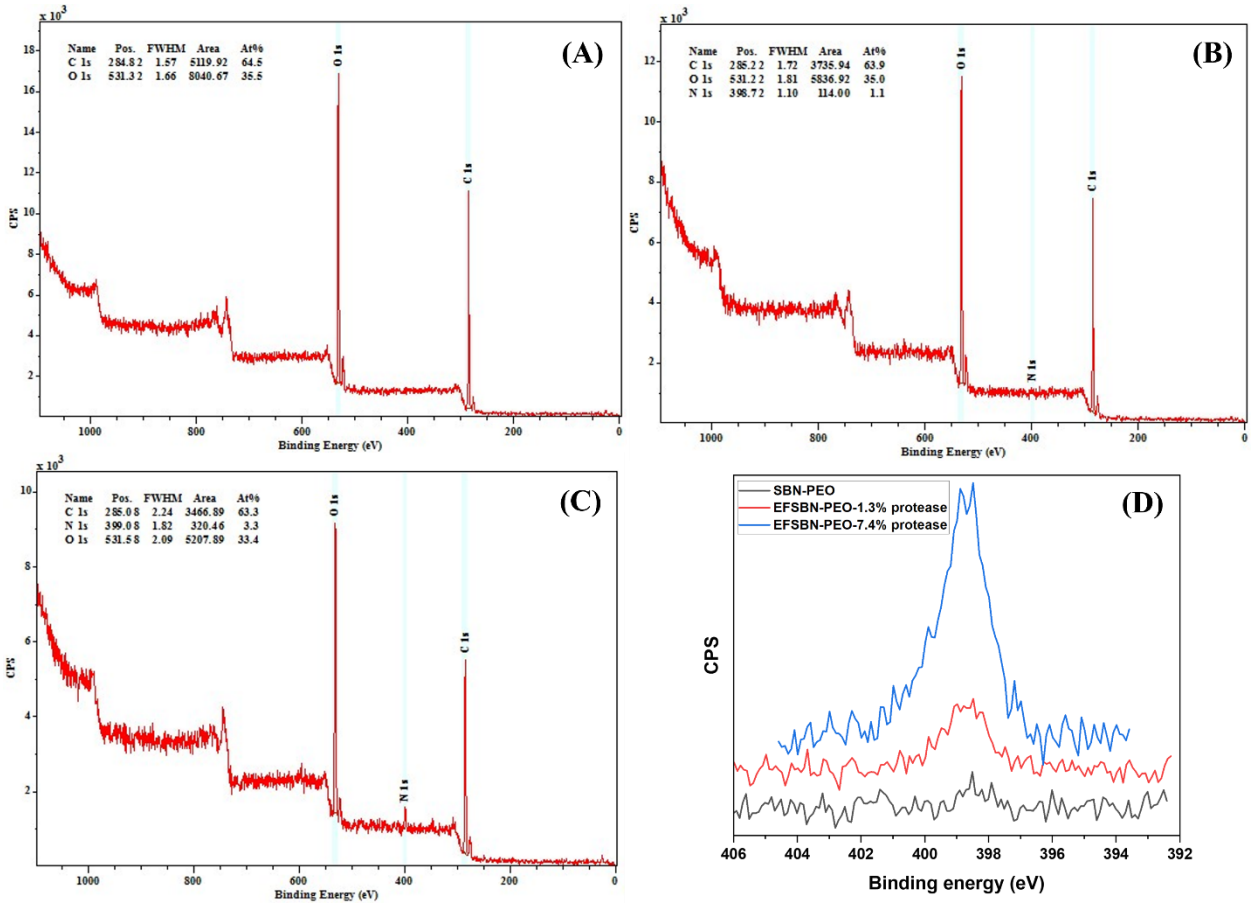

Figure 2.9: XPS spectra of (A) SBN-PEO, (B) 1.3 % SA-EFSBN-PEO, (C) 7.4 % SA-EFSBN-PEO, and (D) N1s peaks of the three samples.

2.3.7. Enzyme position and distribution analysis in EFSBN-PEO by ToF-SIMS

The distribution and position of enzymes in an immobilized carrier is an important parameter for biocatalyst reaction design. The successful immobilization of protease into PEO webs was confirmed using Time-of-Flight Secondary Ion Mass Spectrometry (ToF-SIMS). The ToF-SIMS spectra and distribution maps revealed the distribution and position of the immobilized protease. The high-resolution ToF-SIMS spectra of positive ions and negative ions are shown in **Figure 2.10** and **Figure 2.11**, respectively. The clearly visible characteristic signals from ethylene oxide, namely CH_3O^+, $C_2H_5O^{+,}$ and $C_2H_3O^-$, confirm the detection of PEO polymer. Signals arising from

amide bond cleavage, including CH_4N^+, CN^- and CNO^-, confirm the presence of protein (enzyme) in the PEO webs. However, the intensity (height) of the nitrogen compound peaks depends highly on enzyme loading. The 7.4 % (w/w) protein-loaded EFSBN-PEO webs showed these peaks clearly. In contrast, low protein-loaded webs did not show significant nitrogen peak intensity. The 1.3 % protease EFSBN-PEO web ToF-SIMS spectra are similar to SBN-PEO web spectra which indicated the EFSBN-PEO nanofibers did not have enough protein molecules on the surface for detection. ToF-SIMS is limited to detecting ion fragments within 1-2 nm depth of the surface of a specimen. So, for low enzyme-loaded EFSBN-PEO webs, the ToF-SIMS results indicate that most enzymes are located inside the nanofibers. At high enzyme loading, more enzymes forces toward surface and the ToF-SIMS spectra for 7.4 % (w/w) protein-loaded EFSBN-PEO webs revealed that protein is present on the fiber surfaces.

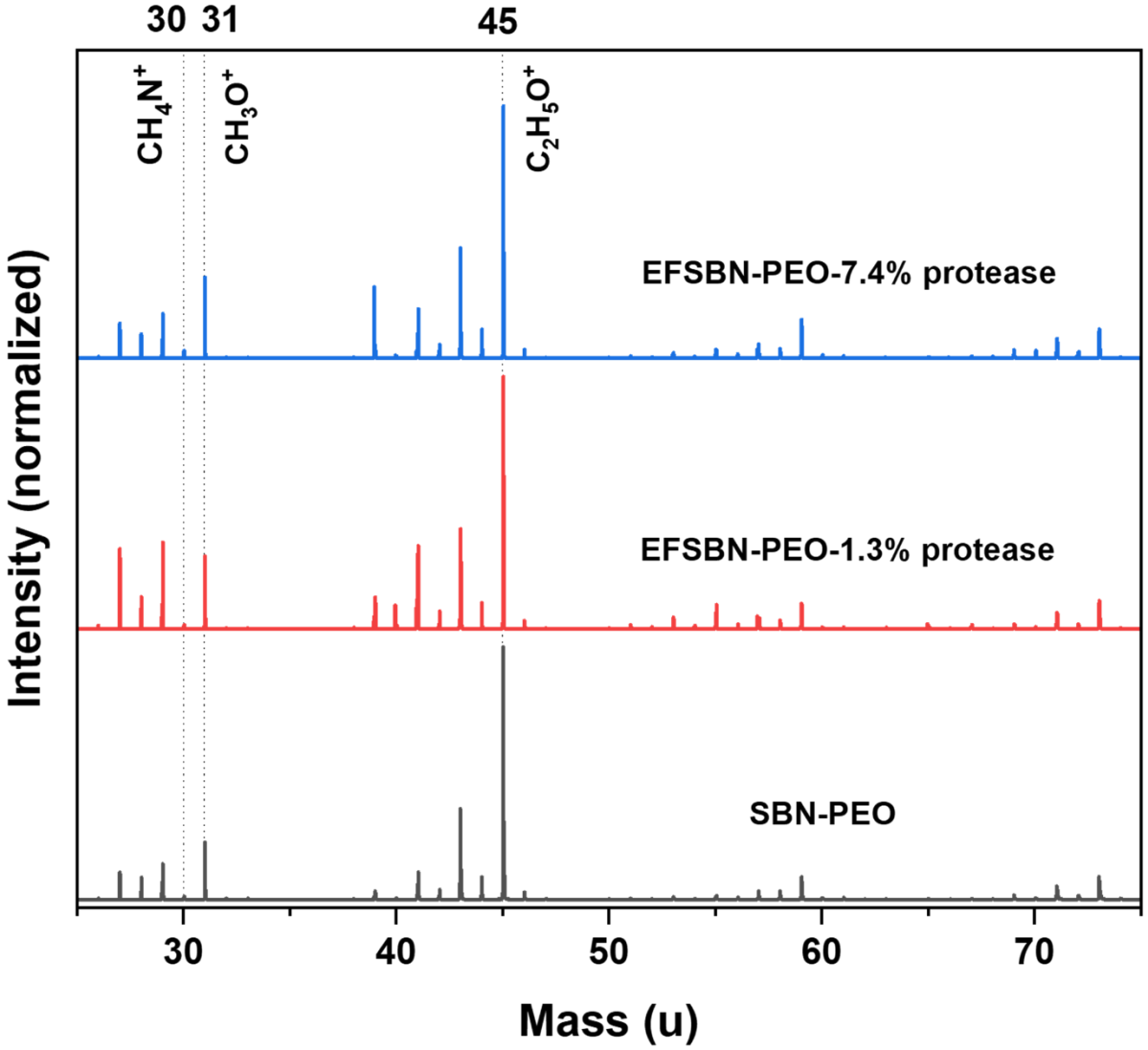

Figure 2.10: High-resolution ToF-SIMS spectra (positive ions) of SBN-PEO and protease EFSBN-PEO webs.

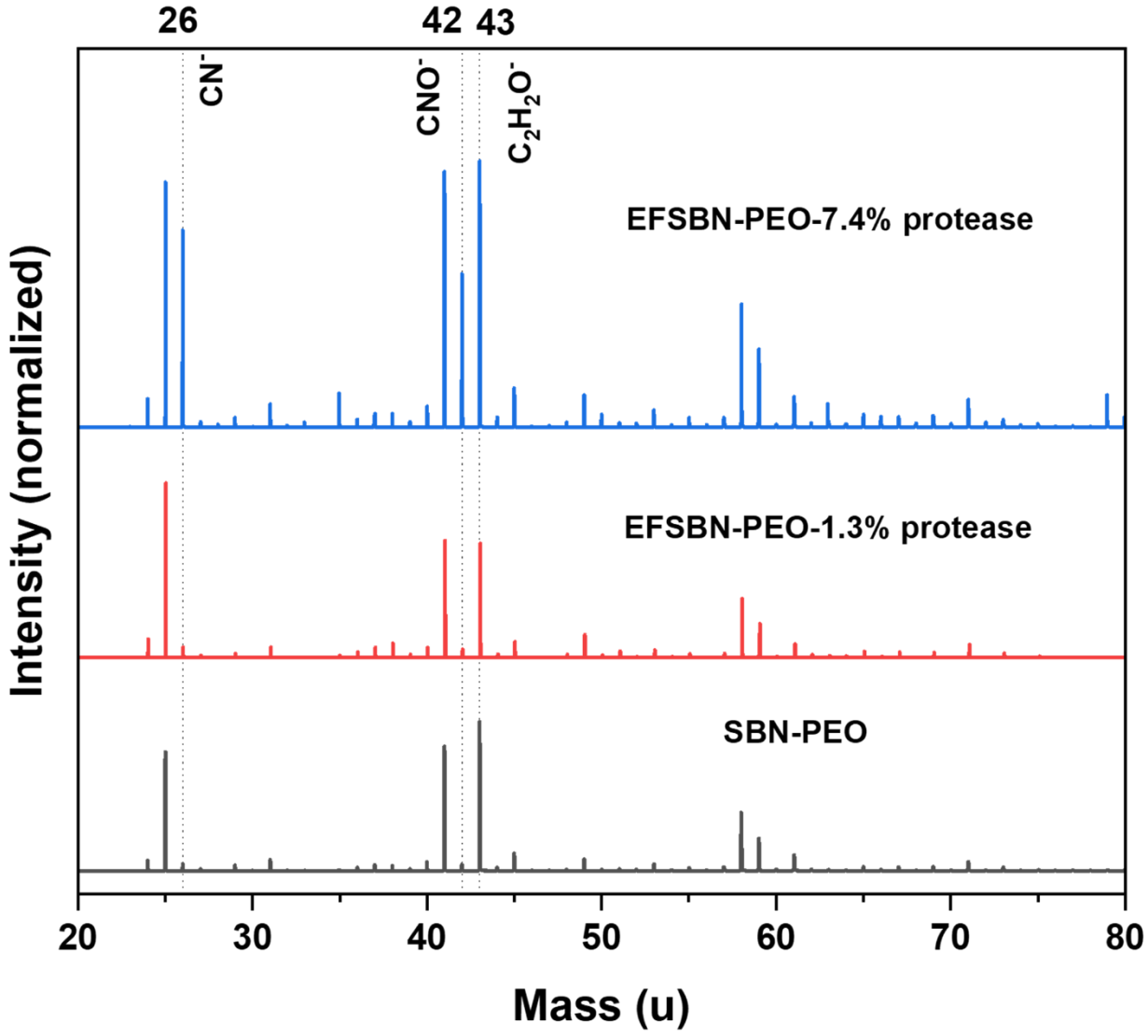

Figure 2.11: High-resolution ToF-SIMS spectra (negative ions) of SBN-PEO and protease EFSBN-PEO webs.

ToF-SIMS distribution maps characterized the distribution of protease in the EFSBN-PEO webs. The ToF-SIMS distribution maps of positive and negative ions of SBN-PEO, 1.3 % (w/w) protease EFSBN-PEO and 7.4 % (w/w) protease EFSBN-PEO are shown in Appendices (**Figure A 2.1 – A 2. 4**). These distribution maps again indicated that most proteases were located inside the fibers. The overlaid image of the distribution map of 7.4 % (w/w) protease EFSBN-PEO is presented in

Figure 2.12. The homogeneous green color distribution (CH_4N^+ and $C_4H_{10}N^+$) indicates subtilisin A protease was homogeneously distributed in the nanofibrous webs.

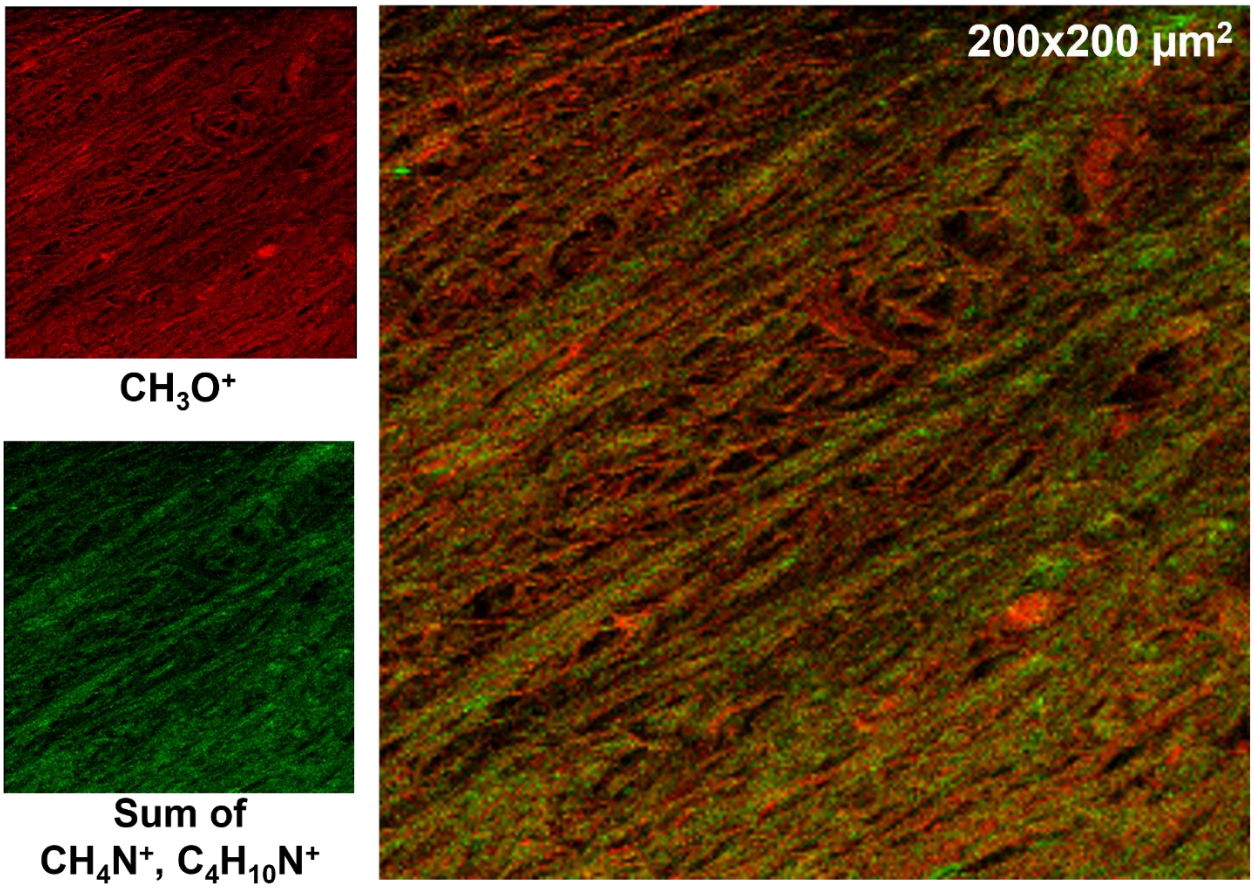

Figure 2.12: ToF-SIMS positive ion distribution maps and overlaid image for a 7.4 % (w/w) protease EFSBN-PEO web.

2.3.8. Enzyme distribution in EFSBN-PEO by confocal microscopy

Uniform distribution of enzyme entrapment in nanofibrous webs is a very important parameter for achieving maximum carrier materials utilization and consistent delivery of enzymes into the intended application. To observe the distribution of entrapped protease in EFSBN-PEO, subtilisin A protease was labeled with fluorescein isothiocyanate (FITC), and the resulting FITC-tagged

protease was entrapped by solution blowing in EFSBN-PEO webs which were then analyzed by laser scanning confocal microscopy (**Figure 2.13)**. These images illustrate that protease distribution in EFSBN was homogeneous at a macroscopic scale throughout the webs. This was achieved because the aqueous protease solution formed a homogeneous solution with the aqueous PEO polymer solution leading to a homogeneous polymer-solvent-enzyme solution. After solution blowing, the enzyme homogeneity remained in the dried PEO webs, indicating that solution blowing of enzyme-loaded PEO solutions is an excellent immobilization fabrication process.

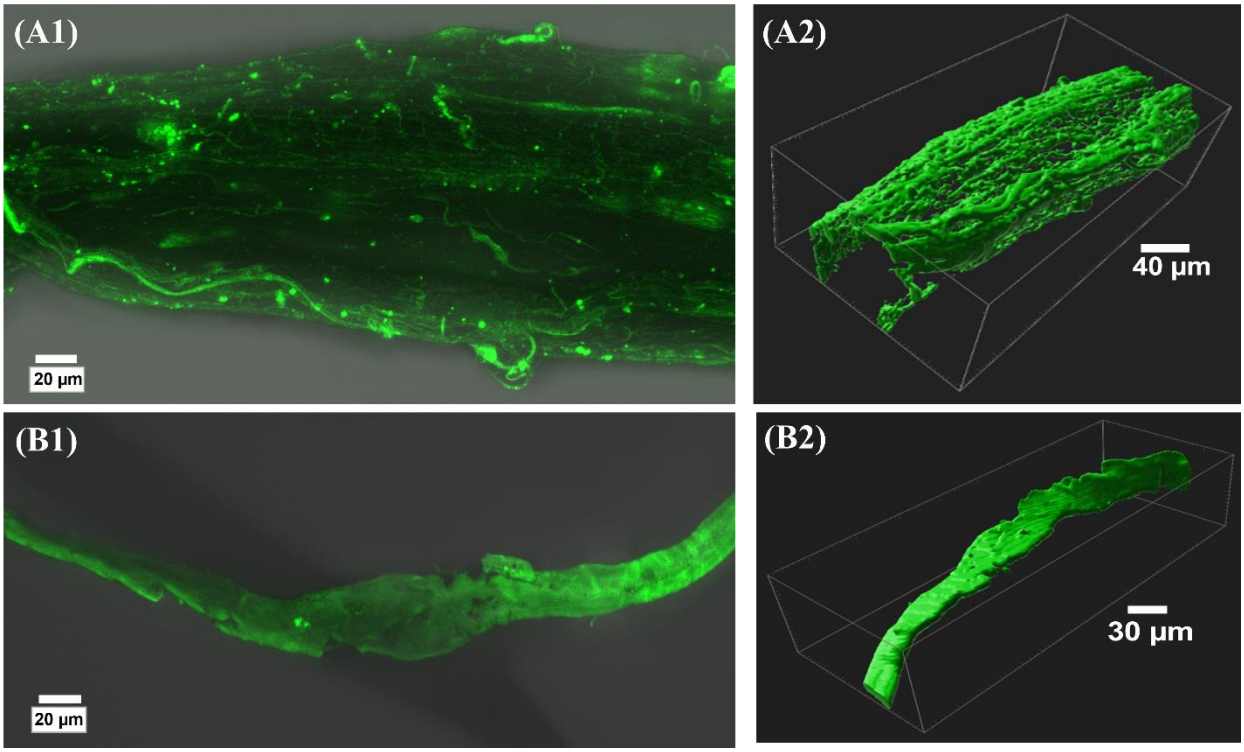

Figure 2.13: Laser scanning confocal microscopy images: raw images of the distribution of FITC-tagged protease encapsulated EFSBN-PEO webs at two different points ((A1: a bundle of fluffy fibers) and (B1: a bundle of stick fibers)) and processed images of distribution of FITC-tagged protease encapsulated EFSBN-PEO webs ((A1: a bundle of fluffy fiber) and (B1: a bundle of stick fibers)).

2.3.9. Storage stability of EFSBN-PEO and native protease in buffer

Dissolved enzymes are quite sensitive to environmental conditions and may lose their activities easily compared to immobilized enzymes. Therefore, it is important to characterize enzyme storage stability for practical applications. Enzyme storage stability has been correlated to structural stability over time. Frequently, by physically stabilizing the enzyme structure, the storage stability of enzymes increases on immobilization with polymeric carriers.[82] Storage stability tests were carried out by placing samples of each enzyme-loaded web at room temperature (~22 ℃) and at 4 ℃ and measuring the remaining activity over time. Activity found at each time point was calculated with the initial activity considered as 100%. Results are presented in **Figure 2.14** and **Figure 2.15** for 1.3 % (w/w) and 3.0 (w/w) protease-loaded EFSBN-PEO webs respectively. Results show that protease was stable for a long time in PEO webs, and an advantage of solution spinning with PEO is that PEO may act as a lyoprotectant[64] to preserve enzyme structure during spinning as well as storing. Enzyme activity detected in EFSBN increased slightly (> 100% activity) after seven days of storage which may be related to conformational stress and relaxation experienced by the enzyme during and after the solution spinning process. Solution spinning is a very rapid fabrication process that could cause enzyme to become trapped in a non-optimal deformed conformation when the solvent evaporates. After relaxation during storage, enzyme could temporarily regain a more optimal conformation and thereafter its conformation would be influenced by the subsequent storage conditions. Further experiments would be needed to determine if this hypothesis is valid. When redissolved in buffer, the EFSBN webs showed at least 60% of their initial activity after 300 days, which is higher than the residual activities of immobilized protease in various polymeric supports reported in the literature as only

33-57% after a much shorter storage period of 30 days at 4 °C.[124,152,174] This result revealed that immobilized protease in EFSBN could be conveniently stored at ambient temperature or in refrigerators. The produced EFSBN is a unique storage technique in a quick-dissolving solid form rather than typical liquid enzymes or lyophilized forms.

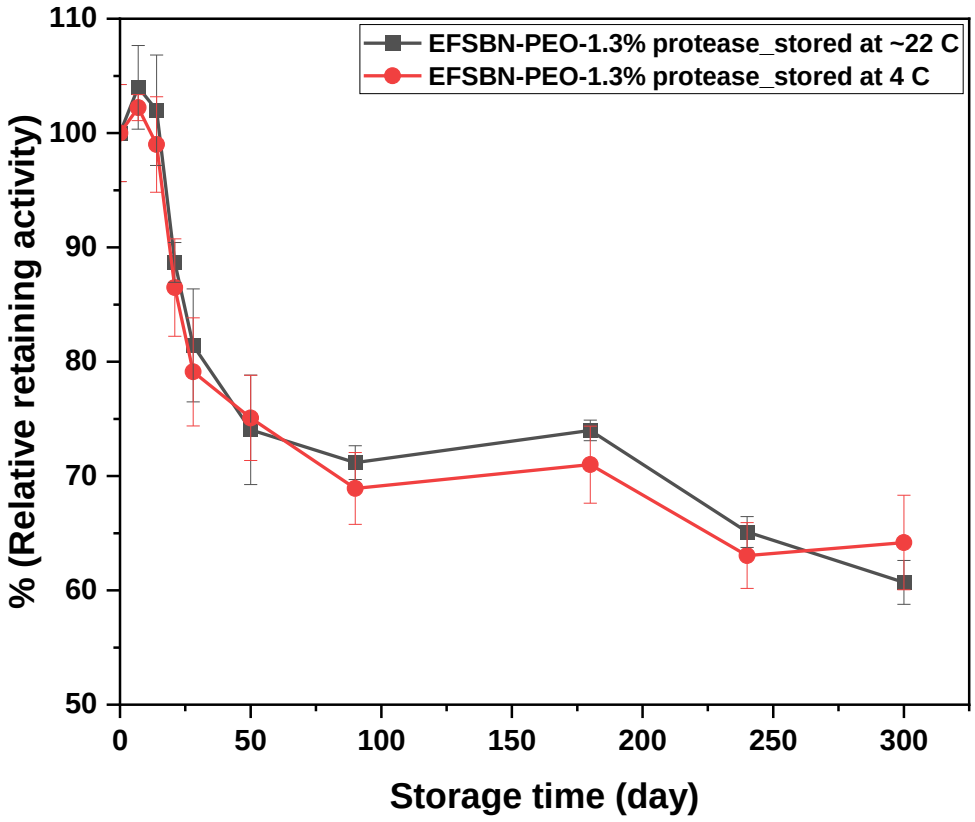

Figure 2.14: Storage stability (retaining activity with time) of 1.3 % (w/w) protease functionalized polyethylene oxide solution blown webs.

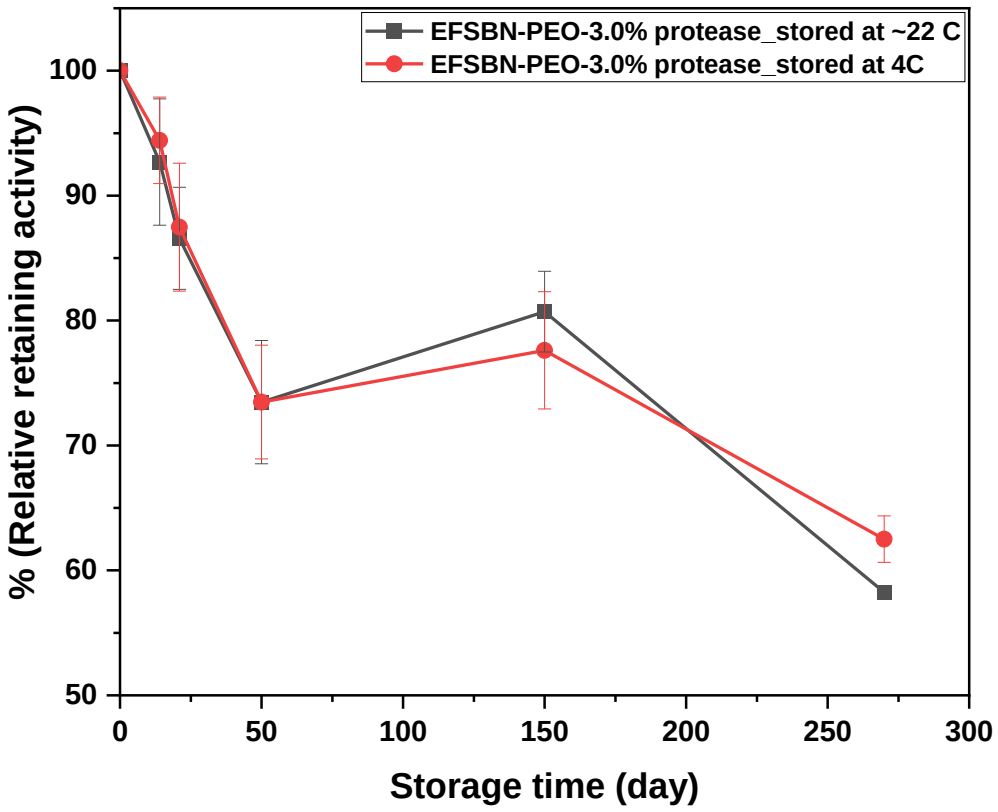

Figure 2.15: Storage stability of 3.0% (w/w) protease-EFSBN-PEO webs at ambient temperature (~22 ℃) and 4 ℃.

The storage stabilities of free subtilisin A protease and encapsulated subtilisin A are also compared and the relative remaining activity at different storage times is presented in **Figure 2.16.** The free subtilisin A protease (as it was supplied), diluted free subtilisin A protease (1µl/ml) in Tris HCl buffer (pH = 8.0, 0.1 M), and protease EFSBN were stored at room temperature (~ 22 ℃). The remaining relative activities of immobilized subtilisin A and free subtilisin A (as it was supplied) after 180 days were 74±0.90% and 85±0.54%, respectively. The commercial free protease retained a high level of activity because the as-supplied liquid protease formulation

contained glycerol that acts as a stabilizer by reducing water activity and preventing protease self-hydrolysis.[346] On the other hand, after the as-supplied protease was diluted in buffer, the stabilizer effectiveness was lost, triggering proteolysis, and the protease activity decreased rapidly.[120,347] The relative remaining activity of diluted free protease was only around 10% of the initial activity after seven days. The storage stability outcome for protease in EFSBN webs showed that immobilizing enzymes within PEO nonwovens can preserve good storage stability at room temperature without adding additional stabilizers. Avoiding refrigeration is important for the formulation of products and energy efficiency in delivering enzymes to different applications, so these extended storage stability results again reveal enzyme entrapment using PEO solution blown nonwoven webs as unique and desirable enzyme storage and delivery option for ambient temperature scenarios.

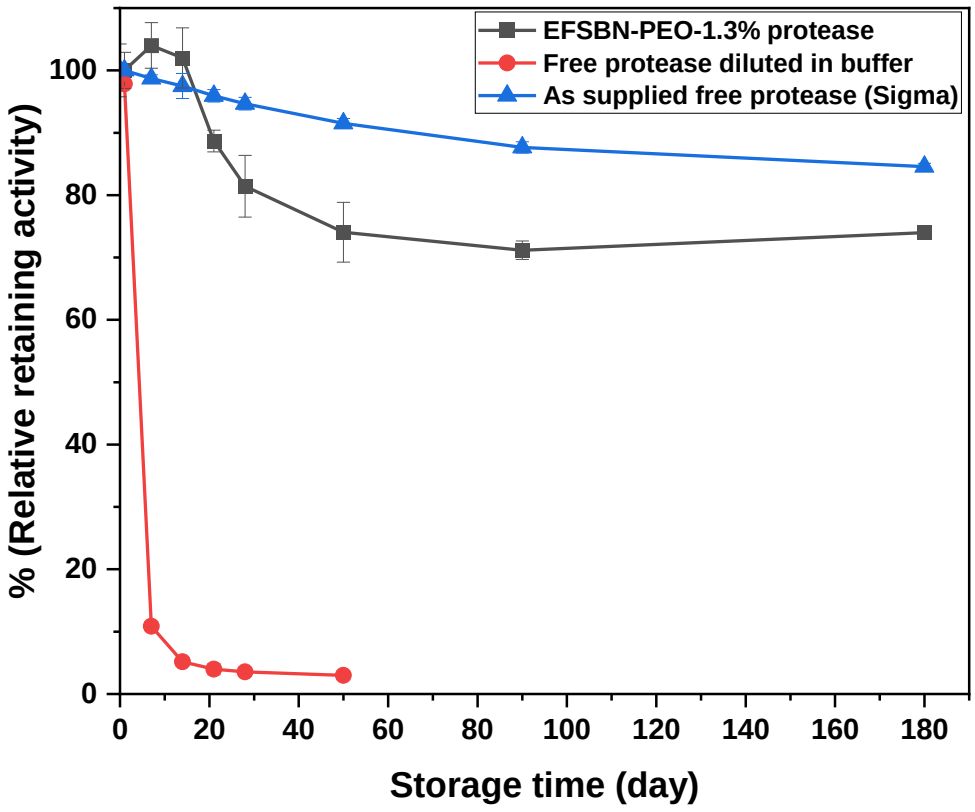

Figure 2.16: Ambient storage stability of supplied free subtilisin A, diluted free subtilisin A (1µl/ml) in Tris HCl buffer (pH = 8.0, 0.1 M) and 1.3 % (w/w) subtilisin A protease-EFSBN-PEO solid webs.

2.3.10. Thermal stability of EFSBN-PEO and native protease in buffer

The thermal stability of entrapped protease is one the most important factors for its application and storage at a higher temperature for prolonged periods. Enzyme entrapment in a suitable carrier can minimize enzyme conformational changes when exposed to harsh environments such as high temperatures and prevent the enzyme structure from denaturing (unfolding). In this study, free liquid protease and immobilized protease in solid EFSBN webs were incubated at 65

°C for up to 12 hr to determine the thermal stability of protease. The relative remaining activities of free liquid protease (as supplied), diluted free protease (1µl/ml) in Tris HCl buffer (pH = 8.0, 0.1 M), and immobilized protease (1.3 % protease EFSBN and 3.0% protease EFSBN) are presented in **Figure 2.17**. Entrapped subtilisin A protease showed excellent thermal stability for up to 12 hrs. This higher thermal stability can be attributed to preventing thermal inactivation by preventing entrapped enzyme molecules from unfolding within the dry nanofibers. A similar observation has been reported for protease (from *Aspergillus niger*) entrapped in polyacrylamide beads.[124] The as-supplied free protease also showed excellent thermal stability over time, similar to immobilized protease. Again, this is attributed to the presence of glycerol stabilizer in the product. In contrast, the diluted free protease showed a steep decline in residual activity and lost total activity within 4 hrs at the elevated temperature. Dilution enhances self-hydrolysis and protease autolysis.[348] leads to a rapid enzyme activity decline. The extended thermal stability results at elevated temperatures again emphasize the benefit of using PEO solution blown nonwoven webs as a unique water-soluble solid carrier for protease entrapment without additional stabilizers.

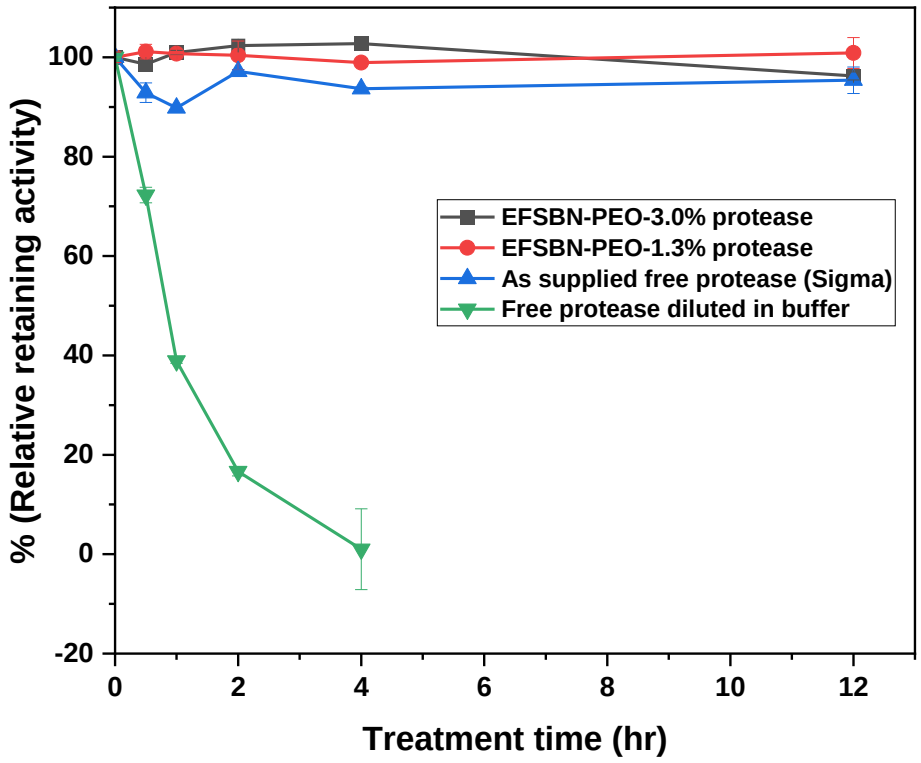

Figure 2.17: Thermal stability of free subtilisin A protease and encapsulated subtilisin A protease in EFSBN-PEO webs at 65 ℃.

2.4. Conclusions

Solution blown nonwovens (SBN) and enzyme functionalized solution blown nonwovens (EFBSN) were successfully prepared from solutions of PEO (aqueous) and liquid subtilisin A protease by a single step solution blowing technique. In this study, the operating conditions for solution blow spinning were optimized across several parameters during formation of PEO-only fibers, and these same optimized parameters were then used to produce enzyme-loaded PEO webs. The results demonstrated that solution blow spinning is a promising single-step fabrication technique for enzyme entrapment from polymer-solvent-enzyme compatible triads. SEM micrographs revealed a more irregular nano- and micro-fibrous nonwoven structure of EFSBN compared to SBN. Protease entrapment in the fibers changed the fiber morphology toward a beads-on-string appearance compared to the uniform diameter of polymer-only fibers. Substantial enzyme activity was detected in EFSBN webs after the solution blowing process and after storage at ambient dry conditions. The protease assay showed that EFSBN retained about 90% activity of the free enzyme activity. FTIR spectra, Lowry protein assay, and XPS spectra confirmed the presence of protein in the nanofibrous webs. However, protein losses appear to occur during solution blowing at higher enzyme loading conditions and clarifying the reason for this should be explored in future work. ToF-SIMS and laser confocal microscopy revealed that immobilized enzymes were mainly located inside the fibers and homogeneously distributed throughout the webs. Protease entrapped in solid dry PEO webs exhibited similar thermal stability compared to the corresponding commercial liquid protease and better stability than buffer-diluted free protease. Similarly, immobilized protease retained longer storage stability than buffer-diluted free protease. Subtilisin A protease entrapped in dry PEO retained more than 60% activity after

300 days, with similar remaining activity values found for both ambient and refrigerated storage. Therefore, protease immobilization via entrapment in PEO nanofibers by solution blowing is a simple, efficient process for loading a wide range of enzyme amounts in a rapidly water-soluble solid-state preparation that preserves a high level of enzyme activity over long periods of ambient storage without any added stabilizer. A specific application where is could be useful is in quick-dissolving solid detergent formulations for laundry or dishwashing. Future studies could extend the SBS parametric test ranges, such as by increasing the air temperature for more rapid solvent evaporation that could potentially lead to higher throughput, and by investigating polymer solution fluid properties in the presence of varying enzyme concentrations. These variables could impact enzyme stability and fiber morphology. This technology can also be used with other enzymes, polymers and solvents, creating a broad category of enzyme functionalized solution blown nonwovens with unique storage and delivery options for numerous applications within industrial, medical, food, packaging, sensing, and consumer products and processes.

Chapter 3: Encapsulation of *Candida Antarctica* lipase B in polycaprolactone nanofiber by solution blown spinning to produce degradable enzymatic nonwoven web.

Abstract:

With increasing polymer wastes entering into environments, the disposal of plastic waste has become an imminent environmental problem. In this work, complete, rapid, and controllable enzymatic degradable nanofibrous nonwoven webs were developed. Lipase (CALB) from *Candida sp.* was successfully entrapped in polycaprolactone (PCL) nanofibrous nonwoven webs via solution-blown spinning of a compatible water-in-oil triad microemulsion of PCL-chloroform-CALB. A wide concentration range (0.53-1.92 wt% protein) of CALB content nanofibrous webs was produced. CALB enzymes survived in the polymer solution organic solvent, and, after the solution spinning process, the immobilized CALB retained around 50% of the free enzyme activity. Residual lipase activity in the webs was measured by degrading fibers in tris buffer (100 mM, pH 8.0) and comparing the released enzyme activity to non-immobilized free enzyme using a p-nitrophenyl acetate substrate-based assay. The presence of enzyme protein in the solid nanofibers was detected by Fourier Transform Infrared Spectroscopy (FTIR). Time of flight-secondary ions mass spectroscopy (ToF-SIMS) and laser confocal microscopy revealed that the immobilized enzymes were mainly positioned inside the fibers and non-homogeneously distributed (enzymes cling to each other) throughout the webs. Enzymatic degradation studies were conducted by incubating different CALB-enzyme functionalized solution-blown nonwoven (EFSBN)-PCL webs in Tris-HCl buffer (100 mM, pH 8.0) at 40 °C and ambient temperature (~22 °C). It is noteworthy to mention that the enzymatic degradation of EFSBN-PCL webs was

controllable. Because of the nanofibrous structure of the webs and the distribution of enzymes throughout the webs, EFSBN-PCL webs degraded very rapidly when exposed to water. Depending on enzyme loading (1.92 to 0.53 (wt%), EFSBN-PCL webs were degraded within 15 to 60 mins. Scanning electron microscopy (SEM) images of partially degraded webs showed that thinner fibers disappeared first. Immobilized CALB in solid nanofiber webs exhibited long storage stability at room (~22 °C) and refrigeration (4 °C) temperature, with around 60% remaining catalytic activity after 120 days compared to the initial activity. While stability under ambient environments demonstrates options for safe storage and applications such as packaging materials, the unique degradation properties of EFSBN-PCL nonwoven webs can be exploited for simple waste management after use.

Keywords: CALB, enzymatic degradation, entrapment, immobilization, polycaprolactone, solution blow spinning.

3.1. Introduction

Petrochemical polymers such as polyethylene and polypropylene have been widely used in various packaging materials owing to their good thermomechanical and barrier properties, low cost, and large production rates.[349] However, these synthetic polymer-based packaging's become a major source of waste after use due to their very poor biodegradability.[350] Material biodegradability has been widely focused on because of the renewed attention to environmental protection issues.[351,352] So, the packaging materials should biodegrade after their useful life without causing environmental waste problems. Hence, great attention has been directed toward fully biodegradable materials that offer a feasible alternative to traditional polymeric

materials when recycling is not cost-effective or technically possible.[353] In this context, aliphatic polyesters, including poly(caprolactone) (PCL), poly(lactic) acid (PLA), poly(glycolic acid), etc., have been the subject of increasing focus because of their biodegradability and biocompatibility.[354] They are used in packaging, agriculture, medicine, and other areas. Among them, PCL has attracted a lot of attention owing to its exceptional properties, such as its biodegradability, compatibility with a wide range of other polymers, good processibility, enabling the fabrication of various structures and forms, and its relatively low cost.[299,355,356] As a result, PCL becomes an excellent candidate for biodegradable packaging,[357] controlled-release drug delivery,[358] tissue engineering[359], and other biomaterial applications.[360]

The major limitation in the applicability of PCL scaffolds is a slow degradation rate, mainly because of their hydrophobicity. The five methylene repeating units moieties of PCL cause more hydrophobicity in PCL than other polyesters.[289] The degradation of PCL starts in the amorphous region where water transport enables the hydrolysis of ester bonds leading to chain scission resulting in the formation of shorter chains, oligomers, and caproic acids.[361] Due to the hydrophobic and semi-crystalline nature, the rate of hydration and subsequent hydrolytic cleavage is low; hence, PCL-based polymer scaffolds require up to 4 years to degrade completely.[362] This slow degradation of PCL restricts its use to a limited set of applications requiring long-life materials. However, the PCL degradation rate can be regulated by embedding an enzyme within the PCL matrix when that enzyme is active for matrix hydrolysis. In addition, enzymatic degradation starts at the surface of the polymer. The lipases and esterase enzymes attach to the polymer surface in a much shorter time and start before hydrolyzing surface ester

bonds to form shorter chain polymers and oligomers.[363] The degradation rate depends on the enzyme used, polymer composition, and crystallinity and is generally complete after a few days.[364] Shi *et al.* studied PCL film degradation in a lipase buffer solution.[365] The PCL film lost 87% of its initial weight after incubation at 37 ℃ for 3 days in the presence of 45 U/ml lipase solution. Ganesh *et al*. studied lipase-embedded PCL degradation where 1.6 and 6.5 wt% *Candida antarctica* lipase B (CALB) were encapsulated in PCL films.[107] CALB-embedded films were incubated in phosphate buffer solution (20 mM, pH 7.10) with shaking (200 rpm) at 37 °C. The 6.5% CALB-loaded PCL film degraded completely within 24 hr while 1.6 wt% CALB-loaded PCL films required 17 days. So, it is established that PCL's enzymatic degradation is faster than pristine PCL hydrolysis degradation. However, a facile and economically cost-effective method to produce enzyme-loaded PCL matrix is needed.

Solution blow spinning (SBS) holds promise as a potential technique to produce a cost-effective lipase enzyme PCL matrix. In literature, a number of PCL-polymer blends were trialed in SBS process.[366–369] SBS is a fiber processing mechanism, like electrospinning, that produces polymeric micro-, submicron- and nanofibers in a continuous process, producing fibers with different properties depending on the polymers used.[326,328] In solution blowing, high-pressure gas is applied to evaporate the solvent from the polymer solution, whereas a high electric voltage is applied in electrospinning. A solution blow spinning unit with a single annular die, including a spinning nozzle with an annular gas cavity surrounding it, is illustrated in **Figure 2.1**. The detailed mechanism is explained in **Section 2.1.** SBS produces fiber morphology that is similar to

electrospinning, but at a much larger production rate and reduced cost.[193,306] The higher production rate could make SBS processes viable for producing mass fiber.

Moreover, the high surface area of SBS webs would provide a high enzyme loading, and the associated high porosity of SBS webs provides accessibility to enzyme active sites resulting in low diffusion resistance. Some works report enzyme entrapment or encapsulation into an electrospun nanofiber.[53,370] So, like electrospinning, it is expected that the solution-spinning process could also employ enzyme encapsulation. The current work is the first to investigate direct enzyme immobilization in PCL solution blown webs.

The PCL-degrading enzyme, lipase from *Candida sp.* (CALB), was selected and entrapped in PCL nanofibrous webs. This work reported the preparation of CALB enzyme-functionalized solution-blown nonwoven polycaprolactone (CALB-EFSBN-PCL) nanofibrous webs by solution blow spinning. The preparation of an enzyme-compatible PCL spinning solution using an anionic surfactant was also described. The results from studying enzyme position and distribution in fibers, immobilized enzyme activity, storage stability, and enzymatic degradability of webs are reported.

3.2. Experimental Section

3.2.1. Materials

Lipase from *Candida sp.* (CALB) Recombinant, expressed in *Aspergillus niger* was purchased from Sigma-Aldrich as a liquid enzyme product (L3170) and used as supplied. Polycaprolactone (M_n = 45000 Da and 80,000 Da), p-nitrophenyl acetate, p-nitrophenyl, Bis(2-ethylhexyl) sulfosuccinate sodium salt (AOT), chloroform, and N,N-dimethylformamide (DMF) were purchased from Sigma-Millipore (Hampton, NH, USA). Pierce Rapid Gold BCA Protein Assay Kit (Catalog Numbers A53225, A53226, and A53227) (Thermo-Fisher Scientific, Waltham, MA, USA) was used to determine the protein concentration in the produced EFSBN using the bovine serum albumin (BSA) standard provided in the kit.

3.2.2. SBN-PCL and EFSBN-PCL webs production

Solution-blown nonwoven webs were produced using the same instrument and procedure described in **Section 2.2.2**. The production process had two main steps: 1) spinning solution preparation and 2) solution blow spinning. The solvent was preloaded by adding 100 mg Bis(2-ethylhexyl) sulfosuccinate sodium salt (AOT) anionic surfactant to 100 ml of the solvent. The polycaprolactone (PCL) (M_n = 45000 Da and 80000 Da) spinning solutions were prepared by dissolving PCL pellets (1.5 g) in AOT surfactant-loaded solvents (chloroform, DMF, and toluene, 10 ml) with continuous (2 hrs) stirring (100 rpm). The liquid Lipase (CALB) from *Candida sp.* (75-1500 µl) was added to the PCL-AOT-chloroform solution and formed a water-in-oil microemulsion through vortexing (2000 rpm, 1.5 mins) and stirring (500 rpm, 3.5 mins). The solution comprising PCL, chloroform, AOT surfactant, and CALB was then subjected to solution blowing. A schematic

flow diagram of EFSBN-PCL production is presented in **Figure 3.1**. The solution-blown apparatus was the same as described in chapter 2, as illustrated in **Figure 2.1**, consisting of a single annular die with an annular gas cavity surrounding a spinning nozzle. The CALB dispersed PCL solution (5 ml, 15 w/v%) was supplied to the inner nozzle with the control of a peristaltic pump, and compressed air (207 kPa/30 psi) was delivered to the outer nozzle. The process maintained the polymer solution feed rate and air temperature at 0.5 ml/min and 40 ℃, respectively. The collector was positioned at a fixed working distance from the nozzle of 100 mm. A pressure regulator controlled the pressurized air, which varied according to the experiment. The prepared solution-blown webs were stored at room temperature (~22 ℃) or 4 ℃ until further analysis.

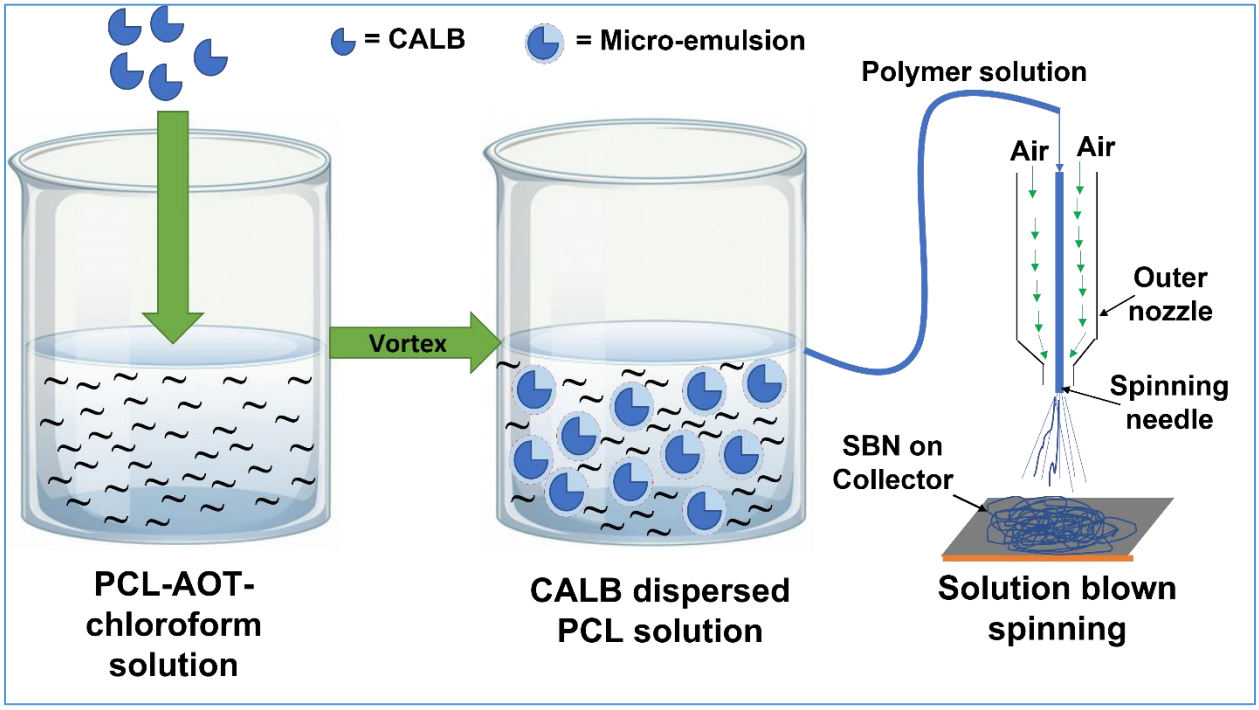

Figure 3.1: Schematic flow diagram of the preparation of SBN-PCL and EFSBN-PCL by solution-blown spinning process.

3.2.3. Protein content and immobilization yield of EFSBN-PCL

The protein (enzyme) content in EFSBN-PCL was determined by the same Lowry assay method[334] described in **Section 2.2.4**. The technique was performed using a Thermo scientific Pierce™ Rapid Gold Bicinchoninic Acid (BCA) Protein Assay Kit, which develops an orange-gold color in the presence of two molecules of BCA and one cuprous ion. The stock solution preparation was slightly different from the described solvent preparation in **Section 2.2.4**. EFSBN-PCL webs were first incubated at 40 ℃ in tris buffer (pH 8.0, 0.1 M) for 120 mins to degrade webs wholly. Then, the degraded and dissolved webs solution was used as the unknown protein stock solution in the test protocol. A series of dilutions of known concentration (50-1500 µg/ml) were prepared from BSA protein and assayed alongside the unknown protein stock solution**.** Absorbance was measured at 480 nm, and protein content for the unknown was determined based on the BSA standard curve. The percent protein content in an EFSBN sample was calculated according to the following formula:

$$\text{Protein content } (\%) = \frac{\text{measured protein,}\frac{\text{mg}}{\text{ml}} * \text{redissolved volume,ml} * 100}{\text{weight of redissolved EFSBN,mg}} \quad \text{.....(3.1)}$$

The immobilization yield of EFSBN-PCL webs was calculated from the ratio of the measured amount of protein content (amount of protein detected in the final webs) in the EFSBN-PCL to the theoretical protein loading (amount of protein added to the spinning solution) in the web. The immobilization yield percentage is calculated using the following formula:

$$\text{Immobilization yield } (\%) = \frac{\text{Measured protein content in EFSBN} * 100}{\text{Theoretical protein in the spinning solution}} \quad \text{.....(3.2)}$$

3.2.4. Lipase assay of immobilized CALB enzymes

The lipase activity of immobilized CALB was measured using a p-nitrophenyl acetate substrate-based assay method following a modification of the determination of carbonic anhydrase activity reported in previous work by Shen *et al*.[36] The protocol was adapted for microcentrifuge tube incubation. In the EFSBN-PCL web dissolution step, a suitable amount (approximately 10-15 mg, exactly weighed) of EFSBN-PCL web was placed into a 1.5 ml microcentrifuge vial and incubated with 1.20 ml Tris HCl buffer (100 mM, pH 8.0) for 120 mins at 40 ℃ during which time EFSBN-PCL fibers were wholly dissolved to produce a stock solution. If enzyme is not present in the webs to hydrolyze the polymer, SBN-PCL does not dissolve at these conditions. The p-nitrophenyl acetate substrate was first dissolved in ethanol to prepare a 100 mM substrate stock solution and kept at -4 ℃ for further assay measurements. Before each set of an assay, 100 mM p-NPAc was diluted with deionized water to a final concentration of 8 mM. In the incubation step, 75 µl of EFSBN-PCL redissolved stock solution and 400 µl Tris HCl buffer (100 mM, pH 8.0) were mixed and preincubated for 5 mins. For free CALB activity, the free CALB liquid enzyme sample was first diluted (10,000 times) in 100 mM Tris buffer (pH 8.0); then, 475 µl of the dilution was added to a 1500 µl microcentrifuge tube and pre-incubated for 5 mins at 45 ℃. Then, 25 µl 8 mM p-NPAc substrate solution was added to the free CALB and immobilized CALB solutions and mixed thoroughly by gentle manual mixing. The final solution (total volume 500 µl) was incubated for 30 minutes at 45 ℃. Active CALB catalyzes the hydrolysis of p-NPAc. After incubation, the reaction was stopped by placing microcentrifuge tubes into ice water. Absorbance measurements of the assay solutions determines the concentration of p-nitrophenol (p-NP), the yellow-colored product of p-NPAc hydrolysis, with an absorbance maximum of 405 nm. Three replicates of each

sample were measured. The blank control was made by maintaining the same procedure except adding an equivalent amount of SBN-PCL (neat PCL web) instead of EFSBN-PCL. All solutions were kept in the same conditions throughout the assay process. A p-NP standard curve was created by plotting absorbance versus known concentrations of p-NP (5-50 µg/ml). The micromoles of p-NP equivalents liberated were determined by using the standard curve. One unit (U) of lipase activity is defined as the amount of enzyme that catalyzes the release of 1.0 µmole of p-NP per min from the p-NPAc substrate at 40 ℃ in the presence of 100 mM pH 8.0 Tris-HCl buffer.

The lipase assay of the free liquid enzyme upon dilution was calculated based on the following equations:

$$\text{U/ml} = \frac{\mu\text{mole p}-\text{NP equivalent release} * \text{volume of total assay,ml}}{\text{Time}_{,\text{min}} * \text{volume of enzyme used,ml}} * \text{dilution} \quad \ldots\ldots\ldots\ldots\ldots\ldots\ldots\ldots\ldots\ldots\ldots\ldots (3.3)$$

$$\text{U/mg}_{\text{protein}} = \frac{\text{U/ml}}{\text{mg of}\frac{\text{protein}}{\text{ml}}\text{of liquid CALB}} \quad \ldots\ldots\ldots\ldots\ldots\ldots\ldots\ldots\ldots\ldots\ldots\ldots\ldots\ldots\ldots\ldots\ldots\ldots\ldots\ldots\ldots\ldots (3.4)$$

The lipase assay of immobilized CALB per mg of the EFSBN-PCL webs protein,

$$\text{U/mg}_{\text{EFSBNs protein}} = \frac{\mu\text{mole of p}-\text{NP equivalent release} * \text{volume of total assay,ml}}{\text{Time,min} * \text{EFSBN protein used in assay,mg} * \text{volume of enzyme solution,ml}} \quad \ldots\ldots\ldots\ldots (3.5)$$

The relative activity of immobilized CALB was calculated as the percentage of the free lipase activity and calculated as follows:

$$\text{Relative activity (\%)} = \frac{\text{Activity of immobilized lipase}}{\text{Activity of free lipase}} * 100 \quad \ldots\ldots\ldots\ldots\ldots\ldots\ldots\ldots\ldots\ldots\ldots\ldots\ldots\ldots\ldots\ldots\ldots\ldots\ldots\ldots (3.6)$$

3.2.5. FTIR spectroscopy analysis of SBN-PCL and EFSBN-PCL

The presence of enzymes in the EFSBN-PCL was characterized by FTIR Spectroscopy (iS50, ThermoFisher Scientific, USA), with a build-in diamond crystal Attenuated Total Reflection sampling head. Spectra were collected for dried SBN-PCL webs, and EFSBN-PCL webs at room

temperature from 500 to 4000 cm^{-1} with 64 scans and 4 cm^{-1} resolution. All specimens were stored in a desiccator for two days before measurement to minimize moisture in the samples.

3.2.6. Enzyme distribution in EFSBN-PCL by confocal microscopy

CALB was conjugated to fluorescein isothiocyanate (FITC) following the "large scale conjugation" procedure described in the Sigma Fluoro-tag-FITC conjugation kit. The FITC-tag-CALB has two absorbances, at 280 nm and 495 nm. The eluent fractions containing these two absorbances were collected. Sephadex G-25M column and phosphate buffered saline solution was used as the elution solvent. The FITC-tag- CALB was dispersed in PCL-AOT-chloroform solution and subjected to the same solution-blowing conditions as EFSBN-PCL webs. The FITC- CALB entrapped EFSBN-PCL webs were placed on a glass slide and mounted under a No. 1.5 cover glass held up by modeling clay spacers to prevent sample compression. The 0.32 % (w/w) FITC-tag-CALB EFSBN-PCL and 0.50 % (w/w) FITC-tagged-CALB EFSBN-PCL webs were imaged by a Zeiss LSM 880 laser scanning confocal microscope using a 488 nm excitation laser to detect the FITC signal. The z-series images were collected using a 20x dry objective with NA=0.8 and 2 µm intervals. The z-series were further processed using Imaris 9.9 software (Bitplane, Zurich, Switzerland) to remove the background signal. Results show the location of CALB in EFSBN-PCL webs.

3.2.7. Surface analysis using ToF-SIMS

The surface analysis of SBN-PCL and EFSBN-PCL was done with the same instrument and procedure described in **Section 2.2.8**. The surface analysis of EFSBN-PCL was performed using a TOF SIMS V (ION TOF, Inc. Chestnut Ridge, NY) instrument equipped with a Bi_n^{m+} (n = 1-5, m = 1,

2) liquid metal ion gun, Cs^+ sputtering gun, and electron flood gun for charge compensation. Both the Bi and Cs ion columns were oriented at 45° with respect to the sample surface normal. The analysis chamber pressure was maintained below 5.0 x 10^{-9} mbar to avoid contamination of the surfaces to be analyzed. In the high lateral resolution mass spectral images acquired in this study, a Burst Alignment setting of 25 keV Bi^{3+} ion beam was used to raster in a pixel region of 256 by 256 pixels. The negative secondary ion mass spectra obtained were calibrated using C^-, O^-, OH^-, Cn^-, respectively. The positive secondary ion mass spectra were calibrated using C^+, $C_2H_3^+$, $C_3H_5^+$, $C_4H_7^+$.

3.2.8. EFSBN-PCL degradation analysis

Degradation studies of EFSBN-PCL webs were carried out under a batch process. SBN-PCL and EFSBN-PCL webs (~15 mg) were placed in 1500 µl microcentrifuge tubes containing 1000 µl Tris-HCl buffer solution (100 mM, pH 8.0). Incubations were performed with manual shaking (every 5 mins intervals) in a dry bath incubator (Isotemp, Fisher Scientific) at 40 ℃. All tubes were removed from the incubator every 15 mins to take a visual picture after which they were replaced in the incubator. The whole incubation process time was 60 mins. Degradation studies of EFSBN-PCL webs at room temperature incubation were also observed. The webs (~15 mg) were immersed in microcentrifuge tubes containing the same tris buffer (1000 µl). The microcentrifuge tubes were then placed in tube holders at room temperature (~22 ℃) for 24 hrs, and a picture was taken for visual comparison. For morphological analysis of degraded webs, fibers were removed from microcentrifuge tubes after 30 mins incubation, dried, and stored for SEM analysis.

3.2.9. Morphological analysis of SBN-PCL, EFSBN-PCL, and degraded EFSBN-PCL using SEM

Morphologies of SBN-PCL and EFSBN-PCL samples were investigated using field-emission scanning electron microscopy (FESEM) (FEI Verios 460L, USA) with an accelerating voltage of 500 V and a current of 2 pA. The morphology of EFSBN-PCL degradation with time was also observed using this instrument.

3.2.10. Storage stability of free and immobilized CALB-EFSBN-PCL

The storage stability of immobilized CALB and liquid-free CALB (Sigma) was evaluated by the modified method of Pereira *et al* [104]. The EFSBN-PCL webs were kept in a zip bag, stored at room temperature (~22 °C), and refrigerated (4 ℃). The as-supplied free liquid CALB and free CALB diluted (0.1 µl/ml) in tris buffer (0.1 M, pH 8.0) were also stored at room temperature (~22 °C). Samples were stored for 0-120 days, and lipase activity was determined as described in **Section 3.2.4**. Residual activity was the ratio of measured activity at a time point to the initial activity at time zero, expressed as a percentage (Eqn. 3.7).

$$\text{Relative residual activity } (\%) = \frac{\text{Measured activity of stored sample}}{\text{Initial sample activity}} * 100\% \ldots\ldots\ldots\ldots . (3.7)$$

3.3. Results and Discussion

3.3.1. SBN-PCL and EFSBN-PCL preparation by solution spinning process

The first step in selecting solution blowing process parameters for producing EFSBN-PCL webs was to investigate the effects of solvents on SBN-PCL webs formation. For this purpose, three solvents, chloroform, DMF, and toluene, were used to form a polymer solution and trialed by solution-blown spinning to choose the most appropriate solvent. All solvents completely dissolved PCL pellets and SBN-PCL samples were produced from those solutions, presented in **Figure 3.2**. The solution blown spinning process parameters were kept constant throughout the SBN-PCL and EFSBN-PCL production, as follows: polymer concentration 15 (w/v)%, solution throughput 0.5 ml/min, die to collector distance (DCD) 100 mm, air pressure 207 kPa (30 psi), and air temperature 40 ℃. PCL-toluene polymer solution formed very few fibers with many beads (**Figure 3.2 A**). The PCL polymer solution using DMF and chloroform solvents formed many fibers without any bead formation (**Figure 3.2 B** and **C**). Cabrera-Padilla *et al.* reported lipase from *Candida rugosa* showed 55% retained activity after 1 hr of contact in 100% chloroform solvent.[258] The total solution spinning time in this work was approximately 15 mins (solution vortexing 1.5 mins, stirring 3.5 mins, and spinning process 10 mins), therefore CALB was expected to retain its active structure in PCL-AOT-chloroform microemulsions within this time. For this reason, chloroform solvent was used in this work to produce the SBN-PCL and EFSBN-PCL webs.

For EFSBN-PCL production, liquid CALB enzyme solution (0.05 -1.0 µl CALB/ml polymer solution) was dispersed in AOT surfactant loaded (1 mg AOT/ml solvent) PCL solution (15 w/v%). The solution spinning process conditions for the enzyme-loaded polymer solution and the polymer-

only solution were the same. However, fiber formation depended on the water phase in the water-in-oil microemulsion polymer solution. For 0.05-0.5 µl CALB/ml polymer solution, EFSBN-PCL webs were produced perfectly in the solution spinning process. For 0.75 µl CALB/ml polymer solution, along with fiber production, a viscous mass accumulated beneath the spinning needle because the higher amount of water phase caused microemulsion instability (**Figure 3.2 D**). Also, water is a challenging solvent for solution spinning because of its comparatively low vapor pressure at the spinning conditions. Therefore, when too much water was present, the spinning process could not evaporate all the solvent quickly enough, resulting in the remaining viscous mass. With even higher enzyme loading (1.0 µl CALB/ml polymer solution), the spinning solution was not able to form fiber because of even more instability of the microemulsion due to the higher amount of water present. A PCL sample of 80 kDa molecular weight was also trialed by solution blown spinning, but it clogged the needle because a higher degree of polymerization (DP) causes more polymer chain entanglement.[371] The optimum conditions for solution blowing were determined to be 0.5 ml/min solution throughput, 207 kPa air pressure, 40 ℃ air temperature, 45 kDa molecular weight, 15 (w/v)% polymer solution, and 100 mm DCD, which were used to produce both SBN and EFSBN webs.

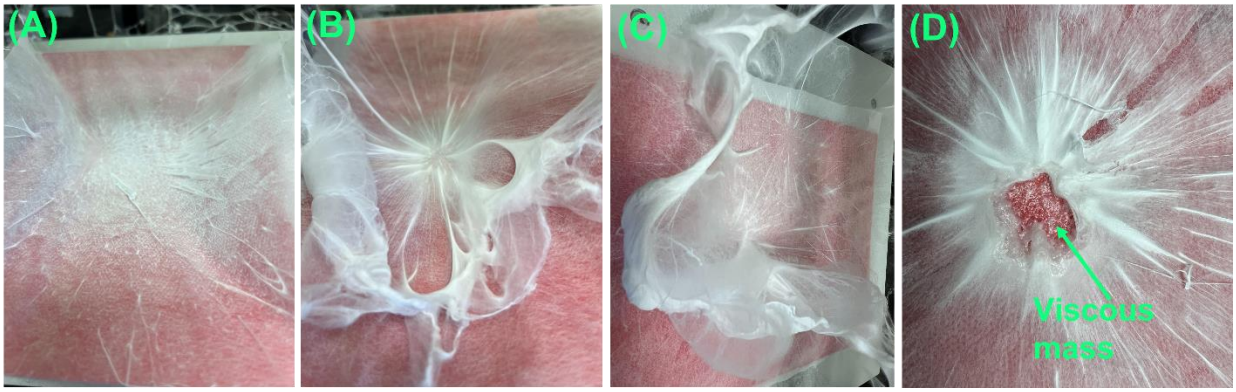

Figure 3.2: SBN-PCL and EFSBN-PCL webs on collectors (A) SBN-PCL produced by using toluene solvent, (B) SBN-PCL produced by using DMF solvent, (C) SBN-PCL produced by using chloroform solvent and (D) 3.0% CALB-EFSBN-PCL produced using chloroform solvent.

3.3.2. FTIR analysis of SBN-PCL and EFSBN-PCL

The solution blown nanofibers (SBN-PCL and EFSBN-PCL) were characterized using FTIR to confirm the chemical constituents of the nanofibrous webs. The infrared absorption peaks of SBN-PCL and EFSBN-PCL webs are presented in **Figure 3.3**. The FTIR spectra of PCL showed the main peak at 1725 cm^{-1} attributed to C=O stretching.[372] PCL also exhibits hydrocarbon peaks, similar to PEO molecules, including strong peaks at 2700-3000 cm^{-1} for symmetric and asymmetric stretching of -CH_2 groups; two strong splitting peaks at 1466 cm^{-1} and 1413 cm^{-1} for CH_2 scissoring (bending mode); two strong splitting peaks at 1359 cm^{-1} and 1341 cm^{-1} for CH_2 wagging; and, two splitting peaks at 1279 cm^{-1} and 1241 cm^{-1} for CH_2 twisting.[336,373,374] The -C-O-C- stretching vibrations yield peaks at three wavenumbers 1042 cm^{-1}, 1107 cm^{-1}, and 1233 cm^{-1} which were present in the samples.[372] Additionally, the double peaks at 1160 cm^{-1} and 1290 cm^{-1} are assigned to C-O and C-C stretching in the amorphous and crystalline phases,[375] and the presence of the strong band at 1290 cm^{-1} (of C-C stretching), indicates crystallinity in nanofibers.

The characteristic peaks of amide I and amide II protein bonds are observed at 1650 cm^{-1} and 1550 cm^{-1}, respectively.[339] The N-H stretching peak of amide A overlaps with OH stretching at 3100-3500 cm^{-1} where the OH stretching peak could come from bound water in an enzyme.[231,340] The considerable amount of water molecules might be present in nanofibrous that keep enzyme molecules as water-in-oil microemulsions. Some water molecules may be entrapped inside individual fibers of the nanofibrous webs together with enzymes as a result of using a water-in-oil microemulsion spinning solution. These presences of water, enzyme binding water, and protein OH groups contribute to the broad OH stretching peak. Dry enzyme-free webs do not show peaks in this region. Likewise, the amides I and II show very small peaks because of the low protease content (1.3% in the EFSBN-PCL webs). However, the amide I peak intensity increases when a background correction from SBN-PCL webs is done.

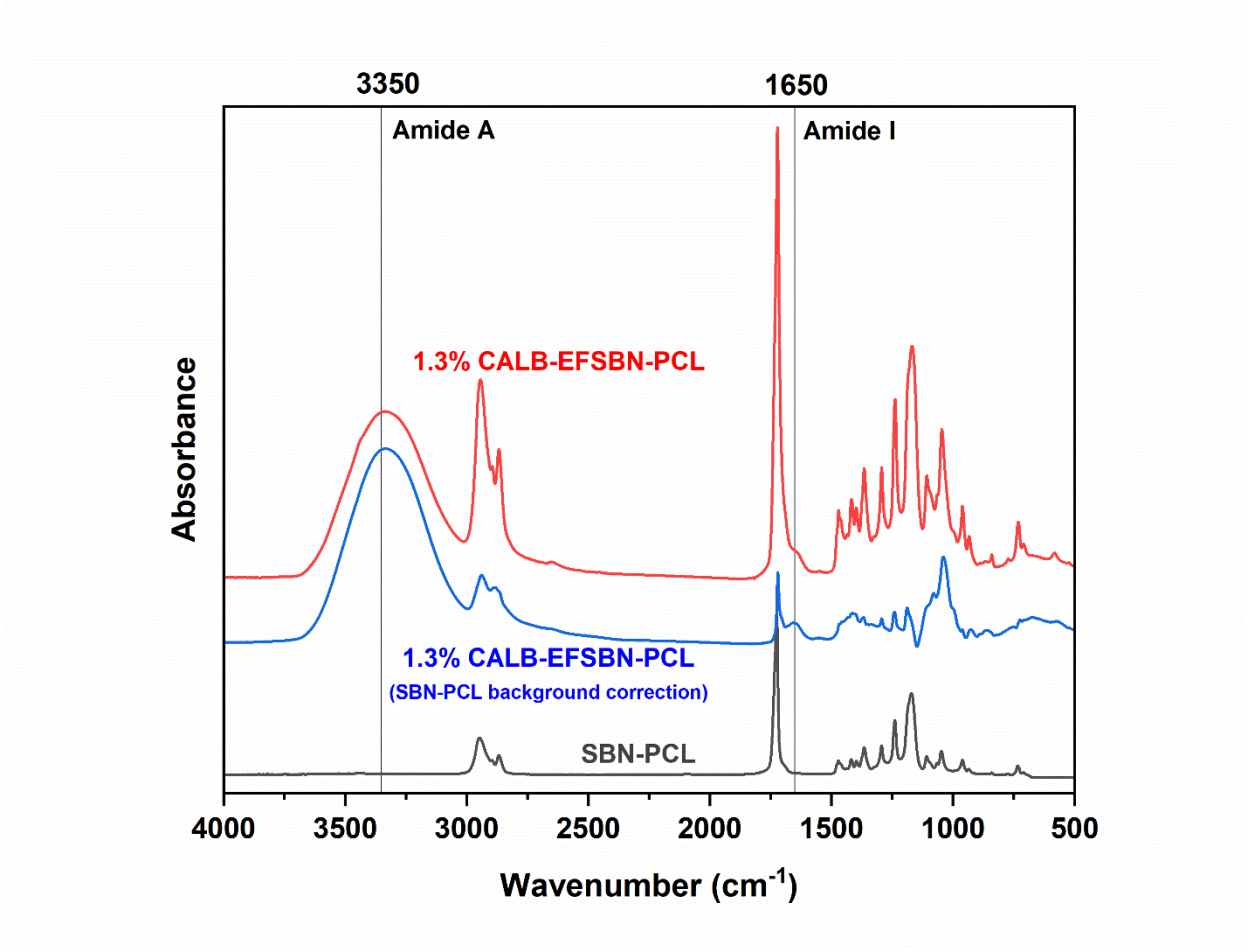

Figure 3.3: FTIR spectrum of SBN-PCL and CALB-EFSBN-PCL webs with normal air background correction (red) and SBN-PCL webs background correction (blue).

3.3.3. Enzyme loading and immobilization yield of EFSBN-PCL

The amount of enzyme loading accommodated by a degradable packaging material is an important parameter for determining degradation time. A range of different CALB (0.53 to 1.92 wt%) loaded EFSBN-PCL webs were prepared. Immobilization yields and corresponding retained protein content in solid webs at different enzyme loading levels in the polymer spinning solutions is shown in **Figure 3.4** measurement of immobilization yield revealed how much enzyme added to the polymer solution was retained after solution blowing. Protein content means the amount

of protein detected in the final webs, and protein loading means the amount of protein initially added to the spinning solution before solution blowing. At low enzyme loading, immobilization yields had a higher value which decreased with increasing CALB loading in the spinning solution. This indicates that at low concentration, it was possible to form a stable water-in-oil microemulsion that could entrap most of the enzyme in the PCL nanofibers. However, the immobilization yield was only around 20% for 8.94 (wt%) protein loading in the spinning solution, which could be caused by instability of the microemulsion (due to high water phase) or inability to dry all solvent during the solution blown process. Additionally, there may have been an artifact error in the Rapid BCA protein determination technique because the control sample had no PCL molecules, whereas the protein content sample contained some degraded PCL. Another explanation for the less than 100% immobilization yields may be that a certain portion of the enzyme is aerosolized and blown away with the high-pressure air. High enzyme loading might lead to less interaction between polymer and enzymes or a decrease in the space available for entrapment, leading to increased enzyme loss to the pressurized airflow. Further work would be needed to clarify the specific cause(s) for the decrease in immobilization yield as enzyme loading increases.

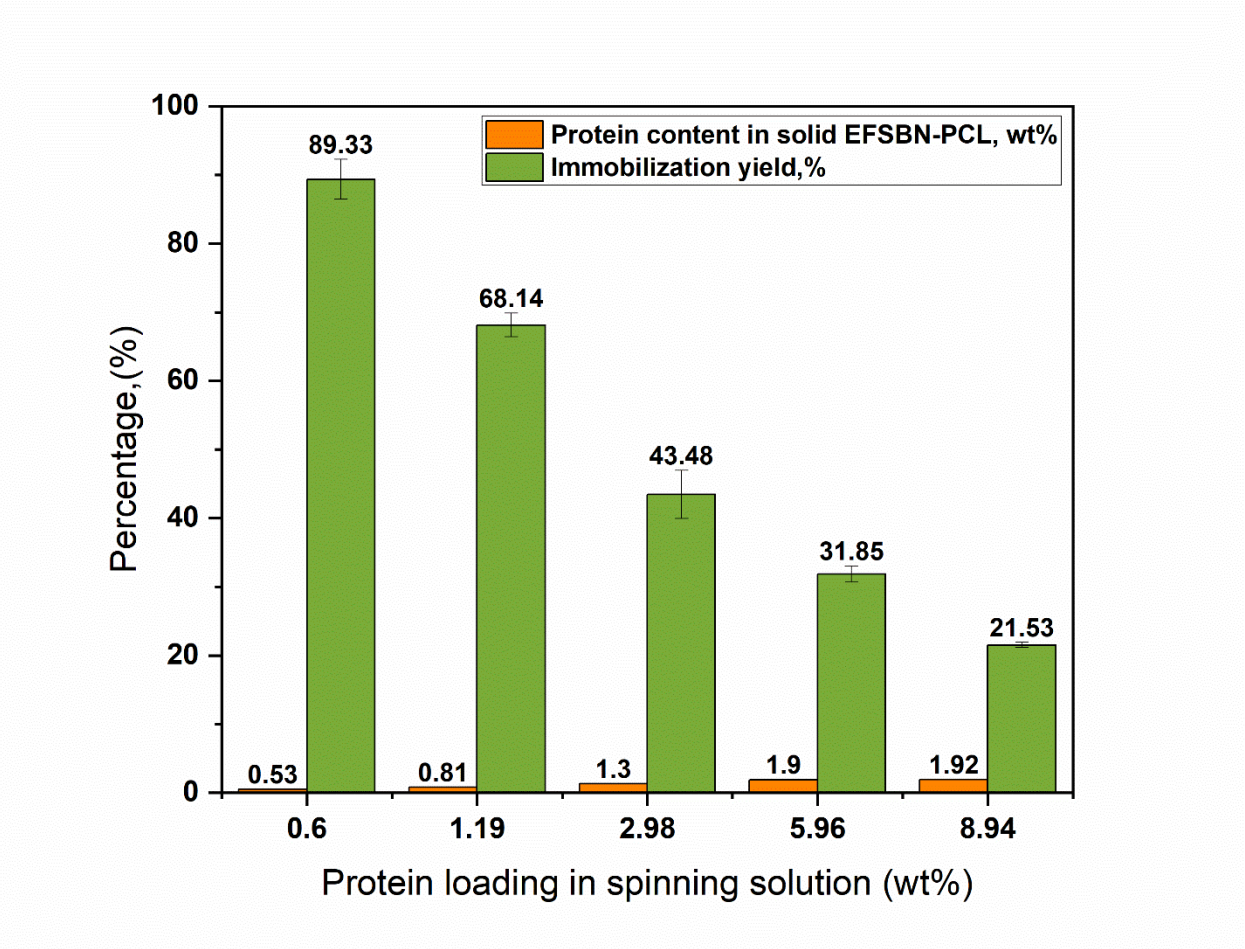

Figure 3.4: Immobilization yield of EFSBN-PCL and retained protein in the solid EFSBN-PCL webs with different enzyme loading in the spinning solution.

3.3.4. CALB-EFSBN-PCL catalytic activity

Immobilized enzyme activity depends on immobilization methods, processing conditions, carrier materials type, and the supporting material's final form. CALB-loaded EFSBN-PCL webs are entirely degradable in buffer (Tris-HCl buffer, 100 mM, pH 8.0) incubation at 40 ℃ which releases CALB into the buffer as a free enzyme. The released enzyme behaves like a free enzyme responding to lipase activity analysis. The activity of the released CALB was calculated based on the protein content detected in the solid webs. Then, the relative activity of enzyme

functionalized webs was measured as the activity of degraded EFSBN-PCL webs compared to the activity of an equivalent amount of free enzyme content, expressed as a percentage. A sample calculation of lipase activity of free CALB and released EFSBN CALB are shown in supplementary data at Appendices (**A 3.1**). The lipase activities of CALB-EFSBN-PCL webs relative to their measured protein content are presented in **Figure 3.5**. The EFSBN-PCL showed around 50% retained catalytic activity, indicating that the enzyme delivered through the solution blowing nozzle was still active in the final solid web products. The retained catalytic activity also indicated that immobilized CALB retained its native structure in PCL-chloroform solution or was able to recover its native functional structure after degrading webs in a buffer. This finding of a high level of retained relative activity reveals that the solution-blown spinning process is an excellent technique for entrapping lipase into a PCL carrier from a PCL-organic solvent solution.

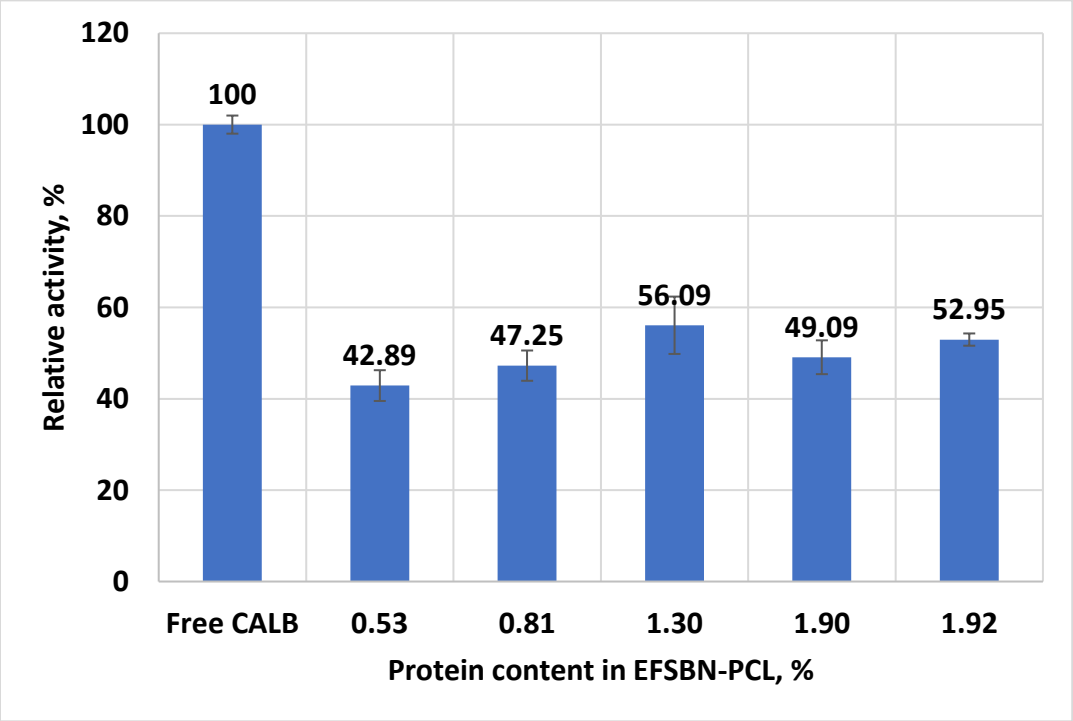

Figure 3.5: Relative catalytic activity of CALB-EFSBN-PCL webs with varying protein content in the solid webs.

3.3.5. Enzyme distribution in EFSBN by confocal microscopy

To determine entrapped CALB distribution in EFSBN-PCL webs, CALB was labeled with fluorescein isothiocyanate (FITC), and the resulting FITC-tagged CALB was entrapped in EFSBN-PCL webs by solution blow spinning. FITC-tagged-CALB-EFSBN-PCL webs were analyzed by laser scanning confocal microscopy. The resulting images of webs with 0.32 and 0.50 (w/w)% entrapped FITC-labeled CALB are displayed in **Figure 3.6** and **Figure 3.7**, respectively. These images illustrate that CALB distribution in EFSBN-PCL was not homogeneous. The microscopic appearance is consistent with aqueous liquid enzyme solution forming a water-in-oil microemulsion in PCL-AOT-chloroform solution. After solution blowing, enzymes remained as aggregates in the dried PCL webs, like in the solution phase. Although the appearance is not homogeneous, this nevertheless indicates that solution blowing of enzyme-loaded PCL solutions is an excellent entrapment process for enzymes.

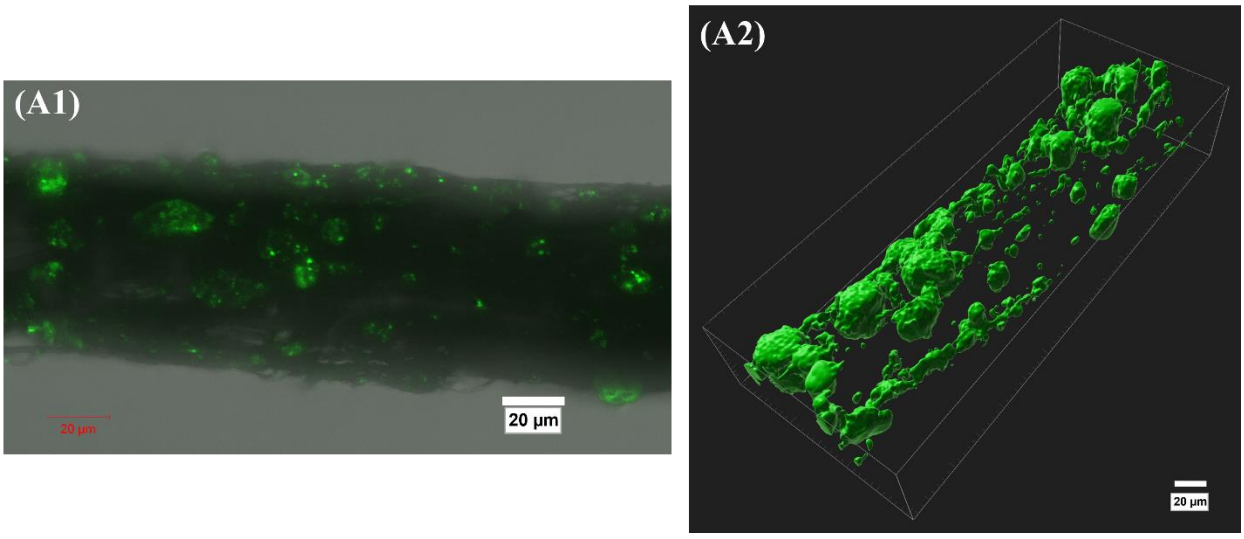

Figure 3.6: Laser scanning confocal microscopy images of the distribution of FITC-tagged-CALB (0.32 w/w%) entrapped EFSBN-PCL webs: (A1) raw image and (A2) z-series image. Green represents the quantity of enzyme distribution along the fiber.

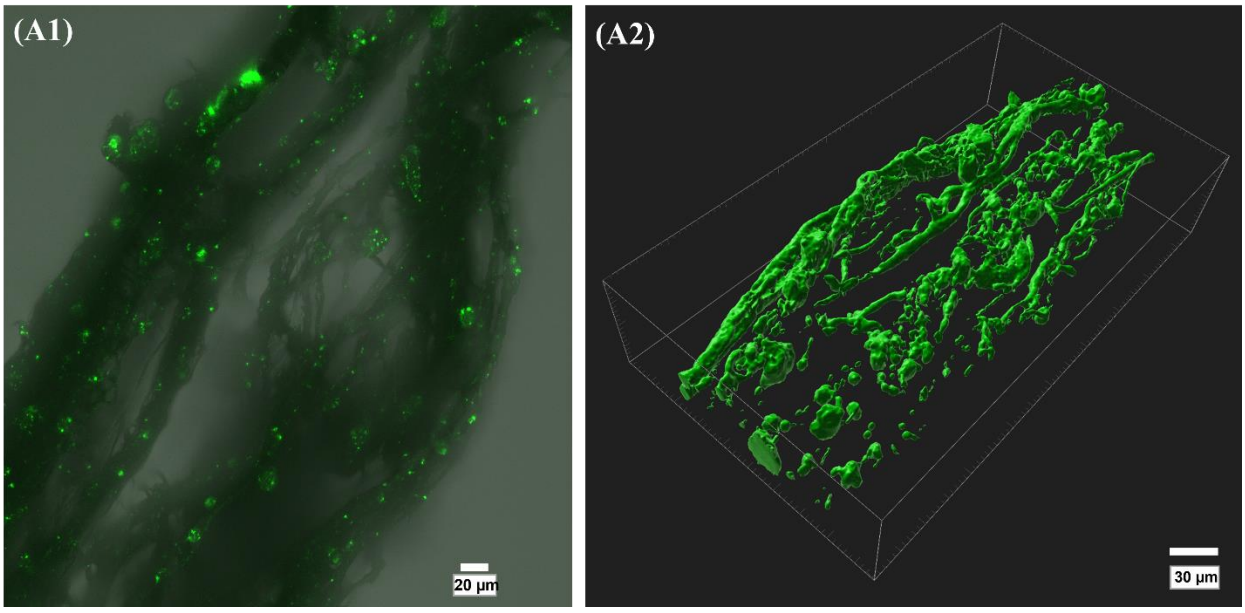

Figure 3.7: Laser scanning confocal microscopy images of the distribution of FITC-tagged-CALB (0.50 w/w%) entrapped EFSBN-PCL webs: (A1) raw image and (A2) z-series image. Green represents the quantity of enzyme distribution along the fiber.

3.3.6. Enzyme position and distribution analysis in EFSBN by ToF-SIMS

The ToF-SIMS spectra and distribution maps revealed the distribution and position of the immobilized lipase. The high lateral resolution mass spectral maps of SBN-PCL webs and 1.30% CALB-EFSBN-PCL webs are shown in **Figure 3.8** and **Figure 3.9**, respectively. The negative ions (CN^- and CNO^-) and total ions ratio of these three samples are shown in **Figure 3.10**. Overall, EFSBN-PCL did not show significant nitrogen peaks intensity that indicated the EFSBN-PCL nanofibers did not have enough protein molecules on the surface for detection. ToF-SIMS is limited to detecting ion fragments within 1-2 nm depth of the surface of a specimen. So, for low enzyme-loaded EFSBN-PCL webs, the ToF-SIMS results indicate that the amount of enzyme on the surface is minimal, and most enzymes are located inside the nanofibers.

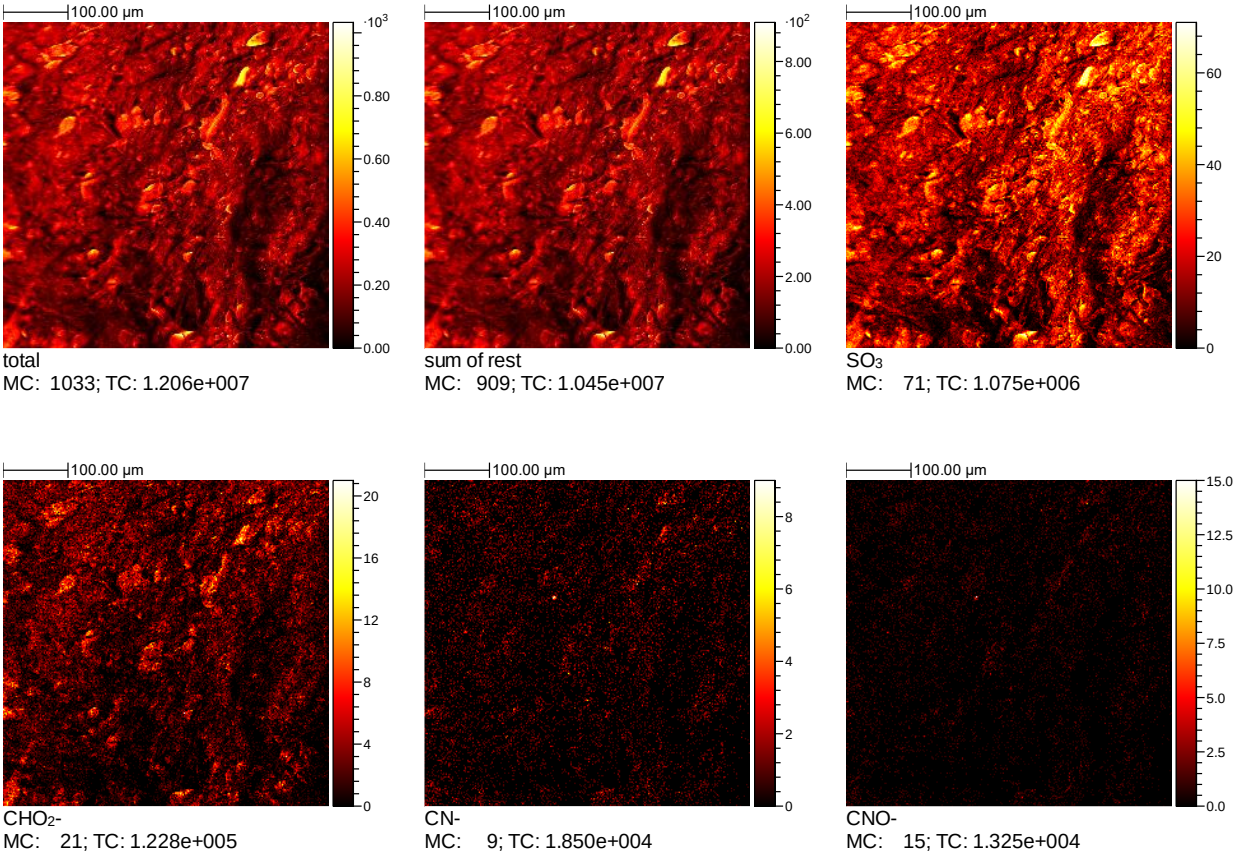

Figure 3.8: ToF-SIMS high lateral resolution mass spectral maps (analysis area 100x100 µm^2) of SBN-PCL webs.

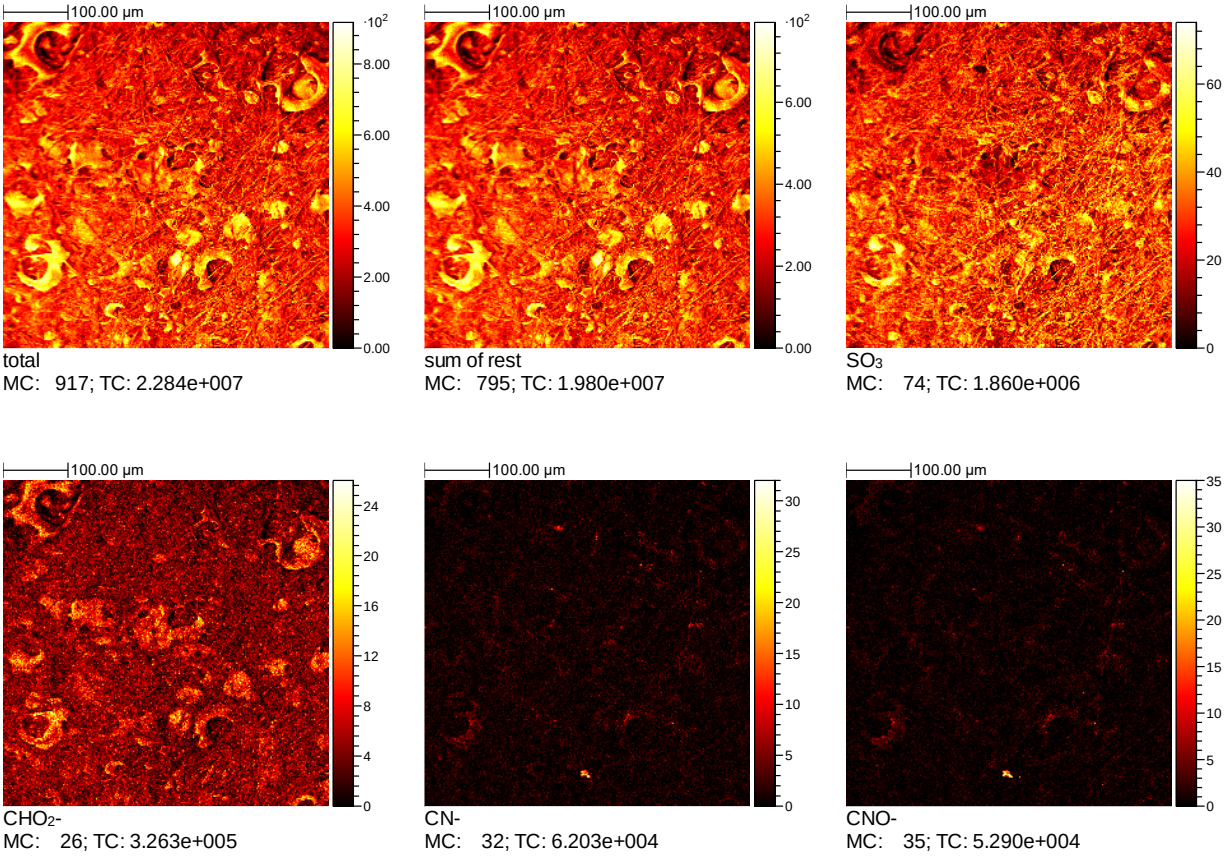

Figure 3.9: ToF-SIMS high lateral resolution mass spectral maps (analysis area 100x100 µm^2) of 0.53% CALB-EFSBN-PCL webs.

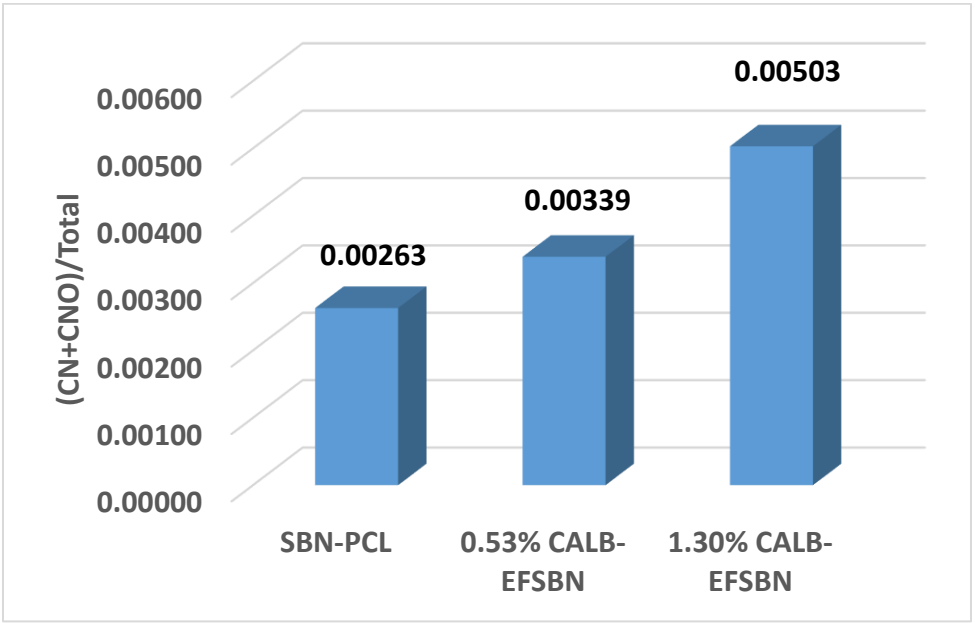

Figure 3.10: (CN+CNO)/total ion count graph of SBN-PCL, 0.53% CALB-EFSBN-PCL and 1.30% CALB-EFSBN-PCL webs.

3.3.7. Enzymatic degradation of EFSBN-PCL

PCL is an excellent candidate for controlled release and other applications, but the slow degradability of PCL limits its use for systems that require shorter lifetimes.[107] Uniform placement of CALB enzyme into PCL carriers and fabrication approaches that create a higher surface area also directly increase the enzymatic degradability of PCL. CALB entrapment into solution-blown PCL nanofibrous nonwoven webs meets the requirement for higher surface area and enzyme distribution throughout the webs. As a result, fast enzymatic degradations of EFSBN-PCL were observed for all loaded webs. The visual degradation test results are presented in **Figure 3.11**. EFSBN-PCL webs were incubated in tris buffer solution (100 mM, 8.0 pH) with handshaking each five mins intervals at 40 ℃. **Figure 3.11** shows that 1.90 and 1.92 wt% CALB-loaded EFSBN-PCL webs degraded so rapidly that by 15 mins these webs were completely degraded. Even the lowest CALB loaded (0.53%) EFSBN-PCL degraded much faster (within 60 mins) than reported for 1.3% CALB embedded PCL films that required 24 hrs to achieve complete degradation.[107]

Packaging materials waste disposal is a massive problem today. EFSBN-PCL would be an excellent addition to develop degradable packaging materials that can be sustainably disposed after use. For potential disposal by soil burial, it is necessary to degrade packaging materials at ambient conditions. For this purpose, EFSBN-PCL webs were immersed in tris buffer (100 mM, 8.0 pH) and kept at room temperature to investigate degradation in the ambient environment. **Figure 3.12** shows the enzymatic degradation of EFSBN-PCL webs at room temperature. Both high and low-loaded CALB- EFSBN-PCL webs were degraded within 24 hrs, which implies EFSBN-PCL could be used as degradable packaging materials or for various agricultural applications, disposed of in soil after use, and degraded rapidly in naturally wet soil or by wetting the soil to trigger degradation.

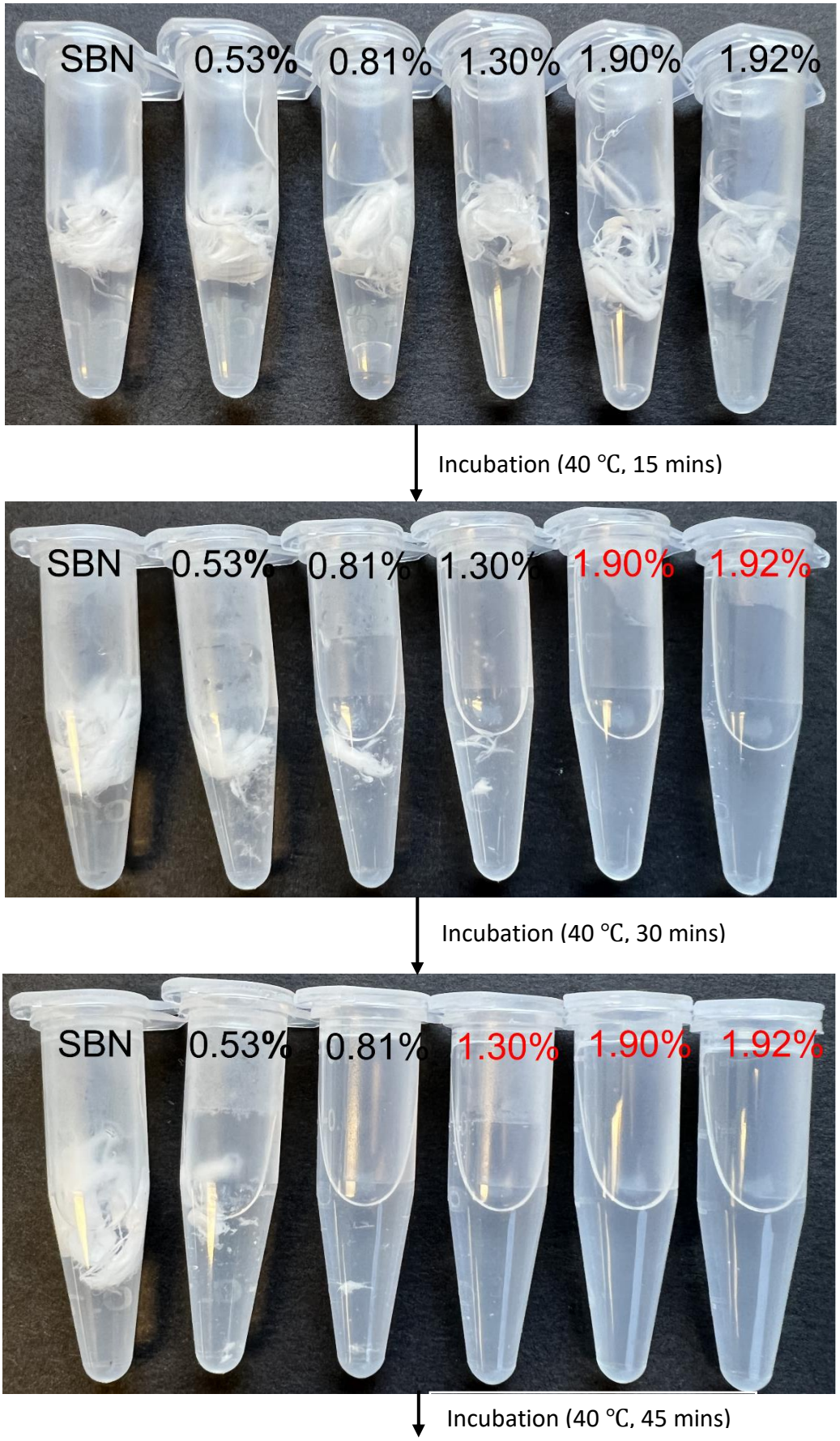
SBN
0.53%
0.81%
1.30%
1.90%
1.92%
Incubation (40 ℃, 15 mins)
SBN
0.53%
0.81%
1.30%
1.90%
1.92%
Incubation (40 ℃, 30 mins)
SBN
0.53%
0.81%
1.30%
1.90%
1.92%
Incubation (40 ℃, 45 mins)

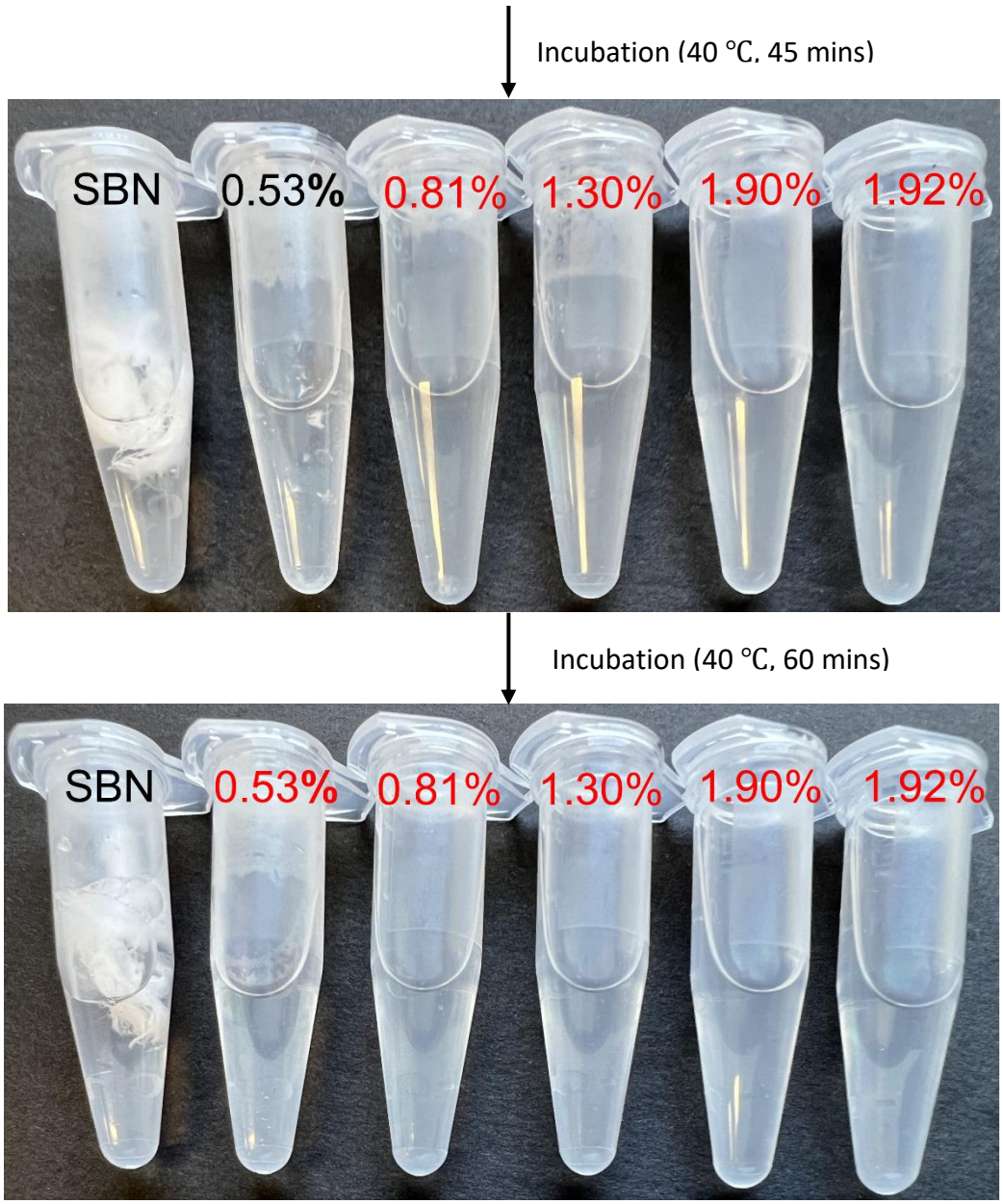

Figure 3.11: Enzymatic degradation of EFSBN-PCL in tris buffer (100 mM, 8.0 pH) incubation at 40 ℃.

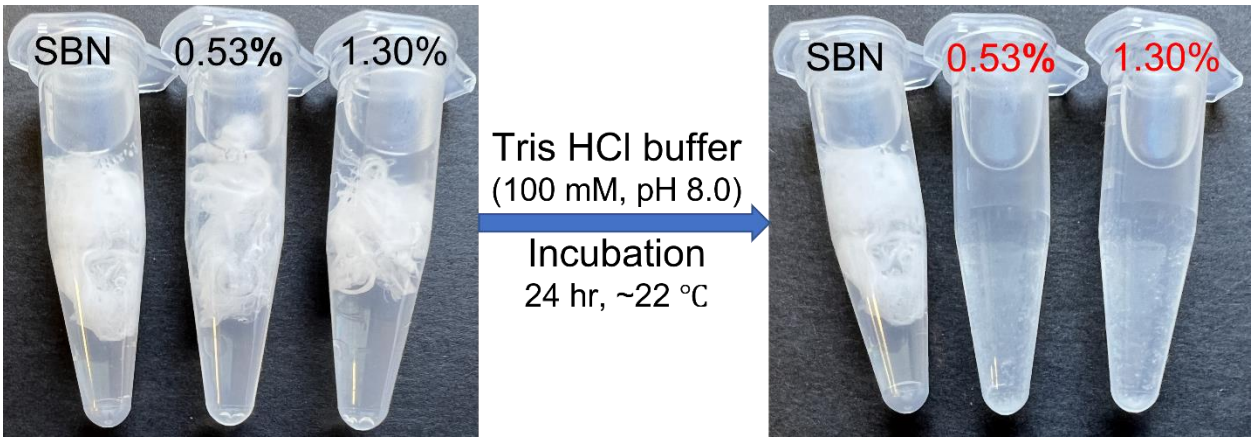

Figure 3.12: SBN-PCL and (0.53%- and 1.30%-) CALB-EFSBN-PCL degradation in a Tris-HCl buffer (pH 8.0, 100 mM) at ambient condition.

3.3.8. Morphology analysis of EFSBN-PCL and partially degraded EFSBN-PCL

The morphology of SBN-PPCL and EFSBN-PCL webs prepared with different CALB loading were characterized by scanning electron microscopy and presented in **Figure 3.13**. The morphology is characteristic of a nonwoven structure with a distribution of micro- and nanofibers forming the web. The surface diameter and web morphology appearance changed as enzyme loading increased. Higher enzyme-loaded webs had comparatively higher diameters and larger standard deviations, revealing that SBN-PCL web fibers were more uniform than EFSBN-PCL webs. In web morphology, higher enzyme loading caused clustering between fibers. Whereas SBN-PCL and 0.53 wt% CALB-EFSBN-PCL webs exhibited almost no clustering between nanofibers, more clustering was observed with increasing protein content in the webs. The irregularities of fiber diameter and appearance of more clustering probably result from the changing amount of aqueous phase in the water-in-oil microemulsion of PCL-AOT-chloroform-CALB compatible spinning solution that increases the solution's resistance to being stretched. Less stretching leads

to larger fiber diameters and slower solvent evaporation, which leads to “stickier” fibers and adhesion between fibers that causes clustering.

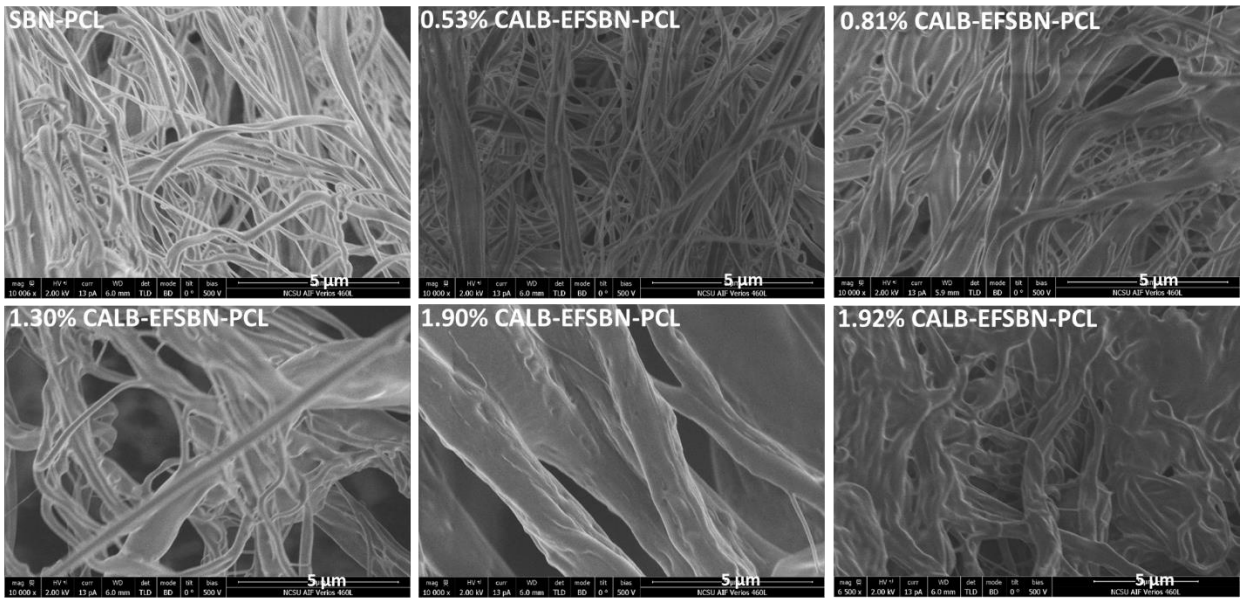

Figure 3.13: SEM micrograph (10000x magnification) of SBN-PCL webs and CALB-EFSBN-PCL webs with varying enzyme loading.

SEM micrographs **Figure 3.14** show the partially degraded EFSBN-PCL nanofiber webs that gives insight to the degradation mechanism. CALB entrapped inside PCL fibers hydrolyzes PCL nanofibers from the inside out in the presence of water, which may result in pore formation. However, pore structures were not observed in partially degraded EFSBN-PCL because CALB distribution in EFSBN-PCL caused uniform degradation of nanofibers. The SEM micrographs also imply that thinner nanofibers degraded quicker, and this phenomenon occurred throughout the whole web, leading to an overall homogeneous degradation. In fact, CALB released from the degradation of thinner nanofibers could then be available to help degrade larger fibers from the outside in. This could be a useful strategy in developing products with controlled degradation

time, by deliberately varying the fiber sizes, or by combining fibers of different sizes with different levels of enzyme loading, including combinations of fibers with and without enzyme.

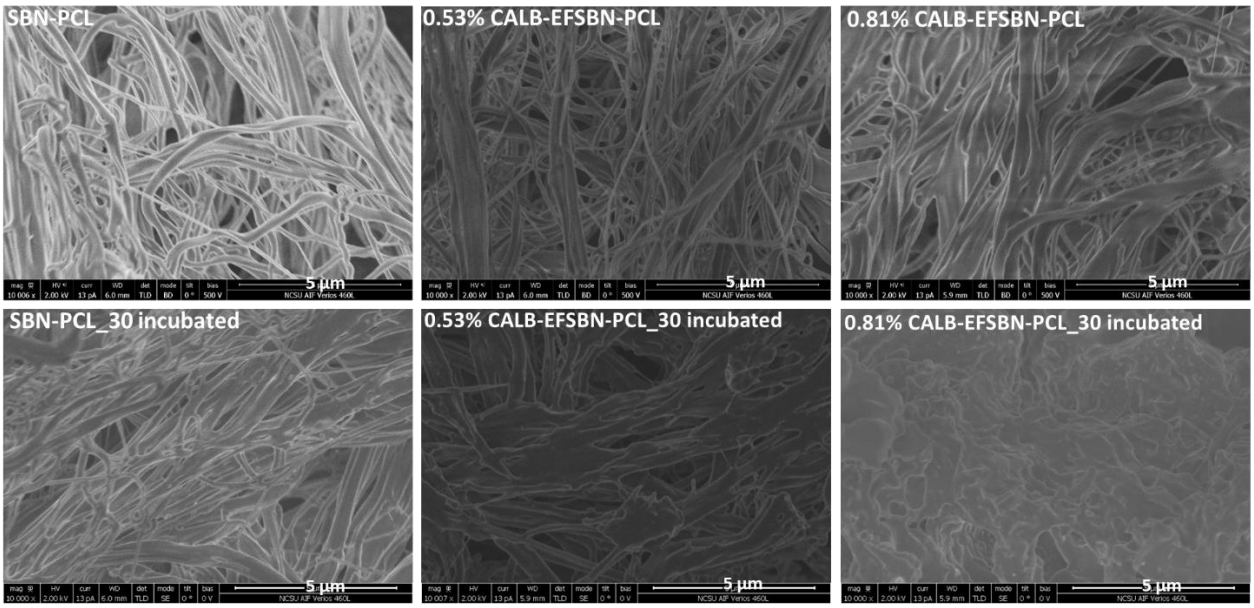

Figure 3.14: SEM micrograph (10000x magnification) of SBN-PCL and EFSBN-PCL webs before and after incubation in Tris-HCl buffer (pH 8.0, 100 mM) at 40 °C for 30 mins.

3.3.9. Storage stability of EFSBN-PCL and free CALB in buffer

Controlled degradation of materials is a fundamental factor in material design and applications. Thus, it is an important question for how many days EFSBN-PCL can be used (e.g., as packaging material) and how the enzyme activity profile changes with time. Storage stability analysis of materials designed using solid EFSBN-PCL should take the application purpose into consideration. Because CALB hydrolyzes the ester bond of PCL in the presence of water or moisture[289], EFSBN-PCL webs might not be stable under moist conditions but could be stable under dry conditions. **Figure 3.15** shows the storage stability of CALB-loaded EFSBN-PCL webs at ambient and refrigerated temperatures. Results show that immobilized CALB was stable for a long time in dry

PCL webs. When redissolved in the buffer, both webs showed around 60% of their initial activity after 120 days. This result revealed that immobilized CALB in EFSBN-PCL can survive at ambient temperature or in refrigerators without degrading PCL webs. The result implies that CALB enzymes retain their structure in dry EFSBN-PCL but don't degrade PCL webs because CALB does not activate without moisture. However, CALB shows activity on wet EFSBN-PCL webs and degrades the ester linkages of the PCL polymer chain. Thus, produced EFSBN-PCL could be used as an enzyme degradable packaging material at an ambient condition. With further evaluation of the availability of caprolactone monomer and oligomer-metabolizing microorganisms in soil, there is the potential for direct disposal of EFSBN-PCL in moist soil for complete biodegradation.

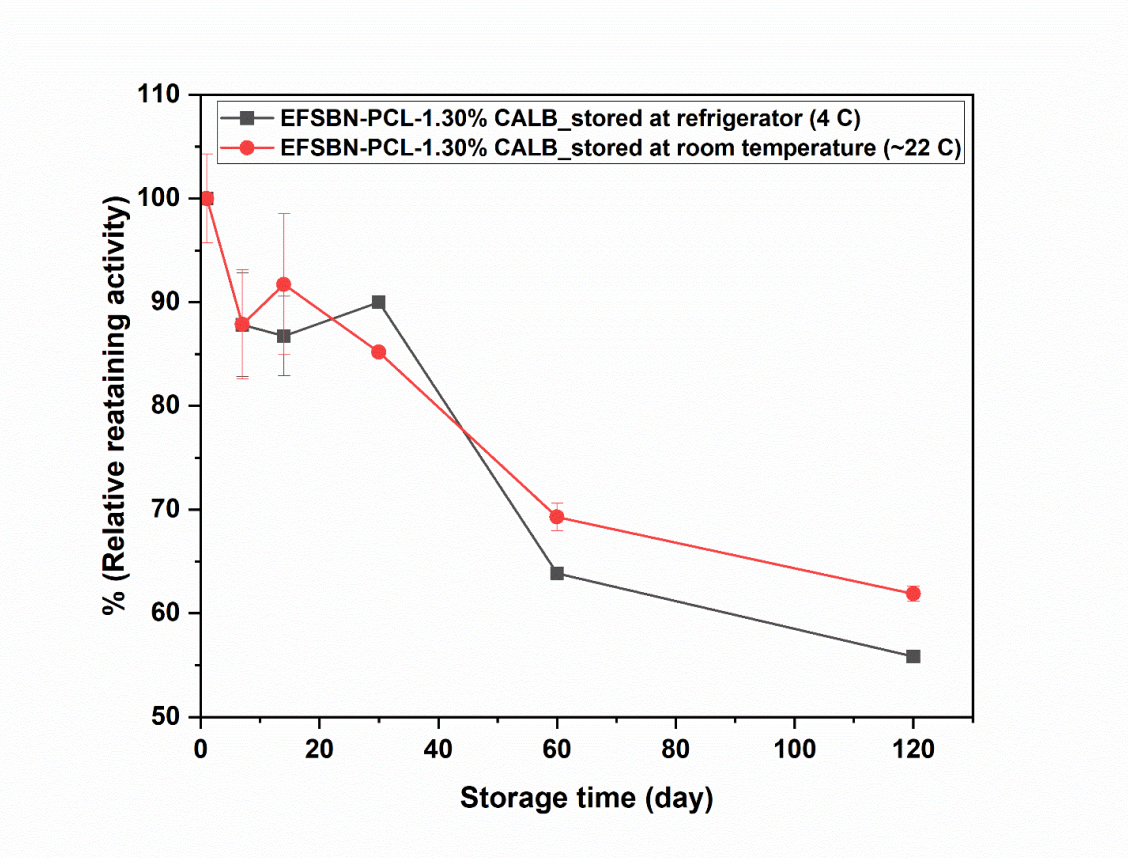

Figure 3.15: Storage stability (retaining activity with time) of 1.3 % (w/w) CALB-EFSBN-PCL webs at ambient and refrigerator temperature.

The storage stabilities of immobilized CALB, free CALB (as supplied), and free CALB diluted in the buffer were also compared. The relative remaining activity at different storage times is presented in **Figure 3.16**. Free CALB (as it was supplied), diluted free CALB (0.1 µl/ml) in Tris HCl buffer (pH = 8.0, 0.1 M), and CALB-EFSBN-PCL were stored at room temperature (~ 22 ℃). The immobilized CALB showed similar storage stability to as-supplied CALB, whereas buffer-diluted CALB had less than 20 % activity after 120 days. The commercial-free CALB might have a stabilizer, and after buffer dilution, the stabilizer effectiveness was lost, which could explain the rapid decrease in hydrolytic activity. The similar (even better) storage stability outcome for CALB in EFSBN-PCL webs compared to stabilized commercial liquid CALB showed that EFSBN-PCL could tolerate ambient conditions for a long time with retained activity. The high level of retained activity implies that EFSBN-PCL can be used for a long time and will still have active enzyme inside when disposed of after use.

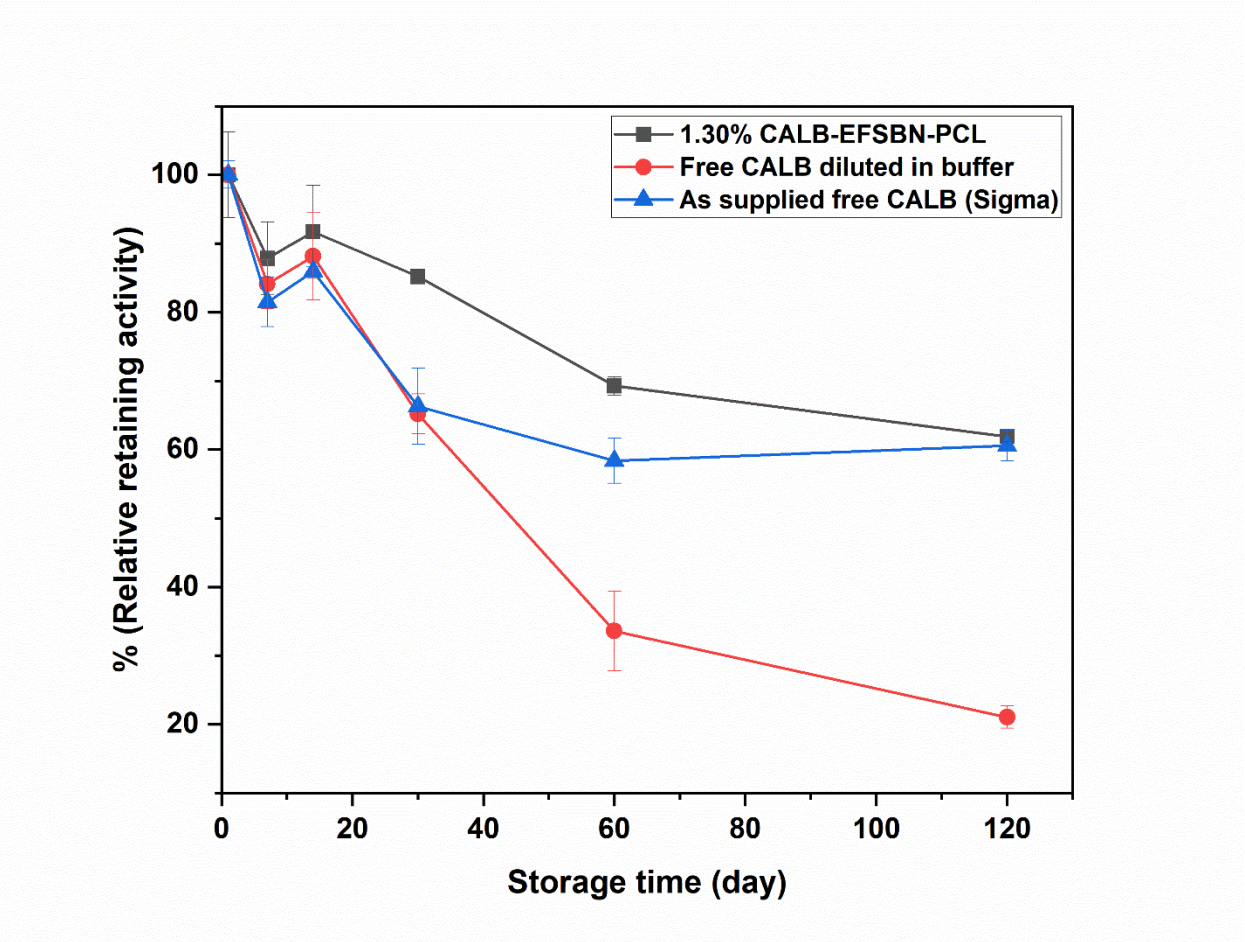

Figure 3.16: Ambient (~22 ℃) storage stability of supplied free CALB, diluted free CALB (0.1 µl/ml) in Tris HCl buffer (pH = 8.0, 100 mM) and 1.30 % (w/w) CALB-EFSBN-PCL solid webs.

3.4. Conclusions

CALB enzyme functionalized solution-blown nonwoven polycaprolactone (CALB-EFSBN-PCL) nanofibrous webs were successfully prepared from water-in-oil microemulsions of PCL-chloroform-CALB compatible triads by a single-step solution blowing technique. The process parameters used, including air pressure, solution flow rate, and die-to-collector distance for solution blow spinning, were the same for PCL-only and CALB-loaded PCL webs. However, the morphologies and diameters of the EFSBN-PCL webs were changed by varying the loading of

aqueous CALB in the spinning solution. SEM micrographs revealed a more irregular and clustered nonwoven structure of EFSBN-PCL compared to SBN-PCL, and the irregularities were more visible in higher CALB-loaded EFSBN-PCL. FTIR spectra and Lowry protein assay results confirmed the presence of protein in the nanofibrous webs. ToF-SIMS surface characterization and laser confocal microscopy imaging revealed that immobilized enzymes were mainly located inside the fibers and non-homogeneously distributed (enzymes cling to each other) throughout the webs. Substantial enzyme activity was detected in EFSBN-PCL webs after the solution-blowing process and after storage at ambient dry conditions. The hydrolytic activity showed that EFSBN-PCL retained about 50% activity of the free CALB activity. Similarly, immobilized CALB retained longer storage stability than buffer-diluted free CALB, and immobilized CALB-EFSBN-PCL webs retained more than 60% activity after 120 days for both ambient and refrigerated storage. An especially interesting finding of this work is the enzymatic degradation of EFSBN-PCL webs. CALB enzymes only hydrolyze PCL in wet conditions, therefore, EFSBN-PCL webs were very stable at ambient dry conditions. This work explored the degradation characteristics of the CALB-EFSBN-PCL webs in tris buffer (100 mM, pH 8.0), which were incubated at predetermined times at 40 ˚C and room temperature (~22 ˚C). At 40 ˚C incubation, high-loaded (1.92 mg protein/100 mg webs) webs degraded entirely in less than 15 mins, and low-loaded (0.53 mg protein/100 mg webs) webs required less than 60 mins for complete enzymatic degradation of the webs. In comparison, at room temperature, complete degradation of both low and high CALB content webs occurred within 24 hrs. The rapid enzymatic degradation implies that EFSBN-PCL webs would become a potential degradable packaging material.

Chapter 4: Immobilization of *Candida antarctica* lipase B on polystyrene solution blown nanofibrous nonwoven webs

Abstract:

Adsorption immobilization of enzymes on hydrophobic carriers, especially nanofibers, is an effective strategy for achieving high loading and catalytic activity. This work successfully adsorbed lipase from Candida sp. (CALB) on solution-blown nonwoven polystyrene (SBN-PS) nanofibers. The SBN-PS fibers were produced by a solution blow spinning (SBS) method that utilizes high-velocity gas to extrude the PS spinning solution and evaporate the solvent to form smooth surface nanofibrous webs with an average fiber diameter of 148±28 nm. A broad range of (1.19-4.45 wt% protein) of CALB enzymes was adsorbed on the surfaces. The presence of enzyme protein on the solid nanofibers was confirmed by Fourier Transform Infrared Spectroscopy (FTIR). Scanning electron microscopy (SEM) showed that fiber morphology didn't change upon immobilization, but a slight increase in fiber diameter was observed. The enzymes were positioned on the surface of the nanofibers, proven by X-ray photoelectron spectroscopy (XPS) and laser confocal microscopy. The hydrolytic activity of CALB was measured using a p-nitrophenyl acetate substrate-based assay, and 4.03 wt% CALB loaded enzyme functionalized solution blown nonwoven polystyrene (CALB-EFSBN-PS) webs retained above 70% of the free enzyme activity. CALB-EFSBN-PS showed wider optimum temperatures for catalytic activity and better thermal stability than free CALB enzymes. During storage in the refrigerator at 4 °C, the activity of CALB-EFSBN-PS webs was measured with time, and the immobilized CALB retained almost all of its initial activity after 90 days of storage. The adsorbed CALB retained more than 70% of its original activity after 15 repetitions of the lipase assay using p-nitrophenyl acetate

substrate in tris buffer (100 mM, pH 8.0). CALB-EFSBN-PS could be a promising biocatalytic functional material due to the low fabrication cost, simple immobilization procedure, and various potential industrial applications.

Keywords: CALB, adsorption, immobilization, polystyrene, reusability, solution blow spinning.

4.1. Introduction

Lipase (EC 3.1.1.3) has been widely used for catalyzing aminolysis, esterification, interesterification, and transesterification reactions and is widely used in the detergent, food, polymer degradation, biodiesel, leather, cosmetic, textile, and pharmaceutical industries.[34,111,148,150,376,377] Among all lipases, lipase B from *Candida antarctica* (CALB) is one of the most recognized biocatalysts because it exhibits high selectivity and affinity to the substrate.[131] Enzymes can be immobilized by attaching to inert, insoluble supporting materials[36] or entrapping them in microspheres.[307] By enzyme immobilization, catalysts can be developed with significant advantages relative to the free enzyme, including easy recovery and possible reuse, improved stability, rapid termination of enzyme-catalyzed reactions, and avoiding protein contamination of the final product.[32]

Lipase immobilization on a water-insoluble carrier is an effective method to improve the biocatalyst performance of the enzyme. Different techniques can be used in the lipase immobilization process, such as adsorption,[148] covalent bonding,[378] encapsulation,[104] and entrapment.[25] Among them, the adsorption operation is simple and low-cost. In industrial applications, lipase, such as the widely used immobilized lipase ‘‘Novozym 435’’, is immobilized

by physical adsorption on a resin, "Lewatit VP OC 1600".[97] The immobilized CALB prepared by physical adsorption has been applied to many fields, such as bio-diesel production,[379] pharmaceutical syntheses,[24] food industry,[380] and industrial ester synthesis.[381] However, enzyme leaching from carrier materials is the main drawback of physical adsorption because of the weak interaction between lipase molecules and carriers. In addition, the adsorption of an enzyme onto a surface can induce conformational changes, which affect the rate and specificity of the catalyst.[148] Therefore, immobilization research has largely focused on matrix selection and optimizing immobilization conditions. Both inorganic and organic carrier materials are widely used for lipase immobilization. The general lipase immobilization carriers are ceramics,[382] glass beads,[383] silica,[384] chitosan,[385] sol-gel,[386] polymeric nanoparticles,[148] polymeric electrospun nanofibers,[387] and polymeric microspheres.[307] Among the polymeric carriers, polystyrene (PS) is a hydrophobic, thermoplastic polymer, low cost, that can be easily synthesized and used as support for lipase adsorption.[111,148,150,307,388,389] Among polymeric carriers, polymeric microspheres and nanomaterials are known to be appropriate carriers for lipase immobilization. Nanomaterials such as nanofibers are viewed as favorable immobilization matrices because they have high surface area that provides high enzyme loading and immobilization yields.[92,164,315] Such high surface area materials could offer additional benefits as a delivery system for adsorbed enzymes and minimizes substrate diffusion.

Solution blow spinning (SBS) is a cost-effective and high fiber yielding method for nanofiber production.[326,328] In this spinning process, high-pressure gas evaporates the solvent from the polymer solution, whereas a comparable technology, electrospinning, requires a high electric

voltage. A solution blow spinning unit with a single annular die, including a spinning nozzle with an annular gas cavity surrounding it, is illustrated in **Figure 2.1**. The detailed mechanism of operation is explained in **Section 2.1.** Miranda *et al*. produced 441±110 nm PS nanofibers from 30 wt% PS solution using toluene solvent for the solution spinning process.[193] Zhang *et al*., prepared 200-1400 nm PS nanofibrous membranes using dichloromethane solvent and solution blow spinning for oil recovery from the water surface.[390] Kasiri ***et al***. produced 424-1619 nm PS nanofibrous SBS nonwoven webs using tetrahydrofuran (THF)/acetone (3:7) solvent and investigated morphological analysis of this superhydrophobic material for oil absorption.[391] So, the SBS process for PS is by now well established. The high surface area of nanofibrous webs and the superhydrophobic nature of PS makes them ideal for physical adsorption applications.

The fascinating superhydrophobic nature of PS, the high surface-to-volume ratio properties of solution-blown nonwoven (SBN), and the cost-effective process of SBS imply the SBN-PS nanofibrous webs are potential carrier materials for CALB adsorption. Hydrophobic binding of CALB on other PS matrices by adsorption has proved successful due to its affinity for water/oil interfaces.[148] Thus, the present work deals with the synthesis of PS nanofibers and their use as a support for the immobilization of CALB. The lipase from *Candida sp.* (CALB) was adsorbed on SBN-PS to produce CALB enzyme functionalized solution blown nonwoven polystyrene (CALB-EFSBN-PS) nanofibrous webs. The effect of the immobilization time and enzyme loading in the immobilization buffer solution and the hydrolytic activity of the corresponding CALB-EFSBN-PS webs were studied. The position and distribution of immobilized CALB, thermal and storage stability, and reusability are also reported in this chapter.

4.2. Experimental Section

4.2.1. Materials

Lipase (CALB) from *Candida sp.* Recombinant, expressed in *Aspergillus niger* was purchased from Sigma-Aldrich as a liquid enzyme product (L3170) and used as supplied. Polystyrene (M_n = 182000 Da), p-nitrophenyl acetate, p-nitrophenyl, Tris-HCl, and toluene were purchased from Sigma-Millipore (Hampton, NH, USA). Pierce Rapid Gold BCA Protein Assay Kit (Catalog Numbers A53225, A53226, and A53227) (Thermo-Fisher Scientific, Waltham, MA, USA) was used to determine the protein concentration in the produced EFSBN using the bovine serum albumin (BSA) standard provided in the kit.

4.2.2. SBN-PS webs production

Solution-blown nonwoven webs of polystyrene (SBN-PS) were produced using the same instrument and procedure described in **Section 2.2.2**. The polystyrene (PS) (M_n = 182000 Da) spinning solutions were prepared by dissolving PS pellets (1.5 g) in toluene solvent with continuous (overnight) stirring (100 rpm). Then, the PS solution was trialed in solution blow spinning using the same apparatus illustrated in **Figure 2.1.** The air temperature was maintained constant at 40 ℃ throughout the process. The effect of concentration, die-to-collector (DCD) distance, solution throughput, and air pressure on fiber morphology and diameter were observed. The experimental setup is described in **Table 4.1**. For observation of PS concentration effects on fiber diameter, PS solutions of 10, 12.5, and 15 (w/v)% were trialed in solution blow spinning. For DCD distance effect analysis, DCD was varied across 100, 150, and 200 mm. The remaining parameters were kept constant during spinning. Similarly, air pressure and solution

throughput effect on fiber morphology were also observed according to the experimental setup in **Table 4.1**.

Table 4.1: Experimental set-up for fiber morphology and diameter analysis of SBN-PS.

Exp.no.	Concentration (w/v)	DCD, mm	Air pressure, kPa	Throughput, ml/min
C 01	10	100	207 (30 psi)	0.5
C 02	12.5	100	207	0.5
C 03	15	100	207	0.5
D 01	15	100	207	0.5
D 02	15	150	207	0.5
D 03	15	200	207	0.5
S 01	15	100	138 (20 psi)	0.5
S 02	15	100	207	0.5
S 03	15	100	276	0.5
S 04	15	100	138	1.0
S 05	15	100	207	1.0
S 06	15	100	276 (40 psi)	1.0
S 07	15	100	138	1.5
S 08	15	100	207	1.5
S 09	15	100	276	1.5

4.2.3. EFSBN-PS webs production

Production of SBN-PS immobilization matrices for creating the novel CALB enzyme functionalized solution-blown nonwoven polystyrene (CALB-EFSBN-PS) webs was done using the modified solution blow spinning method of Pang *et al*.[93]. After the SBN-PS matrix was made, CALB was adsorbed to the fibrous web in a subsequent step. A simplified schematic diagram of the CALB adsorption process on SBN-PS nanofibers is presented in **Figure 4.1**. To evaluate the protein loading capacity of SBN-PS and immobilization yield, approximately 100 mg of SBN-PS was immersed in 10 ml of sodium phosphate buffer (100 mM, pH 7.0) with different CALB concentrations (1.19-11.92 wt%). The adsorption was performed in an incubator shaker (MAXQ

2000, Thermo Scientific) at 50 rpm shaking and 30 ℃ temperature for four hrs. The CALB-EFSBN webs were separated from the solution by a vacuum membrane filter unit and washed until no protein was detected in the filtrate. The wet CALB-EFSBN-PS webs were dried in a convection oven at 45 ℃ for 48 hrs and stored at 4 ℃ until further analysis.

To evaluate the incubation time effect on adsorption, a similar amount (~100 mg) of SBN-PS webs were immersed in 10 ml of 5.96% (wt) CALB in sodium phosphate buffer ((100 mM, pH 7.0) and incubated at the same shaking rate and temperature for different times (1-24 hrs). Then, EFSBN webs were filtered and dried as described above.

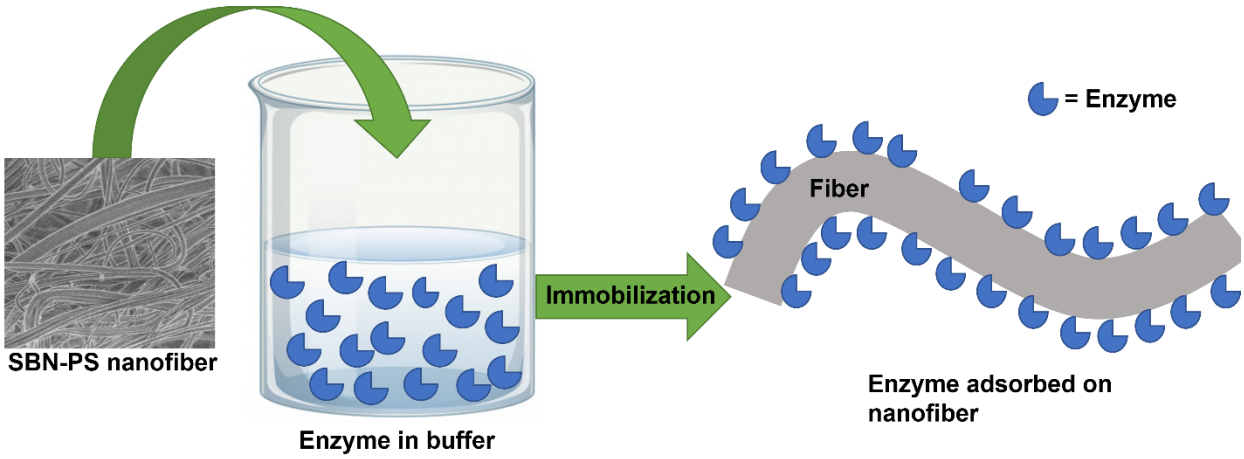

Figure 4.1: Schematic diagram of CALB adsorption on SBN-PS.

The initial protein loading in the buffer and remaining protein in the filtrate were measured by Thermo scientific Pierce™ Rapid Gold Bicinchoninic Acid (BCA) Protein Assay Kit (process described in **Section 2.2.4**). The percent protein content in an EFSBN-PS sample was calculated according to the following formula:

$$\text{Protein content } (\%) = \frac{\text{Total protein in filtrate, mg} * 100}{\text{Total protein loading,mg} * \text{weight of SBN}-\text{PS,mg}} \quad \text{.....(4.1)}$$

The immobilization yield of EFSBN-PS webs was calculated from the ratio of the measured amount of protein content (amount of protein adsorbed in the final webs) on the EFSBN-PS to the theoretical protein loading (amount of protein added to the CALB-buffer solution). The immobilization yield percentage is calculated using the following formula:

$$\text{Immobilization yield } (\%) = \frac{\text{Total protein adsorbed on EFSBN}-\text{PS, mg} * 100}{\text{Total protein loading in buffer, mg}} \quad \text{.....(4.2)}$$

4.2.4. Lipase assay of immobilized CALB on EFSBN-PS

The lipase activity of immobilized CALB was measured using a p-nitrophenyl acetate substrate-based assay method following a modification of the CALB assay described in **Section 3.2.4**. A suitable amount (approximately 3-5 mg, exactly weighed) of CALB-EFSBN-PS web was placed into a 1500 µl microcentrifuge tube and soaked in 475 µl Tris HCl buffer (100 mM, pH 8.0) for 10 mins at room temperature. Then, tubes were pre-incubated for 5 mins at 45 ℃. After preincubation, 25 µl 8 mM p-nitrophenyl acetate (p-NPAc) substrate solution was added to the tube mixture, vortexed for 10 seconds, and incubated at 45 ℃ at 30 mins. Throughout the process, the mixture was hand shaken for a few seconds every five minutes. After incubation, the reaction was stopped by placing microcentrifuge tubes into ice water. The absorbance determines the concentration of p-nitrophenol (p-NP), a yellow color substance released during p-NPAc hydrolysis, with an absorbance maximum of 405 nm. Three replicates of each sample were measured. The blank control was made by maintaining the same procedure except adding an

equivalent amount of SBN-PS. The p-NP equivalents liberated micromoles were determined using a p-NP standard curve.

The lipase assay of immobilized CALB per mg of the EFSBN-PS webs protein,

$$U/mg_{\text{EFSBNs protein}} = \frac{\mu\text{mole of p-NP equivalent release} * \text{volume of total assay,ml}}{\text{Time,min} * \text{EFSBN protein used in assay,mg} * \text{EFSBN soaked buffer,ml}} \ldots\ldots\ldots\ldots\ldots\ldots (4.3)$$

The relative activity of immobilized CALB was calculated as the percentage of the free lipase activity and calculated as follows:

$$\text{Relative activity } (\%) = \frac{\text{Activity of immobilized lipase}}{\text{Activity of free lipase}} * 100 \ldots\ldots\ldots\ldots\ldots\ldots\ldots\ldots\ldots\ldots\ldots\ldots\ldots\ldots\ldots\ldots\ldots\ldots (4.4)$$

4.2.5. FTIR spectroscopy analysis of SBN-PS and EFSBN-PS

The presence of enzymes in the EFSBN-PS was characterized by FTIR Spectroscopy (iS50, ThermoFisher Scientific, USA), with a built-in diamond crystal Attenuated Total Reflection sampling head. Spectra were collected for dried SBN-PS and CALB-EFSBN-PS webs at room temperature from 500 to 4000 cm^{-1} with 64 scans and 4 cm^{-1} resolution. All specimens were stored in a desiccator for two days before measurement to minimize moisture in the samples.

4.2.6. Morphology of SBN-PS and CALB-EFSBN-PS

Morphologies of SBN-PS and CALB-EFSBN-PS samples were investigated using field-emission scanning electron microscopy (FESEM) (FEI Verios 460L, USA) with an accelerating voltage of 500 V and a current of 2 pA. Images were analyzed using ImageJ software (NIH, USA), measuring the average diameter of fibers in at least 100 places on each SEM micrograph.

4.2.7. Enzyme distribution in EFSBN-PS by confocal microscopy

CALB was conjugated to fluorescein isothiocyanate (FITC) following the "large scale conjugation" procedure described in the Sigma Fluoro-tag-FITC conjugation kit (process described in **Section 3.2.6**). FITC-tagged-CALB was adsorbed onto SBN-PS nanofibers according to the method described in **Section 4.2.3**. The FITC-tagged-CALB adsorbed EFSBN-PS webs were placed on a glass slide and mounted under a No. 1.5 cover glass held up by modeling clay spacers to prevent sample compression and imaged by a Zeiss LSM 880 laser scanning confocal microscope using a 488 nm excitation laser to detect the FITC signal. The z-series images were collected using a 20x dry objective with NA=0.8 and 2 µm intervals. The z-series were further processed using Imaris 9.9 software (Bitplane, Zurich, Switzerland) to remove the background signal. Results show the location of CALB on EFSBN-PS webs.

4.2.8. Surface analysis of CALB-EFSBN-PS using XPS

The surface composition of EFSBN-PS and SBN-PS webs was characterized by X-ray photoelectron spectroscopy (XPS) using an XPS/UVS-SPECS system with PHOIBOS 150 analyzer under a pressure of about 3 x 10^{-10} mbar. The instrument was equipped with a MgKα X-ray (hν = 1253.6 eV) and AlKα X-ray (hν = 1486.7 eV) sources. The data were acquired using the MgKα X-ray source operating at 10 kV and 30 mA (300 W) and analyzed with the CasaXPS software. XPS spectra of survey scan were recorded with a pass energy of 24 eV in a 0.5 eV step, and high-resolution scans were recorded with a pass energy of 20 eV in a 0.1 eV step. The C1s peak was used as an internal reference with a binding energy of 285 eV.

4.2.9. Optimum temperature and thermal stability of CALB-EFSBN-PS

The optimum temperatures for lipase assay of immobilized and free CALB were determined by measuring the hydrolytic activity of immobilized CALB and free CALB for different incubation temperatures (30-70 ℃). Thermal stability tests were performed by incubating solid CALB-EFSBN-PS webs soaked in tris buffer (0.1 M, pH 8.0) and the same buffer with diluted free CALB (1 µl/ml) (three replicates of each trial in 1500 µl microcentrifuge tube) at 45 ℃ for different times (1-24 hrs). After thermal treatment, substrate p-NPAc was added to the microcentrifuge tube, and lipase was assayed according to the method described in **Section 4.2.4**. The thermal stability of the enzyme's liquid and immobilized solid forms was expressed as the residual activity after thermal treatment. Residual activity was the ratio of measured activity at a time point to the initial activity at time zero, expressed as a percentage (Eqn. 3.7).

$$\text{Relative residual activity } (\%) = \frac{\text{Measured activity after treatment}}{\text{Initial sample activity}} * 100\% \dots\dots\dots\dots\dots (4.5)$$

4.2.10. Storage stability of CALB-EFSBN-PS

The storage stability of immobilized CALB-EFSBN-PS was evaluated by the modified method of Pereira *et al.* [104]. The EFSBN-PS webs were kept at 4 ℃ and lipase activity was measured over time (0-90 days) according to the method described in **Section 4.2.4**. Residual activity was the ratio of measured activity at a time point to the initial activity at time zero, expressed as a percentage (Eqn. 4.6).

$$\text{Relative residual activity } (\%) = \frac{\text{Measured activity of stored sample}}{\text{Initial sample activity}} * 100\%. \dots\dots\dots\dots. (4.6)$$

4.2.11. Reusability of CALB-EFSBN-PS

The enzyme reusability was measured 15 times by repetitions of the lipase assay. Three replicates of solid CALB-EFSBN-PCL and SBN-PS webs (approximately 5 mg, exactly weighed) were immersed in a 475 µl tris-HCl buffer (100 mM, pH 8.0) and preincubated for 5 mins at 45 ℃. Then, mixtures were incubated with 25 µl 8 mM p-nitrophenyl acetate (p-NPAc) substrate) at 45 ℃ for 30 mins. After each lipase assay, solid webs were removed from the substrate solution and washed with the same buffer three times. The webs were reintroduced into a fresh buffer, preincubated, and incubated with the substrate. After each lipase activity trial, the absorbance was measured at 405 nm (p-nitrophenol release) and activity was determined. The first trial activity was considered 100%. The residual activity of each reuse cycle assay was calculated using Eqn. 4.7.

$$\text{Relative residual activity } (\%) = \frac{\text{Measured activity of reuse cycle}}{\text{Initial cycle activity}} * 100\% \ldots\ldots\ldots\ldots\ldots\ldots (4.7)$$

4.3. Results and Discussion

4.3.1. SBN-PS preparation by solution spinning process

In the solution blow spinning (SBS), the high-pressure air in the outer nozzle creates a driving force that attenuates the polymer solution. The attenuation induces shearing of the polymer solution at the gas-liquid interface leading to the formation of fibers accompanied by solvent evaporation while the solidified fibers are collected on the target.[392] The ability to form stable and continuous fibers is governed by spinning parameters such as polymer concentration, solution flow rate, air pressure, air temperature, and die-to-collector distance. **Table 4.2** shows

the average fiber diameter along with solution spinning parameters. The SEM micrographs of all SBN-PS trials are presented in Appendices (**Figure A 4.1- Figure A 4.5**). The average molecular weight of PS was 19200 Da, and the air temperature (40 ℃) was kept constant for all trials. For the first three trials (C 01-03), it was revealed that the fiber morphology largely depends on polymer concentration, and average fiber diameter increased with increasing PS concentration. However, low-concentration polymer solution has a higher amount of solvent, requiring more driving force to evaporate. The die-to-collector (DCD) distance analysis (trials D01-03) found no significant change in fiber morphology and average fiber diameter. However, high solution throughput might require high DCD for complete evaporation of the solvent. The solution throughput is another crucial parameter for controlling fiber morphology. Fiber diameter was observed to increase with increasing solution throughput. However, high solution throughput could not evaporate all solvents from the PS solution, creating beads in the web morphology. For instance, all solution throughput trials at 1.5 ml/min produced a viscous mass on the collector and a bead morphology was observed in SEM images. The air pressure was also crucial in getting fiber in solution blow spinning. High-pressure air induces more driving force and evaporates more solvent from the polymer solution. As a result, thinner fibers were observed at high air pressure, but high-pressure air also possesses a high possibility of blow-away fiber with air, decreasing the fiber production yield. The SBN-PS produced from 0.5 ml/min solution throughput, 207 kPa air pressure, 40 ℃ air temperature, 182 kDa molecular weight PS, 15 (w/v)% polymer solution, and 100 mm DCD, were optimal for producing uniform webs for CALB immobilization.

Table 4.2: Average fiber diameter of SBN-PS at different solution blow spinning process parameter conditions.

Exp.no.	Concentration (w/v)	DCD, mm	Air pressure, kPa	Throughput, ml/min	Average fiber diameter, nm
C 01*	10	100	207	0.5	78±32
C 02	12.5	100	207	0.5	102±45
C 03	15	100	207	0.5	143±28
D 01	15	100	207	0.5	143±28
D 02	15	150	207	0.5	155±39
D 03	15	200	207	0.5	150±61
S 01	15	100	138	0.5	142±28
S 02	15	100	207	0.5	143±28
S 03	15	100	276	0.5	126±32
S 04*	15	100	138	1.0	176±66
S 05	15	100	207	1.0	152±22
S 06	15	100	276	1.0	157±29
S 07*	15	100	138	1.5	160±47
S 08*	15	100	207	1.5	157±56
S 09*	15	100	276	1.5	167±41

*Observed viscous mass on the collector.

4.3.2. Enzyme loading and immobilization yield of EFSBN-PS

The amount of enzyme loading on a carrier material is an important parameter for distinguishing the material as a "good" carrier. A wide range of CALB (0.98 to 4.45 % wt) adsorbed on the SBN-PS nanofiber surface indicates that SBN-PS is a suitable carrier for enzyme immobilization by physical adsorption. Immobilization yields at different enzyme loading levels in the CALB buffer solutions and corresponding retained protein content on the solid webs are presented in **Figure 4.2**. Immobilization yield revealed how much enzymes adsorbed on the SBN-PS surface from the CALB buffer solution. Enzyme loading above the saturation point causes lower immobilization yield. As a result, lower immobilization yields were found at higher CALB-loaded buffer solutions. For all immobilization trials, the same quantity of SBN-PS webs and amount of buffer (different

CALB loaded) were used. The adsorbed protein content was low at lower enzyme loading, but immobilization yield was high because most of the enzymes adsorbed on the surfaces. Moreover, high enzyme loading in the buffer had higher adsorbed protein on the nanofiber surface but lower immobilization yield because the surface of the nanofiber became saturated, and the remaining enzymes in the buffer resulted in lower immobilization yields.

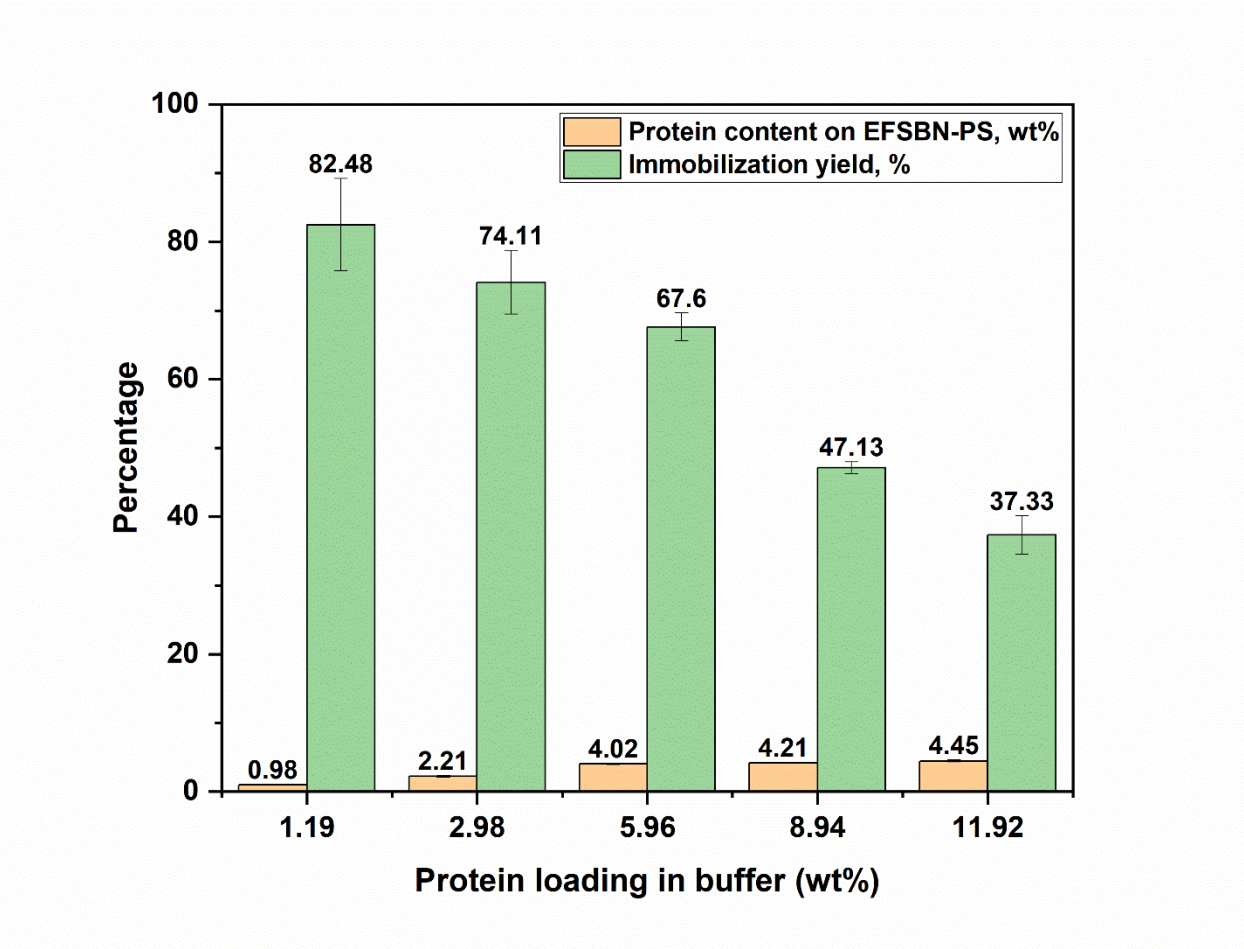

Figure 4.2: Immobilization yield of EFSBN-PS and retained protein on the solid CALB-EFSBN-PS webs with different enzyme loading in the buffer solution.

The enzyme adsorption rate on the nanofiber surface was also determined by immobilizing CALB on SBN-PS at different times (1-24 hr). **Figure 4.3** presents protein content with immobilization time. CALB adsorbed rapidly on the PS nanofiber surface, and the adsorption amount at longer times did not significantly change. The strong hydrophobic nature PS webs enable this rapid CALB adsorption on the SBN-PS nanofibers surface by hydrophobic forces.

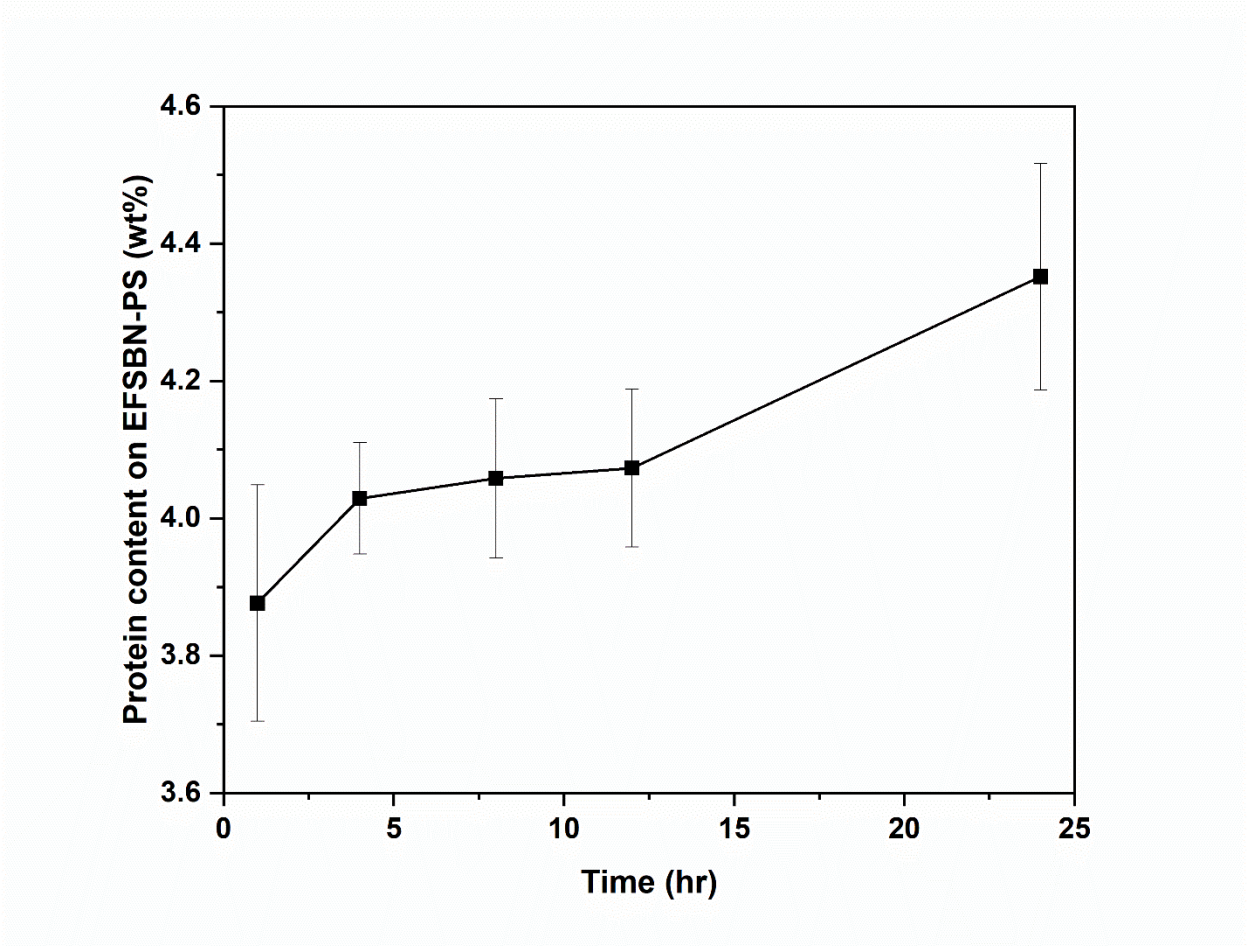

Figure 4.3: CALB protein (wt%) adsorption on SBN-PS with the time of adsorption treatment (5.96 wt% CALB protein loading in sodium phosphate buffer, 100 mM, pH 7.0).

4.3.3. FTIR analysis of SBN-PS and EFSBN-PS

FTIR characterization confirmed the presence of the phenyl group from PS polymer and the amide group from enzyme protein. The infrared absorption peaks of SBN-PS and CALB-EFSBN-PS webs are presented in **Figure 4.4**. The phenyl group (-C=C-) shows peaks at 1600, 1492, and 1450 $cm^{-1,}$ and the peak located at 3026 cm^{-1} corresponds to stretching vibrations of =C-H on phenyl radical, confirming the PS molecules in the webs.[111] To verify the CALB adsorption, FTIR spectra of SBN-PS and CALB-EFSBN-PS were compared. The CALB-EFSBN-PS spectra showed two distinct absorption peaks that are not observed in SBN-PS webs. The characteristic peak of amide I of protein is observed at 1650 cm^{-1}.[339] The N-H stretching peak of amide A overlaps with OH stretching at 3100-3500 cm^{-1} where the OH stretching peak could come from bound water in an enzyme.[231,340] These presences of water, enzyme binding water, and protein OH group contribute to the broad OH stretching peak. These results confirm the presence of the CALB enzyme on the SBN-PS nanofibers' surface.

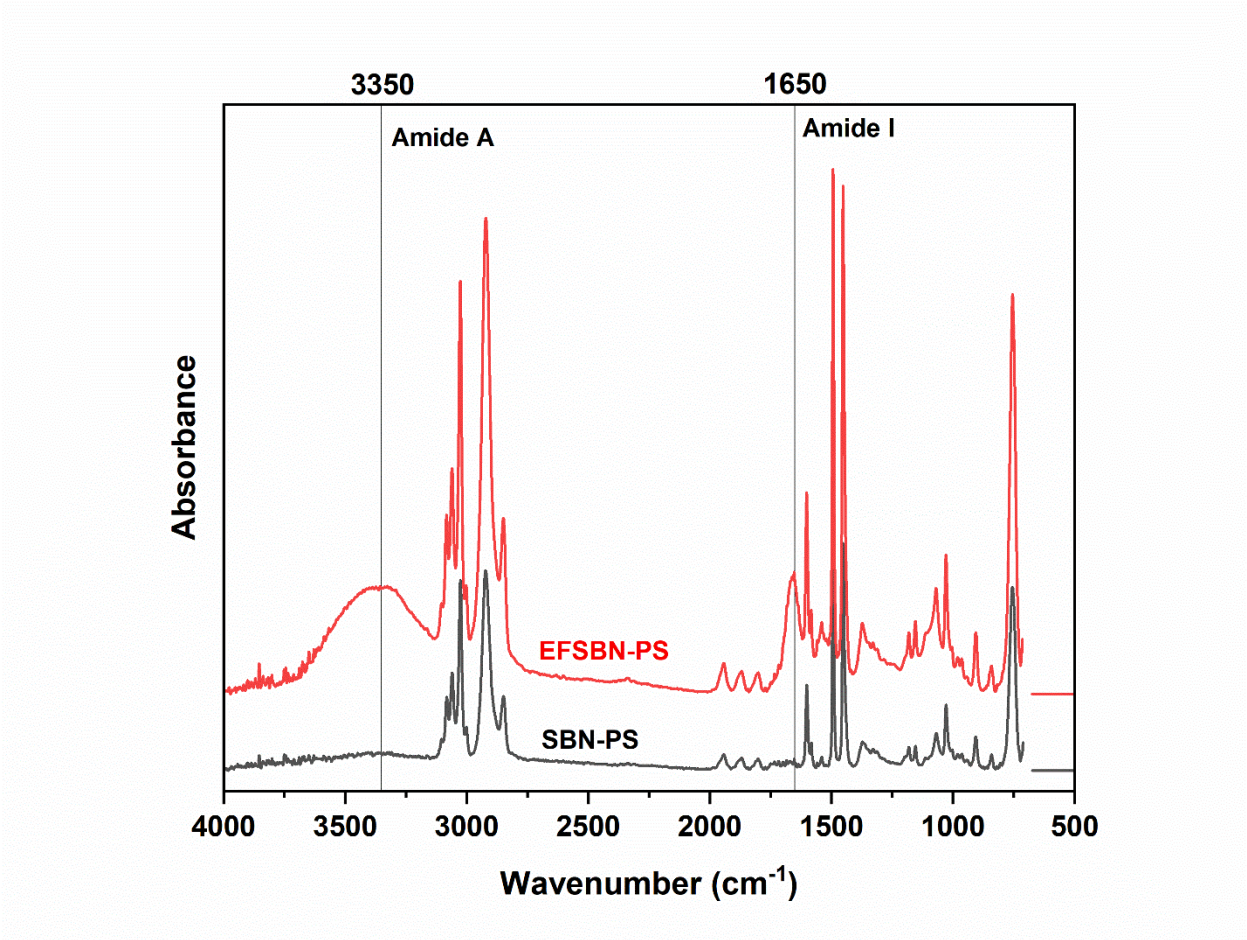

Figure 4.4: FTIR spectrum of SBN-PS and 4.03% CALB-EFSBN-PS webs.

4.3.4. CALB-EFSBN-PS surface analysis by XPS

The surface composition of SBN-PS and 4.03 wt% CALB-EFSBN-PS webs were characterized by X-ray photoelectron spectroscopy (XPS), as shown in **Figure 4.5**. The main peak of C_{1s} is found only in the SBN-PS spectrum, while the CALB-EFSBN-PS spectrum has three peaks of C_{1s}, N_{1s}, and O_{1s}. Since SBN-PS contains the C_{1s} peak only and the comes from the presence of protein[345] on the webs, the presence of N_{1s} signal confirms CALB was successfully immobilized on the PS nanofiber surface. The presence of the N_{1s} signal in XPS spectra further validates the FTIR results indicating the presence of CALB on the EFSBN-PS webs.

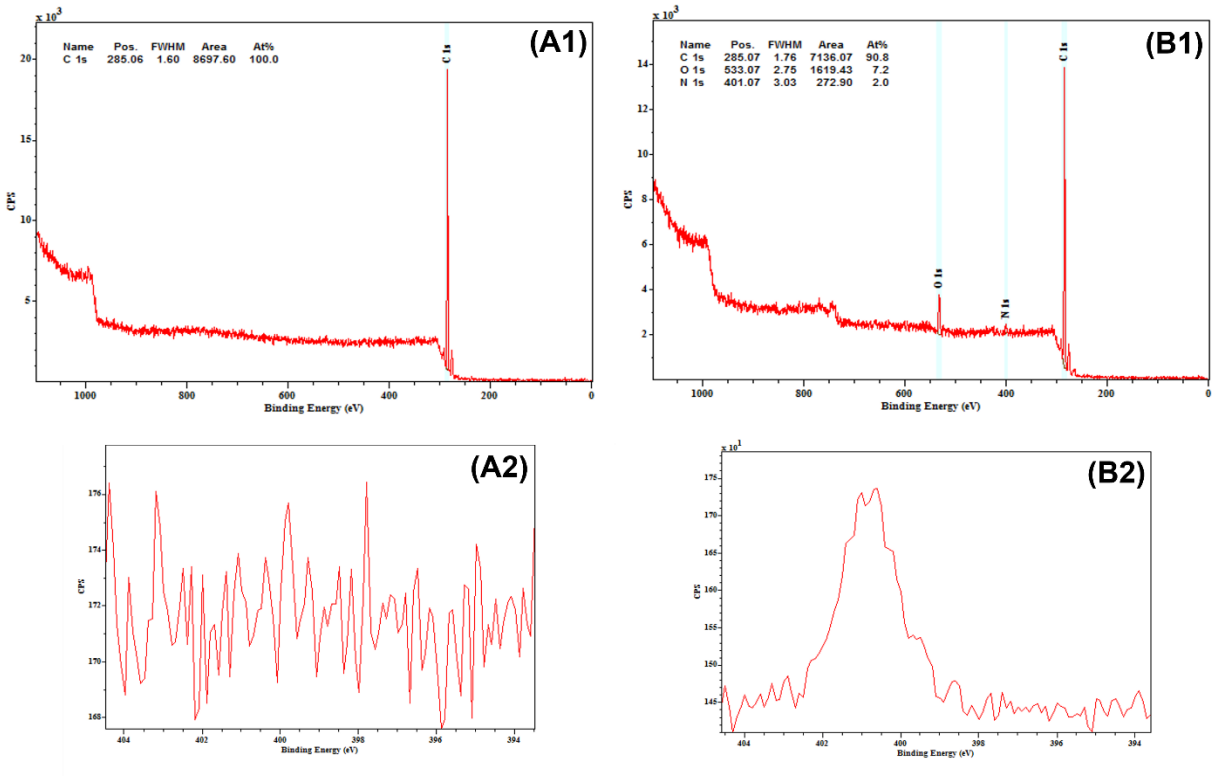

Figure 4.5: XPS spectra of (A1) SBN-PS, (B1) 4.03 % CALB-EFSBN-PS webs, (A2) N 1s peak of SBN-PS and (B2) N 1s peak of 4.03% CALB-EFSBN-PS webs.

4.3.5. Fiber morphology of SBN-PS and CALB-EFSBN-PS by scanning electron microscopy

The fiber morphology of SBN-PS and CALB-EFSBN-PS webs was characterized by scanning electron microscopy. Micrographs of the webs are presented in **Figure 4.6**. SEM micrographs show that SBN-PS nanofibers were nonwoven structures with smooth and no porous surfaces. After the CALB immobilization, no visible change in the surface morphology of EFSBN-PS nanofibers was observed, meaning the adsorption of CALB molecules occurred as a thin layer. The hydrophobic nature of the SBN-PS nanofibers implies that hydrophobic interactions govern the CALB enzyme adsorption.[148]

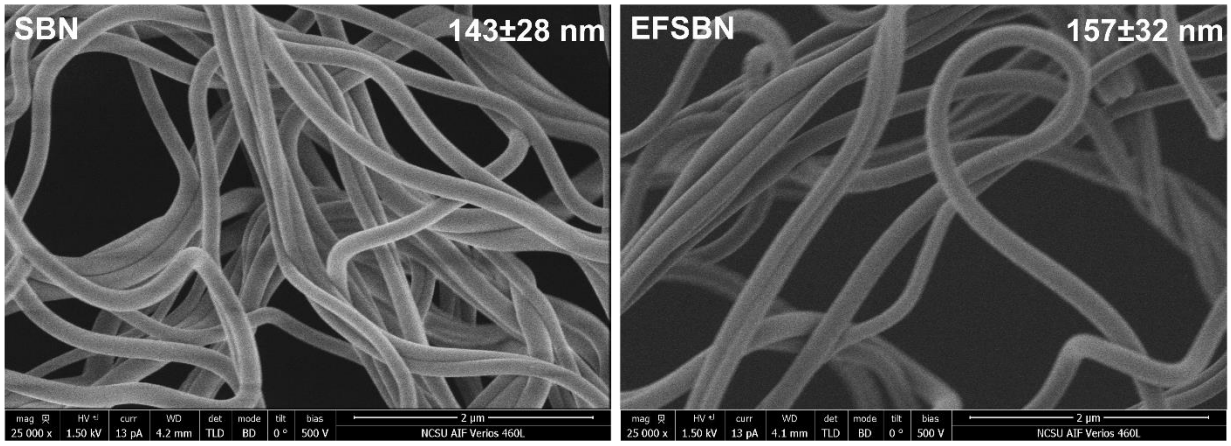

Figure 4.6: SEM micrograph of SBN-PS webs and 4.03% CALB-EFSBN-PS webs at 25000x magnification.

4.3.6. Enzyme distribution on CALB-EFSBN-PS by confocal microscopy

The uniform distribution of immobilized enzymes in carriers is an important parameter for achieving maximum carrier materials utilization and optimum catalytic activity from immobilized enzymes. To observe the distribution of adsorbed CALB on EFSBN-PS, CALB was labeled with fluorescein isothiocyanate (FITC), and the resulting FITC-tagged-CALB adsorbed EFSBN-PS webs were then analyzed by laser scanning confocal microscopy (**Figure 4.7)**. These images illustrate that CALB distribution in EFSBN-PS was homogeneous at a microscopic scale throughout the webs. The hydrophobic nature of SBN-PS nanofibers attracted (hydrophobic interaction) the enzyme protein throughout the nanofiber surface and achieved homogenous adsorption.[150] The homogenous distribution again implies CALB immobilization by adsorption on the nanofiber surface.

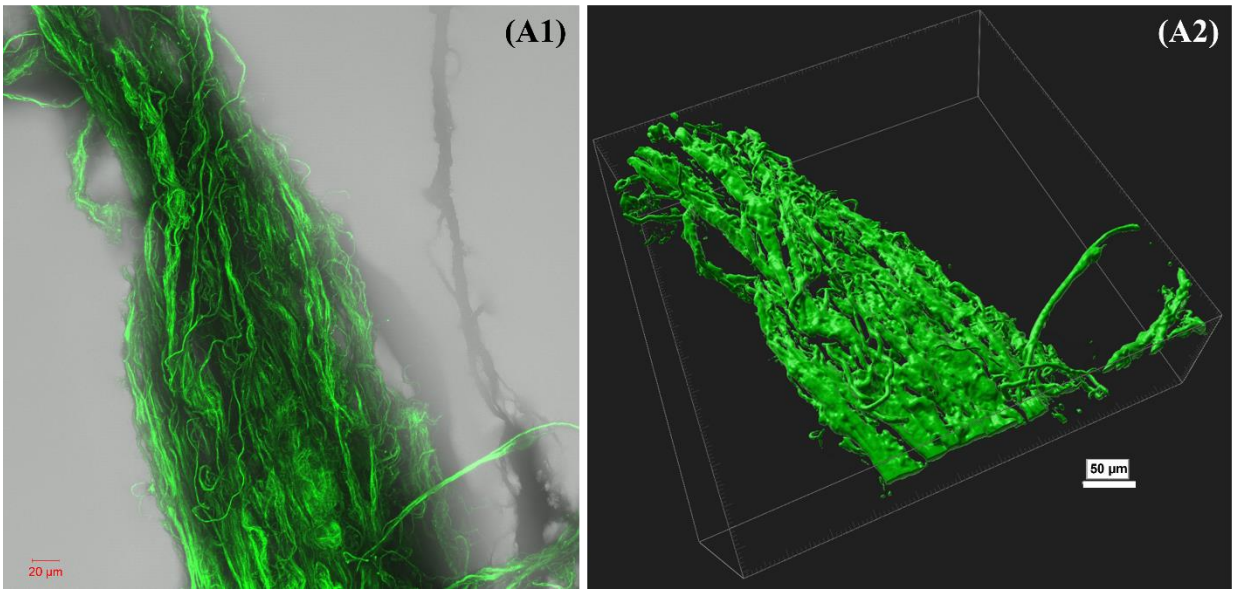

Figure 4.7: Laser scanning confocal microscopy images of the distribution of FITC-tagged-CALB (2.74 wt%) adsorbed-EFSBN-PS webs: (A1) raw image and (A2) z-series image. Green represents the quantity of enzyme distribution along the fiber.

4.3.7. CALB-EFSBN-PCL catalytic activity

The hydrolytic (lipase) activity assay was performed for free CALB, and different CALB-loaded EFSBN-PS and results were compared with the activity obtained for free CALB. **Figure 4.8** shows the relative activities of CALB-EFSBN-PS webs relative to their measured protein content. The immobilized CALB showed excellent retention of hydrolytic activity after immobilization, which implies immobilization did not impact the enzyme's native structure. Adsorption immobilization is considered to have the lowest impact on enzyme structure and shows maximum activity compared to other immobilization methods.[79] Higher relative enzyme activity would therefore be expected when comparing between protease-EFSBN-PEO and CALB-EFSBN-PCL. The substrate diffusion barrier to the immobilized enzymes active pocket might be one of the reasons to get lower activity. On the other hand, with a free CALB hydrolytic activity assay, no diffusion barrier

happened. However, decreasing the diffusion barrier (e.g., continuous shaking or stirring) between solid CALB-EFSBN-PS reaction sites and liquid substrate would increase the hydrolytic activity and relative activity.

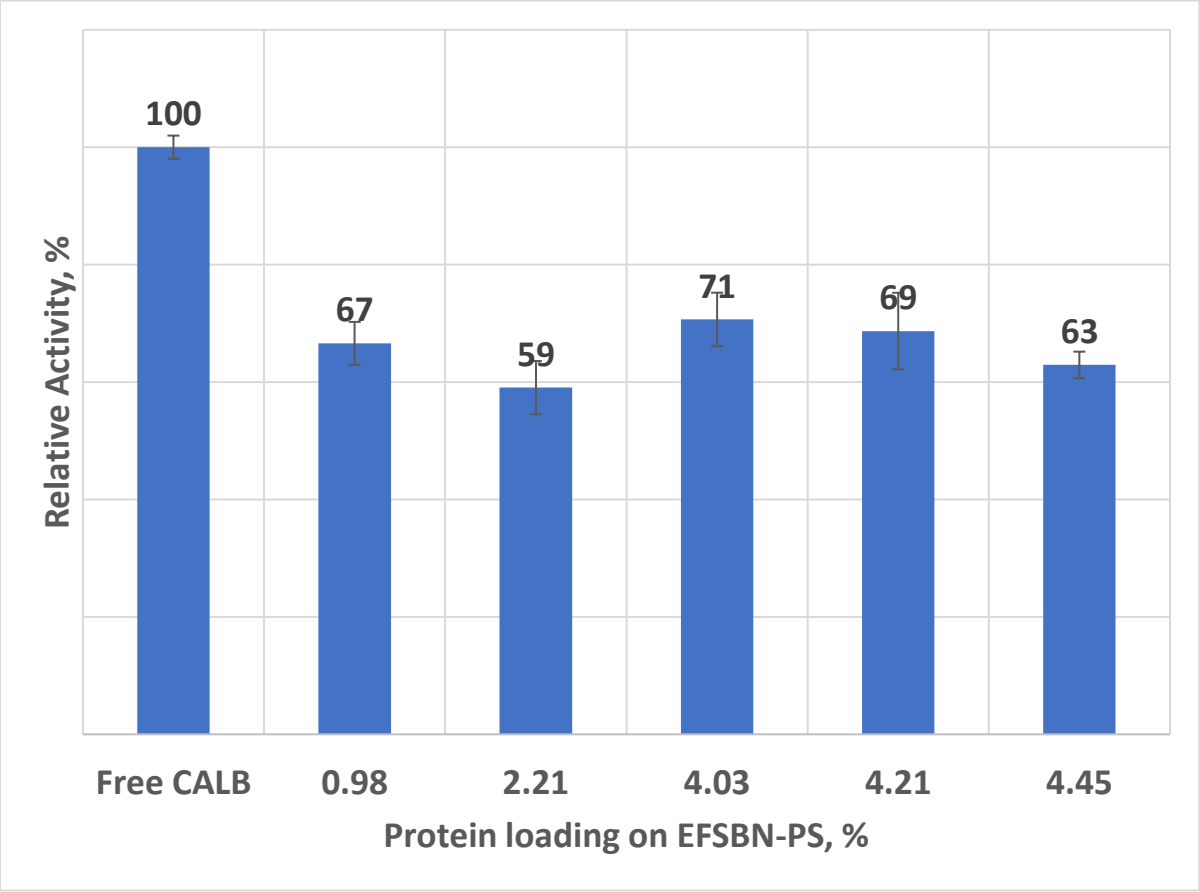

Figure 4.8: Relative catalytic activity of CALB-EFSBN-PS webs to free CALB activity with varying protein content in the solid webs.

4.3.8. Optimum temperature and thermal stability of free CALB and CALB-EFSBN-PS

The effect of temperature on the free CALB and adsorbed CALB-EFSBN-PS hydrolytic activity has been studied in the range of 30 to 70 ℃. The optimum temperature for both free CALB and immobilized CALB was around 40 ℃ (**Figure 4.9**). Free CALB and immobilized CALB had the same

trend before the optimum temperature (40 °C), while CALB-EFSBN-PS showed better performance in higher temperatures. In lower temperatures, conformational changes do not occur; also, the relative activity of immobilized and free enzymes shows the same trends, but at higher temperatures, conformational changes are reported to occur in the free enzyme,[149] therefore, the activity of the free enzyme decreased because of denaturation phenomena. CALB-EFSBN-PS showed a wider temperature activity profile than free CALB, which implies more industrial applicability of immobilized CALB.

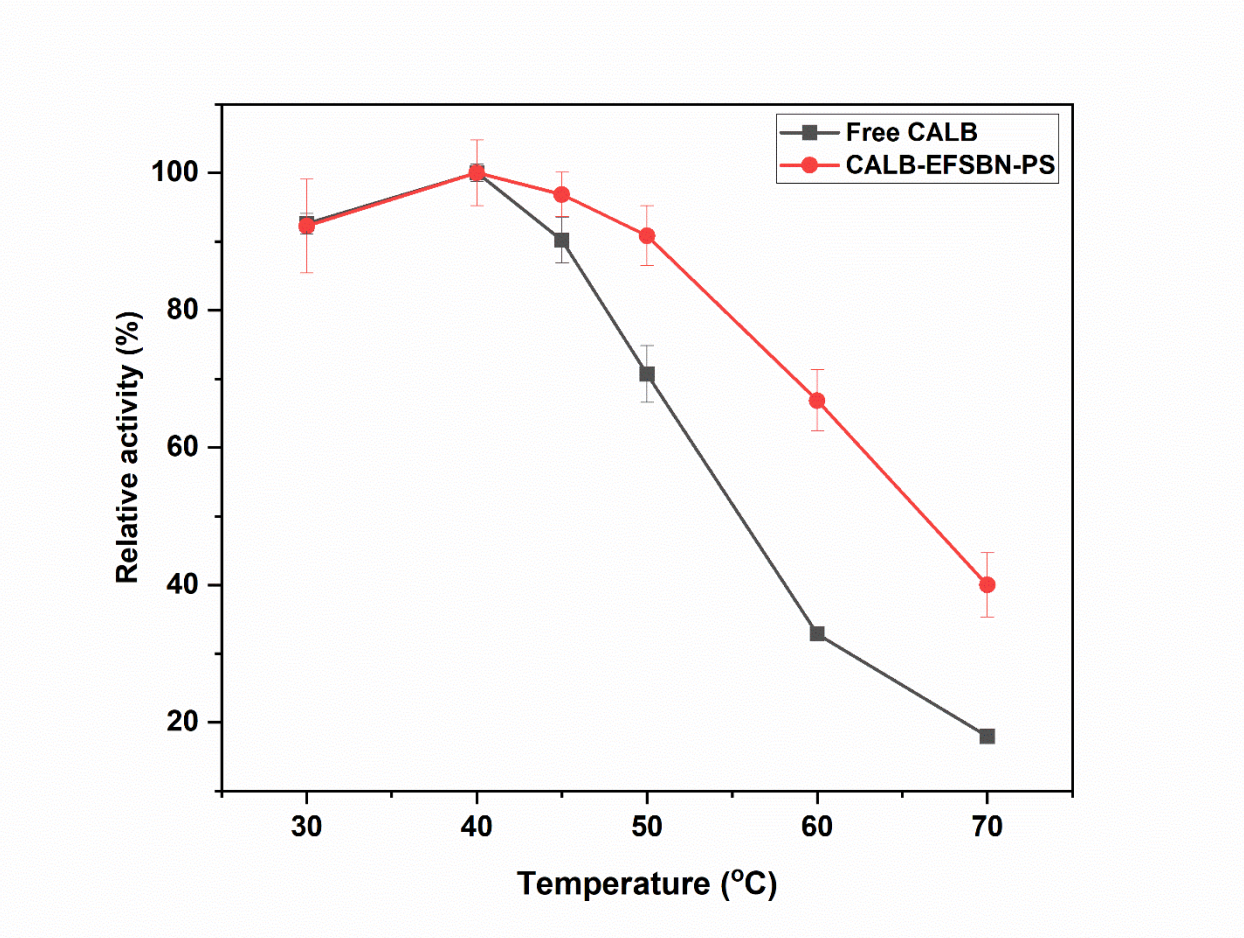

Figure 4.9: Optimum temperature comparison of free CALB and immobilized CALB (4.03 wt%) on EFSBN-PS.

The thermal stability of immobilized enzymes is another important factor for their application and storage at higher temperatures for prolonged periods. In this study, free CALB diluted (1 µl/ml) in tris buffer (100 mM, pH 8.0) and soaked solid EFSBN-PS webs in the same buffer were incubated at 45 ℃ for up to 12 hr to determine the thermal stability of lipase. The relative remaining activities of free CALB and immobilized CALB are presented in **Figure 4.10.** Both enzymes lost their hydrolytic activity with time, but immobilized CALB had more stability than free CALB. This higher thermal stability to thermal inactivation can be attributed to the dry nanofiber matrix helps prevent immobilized enzyme molecules from unfolding. Therefore, immobilization led to a considerable increase in thermal stability, which is often seen with immobilized enzymes.[99]

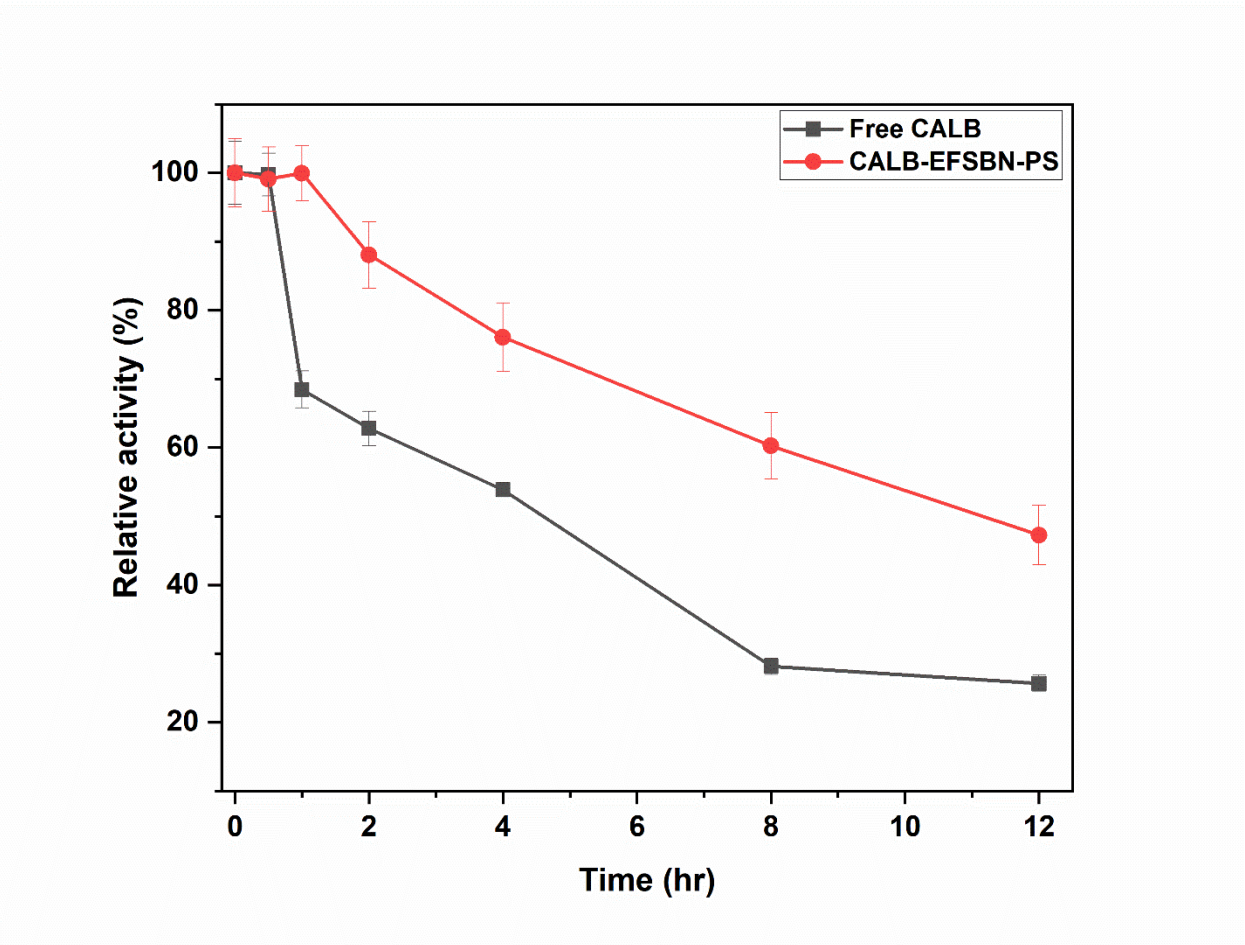

Figure 4.10: Thermal stability of free CALB and adsorbed CALB (4.03 wt%) on EFSBN-PS nanofiber webs at 45 ℃.

4.3.9. Storage stability of EFSBN-PCL and free CALB in buffer

Enzyme storage stability has been correlated to structural stability and remaining activity over time at storage conditions. Frequently, by physically stabilizing the enzyme structure, the storage stability of enzymes increases on immobilization with polymeric carriers.[82] Storage stability tests were performed by placing samples of each enzyme-loaded web at 4 ℃ and measuring the remaining activity over time. Activity found at each time point was calculated with the initial activity considered as 100%. The storage stability of 4.03 wt% CALB-loaded EFSBN-PS is presented in **Figure 4.11.** The result shows immobilized CALB had excellent stability for 90 days, almost fully

maintaining its initial activity. Therefore, the immobilization of CALB on SBN-PS nanofibers improves the stability of CALB and helps to maintain its activity for a longer time.

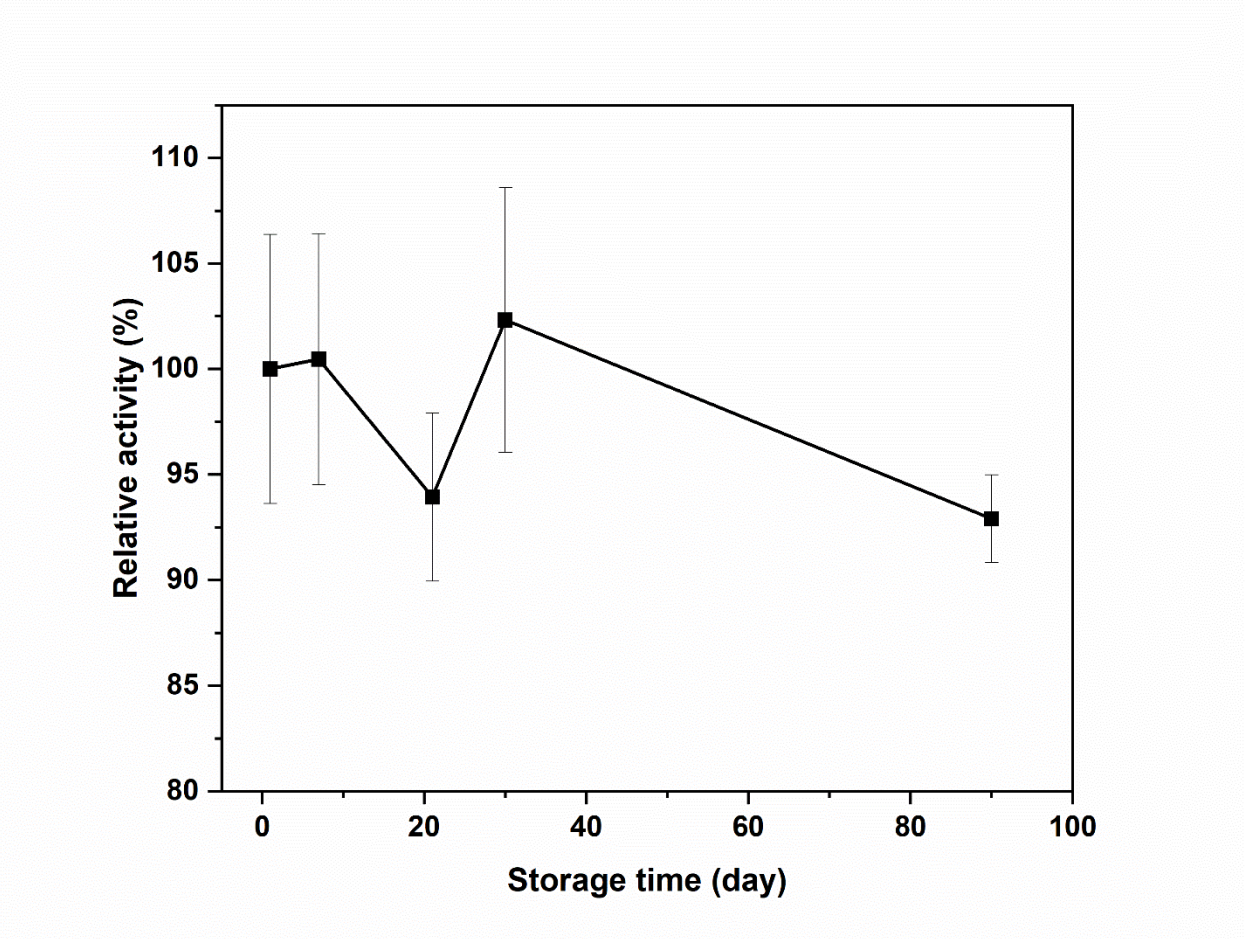

Figure 4.11: Storage stability (retaining activity with time) of 4.03 wt% CALB-EFSBN-PS webs at refrigerator temperature (4 ℃).

4.3.10. Reusability of EFSBN-PS

Reuse is one of the most important parameters to evaluate immobilized enzymes' economic viability and industrial application. Improvement in operational stability makes the use of immobilized enzymes more advantageous than soluble enzymes. However, adsorbed enzymes suffer from the problem of leaching and activity loss. Reusability testing reveals the degree of leaching and activity loss with repeatable applications. The immobilized CALB activity decreased

very slowly after it was repeatedly reused (**Figure 4.12**) The enzyme retained around 70 % of its initial activity after 15 reuse cycles. However, the first use cycle lost activity by about 15%, which might be the leaching out of loosely bound protein on the surface. After first use, immobilized CALB enzymes behave as though they are firmly attached to the nanofiber surface, revealing a robust hydrophobic interaction between enzymes and the PS nanofiber carrier. So, the CALB-EFSBN-PS is an excellent immobilized carrier with good thermal stability, storage stability, and reusability, making it a perfect biocatalyst for more harsh conditions.

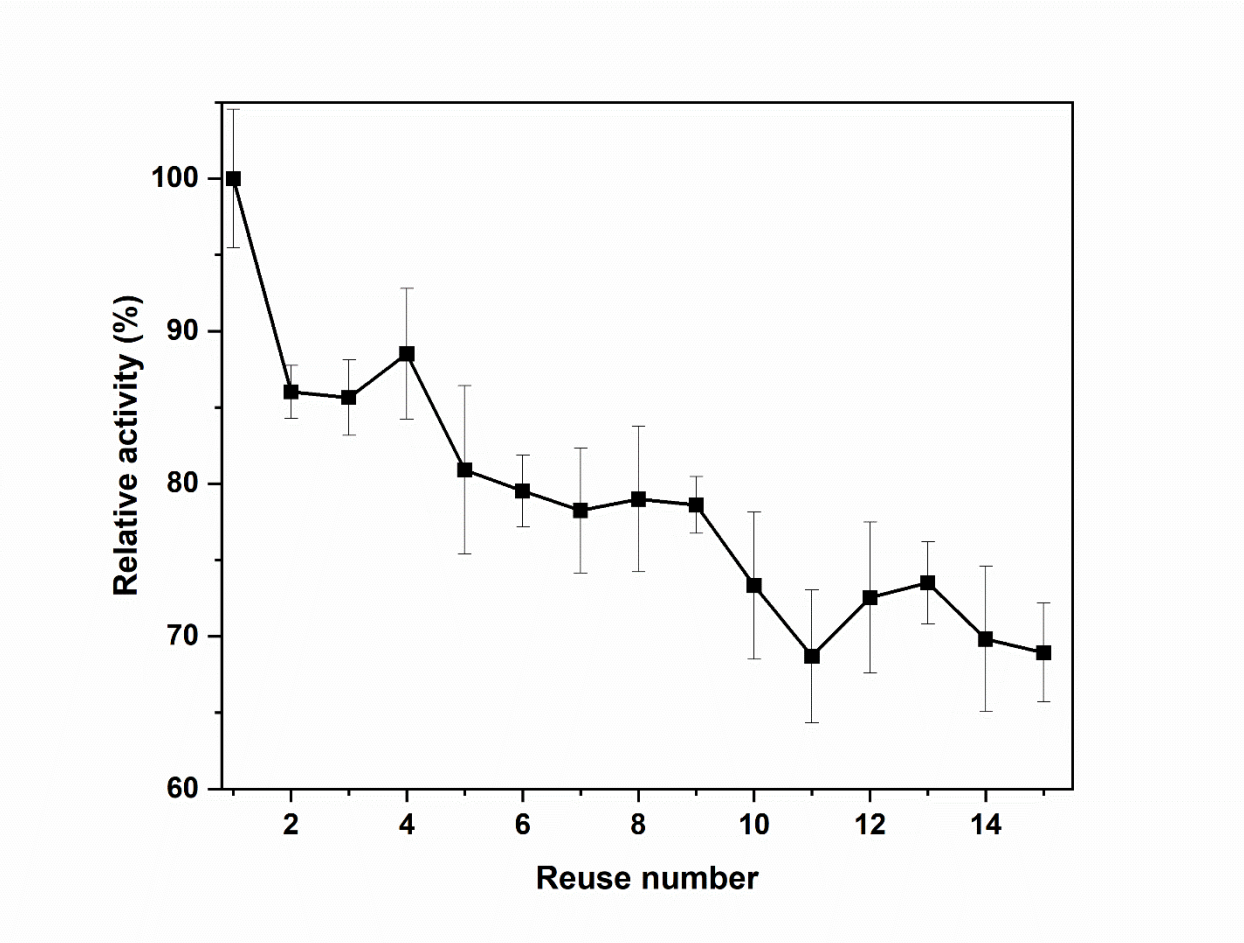

Figure 4.12: Reusability of 4.03 wt% CALB-EFSBN-PS nanofiber webs at lipase assay trials.

4.4. Conclusions

Polystyrene solution-blown nanofibrous nonwoven webs are an excellent support for CALB immobilization because of the following: (a) SBN-PS nanofibers can be prepared economically in a short time in large amounts with a uniform smooth surface; (b) they can immobilize large amounts of protein (4.45 mg protein/100 mg SBN-PS webs); and, (c) they can immobilize the enzymes without any modification by simple adsorption binding due to the highly hydrophobic nature of PS. In this study, the solid immobilization carrier SBN-PS nanofibers webs were produced by the solution blow spinning (SBS) process. SBS is a practical and feasible method to produce nanofibers at high rates without the use of high-voltage electrical charges. The morphologies and diameters of the fibers depended on the process parameters, such as the solution flow rate, air pressure, air temperature, die-to-collector distance, and spinning (PS polymer) solution. The solution concentration and air pressure greatly influenced the fiber diameter and web uniformity, respectively. Lipase from *Candida sp*. (CALB) lipase was strongly adsorbed on polystyrene solution-blown nanofibrous webs. SBN-PS was a good support material for lipase immobilization in terms of protein loadings, activity yield, and operational and thermal stability of enzymes. The highest amount of protein immobilization on SBN-PS nanofibers was 4.45 mg protein/100 mg webs (or 4.45% by mass). Immobilization yield decreased with increasing enzyme concentration in the buffer solution. The highest immobilization yield of 82% was found at low enzyme loading indicating high enzyme affinity to PS. Across the full protein loading range (0.98-4.45 wt%), enzyme activity measurements were relatively constant (59-71%). Combined with XPS surface analysis and laser confocal microscopy imaging, the position and distribution of the CALB on the PCL nanofibers were revealed, and homogeneously distributed

adsorption was confirmed. The SEM micrograph analysis revealed no change in web morphology after immobilization which implied that the hydrophobic interactions were the driving force of the immobilization process. Immobilized CALB enzymes retained almost similar activity to the freshly prepared EFSBN-PS webs after 90 days of storage at 4 °C. In addition, the operational stability was kept at over 70% of its initial activity after 15 cycles of reuse. Immobilized CALB showed wider optimum catalytic activity and high thermal stability compared to the free soluble enzyme, an important parameter for industrial applications. The methodology developed in this research work is simple and effective; the newly immobilized lipase could be used in several applications, such as oil hydrolysis and biodiesel synthesis.

Chapter 5: Outlook and Path Forward

This dissertation research developed a new class of enzyme-functionalized solution-blown nonwoven bio-catalytic materials by combing synthetic polymers and enzyme biocatalysts. This work would have implications in various fields, including the washing industry, degradable packaging, filtration industry, and other applications. The field of solution blow spinning (SBS) has flourished within the last 7-8 years, many polymers have been trialed with the SBS process, and new application fields have also grown. However, we are the pioneer of the single-step co-immobilization of enzymes using the solution-blown spinning process. In this work, we studied the SBS process for three functionally different polymers (PEO, water-soluble; PCL, water-insoluble and biodegradable; and PS, water-insoluble and durable). This opens a vast window where other enzyme-compatible polymer pairs can be explored to produce enzyme-functionalized solution blown nonwovens. Although the made EFSBN webs showed excellent activity and stability in lab-scale preparation, the author believes significant advancement is still needed to commercialize the EFSBN. For instance, limitations like the low production rate of EFSBN-PEO webs, relatively large fiber diameter and beads formations for high enzyme loading EFSBN, and the stability of water-in-oil micro-emulsion of the bulk quantity aqueous enzyme in polymer organic solvent solution need to be addressed. To overcome these challenges, a variety of areas of improvement are discussed below that the author believes to be key elements for future research.

Chapter 2 studied the preparation, physiochemical properties, activity, and anticipated validated application features of protease-EFSBN-PEO nanofibrous webs. A wide range (0.62-7.43 wt%) of

enzymes were included directly in the PEO solution blown nanofibrous webs, however, the position of enzymes in nanofibers (inside or outside) still needs further validation. For low protease loaded (e.g., 1.3 wt%)-EFSBN-EFBN-PEO, ToF-SIMS analysis did not detect significant protein molecules on the nanofibers surfaces (depth of analysis 2 nm), implying that enzymes are embedded inside the fibers, which is consistent with the detected level of enzyme activity. On the other hand, ToF-SIMS produced characteristic nitrogen ion signals for high protease loaded (e.g., 7.4 wt%)-EFSBN-PEO webs, confirming the presence of enzymes at the fiber surfaces. The XPS analysis penetrates deeper into the sample (~10 nm depth) and found protein presence for both low and high enzyme-loading EFSBN-PEO. Together, the ToF-SIMS and XPS analyses imply that enzymes are mainly located inside the fiber, and this is consistent with enzyme activity analysis. Still, additional evidence (e.g., TEM analysis) is recommended for determining the exact position of enzymes in nanofibers. Regardless of the exact distribution of enzymes through the fiber cross section, the produced EFSBN webs had excellent catalytic activity and stability, but the fiber production rate was low. The high surface tension of water and hydrogen bonding with the PEO chains makes it a difficult solvent to evaporate from the polymer solution and solidify the polymer. In future work, the spinning solution formulation could be modified to reduce the surface tension of the solvent and accelerate solvent evaporation in SBS. Developing a multi-needle solution spinning process would be interesting to increase the fiber production rate. Studies involving other aqueous-soluble polymers, such as polyvinyl alcohol (PVA) or blends such as PEO-PVA, and enzymes, such as lipases, would be interesting to consider. In addition, protease-EFSBN-PEO webs would likely be a successful application in the laundry industry, but it needs to be explored. Another interesting area would be using water-soluble enzyme-entrapped

solution-blown nonwoven webs (e.g., CALB-EFSBN) in organic media reactions (such as transesterification).

Chapter 3 developed a rapid enzymatic degradable material (EFSBN-PCL webs using chloroform solvent) by solution blow spinning. Such a system is highly relevant for the degradable packaging industry. The next step would be a feasibility study of EFSBN-PCL webs for degradable packaging applications. In this work, SBN-PCL webs were also successfully produced using dichloromethane (DCM) solvent, but a full battery of testing was not carried out. Therefore, further trials for creating EFSBN-PCL using DCM solvent should be explored. Other polymer-solvent-enzyme triads (e.g., α-chymotrypsin-toluene-polystyrene) could also be explored for producing EFSBN. In addition, the literature review discussed a two-solvent approach to produce enzyme-compatible polymer solution triads that could be researched for making enzyme-functionalized solution blown nonwovens by solution blow spinning.

Chapter 4 described a process where CALB was physically adsorbed on SBN-PS nanofibrous webs by two-step post-immobilization method (step-1: SBN-PS fabrication and step 2: CALB immobilization to produce EFSBN-PS). While the two-step method was very effective, it is still interesting to consider whether a single-step co-immobilization, as the most straightforward approach to entrap enzymes, could be developed for enzyme entrapment in durable polymers (PS) by the SBS process. A known challenge with this approach is that enzyme active sites could be blocked by hydrophobic polymer matrices during material fabrication, and more research is

needed to overcome this issue. Imparting matrix porosity and increasing surface area are two approaches that can help.

Thus, there is still much to be accomplished in the research area of selecting polymer-solvent-enzyme combinations and optimized corresponding solution blow spinning parameters, and we look forward to seeing future innovations.

REFERENCES

(1) Kumar, A.; Gudiukaite, R.; Gricajeva, A.; Sadauskas, M.; Malunavicius, V.; Kamyab, H.; Sharma, S.; Sharma, T.; Pant, D. Microbial Lipolytic Enzymes – Promising Energy-Efficient Biocatalysts in Bioremediation. *Energy* **2020**, *192*, 116674. https://doi.org/10.1016/j.energy.2019.116674.

(2) Milczek, E. M. Commercial Applications for Enzyme-Mediated Protein Conjugation: New Developments in Enzymatic Processes to Deliver Functionalized Proteins on the Commercial Scale. *Chem. Rev.* **2018**, *118* (1), 119–141. https://doi.org/10.1021/acs.chemrev.6b00832.

(3) Gruber, P.; Marques, M. P. C.; Sulzer, P.; Wohlgemuth, R.; Mayr, T.; Baganz, F.; Szita, N. Real-Time PH Monitoring of Industrially Relevant Enzymatic Reactions in a Microfluidic Side-Entry Reactor (MSER) Shows Potential for PH Control. *Biotechnol. J.* **2017**, *12* (6), 1–13. https://doi.org/10.1002/biot.201600475.

(4) Khan, M. N.; Luna, I. Z.; Islam, M. M.; Sharmeen, S.; Salem, K. S.; Rashid, T. U.; Zaman, A.; Haque, P.; Rahman, M. M. Cellulase in Waste Management Applications. In *New and Future Developments in Microbial Biotechnology and Bioengineering*; Elsevier, 2016; pp 237–256. https://doi.org/10.1016/B978-0-444-63507-5.00021-6.

(5) Wu, S.; Snajdrova, R.; Moore, J. C.; Baldenius, K.; Bornscheuer, U. T. Biocatalysis: Enzymatic Synthesis for Industrial Applications. *Angew. Chemie - Int. Ed.* **2021**, *60* (1), 88–119. https://doi.org/10.1002/anie.202006648.

(6) Kaluzna, I.; Schmitges, T.; Straatman, H.; Van Tegelen, D.; Müller, M.; Schürmann, M.; Mink, D. Enabling Selective and Sustainable P450 Oxygenation Technology. Production of

4-Hydroxy-α-Isophorone on Kilogram Scale. *Org. Process Res. Dev.* **2016**, *20* (4), 814–819. https://doi.org/10.1021/acs.oprd.5b00282.

(7) Bastürk, E.; Demir, S.; Danis, O.; Kahraman, M. V. Covalent Immobilization of α-Amylase onto Thermally Crosslinked Electrospun PVA/PAA Nanofibrous Hybrid Membranes. *Journal of Applied Polymer Science*. 2013, pp 349–355. https://doi.org/10.1002/app.37901.

(8) Rojas-Mercado, A. S.; Moreno-Cortez, I. E.; Lucio-Porto, R.; Pavón, L. L. Encapsulation and Immobilization of Ficin Extract in Electrospun Polymeric Nanofibers. *Int. J. Biol. Macromol.* **2018**, *118*, 2287–2295. https://doi.org/10.1016/j.ijbiomac.2018.07.113.

(9) Ingle, A. P.; Rathod, J.; Pandit, R.; da Silva, S. S.; Rai, M. Comparative Evaluation of Free and Immobilized Cellulase for Enzymatic Hydrolysis of Lignocellulosic Biomass for Sustainable Bioethanol Production. *Cellulose* **2017**, *24* (12), 5529–5540. https://doi.org/10.1007/s10570-017-1517-1.

(10) Sel, E.; Ulu, A.; Ateş, B.; Köytepe, S. Comparative Study of Catalase Immobilization via Adsorption on P(MMA-Co-PEG500MA) Structures as an Effective Polymer Support. *Polym. Bull.* **2021**, *78* (5), 2663–2684. https://doi.org/10.1007/s00289-020-03233-0.

(11) Lai, E.; Wang, Y.; Wei, Y.; Li, G.; Ma, G. Covalent Immobilization of Trypsin onto Thermo-Sensitive Poly(N-Isopropylacrylamide-Co-Acrylic Acid) Microspheres with High Activity and Stability. *J. Appl. Polym. Sci.* **2016**, *133* (21), 1–9. https://doi.org/10.1002/app.43343.

(12) Rao, N. N.; Lu, S.; Ju, F. Continuous Biocatalytic Processes. *Org. Process Res. Dev.* **2009**, *13* (3), 607–616.

(13) Mateo, C.; Palomo, J. M.; Fernandez-Lorente, G.; Guisan, J. M.; Fernandez-Lafuente, R.

Improvement of Enzyme Activity, Stability and Selectivity via Immobilization Techniques. *Enzyme Microb. Technol.* **2007**, *40* (6), 1451–1463. https://doi.org/10.1016/j.enzmictec.2007.01.018.

(14) Rodrigues, R. C.; Ortiz, C.; Berenguer-Murcia, Á.; Torres, R.; Fernández-Lafuente, R. Modifying Enzyme Activity and Selectivity by Immobilization. *Chem. Soc. Rev.* **2013**, *42* (15), 6290–6307. https://doi.org/10.1039/c2cs35231a.

(15) Yushkova, E. D.; Nazarova, E. A.; Matyuhina, A. V.; Noskova, A. O.; Shavronskaya, D. O.; Vinogradov, V. V.; Skvortsova, N. N.; Krivoshapkina, E. F. Application of Immobilized Enzymes in Food Industry. *J. Agric. Food Chem.* **2019**, *67* (42), 11553–11567. https://doi.org/10.1021/acs.jafc.9b04385.

(16) Hayes, S. T.; Assaf, G.; Checksfield, G.; Cheung, C.; Critcher, D.; Harris, L.; Howard, R.; Mathew, S.; Regius, C.; Scotney, G.; Scott, A. Commercial Synthesis of (S,S)-Reboxetine Succinate: A Journey to Find the Cheapest Commercial Chemistry for Manufacture. *Org. Process Res. Dev.* **2011**, *15* (6), 1305–1314. https://doi.org/10.1021/op200181f.

(17) Lopes, M. M.; Coutinho, T. C.; Malafatti, J. O. D.; Paris, E. C.; Sousa, C. P. de; Farinas, C. S. Immobilization of Phytase on Zeolite Modified with Iron(II) for Use in the Animal Feed and Food Industry Sectors. *Process Biochem.* **2021**, *100* (November 2020), 260–271. https://doi.org/10.1016/j.procbio.2020.10.017.

(18) Fortes, C. C. S.; Daniel-da-Silva, A. L.; Xavier, A. M. R. B.; Tavares, A. P. M. Optimization of Enzyme Immobilization on Functionalized Magnetic Nanoparticles for Laccase Biocatalytic Reactions. *Chem. Eng. Process. Process Intensif.* **2017**, *117* (March), 1–8. https://doi.org/10.1016/j.cep.2017.03.009.

(19) Tufvesson, P.; Lima-Ramos, J.; Nordblad, M.; Woodley, J. M. Guidelines and Cost Analysis for Catalyst Production in Biocatalytic Processes. *Org. Process Res. Dev.* **2011**, *15* (1), 266–274. https://doi.org/10.1021/op1002165.

(20) Truppo, M. D. Biocatalysis in the Pharmaceutical Industry: The Need for Speed. *ACS Med. Chem. Lett.* **2017**, *8* (5), 476–480. https://doi.org/10.1021/acsmedchemlett.7b00114.

(21) Bhosale, S. H.; Rao, M. B.; Deshpande, V. V. Molecular and Industrial Aspects of Glucose Isomerase. *Microbiol. Rev.* **1996**, *60* (2), 280–300. https://doi.org/10.1128/mmbr.60.2.280-300.1996.

(22) Coutinho, T. C.; Tardioli, P. W.; Farinas, C. S. Phytase Immobilization on Hydroxyapatite Nanoparticles Improves Its Properties for Use in Animal Feed. *Appl. Biochem. Biotechnol.* **2020**, *190* (1), 270–292. https://doi.org/10.1007/s12010-019-03116-9.

(23) Soleimani, M.; Khani, A.; Najafzadeh, K. α-Amylase Immobilization on the Silica Nanoparticles for Cleaning Performance towards Starch Soils in Laundry Detergents. *J. Mol. Catal. B Enzym.* **2012**, *74* (1–2), 1–5. https://doi.org/10.1016/j.molcatb.2011.07.011.

(24) Basso, A.; Serban, S. Industrial Applications of Immobilized Enzymes—A Review. *Mol. Catal.* **2019**, *479* (March), 110607. https://doi.org/10.1016/j.mcat.2019.110607.

(25) Lu, S.; Wang, X.; Lu, Q.; Hu, X.; Uppal, N.; Omenetto, F. G.; Kaplan, D. L. Stabilization of Enzymes in Silk Films. *Biomacromolecules* **2009**, *10* (5), 1032–1042. https://doi.org/10.1021/bm800956n.

(26) Sulaiman, S.; Cieh, N. L.; Mokhtar, M. N.; Naim, M. N.; Kamal, S. M. M. Covalent Immobilization of Cyclodextrin Glucanotransferase on Kenaf Cellulose Nanofiber and Its

Application in Ultrafiltration Membrane System. *Process Biochem.* **2017**, *55*, 85–95. https://doi.org/10.1016/j.procbio.2017.01.025.

(27) Wu, R.; He, B. H.; Zhao, G. L.; Qian, L. Y.; Li, X. F. Immobilization of Pectinase on Oxidized Pulp Fiber and Its Application in Whitewater Treatment. *Carbohydr. Polym.* **2013**, *97* (2), 523–529. https://doi.org/10.1016/j.carbpol.2013.05.019.

(28) Khan, M. N.; Luna, I. Z.; Islam, M. M.; Sharmeen, S.; Salem, K. S.; Rashid, T. U.; Zaman, A.; Haque, P.; Rahman, M. M. Cellulase in Waste Management Applications. In *New and Future Developments in Microbial Biotechnology and Bioengineering*; Elsevier, 2016; pp 237–256. https://doi.org/10.1016/B978-0-444-63507-5.00021-6.

(29) Thomas, S.; Kirk, O.; Borchert, O. V.; Fuglsang, C. C.; Pedersen, S.; Slamon, S.; Olsen, H. S.; Deinhammer, R. and Lund, H. Enzymes for Technical Applications. In *Polysaccharides and polyamides in the food industry: properties, production, and patents*; Steinbuchel, A.; Rhee, S. K., Ed.; WILEY-VCH Verlag GMBH & Co. KGaA, 2005; pp 557–617.

(30) Cristóvão, R. O.; Silvério, S. C.; Tavares, A. P. M.; Brígida, A. I. S.; Loureiro, J. M.; Boaventura, R. A. R.; Macedo, E. A.; Coelho, M. A. Z. Green Coconut Fiber: A Novel Carrier for the Immobilization of Commercial Laccase by Covalent Attachment for Textile Dyes Decolourization. *World J. Microbiol. Biotechnol.* **2012**, *28* (9), 2827–2838. https://doi.org/10.1007/s11274-012-1092-4.

(31) Sathishkumar, P.; Kamala-Kannan, S.; Cho, M.; Kim, J. S.; Hadibarata, T.; Salim, M. R.; Oh, B. T. Laccase Immobilization on Cellulose Nanofiber: The Catalytic Efficiency and Recyclic Application for Simulated Dye Effluent Treatment. *J. Mol. Catal. B Enzym.* **2014**, *100*, 111–120. https://doi.org/10.1016/j.molcatb.2013.12.008.

(32) Jin, L. H.; Li, Y.; Ren, X. H.; Lee, J. H. Immobilization of Lactase onto Various Polymer Nanofibers for Enzyme Stabilization and Recycling. *J. Microbiol. Biotechnol.* **2015**, *25* (8), 1291–1298. https://doi.org/10.4014/jmb.1501.01012.

(33) Amaly, N.; Si, Y.; Chen, Y.; El-Moghazy, A. Y.; Zhao, C.; Zhang, R.; Sun, G. Reusable Anionic Sulfonate Functionalized Nanofibrous Membranes for Cellulase Enzyme Adsorption and Separation. *Colloids Surfaces B Biointerfaces* **2018**, *170* (May), 588–595. https://doi.org/10.1016/j.colsurfb.2018.06.019.

(34) Chen, P. C.; Huang, X. J.; Huang, F.; Ou, Y.; Chen, M. R.; Xu, Z. K. Immobilization of Lipase onto Cellulose Ultrafine Fiber Membrane for Oil Hydrolysis in High Performance Bioreactor. *Cellulose* **2011**, *18* (6), 1563–1571. https://doi.org/10.1007/s10570-011-9593-0.

(35) Zhang, Y. T.; Zhang, L.; Chen, H. L.; Zhang, H. M. Selective Separation of Low Concentration CO2 Using Hydrogel Immobilized CA Enzyme Based Hollow Fiber Membrane Reactors. *Chem. Eng. Sci.* **2010**, *65* (10), 3199–3207. https://doi.org/10.1016/j.ces.2010.02.010.

(36) Shen, J.; Yuan, Y.; Salmon, S. Carbonic Anhydrase Immobilized on Textile Structured Packing Using Chitosan Entrapment for CO 2 Capture. *ACS Sustain. Chem. Eng.* **2022**, *10* (23), 7772–7785. https://doi.org/10.1021/acssuschemeng.2c02545.

(37) Almeida, F. L. C.; Castro, M. P. J.; Travália, B. M.; Forte, M. B. S. Trends in Lipase Immobilization: Bibliometric Review and Patent Analysis. *Process Biochem.* **2021**, *110* (July), 37–51. https://doi.org/10.1016/j.procbio.2021.07.005.

(38) Alvarado-Ramírez, L.; Rostro-Alanis, M.; Rodríguez-Rodríguez, J.; Castillo-Zacarías, C.;

Sosa-Hernández, J. E.; Barceló, D.; Iqbal, H. M. N.; Parra-Saldívar, R. Exploring Current Tendencies in Techniques and Materials for Immobilization of Laccases – A Review. *Int. J. Biol. Macromol.* **2021**, *181*, 683–696. https://doi.org/10.1016/j.ijbiomac.2021.03.175.

(39) Imam, H. T.; Marr, P. C.; Marr, A. C. Enzyme Entrapment, Biocatalyst Immobilization without Covalent Attachment. *Green Chem.* **2021**, *23* (14), 4980–5005. https://doi.org/10.1039/d1gc01852c.

(40) geor malar, C.; Seenuvasan, M.; Kumar, K. S.; Kumar, A.; Parthiban, R. Review on Surface Modification of Nanocarriers to Overcome Diffusion Limitations: An Enzyme Immobilization Aspect. *Biochem. Eng. J.* **2020**, *158* (March), 107574. https://doi.org/10.1016/j.bej.2020.107574.

(41) Molina-Fernández, C.; Luis, P. Immobilization of Carbonic Anhydrase for CO2 Capture and Its Industrial Implementation: A Review. *J. CO2 Util.* **2021**, *47* (December 2020), 101475. https://doi.org/10.1016/j.jcou.2021.101475.

(42) Verma, M. L.; Kumar, S.; Das, A.; Randhawa, J. S.; Chamundeeswari, M. Chitin and Chitosan-Based Support Materials for Enzyme Immobilization and Biotechnological Applications. *Environ. Chem. Lett.* **2020**, *18* (2), 315–323. https://doi.org/10.1007/s10311-019-00942-5.

(43) Gennari, A.; Führ, A. J.; Volpato, G.; Volken de Souza, C. F. Magnetic Cellulose: Versatile Support for Enzyme Immobilization - A Review. *Carbohydr. Polym.* **2020**, *246* (March), 116646. https://doi.org/10.1016/j.carbpol.2020.116646.

(44) Girelli, A. M.; Astolfi, M. L.; Scuto, F. R. Agro-Industrial Wastes as Potential Carriers for Enzyme Immobilization: A Review. *Chemosphere* **2020**, *244*, 125368.

https://doi.org/10.1016/j.chemosphere.2019.125368.

(45) Liang, S.; Wu, X. L.; Xiong, J.; Zong, M. H.; Lou, W. Y. Metal-Organic Frameworks as Novel Matrices for Efficient Enzyme Immobilization: An Update Review. *Coord. Chem. Rev.* **2020**, *406*, 213149. https://doi.org/10.1016/j.ccr.2019.213149.

(46) Liu, J.; Ma, R. T.; Shi, Y. P. "Recent Advances on Support Materials for Lipase Immobilization and Applicability as Biocatalysts in Inhibitors Screening Methods"-A Review. *Anal. Chim. Acta* **2020**, *1101*, 9–22. https://doi.org/10.1016/j.aca.2019.11.073.

(47) Sharifi, M.; Sohrabi, M. J.; Hosseinali, S. H.; Hasan, A.; Kani, P. H.; Talaei, A. J.; Karim, A. Y.; Nanakali, N. M. Q.; Salihi, A.; Aziz, F. M.; Yan, B.; Khan, R. H.; Saboury, A. A.; Falahati, M. Enzyme Immobilization onto the Nanomaterials: Application in Enzyme Stability and Prodrug-Activated Cancer Therapy. *Int. J. Biol. Macromol.* **2020**, *143*, 665–676. https://doi.org/10.1016/j.ijbiomac.2019.12.064.

(48) Wong, J. X.; Ogura, K.; Chen, S.; Rehm, B. H. A. Bioengineered Polyhydroxyalkanoates as Immobilized Enzyme Scaffolds for Industrial Applications. *Front. Bioeng. Biotechnol.* **2020**, *8* (March). https://doi.org/10.3389/fbioe.2020.00156.

(49) Bilal, M.; Asgher, M.; Cheng, H.; Yan, Y.; Iqbal, H. M. N. Multi-Point Enzyme Immobilization, Surface Chemistry, and Novel Platforms: A Paradigm Shift in Biocatalyst Design. *Crit. Rev. Biotechnol.* **2019**, *39* (2), 202–219. https://doi.org/10.1080/07388551.2018.1531822.

(50) Chapman, R.; Stenzel, M. H. All Wrapped up: Stabilization of Enzymes within Single Enzyme Nanoparticles. *J. Am. Chem. Soc.* **2019**, *141* (7), 2754–2769. https://doi.org/10.1021/jacs.8b10338.

(51) Hong, T.; Liu, W.; Li, M.; Chen, C. Recent Advances in the Fabrication and Application of Nanomaterial-Based Enzymatic Microsystems in Chemical and Biological Sciences. *Anal. Chim. Acta* **2019**, *1067*, 31–47. https://doi.org/10.1016/j.aca.2019.02.031.

(52) Lu, Y.; Lv, Q.; Liu, B.; Liu, J. Immobilized Candida Antarctica Lipase B Catalyzed Synthesis of Biodegradable Polymers for Biomedical Applications. *Biomater. Sci.* **2019**, *7* (12), 4963–4983. https://doi.org/10.1039/c9bm00716d.

(53) Sun, Y.; Cheng, S.; Lu, W.; Wang, Y.; Zhang, P.; Yao, Q. Electrospun Fibers and Their Application in Drug Controlled Release, Biological Dressings, Tissue Repair, and Enzyme Immobilization. *RSC Adv.* **2019**, *9* (44), 25712–25729. https://doi.org/10.1039/c9ra05012d.

(54) Thangaraj, B.; Solomon, P. R. Immobilization of Lipases – A Review. Part I: Enzyme Immobilization. *ChemBioEng Rev.* **2019**, *6* (5), 157–166. https://doi.org/10.1002/cben.201900016.

(55) Thangaraj, B.; Solomon, P. R. Immobilization of Lipases – A Review. Part II: Carrier Materials. *ChemBioEng Rev.* **2019**, *6* (5), 167–194. https://doi.org/10.1002/cben.201900017.

(56) Zhang, H.; Li, H.; Xu, C. C.; Yang, S. Heterogeneously Chemo/Enzyme-Functionalized Porous Polymeric Catalysts of High-Performance for Efficient Biodiesel Production. *ACS Catal.* **2019**, *9* (12), 10990–11029. https://doi.org/10.1021/acscatal.9b02748.

(57) Neeraj, G.; Ravi, S.; Somdutt, R.; Ravi, S. A. K.; Kumar, V. V. Immobilized Inulinase: A New Horizon of Paramount Importance Driving the Production of Sweetener and Prebiotics. *Crit. Rev. Biotechnol.* **2018**, *38* (3), 409–422.

https://doi.org/10.1080/07388551.2017.1359146.

(58) Martinović, T.; Josić, D. Polymethacrylate-Based Monoliths as Stationary Phases for Separation of Biopolymers and Immobilization of Enzymes. *Electrophoresis* **2017**, *38* (22–23), 2821–2826. https://doi.org/10.1002/elps.201700255.

(59) Sulaiman, S.; Mokhtar, M. N.; Naim, M. N.; Baharuddin, A. S.; Sulaiman, A. A Review: Potential Usage of Cellulose Nanofibers (CNF) for Enzyme Immobilization via Covalent Interactions. *Appl. Biochem. Biotechnol.* **2014**, *175* (4), 1817–1842. https://doi.org/10.1007/s12010-014-1417-x.

(60) Jesionowski, T.; Zdarta, J.; Krajewska, B. Enzyme Immobilization by Adsorption: A Review. *Adsorption* **2014**, *20* (5–6), 801–821. https://doi.org/10.1007/s10450-014-9623-y.

(61) Homaei, A. A.; Sariri, R.; Vianello, F.; Stevanato, R. Enzyme Immobilization: An Update. *J. Chem. Biol.* **2013**, *6* (4), 185–205. https://doi.org/10.1007/s12154-013-0102-9.

(62) Ansari, S. A.; Husain, Q. Potential Applications of Enzymes Immobilized on/in Nano Materials: A Review. *Biotechnol. Adv.* **2012**, *30* (3), 512–523. https://doi.org/10.1016/j.biotechadv.2011.09.005.

(63) Wang, Z. G.; Wan, L. S.; Liu, Z. M.; Huang, X. J.; Xu, Z. K. Enzyme Immobilization on Electrospun Polymer Nanofibers: An Overview. *J. Mol. Catal. B Enzym.* **2009**, *56* (4), 189–195. https://doi.org/10.1016/j.molcatb.2008.05.005.

(64) Klibanov, A. M. Improving Enzymes by Uisng Them in Organic Solvents. *Nature* **2001**, *409*, 241–246.

(65) Krishna, S. H. Developments and Trends in Enzyme Catalysis in Nonconventional Media. *Biotechnol. Adv.* **2002**, *20* (3–4), 239–267.

(66) Stepankova, V.; Bidmanova, S.; Koudelakova, T.; Prokop, Z.; Chaloupkova, R.; Damborsky, J. Strategies for Stabilization of Enzymes in Organic Solvents. *ACS Catal.* **2013**, *3* (12), 2823–2836. https://doi.org/10.1021/cs400684x.

(67) Silva, C.; Martins, M.; Jing, S.; Fu, J.; Cavaco-Paulo, A. Practical Insights on Enzyme Stabilization. *Crit. Rev. Biotechnol.* **2018**, *38* (3), 335–350. https://doi.org/10.1080/07388551.2017.1355294.

(68) Salihu, A.; Alam, M. Z. Solvent Tolerant Lipases: A Review. *Process Biochem.* **2015**, *50* (1), 86–96. https://doi.org/10.1016/j.procbio.2014.10.019.

(69) Rehm, F.; Chen, S.; Rehm, B. Enzyme Engineering for In Situ Immobilization. *Molecules* **2016**, *21* (10), 1370. https://doi.org/10.3390/molecules21101370.

(70) Salem, K. S.; Rashid, T. U.; Asaduzzaman; Islam, M. M.; Khan, M. N.; Sharmeen, S.; Rahman, M. M.; Haque, P. Recent Updates on Immobilization of Microbial Cellulase. In *New and Future Developments in Microbial Biotechnology and Bioengineering*; Elsevier, 2016; pp 107–139. https://doi.org/10.1016/B978-0-444-63507-5.00011-3.

(71) Liu, D. M.; Chen, J.; Shi, Y. P. Advances on Methods and Easy Separated Support Materials for Enzymes Immobilization. *TrAC - Trends Anal. Chem.* **2018**, *102*, 332–342. https://doi.org/10.1016/j.trac.2018.03.011.

(72) Nawaz, M. A.; Pervez, S.; Rehman, H. U.; Jamal, M.; Jan, T.; Hazrat, A.; Attaullah, M.; Khan, W.; Qader, S. A. U. Utilization of Different Polymers for the Improvement of Catalytic Properties and Recycling Efficiency of Bacterial Maltase. *Int. J. Biol. Macromol.* **2020**, *163*, 1344–1352. https://doi.org/10.1016/j.ijbiomac.2020.07.166.

(73) Thangaraj, B.; Solomon, P. R. Immobilization of Lipases – A Review. Part I: Enzyme

Immobilization. *ChemBioEng Rev.* **2019**, *6* (5), 157–166. https://doi.org/10.1002/cben.201900016.

(74) Primožič, M.; Kravanja, G.; Knez, Ž.; Crnjac, A.; Leitgeb, M. Immobilized Laccase in the Form of (Magnetic) Cross-Linked Enzyme Aggregates for Sustainable Diclofenac (Bio)Degradation. *J. Clean. Prod.* **2020**, *275*, 124121. https://doi.org/10.1016/j.jclepro.2020.124121.

(75) Sheldon, R. A.; van Pelt, S. Enzyme Immobilisation in Biocatalysis: Why, What and How. *Chem. Soc. Rev.* **2013**, *42* (15), 6223–6235. https://doi.org/10.1039/c3cs60075k.

(76) Galliani, M.; Santi, M.; Del Grosso, A.; Cecchettini, A.; Santorelli, F. M.; Hofmann, S. L.; Lu, J. Y.; Angella, L.; Cecchini, M.; Signore, G. Cross-Linked Enzyme Aggregates as Versatile Tool for Enzyme Delivery: Application to Polymeric Nanoparticles. *Bioconjug. Chem.* **2018**, *29* (7), 2225–2231. https://doi.org/10.1021/acs.bioconjchem.8b00206.

(77) Sheldon, R. A.; Schoevaart, R.; Van Langen, L. M. Cross-Linked Enzyme Aggregates (CLEAs): A Novel and Versatile Method for Enzyme Immobilization (a Review). *Biocatal. Biotransformation* **2005**, *23* (3–4), 141–147. https://doi.org/10.1080/10242420500183378.

(78) Xie, W.; Xiong, J.; Xiang, G. Enzyme Immobilization on Functionalized Monolithic CNTs-Ni Foam Composite for Highly Active and Stable Biocatalysis in Organic Solvent. *Mol. Catal.* **2020**, *483* (July 2019), 110714. https://doi.org/10.1016/j.mcat.2019.110714.

(79) Sassolas, A.; Blum, L. J.; Leca-Bouvier, B. D. Immobilization Strategies to Develop Enzymatic Biosensors. *Biotechnol. Adv.* **2012**, *30* (3), 489–511. https://doi.org/10.1016/j.biotechadv.2011.09.003.

(80) Aranaz, I.; Acosta, N.; Heras, A. Enzymatic D-p-Hydrophenyl Glycine Synthesis Using Chitin and Chitosan as Supports for Biocatalyst Immobilization. *Biocatal. Biotransformation* **2018**, *36* (2), 89–101. https://doi.org/10.1080/10242422.2017.1366991.

(81) Golshaei, R.; Karazehir, T.; Ghoreishi, S. M.; Ates, M.; Sarac, A. S. Glucose Oxidase Immobilization onto Au/Poly[Anthranilic Acid-Co-3-Carboxy-N-(2-Thenylidene)Aniline]/PVAc Electrospun Nanofibers. *Polym. Bull.* **2017**, *74* (5), 1493–1517. https://doi.org/10.1007/s00289-016-1786-0.

(82) Baştürk, E.; Demir, S.; Danış, Ö.; Kahraman, M. V. Covalent Immobilization of α-Amylase onto Thermally Crosslinked Electrospun PVA/PAA Nanofibrous Hybrid Membranes. *J. Appl. Polym. Sci.* **2013**, *127* (1), 349–355. https://doi.org/10.1002/app.37901.

(83) Monier, M.; El-Sokkary, A. M. A.; Sarhan, A. A. Immobilization of Candida Rugosa Lipase on Modified Natural Wool Fibers. *React. Funct. Polym.* **2010**, *70* (2), 122–128. https://doi.org/10.1016/j.reactfunctpolym.2009.11.004.

(84) Li, X.; Wang, X.; Ye, G.; Xia, W.; Wang, X. Polystyrene-Based Diazonium Salt as Adhesive: A New Approach for Enzyme Immobilization on Polymeric Supports. *Polymer (Guildf).* **2010**, *51* (4), 860–867. https://doi.org/10.1016/j.polymer.2009.12.036.

(85) Arslan, M. Immobilization Horseradish Peroxidase on Amine-Functionalized Glycidyl Methacrylate-g-Poly(Ethylene Terephthalate) Fibers for Use in Azo Dye Decolorization. *Polym. Bull.* **2011**, *66* (7), 865–879. https://doi.org/10.1007/s00289-010-0316-8.

(86) Talingtaisong, S.; Vongsetskul, T.; Panatdasirisuk, W.; Tangboriboonrat, P. Gauze-Reinforced Electrospun Regenerated Cellulose Ultrafine Fibers for Immobilizing

Bromelain. *Cellulose* **2017**, *24* (7), 2967–2975. https://doi.org/10.1007/s10570-017-1307-9.

(87) Tavernini, L.; Ottone, C.; Illanes, A.; Wilson, L. Entrapment of Enzyme Aggregates in Chitosan Beads for Aroma Release in White Wines. *Int. J. Biol. Macromol.* **2020**, *154*, 1082–1090. https://doi.org/10.1016/j.ijbiomac.2020.03.031.

(88) Zdarta, J.; Meyer, A.; Jesionowski, T.; Pinelo, M. A General Overview of Support Materials for Enzyme Immobilization: Characteristics, Properties, Practical Utility. *Catalysts* **2018**, *8* (2), 92. https://doi.org/10.3390/catal8020092.

(89) Cen, Y. K.; Liu, Y. X.; Xue, Y. P.; Zheng, Y. G. Immobilization of Enzymes in/on Membranes and Their Applications. *Adv. Synth. Catal.* **2019**, *361* (24), 5500–5515. https://doi.org/10.1002/adsc.201900439.

(90) Nguyen, H. H.; Kim, M. An Overview of Techniques in Enzyme Immobilization. *Appl. Sci. Converg. Technol.* **2017**, *26* (6), 157–163. https://doi.org/10.5757/ASCT.2017.26.6.157.

(91) Zhang, T.; Xu, X. L.; Jin, Y. N.; Wu, J.; Xu, Z. K. Immobilization of Horseradish Peroxidase (HRP) on Polyimide Nanofibers Blending with Carbon Nanotubes. *J. Mol. Catal. B Enzym.* **2014**, *106*, 56–62. https://doi.org/10.1016/j.molcatb.2014.04.015.

(92) Demirkan, E.; Avci, T.; Aykut, Y. Protease Immobilization on Cellulose Monoacetate/Chitosan-Blended Nanofibers. *J. Ind. Text.* **2018**, *47* (8), 2092–2111. https://doi.org/10.1177/1528083717720205.

(93) Pang, S.; Wu, Y.; Zhang, X.; Li, B.; Ouyang, J.; Ding, M. Immobilization of Laccase via Adsorption onto Bimodal Mesoporous Zr-MOF. *Process Biochem.* **2016**, *51* (2), 229–239. https://doi.org/10.1016/j.procbio.2015.11.033.

(94) Tran, D. N.; Balkus, K. J. Perspective of Recent Progress in Immobilization of Enzymes. *ACS Catal.* **2011**, *1* (8), 956–968. https://doi.org/10.1021/cs200124a.

(95) Hudson, S.; Magner, E.; Cooney, J.; Kieran, B. Methodology for the Immobilization of Enzymes onto Mesoporous Materials. *J. Phys. Chem. B* **2005**, *109* (41), 19496–19506. https://doi.org/10.1021/jp052102n.

(96) Mei, Y.; Miller, L.; Gao, W.; Gross, R. A. Imaging the Distribution and Secondary Structure of Immobilized Enzymes Using Infrared Microspectroscopy. *Biomacromolecules* **2003**, *4* (1), 70–74. https://doi.org/10.1021/bm025611t.

(97) Ortiz, C.; Ferreira, M. L.; Barbosa, O.; Dos Santos, J. C. S.; Rodrigues, R. C.; Berenguer-Murcia, Á.; Briand, L. E.; Fernandez-Lafuente, R. Novozym 435: The “Perfect” Lipase Immobilized Biocatalyst? *Catal. Sci. Technol.* **2019**, *9* (10), 2380–2420. https://doi.org/10.1039/c9cy00415g.

(98) Essa, H.; Magner, E.; Cooney, J.; Hodnett, B. K. Influence of PH and Ionic Strength on the Adsorption, Leaching and Activity of Myoglobin Immobilized onto Ordered Mesoporous Silicates. *J. Mol. Catal. B Enzym.* **2007**, *49* (1–4), 61–68. https://doi.org/10.1016/j.molcatb.2007.07.005.

(99) Cipolatti, E. P.; Valério, A.; Nicoletti, G.; Theilacker, E.; Araújo, P. H. H.; Sayer, C.; Ninow, J. L.; De Oliveira, D. Immobilization of Candida Antarctica Lipase B on PEGylated Poly(Urea-Urethane) Nanoparticles by Step Miniemulsion Polymerization. *J. Mol. Catal. B Enzym.* **2014**, *109*, 116–121. https://doi.org/10.1016/j.molcatb.2014.08.017.

(100) Simon, P.; Lima, J. S.; Valério, A.; De Oliveira, D.; Araújo, P. H. H.; Sayer, C.; De Souza, A. A. U.; Guelli U De Souza, S. M. A. Cellulase Immobilization on Poly(Methyl Methacrylate)

Nanoparticles by Miniemulsion Polymerization. *Brazilian J. Chem. Eng.* **2018**, *35* (2), 649–658. https://doi.org/10.1590/0104-6632.20180352s20160094.

(101) Melo, M. N.; Pereira, F. M.; Rocha, M. A.; Ribeiro, J. G.; Diz, F. M.; Monteiro, W. F.; Ligabue, R. A.; Severino, P.; Fricks, A. T. Immobilization and Characterization of Horseradish Peroxidase into Chitosan and Chitosan/PEG Nanoparticles: A Comparative Study. *Process Biochem.* **2020**, *98* (August), 160–171. https://doi.org/10.1016/j.procbio.2020.08.007.

(102) Valério, A.; Nicoletti, G.; Cipolatti, E. P.; Ninow, J. L.; Araújo, P. H. H.; Sayer, C.; de Oliveira, D. Kinetic Study of Candida Antarctica Lipase B Immobilization Using Poly(Methyl Methacrylate) Nanoparticles Obtained by Miniemulsion Polymerization as Support. *Appl. Biochem. Biotechnol.* **2015**, *175* (6), 2961–2971. https://doi.org/10.1007/s12010-015-1478-5.

(103) Chiaradia, V.; Valério, A.; De Oliveira, D.; Araújo, P. H. H.; Sayer, C. Simultaneous Single-Step Immobilization of Candida Antarctica Lipase B and Incorporation of Magnetic Nanoparticles on Poly(Urea-Urethane) Nanoparticles by Interfacial Miniemulsion Polymerization. *J. Mol. Catal. B Enzym.* **2016**, *131*, 31–35. https://doi.org/10.1016/j.molcatb.2016.06.004.

(104) Pereira, A. da S.; Diniz, M. M.; De Jong, G.; Gama Filho, H. S.; dos Anjos, M. J.; Finotelli, P. V.; Fontes-Sant'Ana, G. C.; Amaral, P. F. F. Chitosan-Alginate Beads as Encapsulating Agents for Yarrowia Lipolytica Lipase: Morphological, Physico-Chemical and Kinetic Characteristics. *Int. J. Biol. Macromol.* **2019**, *139*, 621–630. https://doi.org/10.1016/j.ijbiomac.2019.08.009.

(105) Tamo, A. K.; Doench, I.; Helguera, A. M.; Hoenders, D.; Walther, A.; Madrazo, A. O. Biodegradation of Crystalline Cellulose Nanofibers by Means of Enzyme Immobilized-Alginate Beads and Microparticles. *Polymers (Basel).* **2020**, *12* (7), 1–24. https://doi.org/10.3390/polym12071522.

(106) Nyari, N. L. D.; Fernandes, I. A.; Bustamante-Vargas, C. E.; Steffens, C.; De Oliveira, D.; Zeni, J.; Rigo, E.; Dallago, R. M. In Situ Immobilization of Candida Antarctica B Lipase in Polyurethane Foam Support. *J. Mol. Catal. B Enzym.* **2016**, *124*, 52–61. https://doi.org/10.1016/j.molcatb.2015.12.003.

(107) Ganesh, M.; Dave, R. N.; Amoreaux, W. L.; Gross, R. a. Embedded Enzymatic Biomaterial Degradation. *Macromolecules* **2009**, *42*, 6836. https://doi.org/10.1021/ma901481h.

(108) Wu, L.; Yuan, X.; Sheng, J. Immobilization of Cellulase in Nanofibrous PVA Membranes by Electrospinning. *J. Memb. Sci.* **2005**, *250* (1–2), 167–173. https://doi.org/10.1016/j.memsci.2004.10.024.

(109) Vassiliadi, E.; Xenakis, A.; Zoumpanioti, M. Chitosan Hydrogels: A New and Simple Matrix for Lipase Catalysed Biosyntheses. *Mol. Catal.* **2018**, *445*, 206–212. https://doi.org/10.1016/j.mcat.2017.11.031.

(110) Herricks, T. E.; Kim, S. H.; Kim, J.; Li, D.; Kwak, J. H.; Grate, J. W.; Kim, S. H.; Xia, Y. Direct Fabrication of Enzyme-Carrying Polymer Nanofibers by Electrospinning. *J. Mater. Chem.* **2005**, *15* (31), 3241–3245. https://doi.org/10.1039/b503660g.

(111) Dantas, A.; Valério, A.; Ninow, J. L.; de Oliveira, J. V.; de Oliveira, D. Potential Application of Thermomyces Lanuginosus Lipase (TLL) Immobilized on Nonporous Polystyrene Particles. *Environ. Prog. Sustain. Energy* **2019**, *38* (2), 608–613.

https://doi.org/10.1002/ep.12953.

(112) Betancor, L.; Luckarift, H. R. Co-Immobilized Coupled Enzyme Systems in Biotechnology. *Biotechnol. Genet. Eng. Rev.* **2010**, *27* (1), 95–114. https://doi.org/10.1080/02648725.2010.10648146.

(113) Torres, P.; Batista-Viera, F. Production of D-Tagatose and D-Fructose from Whey by Co-Immobilized Enzymatic System. *Mol. Catal.* **2019**, *463* (July 2018), 99–109. https://doi.org/10.1016/j.mcat.2018.11.017.

(114) Richetti, A.; Munaretto, C. B.; Lerin, L. A.; Batistella, L.; Vladimir Oliveira, J.; Dallago, R. M.; Astolfi, V.; Luccio, M. Di; Mazutti, M. A.; De Oliveira, D.; Treichel, H. Immobilization of Inulinase from Kluyveromyces Marxianus NRRL Y-7571 Using Modified Sodium Alginate Beads. *Bioprocess Biosyst. Eng.* **2012**, *35* (3), 383–388. https://doi.org/10.1007/s00449-011-0576-1.

(115) Yachmenev, V. G.; Blanchard, E. J.; Lambert, A. H. Use of Ultrasonic Energy in the Enzymatic Treatment of Cotton Fabric. *Ind. Eng. Chem. Res.* **1998**, *37* (10), 3919–3923. https://doi.org/10.1021/ie980274j.

(116) Erickson, H. P. Size and Shape of Protein Molecules at the Nanometer Level Determined by Sedimentation, Gel Filtration, and Electron Microscopy. *Biol. Proced. Online* **2009**, *11* (1), 32–51. https://doi.org/10.1007/s12575-009-9008-x.

(117) Patel, A. C.; Li, S.; Yuan, J. M.; Wei, Y. In Situ Encapsulation of Horseradish Peroxidase in Electrospun Porous Silica Fibers for Potential Biosensor Applications. *Nano Lett.* **2006**, *6* (5), 1042–1046. https://doi.org/10.1021/nl0604560.

(118) Yang, Q.; Yan, Y.; Yang, X.; Liao, G.; Wang, D.; Xia, H. Enzyme Immobilization in Cage-like

3D-Network PVA-H and GO Modified PVA-H (GO@PVA-H) with Stable Conformation and High Activity. *Chem. Eng. J.* **2019**, *372* (March), 946–955. https://doi.org/10.1016/j.cej.2019.04.216.

(119) Bilal, M.; Iqbal, H. M. N.; Hu, H.; Wang, W.; Zhang, X. Enhanced Bio-Catalytic Performance and Dye Degradation Potential of Chitosan-Encapsulated Horseradish Peroxidase in a Packed Bed Reactor System. *Sci. Total Environ.* **2017**, *575*, 1352–1360. https://doi.org/10.1016/j.scitotenv.2016.09.215.

(120) Sattar, H.; Aman, A.; Qader, S. A. U. Agar-Agar Immobilization: An Alternative Approach for the Entrapment of Protease to Improve the Catalytic Efficiency, Thermal Stability and Recycling Efficiency. *Int. J. Biol. Macromol.* **2018**, *111*, 917–922. https://doi.org/10.1016/j.ijbiomac.2018.01.105.

(121) Munjal, N.; Sawhney, S. . Stability and Properties of Mushroom Tyrosinase Entrapped in Alginate, Polyacrylamide and Gelatin Gels. *Enzyme Microb. Technol.* **2002**, *30* (5), 613–619. https://doi.org/10.1016/S0141-0229(02)00019-4.

(122) Bilal, M.; Iqbal, M.; Hu, H.; Zhang, X. Mutagenicity and Cytotoxicity Assessment of Biodegraded Textile Effluent by Ca-Alginate Encapsulated Manganese Peroxidase. *Biochem. Eng. J.* **2016**, *109*, 153–161. https://doi.org/10.1016/j.bej.2016.01.020.

(123) Nichele, V.; Signoretto, M.; Ghedini, E. β-Galactosidase Entrapment in Silica Gel Matrices for a More Effective Treatment of Lactose Intolerance. *J. Mol. Catal. B Enzym.* **2011**, *71* (1–2), 10–15. https://doi.org/10.1016/j.molcatb.2011.03.002.

(124) Sattar, H.; Aman, A.; Javed, U.; Ul Qader, S. A. Polyacrylamide Beads: Polymer Entrapment Increases the Catalytic Efficiency and Thermal Stability of Protease. *Mol.*

Catal. **2018**, *446*, 81–87. https://doi.org/10.1016/j.mcat.2017.12.022.

(125) Bilal, M.; Asgher, M. Sandal Reactive Dyes Decolorization and Cytotoxicity Reduction Using Manganese Peroxidase Immobilized onto Polyvinyl Alcohol-Alginate Beads. *Chem. Cent. J.* **2015**, *9* (1), 1–14. https://doi.org/10.1186/s13065-015-0125-0.

(126) Harguindeguy, M.; Antonelli, C.; Belleville, M.; Sanchez-Marcano, J.; Pochat-Bohatier, C. Gelatin Supports with Immobilized Laccase as Sustainable Biocatalysts for Water Treatment. *J. Appl. Polym. Sci.* **2021**, *138* (2), 49669. https://doi.org/10.1002/app.49669.

(127) Bayazidi, P.; Almasi, H.; Asl, A. K. Immobilization of Lysozyme on Bacterial Cellulose Nanofibers: Characteristics, Antimicrobial Activity and Morphological Properties. *Int. J. Biol. Macromol.* **2018**, *107*, 2544–2551. https://doi.org/10.1016/j.ijbiomac.2017.10.137.

(128) Nikolic, T.; Korica, M.; Milanovic, J.; Kramar, A.; Petronijevic, Z.; Kostic, M. TEMPO-Oxidized Cotton as a Substrate for Trypsin Immobilization: Impact of Functional Groups on Proteolytic Activity and Stability. *Cellulose* **2017**, *24* (4), 1863–1875. https://doi.org/10.1007/s10570-017-1221-1.

(129) Bilal, M.; Iqbal, H. M. N. Naturally-Derived Biopolymers: Potential Platforms for Enzyme Immobilization. *Int. J. Biol. Macromol.* **2019**, *130*, 462–482. https://doi.org/10.1016/j.ijbiomac.2019.02.152.

(130) Vartiainen, J.; Rättö, M.; Paulussen, S. Antimicrobial Activity of Glucose Oxidase-Immobilized Plasma-Activated Polypropylene Films. *Packag. Technol. Sci.* **2005**, *18* (5), 243–251. https://doi.org/10.1002/pts.695.

(131) Wang, W.; Zhou, W.; Li, J.; Hao, D.; Su, Z.; Ma, G. Comparison of Covalent and Physical Immobilization of Lipase in Gigaporous Polymeric Microspheres. *Bioprocess Biosyst. Eng.*

2015, *38* (11), 2107–2115. https://doi.org/10.1007/s00449-015-1450-3.

(132) Kumar, N; Upadhay, L. Enzyme Immobilization over Polystyrene Surface Using Cysteine Functionalized Copper Nanoparticle as a Linker Molecule. *Appl. Biochem. Biotechnol.* **2020**, *191* (3), 1247–1257. https://doi.org/10.1007/s12010-020-03257-2.

(133) Datta, S.; Christena, L. R.; Rajaram, Y. R. S. Enzyme Immobilization: An Overview on Techniques and Support Materials. *3 Biotech* **2013**, *3* (1), 1–9. https://doi.org/10.1007/s13205-012-0071-7.

(134) Shinde, P.; Musameh, M.; Gao, Y.; Robinson, A. J.; Kyratzis, I. (Louis). Immobilization and Stabilization of Alcohol Dehydrogenase on Polyvinyl Alcohol Fibre. *Biotechnol. Reports* **2018**, *19*, e00260. https://doi.org/10.1016/j.btre.2018.e00260.

(135) Braga, A. R. C.; Silva, M. F.; Oliveira, J. V.; Treichel, H.; Kalil, S. J. A New Approach to Evaluate Immobilization of β-Galactosidase on Eupergit® C: Structural, Kinetic, and Thermal Characterization. *Quimica Nova*. 2014, pp 796–803. https://doi.org/10.5935/0100-4042.20140128.

(136) Pečar, D.; Vasić-Rački, D.; Vrsalović Presečki, A. Immobilization of Glucose Oxidase on Eupergit C: Impact of Aeration, Kinetic and Operational Stability Studies of Free and Immobilized Enzyme. *Chem. Biochem. Eng. Q.* **2018**, *32* (4), 511–522. https://doi.org/10.15255/CABEQ.2018.1391.

(137) Pahujani, S.; Kanwar, S. S.; Chauhan, G.; Gupta, R. Glutaraldehyde Activation of Polymer Nylon-6 for Lipase Immobilization: Enzyme Characteristics and Stability. *Bioresour. Technol.* **2008**, *99* (7), 2566–2570. https://doi.org/10.1016/j.biortech.2007.04.042.

(138) Lin, C. C.; Yang, M. C. Urea Permeation and Hydrolysis through Hollow Fiber Dialyzer

Immobilized with Urease: Storage and Operation Properties. *Biomaterials* **2003**, *24* (11), 1989–1994. https://doi.org/10.1016/S0142-9612(02)00611-7.

(139) Ashly, P. C.; Joseph, M. J.; Mohanan, P. V. Activity of Diastase α-Amylase Immobilized on Polyanilines (PANIs). *Food Chem.* **2011**, *127* (4), 1808–1813. https://doi.org/10.1016/j.foodchem.2011.02.068.

(140) Xiangli, Q.; Zhe, L.; Zhiwei, L.; Yinglin, Z.; Zhengjia, Z. Immobilization of Activated Sludge in Poly(Ethylene Glycol) by UV Technology and Its Application in Micro-Polluted Wastewater. *Biochem. Eng. J.* **2010**, *50* (1–2), 71–76. https://doi.org/10.1016/j.bej.2010.03.007.

(141) Sieber, S.; Siegrist, S.; Schwarz, S.; Porta, F.; Schenk, S. H.; Huwyler, J. Immobilization of Enzymes on PLGA Sub-Micrometer Particles by Crosslinked Layer-by-Layer Deposition. *Macromol. Biosci.* **2017**, *17* (8), 1–10. https://doi.org/10.1002/mabi.201700015.

(142) Aykut, Y.; Sevgi, T.; Demirkan, E. Cellulose Monoacetate/Polycaprolactone and Cellulose Monoacetate/Polycaprolactam Blended Nanofibers for Protease Immobilization. *J. Appl. Polym. Sci.* **2017**, *134* (44), 1–9. https://doi.org/10.1002/app.45479.

(143) Labus, K.; Gancarz, I.; Bryjak, J. Immobilization of Laccase and Tyrosinase on Untreated and Plasma-Treated Cellulosic and Polyamide Membranes. *Mater. Sci. Eng. C* **2012**, *32* (2), 228–235. https://doi.org/10.1016/j.msec.2011.10.023.

(144) Huang, X.; Ge, D.; Xu, Z. Preparation and Characterization of Stable Chitosan Nanofibrous Membrane for Lipase Immobilization. *Eur. Polym. J.* **2007**, *43* (9), 3710–3718. https://doi.org/10.1016/j.eurpolymj.2007.06.010.

(145) Siqueira, N. M.; Garcia, K. C.; Bussamara, R.; Both, F. S.; Vainstein, M. H.; Soares, R. M. D.

Poly (Lactic Acid)/Chitosan Fiber Mats: Investigation of Effects of the Support on Lipase Immobilization. *Int. J. Biol. Macromol.* **2015**, *72*, 998–1004. https://doi.org/10.1016/j.ijbiomac.2014.08.048.

(146) Jankowska, K.; Zdarta, J.; Grzywaczyk, A.; Kijeńska-Gawrońska, E.; Biadasz, A.; Jesionowski, T. Electrospun Poly(Methyl Methacrylate)/Polyaniline Fibres as a Support for Laccase Immobilisation and Use in Dye Decolourisation. *Environ. Res.* **2020**, *184* (March), 109332. https://doi.org/10.1016/j.envres.2020.109332.

(147) Markošová, K.; Dolejš, I.; Stloukal, R.; Rios-Solis, L.; Rosenberg, M.; Micheletti, M.; Lye, G. J.; Turner, N. J.; Rebroš, M. Immobilisation and Kinetics of Monoamine Oxidase (MAO-N-D5) Enzyme in Polyvinyl Alcohol Gels. *J. Mol. Catal. B Enzym.* **2016**, *129*, 69–74. https://doi.org/10.1016/j.molcatb.2016.04.009.

(148) Miletić, N.; Abetz, V.; Ebert, K.; Loos, K. Immobilization of Candida Antarctica Lipase B on Polystyrene Nanoparticles. *Macromol. Rapid Commun.* **2010**, *31* (1), 71–74. https://doi.org/10.1002/marc.200900497.

(149) Pesaran, M.; Amoabediny, G. Study on the Stability and Reusability of Glutamate Dehydrogenase Immobilized on Bacterial Cellulose Nanofiber. *Fibers Polym.* **2017**, *18* (2), 240–245. https://doi.org/10.1007/s12221-017-6864-x.

(150) Lima, L. N.; Oliveira, G. C.; Rojas, M. J.; Castro, H. F.; Da Rós, P. C. M.; Mendes, A. A.; Giordano, R. L. C.; Tardioli, P. W. Immobilization of Pseudomonas Fluorescens Lipase on Hydrophobic Supports and Application in Biodiesel Synthesis by Transesterification of Vegetable Oils in Solvent-Free Systems. *J. Ind. Microbiol. Biotechnol.* **2015**, *42* (4), 523–535. https://doi.org/10.1007/s10295-015-1586-9.

(151) Monier, M. Immobilization of β-Galactosidase from Escherichia Coli onto Modified Natural Silk Fibers. *Journal of Applied Polymer Science*. 2013, pp 2923–2931. https://doi.org/10.1002/app.39475.

(152) Shim, E. J.; Lee, S. H.; Song, W. S.; Kim, H. R. Development of an Enzyme-Immobilized Support Using a Polyester Woven Fabric. *Text. Res. J.* **2017**, *87* (1), 3–14. https://doi.org/10.1177/0040517515624874.

(153) Zhu, Y.; Qiu, F.; Rong, J.; Zhang, T.; Mao, K.; Yang, D. Covalent Laccase Immobilization on the Surface of Poly(Vinylidene Fluoride) Polymer Membrane for Enhanced Biocatalytic Removal of Dyes Pollutants from Aqueous Environment. *Colloids Surfaces B Biointerfaces* **2020**, *191* (April), 111025. https://doi.org/10.1016/j.colsurfb.2020.111025.

(154) Tanksale, A.; Chandra, P. M.; Rao, M.; Deshpande, V. Immobilization of Alkaline Protease from Conidiobolus Macrosporus for Reuse and Improved Thermal Stability. *Biotechnol. Lett.* **2001**, *23* (1), 51–54. https://doi.org/10.1023/A:1026782206945.

(155) Zaman, A.; Rashid, T. U.; Khan, M. A.; Rahman, M. M. Preparation and Characterization of Multiwall Carbon Nanotube (MWCNT) Reinforced Chitosan Nanocomposites: Effect of Gamma Radiation. *Bionanoscience* **2014**, *5* (1), 31–38. https://doi.org/10.1007/s12668-014-0159-0.

(156) Salmon, S.; Hudson, S. M. Crystal Morphology, Biosynthesis, and Physical Assembly of Cellulose, Chitin, and Chitosan. *J. Macromol. Sci. - Rev. Macromol. Chem. Phys.* **1997**, *C37* (2), 199–276.

(157) Yuan, Y.; Li, H.; Leite, W.; Zhang, Q.; Bonnesen, P. V.; Labbé, J. L.; Weiss, K. L.; Pingali, S. V.; Hong, K.; Urban, V. S.; Salmon, S. I.; O'Neill, H. Biosynthesis and Characterization of

Deuterated Chitosan in Filamentous Fungus and Yeast. *Carbohydr. Polym.* **2021**, *257* (September 2020), 117637. https://doi.org/10.1016/j.carbpol.2021.117637.

(158) Siar, E.-H.; Arana-Peña, S.; Barbosa, O.; Zidoune, M.; Fernandez-Lafuente, R. Immobilization/Stabilization of Ficin Extract on Glutaraldehyde-Activated Agarose Beads. Variables That Control the Final Stability and Activity in Protein Hydrolyses. *Catalysts* **2018**, *8* (4), 149. https://doi.org/10.3390/catal8040149.

(159) Blandino, A.; Macías, M.; Cantero, D. Immobilization of Glucose Oxidase within Calcium Alginate Gel Capsules. *Process Biochem.* **2001**, *36* (7), 601–606. https://doi.org/10.1016/S0032-9592(00)00240-5.

(160) da Silva, R. M.; Paiva Souza, P. M.; Fernandes, F. A. N.; Gonçalves, L. R. B.; Rodrigues, S. Co-Immobilization of Dextransucrase and Dextranase in Epoxy-Agarose- Tailoring Oligosaccharides Synthesis. *Process Biochem.* **2019**, *78* (January), 71–81. https://doi.org/10.1016/j.procbio.2019.01.009.

(161) Siar, E. H.; Zaak, H.; Kornecki, J. F.; Zidoune, M. N.; Barbosa, O.; Fernandez-Lafuente, R. Stabilization of Ficin Extract by Immobilization on Glyoxyl Agarose. Preliminary Characterization of the Biocatalyst Performance in Hydrolysis of Proteins. *Process Biochem.* **2017**, *58* (March), 98–104. https://doi.org/10.1016/j.procbio.2017.04.009.

(162) Leimbrink, M.; Nikoleit, K. G.; Spitzer, R.; Salmon, S.; Bucholz, T.; Górak, A.; Skiborowski, M. Enzymatic Reactive Absorption of CO2 in MDEA by Means of an Innovative Biocatalyst Delivery System. *Chem. Eng. J.* **2018**, *334* (May 2017), 1195–1205. https://doi.org/10.1016/j.cej.2017.11.034.

(163) Yeon, K. M.; You, J.; Adhikari, M. D.; Hong, S. G.; Lee, I.; Kim, H. S.; Kim, L. N.; Nam, J.;

Kwon, S. J.; Kim, M. Il; Sajomsang, W.; Dordick, J. S.; Kim, J. Enzyme-Immobilized Chitosan Nanoparticles as Environmentally Friendly and Highly Effective Antimicrobial Agents. *Biomacromolecules* **2019**, *20* (7), 2477–2485. https://doi.org/10.1021/acs.biomac.9b00152.

(164) Duru Kamaci, U.; Peksel, A. Fabrication of PVA-Chitosan-Based Nanofibers for Phytase Immobilization to Enhance Enzymatic Activity. *Int. J. Biol. Macromol.* **2020**, *164*, 3315–3322. https://doi.org/10.1016/j.ijbiomac.2020.08.226.

(165) de Melo Brites, M.; Cerón, A. A.; Costa, S. M.; Oliveira, R. C.; Ferraz, H. G.; Catalani, L. H.; Costa, S. A. Bromelain Immobilization in Cellulose Triacetate Nanofiber Membranes from Sugarcane Bagasse by Electrospinning Technique. *Enzyme Microb. Technol.* **2020**, *132*, 109384. https://doi.org/10.1016/j.enzmictec.2019.109384.

(166) Moreno, I.; González-González, V.; Romero-García, J. Control Release of Lactate Dehydrogenase Encapsulated in Poly (Vinyl Alcohol) Nanofibers via Electrospinning. *Eur. Polym. J.* **2011**, *47* (6), 1264–1272. https://doi.org/10.1016/j.eurpolymj.2011.03.005.

(167) Antipova, A. A.; Yudanova, T. N.; Papkov, M. A.; Milyukina, E. N.; Gal'braikh, L. S. Immobilization of Protease Composites with Polyethylene Oxide on Fibre Substrates. *Fibre Chem.* **2010**, *42* (2), 99–102. https://doi.org/10.1007/s10692-010-9231-x.

(168) Piacentini, E.; Yan, M.; Giorno, L. Development of Enzyme-Loaded PVA Microspheres by Membrane Emulsification. *J. Memb. Sci.* **2017**, *524* (October 2016), 79–86. https://doi.org/10.1016/j.memsci.2016.11.008.

(169) Dai, H.; Ou, S.; Liu, Z.; Huang, H. Pineapple Peel Carboxymethyl Cellulose/Polyvinyl Alcohol/Mesoporous Silica SBA-15 Hydrogel Composites for Papain Immobilization.

Carbohydr. Polym. **2017**, *169*, 504–514. https://doi.org/10.1016/j.carbpol.2017.04.057.

(170) Moreno-Cortez, I. E.; Romero-García, J.; González-González, V.; García-Gutierrez, D. I.; Garza-Navarro, M. A.; Cruz-Silva, R. Encapsulation and Immobilization of Papain in Electrospun Nanofibrous Membranes of PVA Cross-Linked with Glutaraldehyde Vapor. *Mater. Sci. Eng. C* **2015**, *52*, 306–314. https://doi.org/10.1016/j.msec.2015.03.049.

(171) Badgujar, K. C.; Dhake, K. P.; Bhanage, B. M. Immobilization of Candida Cylindracea Lipase on Poly Lactic Acid, Polyvinyl Alcohol and Chitosan Based Ternary Blend Film: Characterization, Activity, Stability and Its Application for N-A. *Process Biochem.* **2013**, *48* (9), 1335–1347. https://doi.org/10.1016/j.procbio.2013.06.009.

(172) Han, C.; Goodwine, J.; Romero, N.; Steck, K. S.; Sauer, K.; Doiron, A. Enzyme-Encapsulating Polymeric Nanoparticles: A Potential Adjunctive Therapy in Pseudomonas Aeruginosa Biofilm-Associated Infection Treatment. *Colloids Surfaces B Biointerfaces* **2019**, *184* (March), 110512. https://doi.org/10.1016/j.colsurfb.2019.110512.

(173) Rodríguez-deLuna, S. E.; Moreno-Cortez, I. E.; Garza-Navarro, M. A.; Lucio-Porto, R.; López Pavón, L.; González-González, V. A. Thermal Stability of the Immobilization Process of Horseradish Peroxidase in Electrospun Polymeric Nanofibers. *J. Appl. Polym. Sci.* **2017**, *134* (19), 1–10. https://doi.org/10.1002/app.44811.

(174) Cunha, A. G.; Besteti, M. D.; Manoel, E. A.; Da Silva, A. A. T.; Almeida, R. V.; Simas, A. B. C.; Fernandez-Lafuente, R.; Pinto, J. C.; Freire, D. M. G. Preparation of Core-Shell Polymer Supports to Immobilize Lipase B from Candida Antarctica: Effect of the Support Nature on Catalytic Properties. *J. Mol. Catal. B Enzym.* **2014**, *100*, 59–67. https://doi.org/10.1016/j.molcatb.2013.11.020.

(175) Dai, Y.; Niu, J.; Liu, J.; Yin, L.; Xu, J. In Situ Encapsulation of Laccase in Microfibers by Emulsion Electrospinning: Preparation, Characterization, and Application. *Bioresour. Technol.* **2010**, *101* (23), 8942–8947. https://doi.org/10.1016/j.biortech.2010.07.027.

(176) Carrea, G.; Riva, S. Medium Engineering of Enzymatic Reactions : E Nzyme Selectivity in Organic Solvents Can Differ from That in Water and Properties and Synthetic Applications of Enzymes in Organic Solvents. *Angew.chem.int.ed* **2000**, *39*, 2226–2254.

(177) Lee, M. Y.; Dordick, J. S. Enzyme Activation for Nonaqueous Media. *Curr. Opin. Biotechnol.* **2002**, *13* (4), 376–384. https://doi.org/10.1016/S0958-1669(02)00337-3.

(178) Shenoy, S. L.; Bates, W. D.; Frisch, H. L.; Wnek, G. E. Role of Chain Entanglements on Fiber Formation during Electrospinning of Polymer Solutions: Good Solvent, Non-Specific Polymer-Polymer Interaction Limit. *Polymer (Guildf).* **2005**, *46* (10), 3372–3384. https://doi.org/10.1016/j.polymer.2005.03.011.

(179) Harnau, L. Influence of Intermolecular Interaction on the Dynamics of Good Solvent-Polymer Solutions. *J. Chem. Phys.* **2001**, *115* (4), 1943–1945. https://doi.org/10.1063/1.1383054.

(180) Papadopoulou, E. L.; Pignatelli, F.; Marras, S.; Marini, L.; Davis, A.; Athanassiou, A.; Bayer, I. S. Nylon 6,6/Graphene Nanoplatelet Composite Films Obtained from a New Solvent. *RSC Adv.* **2016**, *6* (8), 6823–6831. https://doi.org/10.1039/c5ra23647a.

(181) McCrary-Dennis, M.; Uddin, M. J.; Okoli, O. I. Synthesis and Characterization of Polystyrene Carbon Nanotube Nanocomposite for Utilization in the Displaced Foam Dispersion Methodology. *Compos. Part B Eng.* **2016**, *98*, 484–495. https://doi.org/10.1016/j.compositesb.2016.05.014.

(182) Nepomuceno, N. C.; Barbosa, M. A.; Bonan, R. F.; Oliveira, J. E.; Sampaio, F. C.; Medeiros, E. S. Antimicrobial Activity of PLA/PEG Nanofibers Containing Terpinen-4-Ol against Aggregatibacter Actinomycetemcomitans. *J. Appl. Polym. Sci.* **2018**, *135* (6), 45782. https://doi.org/10.1002/app.45782.

(183) Zhang, T.; Tian, H.; Yin, X.; Li, Z.; Zhang, X.; Yang, J.; Zhu, L. Solution Blow Spinning of Polylactic Acid to Prepare Fibrous Oil Adsorbents Through Morphology Optimization with Response Surface Methodology. *J. Polym. Environ.* **2020**, *28* (3), 812–825. https://doi.org/10.1007/s10924-019-01617-6.

(184) Zheng, W.; Zheng, W.; Shi, C.; Wang, X. Cylindrical-Electrode-Assisted Solution Blowing for Nanofiber Spinning. *J. Appl. Polym. Sci.* **2019**, *136* (8), 4–7. https://doi.org/10.1002/app.47087.

(185) Pillai, C. K. S.; Paul, W.; Sharma, C. P. Chitin and Chitosan Polymers: Chemistry, Solubility and Fiber Formation. *Prog. Polym. Sci.* **2009**, *34* (7), 641–678. https://doi.org/10.1016/j.progpolymsci.2009.04.001.

(186) Zargar, V.; Asghari, M.; Dashti, A. A Review on Chitin and Chitosan Polymers: Structure, Chemistry, Solubility, Derivatives, and Applications. *ChemBioEng Rev.* **2015**, *2* (3), 204–226. https://doi.org/10.1002/cben.201400025.

(187) Luo, X.; Zhang, L. New Solvents and Functional Materials Prepared from Cellulose Solutions in Alkali/Urea Aqueous System. *Food Res. Int.* **2013**, *52* (1), 387–400. https://doi.org/10.1016/j.foodres.2010.05.016.

(188) *Reference: Polymer Properties*. Aldrich Polymer Products Applicaton & Reference Information.

https://www.sigmaaldrich.com/deepweb/assets/sigmaaldrich/marketing/global/documents/202/447/j_polymer_solutions.pdf (accessed 2021-06-28).

(189) Pawar, S. N.; Edgar, K. J. Chemical Modification of Alginates in Organic Solvent Systems. *Biomacromolecules* **2011**, *12* (11), 4095–4103. https://doi.org/10.1021/bm201152a.

(190) Pawar, S. N.; Edgar, K. J. Alginate Derivatization: A Review of Chemistry, Properties and Applications. *Biomaterials* **2012**, *33* (11), 3279–3305. https://doi.org/10.1016/j.biomaterials.2012.01.007.

(191) Kausar, A. Phase Inversion Technique-Based Polyamide Films and Their Applications: A Comprehensive Review. *Polym. - Plast. Technol. Eng.* **2017**, *56* (13), 1421–1437. https://doi.org/10.1080/03602559.2016.1276593.

(192) Sturm, D. R.; Caputo, K. J.; Liu, S.; Danner, R. P. Solubility of Solvents in Polyethylene below the Melt Temperature. *Fluid Phase Equilib.* **2018**, *470*, 68–74. https://doi.org/10.1016/j.fluid.2017.09.004.

(193) Miranda, K. W. E.; Mattoso, L. H. C.; Bresolin, J. D.; Hubinger, S. Z.; Medeiros, E. S.; de Oliveira, J. E. Polystyrene Bioactive Nanofibers Using Orange Oil as an Ecofriendly Solvent. *J. Appl. Polym. Sci.* **2019**, *136* (15), 1–8. https://doi.org/10.1002/app.47337.

(194) Liebert, T. Cellulose Solvents – Remarkable History ,. In *Cellulose Solvents: For Analysis, Shaping and Chemical Modification ACS Symposium Series; American Chemical Society: Washington, DC*; 2010; pp 3–54.

(195) Da Silva Parize, D. D.; De Oliveira, J. E.; Foschini, M. M.; Marconcini, J. M.; Mattoso, L. H. C. Poly(Lactic Acid) Fibers Obtained by Solution Blow Spinning: Effect of a Greener Solvent on the Fiber Diameter. *J. Appl. Polym. Sci.* **2016**, *133* (18), 1–10.

https://doi.org/10.1002/app.43379.

(196) Costa, R. G. F.; Brichi, G. S.; Ribeiro, C.; Mattoso, L. H. C. Nanocomposite Fibers of Poly(Lactic Acid)/Titanium Dioxide Prepared by Solution Blow Spinning. *Polym. Bull.* **2016**, *73* (11), 2973–2985. https://doi.org/10.1007/s00289-016-1635-1.

(197) Ye, B.; Jia, C.; Li, Z.; Li, L.; Zhao, Q.; Wang, J.; Wu, H. Solution-Blow Spun PLA/SiO2 Nanofiber Membranes toward High Efficiency Oil/Water Separation. *J. Appl. Polym. Sci.* **2020**, No. November 2019, 1–9. https://doi.org/10.1002/app.49103.

(198) Behrens, A. M.; Casey, B. J.; Sikorski, M. J.; Wu, K. L.; Tutak, W.; Sandler, A. D.; Kofinas, P. In Situ Deposition of PLGA Nanofibers via Solution Blow Spinning. *ACS Macro Lett.* **2014**, *3* (3), 249–254. https://doi.org/10.1021/mz500049x.

(199) Gebru, K. A.; Das, C. Effects of Solubility Parameter Differences among PEG, PVP and CA on the Preparation of Ultrafiltration Membranes: Impacts of Solvents and Additives on Morphology, Permeability and Fouling Performances. *Chinese J. Chem. Eng.* **2017**, *25* (7), 911–923. https://doi.org/10.1016/j.cjche.2016.11.017.

(200) Li, M.; Katsouras, I.; Piliego, C.; Glasser, G.; Lieberwirth, I.; Blom, P. W. M.; De Leeuw, D. M. Controlling the Microstructure of Poly(Vinylidene-Fluoride) (PVDF) Thin Films for Microelectronics. *J. Mater. Chem. C* **2013**, *1* (46), 7695–7702. https://doi.org/10.1039/c3tc31774a.

(201) González-Benito, J.; Torres, D.; Ballesteros, C.; Ruiz, V. M.; Teno, J. PVDF Based Nanocomposites Produced by Solution Blow Spinning, Structure and Morphology Induced by the Presence of MWCNT and Their Consequences on Some Properties. *Colloid Polym. Sci.* **2019**, *297* (7–8), 1105–1118. https://doi.org/10.1007/s00396-019-04530-5.

(202) Ruiz, V. M.; Sirera, R.; Martínez, J. M.; González-Benito, J. Solution Blow Spun Graded Dielectrics Based on Poly(Vinylidene Fluoride)/Multi-Walled Carbon Nanotubes Nanocomposites. *Eur. Polym. J.* **2020**, *122* (November 2019), 109397. https://doi.org/10.1016/j.eurpolymj.2019.109397.

(203) Cena, C. R.; Silva, M. J.; Malmonge, L. F.; Malmonge, J. A. Poly(Vinyl Pyrrolidone) Sub-Microfibers Produced by Solution Blow Spinning. *J. Polym. Res.* **2018**, *25* (11), 238. https://doi.org/10.1007/s10965-018-1633-0.

(204) González-Benito, J.; Teno, J.; González-Gaitano, G.; Xu, S.; Chiang, M. Y. PVDF/TiO2 Nanocomposites Prepared by Solution Blow Spinning: Surface Properties and Their Relation with S. Mutans Adhesion. *Polym. Test.* **2017**, *58*, 21–30. https://doi.org/10.1016/j.polymertesting.2016.12.005.

(205) Li, Q.; Xu, Z. L.; Yu, L. Y. Effects of Mixed Solvents and PVDF Types on Performances of PVDF Microporous Membranes. *J. Appl. Polym. Sci.* **2010**, *115* (4), 2277–2287. https://doi.org/10.1002/app.31324.

(206) Liverani, L.; Boccardi, E.; Beltran, A. M.; Boccaccini, A. R. Incorporation of Calcium Containing Mesoporous (MCM-41-Type) Particles in Electrospun PCL Fibers by Using Benign Solvents. *Polymers (Basel).* **2017**, *9* (10), 1–16. https://doi.org/10.3390/polym9100487.

(207) Zhang, T.; Yang, R.; Zhang, X.; Yin, X.; Tian, H.; Zhu, L. Preparation, Oil Adsorption Behavior, and Mechanism of Micro/Nanofibrous Polycaprolactone Membrane Prepared through Solution Blow Spinning. *Polym. Adv. Technol.* **2020**, *31* (4), 686–698. https://doi.org/10.1002/pat.4805.

(208) Zhuang, X.; Jia, K.; Cheng, B.; Guan, K.; Kang, W.; Ren, Y. Preparation of Polyacrylonitrile Nanofibers by Solution Blowing Process. *J. Eng. Fiber. Fabr.* **2013**, *8* (1), 88–93. https://doi.org/10.1177/155892501300800111.

(209) Ren, J.; Huang, X.; Wang, N.; Lu, K.; Zhang, X.; Li, W.; Liu, D. Preparation of Polyaniline-Coated Polyacrylonitrile Fiber Mats and Their Application to Cr(VI) Removal. *Synth. Met.* **2016**, *222*, 255–266. https://doi.org/10.1016/j.synthmet.2016.10.027.

(210) Iorio, M.; Teno, J.; Nicolás, M.; García-González, R.; Peláez, V. H.; González-Gaitano, G.; González-Benito, J. Conformational Changes on PMMA Induced by the Presence of TiO2 Nanoparticles and the Processing by Solution Blow Spinning. *Colloid Polym. Sci.* **2018**, *296* (3), 461–469. https://doi.org/10.1007/s00396-018-4268-0.

(211) Ali, U.; Karim, K. J. B. A.; Buang, N. A. A Review of the Properties and Applications of Poly (Methyl Methacrylate) (PMMA). *Polym. Rev.* **2015**, *55* (4), 678–705. https://doi.org/10.1080/15583724.2015.1031377.

(212) Mahalingam, S.; Raimi-Abraham, B. T.; Craig, D. Q. M.; Edirisinghe, M. Solubility-Spinnability Map and Model for the Preparation of Fibres of Polyethylene (Terephthalate) Using Gyration and Pressure. *Chem. Eng. J.* **2015**, *280*, 344–353. https://doi.org/10.1016/j.cej.2015.05.114.

(213) Liu, Y.; Zhang, G.; Zhuang, X.; Li, S.; Shi, L.; Kang, W.; Cheng, B.; Xu, X. Solution Blown Nylon 6 Nanofibrous Membrane as Scaffold for Nanofiltration. *Polymers (Basel).* **2019**, *11* (2), 1–15. https://doi.org/10.3390/POLYM11020364.

(214) Polat, Y.; Pampal, E. S.; Stojanovska, E.; Simsek, R.; Hassanin, A.; Kilic, A.; Demir, A.; Yilmaz, S. Solution Blowing of Thermoplastic Polyurethane Nanofibers: A Facile Method

to Produce Flexible Porous Materials. *J. Appl. Polym. Sci.* **2016**, *133* (9), 1–9. https://doi.org/10.1002/app.43025.

(215) Kuk, E.; Ha, Y.-M.; Yu, J.; Im, I.-T.; Kim, Y.; Jung, Y. C. Robust and Flexible Polyurethane Composite Nanofibers Incorporating Multi-Walled Carbon Nanotubes Produced by Solution Blow Spinning. *Macromol. Mater. Eng.* **2016**, *301* (4), 364–370. https://doi.org/10.1002/mame.201500298.

(216) Griffiths, T. R.; Pugh, D. C. Correlations among Solvent Polarity Scales, Dielectric Constant and Dipole Moment, and a Means to Reliable Predictions of Polarity Scale Values from Cu. *Coord. Chem. Rev.* **1979**, *29* (2–3), 129–211. https://doi.org/10.1016/S0010-8545(00)82109-8.

(217) Ahmed, W. Classification of Solvents According to Interaction Mechanisms. *J. Chem. Educ.* **1979**, *56* (12), 795. https://doi.org/10.1021/ed056p795.

(218) Ramos-Villaseñor, J. M.; Rodríguez-Cárdenas, E.; Barrera Díaz, C. E.; Frontana-Uribe, B. A. Review—Use of 1,1,1,3,3,3–Hexafluoro–2–Propanol (HFIP) Co-Solvent Mixtures in Organic Electrosynthesis. *J. Electrochem. Soc.* **2020**, *167* (15), 155509. https://doi.org/10.1149/1945-7111/abb83c.

(219) Salem, K. S.; Starkey, H. R.; Pal, L.; Lucia, L.; Jameel, H. The Topochemistry of Cellulose Nanofibrils as a Function of Mechanical Generation Energy. *ACS Sustain. Chem. Eng.* **2020**, *8* (3), 1471–1478. https://doi.org/10.1021/acssuschemeng.9b05806.

(220) Rashid, T. U.; Rahman, M. M.; Kabir, S.; Shamsuddin, S. M.; Khan, M. A. A New Approach for the Preparation of Chitosan from γ-Irradiation of Prawn Shell: Effects of Radiation on the Characteristics of Chitosan. *Polym. Int.* **2012**, *61* (8), 1302–1308.

https://doi.org/10.1002/pi.4207.

(221) Wang, Y.; Hsieh, Y. L. Immobilization of Lipase Enzyme in Polyvinyl Alcohol (PVA) Nanofibrous Membranes. *J. Memb. Sci.* **2008**, *309* (1–2), 73–81. https://doi.org/10.1016/j.memsci.2007.10.008.

(222) Rudra, R.; Kumar, V.; Kundu, P. P. Acid Catalysed Cross-Linking of Poly Vinyl Alcohol (PVA) by Glutaraldehyde: Effect of Crosslink Density on the Characteristics of PVA Membranes Used in Single Chambered Microbial Fuel Cells. *RSC Adv.* **2015**, *5* (101), 83436–83447. https://doi.org/10.1039/c5ra16068e.

(223) Franco, P.; De Marco, I. The Use of Poly(N-Vinyl Pyrrolidone) in the Delivery of Drugs: A Review. *Polymers (Basel).* **2020**, *12* (5), 18–21. https://doi.org/10.3390/POLYM12051114.

(224) Wagner, I.; Nagy, Z. K.; Vass, P.; Fehér, C.; Barta, Z.; Vigh, T.; Sóti, P. L.; Harasztos, A. H.; Pataki, H.; Balogh, A.; Verreck, G.; Assche, I. Van; Marosi, G. Stable Formulation of Protein-Type Drug in Electrospun Polymeric Fiber Followed by Tableting and Scaling-up Experiments. *Polym. Adv. Technol.* **2015**, *26* (12), 1461–1467. https://doi.org/10.1002/pat.3569.

(225) de Lima, L.; Mendes, A.; Fernandez-Lafuente, R.; Tardioli, P.; Giordano, R. Performance of Different Immobilized Lipases in the Syntheses of Short- and Long-Chain Carboxylic Acid Esters by Esterification Reactions in Organic Media. *Molecules* **2018**, *23* (4), 766. https://doi.org/10.3390/molecules23040766.

(226) Dalla-Vecchia, R.; Sebrão, D.; Nascimento, M. D. G.; Soldi, V. Carboxymethylcellulose and Poly(Vinyl Alcohol) Used as a Film Support for Lipases Immobilization. *Process Biochem.* **2005**, *40* (8), 2677–2682. https://doi.org/10.1016/j.procbio.2004.12.004.

(227) Liu, H.; Wang, S.; Qi, N. Controllable Structure, Properties, and Degradation of the Electrospun PLGA/PLA-Blended Nanofibrous Scaffolds. *J. Appl. Polym. Sci.* **2012**, *125* (S2), E468–E476. https://doi.org/10.1002/app.36757.

(228) de Melo Brites, M.; Cerón, A. A.; Costa, S. M.; Oliveira, R. C.; Ferraz, H. G.; Catalani, L. H.; Costa, S. A. Bromelain Immobilization in Cellulose Triacetate Nanofiber Membranes from Sugarcane Bagasse by Electrospinning Technique. *Enzyme Microb. Technol.* **2020**, *132* (March 2019), 109384. https://doi.org/10.1016/j.enzmictec.2019.109384.

(229) Pervushin, K.; Vamvaca, K.; Vögeli, B.; Hilvert, D. Structure and Dynamics of a Molten Globular Enzyme. *Nat. Struct. Mol. Biol.* **2007**, *14* (12), 1202–1206. https://doi.org/10.1038/nsmb1325.

(230) Brode, P. F.; Erwin, C. R.; Rauch, D. S.; Lucas, D. S.; Rubingh, D. N. Enzyme Behavior at Surfaces. Site-Specific Variants of Subtilisin BPN' with Enhanced Surface Stability. *J. Biol. Chem.* **1994**, *269* (38), 23538–23543. https://doi.org/10.1016/s0021-9258(17)31549-1.

(231) Arjunan, P.; Umland, T.; Dyda, F.; Swaminathan, S.; Furey, W.; Sax, M.; Farrenkopf, B.; Gao, Y.; Zhang, D.; Jordan, F. Crystal Structure of the Thiamin Diphosphate-Dependent Enzyme Pyruvate Decarboxylase from the Yeast Saccharomyces Cerevisiae at 2.3 Å Resolution. *J. Mol. Biol.* **1996**, *256* (3), 590–600. https://doi.org/10.1006/jmbi.1996.0111.

(232) Hartsough, D. S.; Merz, K. M. Protein Flexibility in Aqueous and Nonaqueous Solutions. *J. Am. Chem. Soc.* **1992**, *114* (26), 10113–10116. https://doi.org/10.1021/ja00052a004.

(233) Safarian, S.; Saffarzadeh, M.; Zargar, S. J.; Moosavi-Movahedi, A. A. Molten Globule-like State of Bovine Carbonic Anhydrase in the Presence of Acetonitrile. *J. Biochem.* **2006**, *139* (6), 1025–1033. https://doi.org/10.1093/jb/mvj115.

(234) Yang, L.; Dordick, J. S.; Garde, S. Hydration of Enzyme in Nonaqueous Media Is Consistent with Solvent Dependence of Its Activity. *Biophys. J.* **2004**, *87* (2), 812–821. https://doi.org/10.1529/biophysj.104.041269.

(235) Trodler, P.; Pleiss, J. Modeling Structure and Flexibility of Candida Antarctica Lipase B in Organic Solvents. *BMC Struct. Biol.* **2008**, *8*, 1–10. https://doi.org/10.1186/1472-6807-8-9.

(236) Van Pouderoyen, G.; Eggert, T.; Jaeger, K. E.; Dijkstra, B. W. The Crystal Structure of Bacillus Subtilis Lipase: A Minimal α/β Hydrolase Fold Enzyme. *Journal of Molecular Biology*. 2001, pp 215–226. https://doi.org/10.1006/jmbi.2001.4659.

(237) Zaks, A.; Klibanov, A. M. The Effect of Water on Enzyme Action in Organic Media. *J. Biol. Chem.* **1988**, *263* (17), 8017–8021. https://doi.org/10.1016/s0021-9258(18)68435-2.

(238) Pandey, S.; Singh, S. P. Organic Solvent Tolerance of an α-Amylase from Haloalkaliphilic Bacteria as a Function of PH, Temperature, and Salt Concentrations. *Appl. Biochem. Biotechnol.* **2012**, *166* (7), 1747–1757. https://doi.org/10.1007/s12010-012-9580-4.

(239) Zaks, A.; Klibanov, A. M. Enzymatic Catalysis in Nonaqueous Solvents. *J. Biol. Chem.* **1988**, *263* (7), 3194–3201. https://doi.org/10.1016/s0021-9258(18)69054-4.

(240) Debulis, K.; Klibanov, A. M. Dramatic Enhancement of Enzymatic Activity in Organic Solvents by Lyoprotectants. *Biotechnol. Bioeng.* **1993**, *41* (5), 566–571. https://doi.org/10.1002/bit.260410509.

(241) Klibanov, A. Why Are Enzymes Less Active in Organic Solvents than in Water? *Trends Biotechnol.* **1997**, *15* (3), 97–101. https://doi.org/10.1016/S0167-7799(97)01013-5.

(242) Wangikar, P. P.; Graycar, T. P.; Estell, D. A.; Clark, D. S.; Dordick, J. S. Protein and Solvent

Engineering of Subtilisin BPN' in Nearly Anhydrous Organic Media. *J. Am. Chem. Soc.* **1993**, *115* (26), 12231–12237. https://doi.org/10.1021/ja00079a001.

(243) Wu, X.; Wang, Y.; Tong, B.; Chen, X.; Chen, J. International Journal of Biological Macromolecules Purification and Biochemical Characterization of a Thermostable and Acid-Stable Alpha-Amylase from Bacillus Licheniformis B4-423. *Int. J. Biol. Macromol.* **2018**, *109*, 329–337. https://doi.org/10.1016/j.ijbiomac.2017.12.004.

(244) Shafiei, M.; Ziaee, A.-A.; Amoozegar, M. A. Purification and Characterization of a Halophilic α-Amylase with Increased Activity in the Presence of Organic Solvents from the Moderately Halophilic Nesterenkonia Sp. Strain F. *Extremophiles* **2012**, *16* (4), 627–635. https://doi.org/10.1007/s00792-012-0462-z.

(245) Rehan, M.; Younus, H. Effect of Organic Solvents on the Conformation and Interaction of Catalase and Anticatalase Antibodies. *Int. J. Biol. Macromol.* **2006**, *38* (3–5), 289–295. https://doi.org/10.1016/j.ijbiomac.2006.03.023.

(246) Zhu, T.; Li, R.; Sun, J.; Cui, Y.; Wu, B. Characterization and Efficient Production of a Thermostable, Halostable and Organic Solvent-Stable Cellulase from an Oil Reservoir. *Int. J. Biol. Macromol.* **2020**, *159*, 622–629. https://doi.org/10.1016/j.ijbiomac.2020.05.021.

(247) Gaur, R.; Tiwari, S. Isolation, Production, Purification and Characterization of an Organic-Solvent-Thermostable Alkalophilic Cellulase from Bacillus Vallismortis RG-07. *BMC Biotechnol.* **2015**, *15* (1), 1–12. https://doi.org/10.1186/s12896-015-0129-9.

(248) Irfan, M.; Tayyab, A.; Hasan, F.; Khan, S.; Badshah, M.; Shah, A. A. Production and Characterization of Organic Solvent-Tolerant Cellulase from Bacillus Amyloliquefaciens AK9 Isolated from Hot Spring. *Appl. Biochem. Biotechnol.* **2017**, *182* (4), 1390–1402.

https://doi.org/10.1007/s12010-017-2405-8.

(249) Zhao, L.; Zhou, T.; Li, X.; Fan, S.; You, L. Expression and Characterization of GH3 β-Glucosidase from Aspergillus Niger NL-1 with High Specific Activity, Glucose Inhibition and Solvent Tolerance. *Microbiology (Russian Federation)*. 2013, pp 356–363. https://doi.org/10.1134/S0026261713030181.

(250) Karami, F.; Ghorbani, M.; Sadeghi Mahoonak, A.; Khodarahmi, R. Fast, Inexpensive Purification of β-Glucosidase from Aspergillus Niger and Improved Catalytic/Physicochemical Properties upon the Enzyme Immobilization: Possible Broad Prospects for Industrial Applications. *LWT* **2020**, *118*, 108770. https://doi.org/10.1016/j.lwt.2019.108770.

(251) Narasimha, G.; Sridevi, A.; Ramanjaneyulu, G.; Rajasekhar Reddy, B. Purification and Characterization of β-Glucosidase from Aspergillus Niger. *Int. J. Food Prop.* **2016**, *19* (3), 652–661. https://doi.org/10.1080/10942912.2015.1023398.

(252) Wan, Y. Y.; Lu, R.; Xiao, L.; Du, Y. M.; Miyakoshi, T.; Chen, C. L.; Knill, C. J.; Kennedy, J. F. Effects of Organic Solvents on the Activity of Free and Immobilised Laccase from Rhus Vernicifera. *Int. J. Biol. Macromol.* **2010**, *47* (4), 488–495. https://doi.org/10.1016/j.ijbiomac.2010.07.003.

(253) Lu, L.; Zhao, M.; Wang, T. N.; Zhao, L. Y.; Du, M. H.; Li, T. L.; Li, D. Bin. Characterization and Dye Decolorization Ability of an Alkaline Resistant and Organic Solvents Tolerant Laccase from Bacillus Licheniformis LS04. *Bioresour. Technol.* **2012**, *115*, 35–40. https://doi.org/10.1016/j.biortech.2011.07.111.

(254) Ogino, H.; Nakagawa, S.; Shinya, K.; Muto, T.; Fujimura, N.; Yasuda, M.; Ishikawa, H.

Purification and Characterization of Organic Solvent-Stable Lipase from Organic Solvent-Tolerant Pseudomonas Aeruginosa LST-03. *J. Biosci. Bioeng.* **2000**, *89* (5), 451–457. https://doi.org/10.1016/S1389-1723(00)89095-7.

(255) Essamri, M.; Deyris, V.; Comeau, L. Optimization of Lipase Production by Rhizopus Oryzae and Study on the Stability of Lipase Activity in Organic Solvents. *J. Biotechnol.* **1998**, *60* (1–2), 97–103. https://doi.org/10.1016/S0168-1656(97)00193-4.

(256) Pera, L. M.; Romero, C. M.; Baigori, M. D.; Castro, G. R. Catalytic Properties of Lipase Extracts from Aspergillus Niger. *Food Technol. Biotechnol.* **2006**, *44* (2), 247–252.

(257) Zhang, J.; Tian, M.; Lv, P.; Luo, W.; Wang, Z.; Xu, J.; Wang, Z. High-Efficiency Expression of the Thermophilic Lipase from Geobacillus Thermocatenulatus in Escherichia Coli and Its Application in the Enzymatic Hydrolysis of Rapeseed Oil. *3 Biotech* **2020**, *10* (12), 523. https://doi.org/10.1007/s13205-020-02517-6.

(258) Cabrera-Padilla, R. Y.; Lisboa, M. C.; Fricks, A. T.; Franceschi, E.; Lima, A. S.; Silva, D. P.; Soares, C. M. F. Immobilization of Candida Rugosa Lipase on Poly(3-Hydroxybutyrate-Co-Hydroxyvalerate): A New Eco-Friendly Support. *J. Ind. Microbiol. Biotechnol.* **2012**, *39* (2), 289–298. https://doi.org/10.1007/s10295-011-1027-3.

(259) Mohamed, S. A.; Al-Malki, A. L.; Kumosani, T. A.; El-Shishtawy, R. M. Horseradish Peroxidase and Chitosan: Activation, Immobilization and Comparative Results. *Int. J. Biol. Macromol.* **2013**, *60*, 295–300. https://doi.org/10.1016/j.ijbiomac.2013.06.003.

(260) Singh, P.; Prakash, R.; Shah, K. Effect of Organic Solvents on Peroxidases from Rice and Horseradish: Prospects for Enzyme Based Applications. *Talanta* **2012**, *97*, 204–210. https://doi.org/10.1016/j.talanta.2012.04.018.

(261) Azevedo, A. M.; Prazeres, D. M. F.; Cabral, J. M. S.; Fonseca, L. P. Stability of Free and Immobilised Peroxidase in Aqueous-Organic Solvents Mixtures. *J. Mol. Catal. - B Enzym.* **2001**, *15* (4–6), 147–153. https://doi.org/10.1016/S1381-1177(01)00017-0.

(262) Lam, M. Q.; Nik Mut, N. N.; Thevarajoo, S.; Chen, S. J.; Selvaratnam, C.; Hussin, H.; Jamaluddin, H.; Chong, C. S. Characterization of Detergent Compatible Protease from Halophilic Virgibacillus Sp. CD6. *3 Biotech* **2018**, *8* (2), 1–9. https://doi.org/10.1007/s13205-018-1133-2.

(263) Uttatree, S.; Charoenpanich, J. Isolation and Characterization of a Broad PH- and Temperature-Active, Solvent and Surfactant Stable Protease from a New Strain of Bacillus Subtilis. *Biocatal. Agric. Biotechnol.* **2016**, *8*, 32–38. https://doi.org/10.1016/j.bcab.2016.08.003.

(264) Verma, J.; Pandey, S. Characterization of Partially Purified Alkaline Protease Secreted by Halophilic Bacterium Citricoccus Sp. Isolated from Agricultural Soil of Northern India. *Biocatal. Agric. Biotechnol.* **2019**, *17* (December 2018), 605–612. https://doi.org/10.1016/j.bcab.2019.01.020.

(265) Aslani, E.; Abri, A.; Pazhang, M. Immobilization of Trypsin onto Fe3O4@SiO2 –NH2 and Study of Its Activity and Stability. *Colloids Surfaces B Biointerfaces* **2018**, *170* (June), 553–562. https://doi.org/10.1016/j.colsurfb.2018.06.022.

(266) Pradeep, G. C.; Choi, Y. H.; Choi, Y. S.; Seong, C. N.; Cho, S. S.; Lee, H. J.; Yoo, J. C. A Novel Thermostable Cellulase Free Xylanase Stable in Broad Range of PH from Streptomyces Sp. CS428. *Process Biochem.* **2013**, *48* (8), 1188–1196. https://doi.org/10.1016/j.procbio.2013.06.007.

(267) Wang, S.; Lin, C.; Liu, Y.; Shen, Z.; Jeyaseelan, J.; Qin, W. Characterization of a Starch-Hydrolyzing α-Amylase Produced by Aspergillus Niger WLB42 Mutated by Ethyl Methanesulfonate Treatment. *Int. J. Biochem. Mol. Biol.* **2016**, *7* (1), 1–10.

(268) Zhang, Y. Q.; Li, R. H.; Zhang, H. Bin; Wu, M.; Hu, X. Q. Purification, Characterization, and Application of a Thermostable Dextranase from Talaromyces Pinophilus. *J. Ind. Microbiol. Biotechnol.* **2017**, *44* (2), 317–327. https://doi.org/10.1007/s10295-016-1886-8.

(269) Patil, U.; Mokashe, N.; Chaudhari, A. Detergent-Compatible, Organic Solvent-Tolerant Alkaline Protease from Bacillus Circulans MTCC 7942: Purification and Characterization. *Prep. Biochem. Biotechnol.* **2016**, *46* (1), 56–64. https://doi.org/10.1080/10826068.2014.979205.

(270) Devi, S. G.; Fathima, A. A.; Sanitha, M.; Iyappan, S.; Curtis, W. R.; Ramya, M. Expression and Characterization of Alkaline Protease from the Metagenomic Library of Tannery Activated Sludge. *J. Biosci. Bioeng.* **2016**, *122* (6), 694–700. https://doi.org/10.1016/j.jbiosc.2016.05.012.

(271) Monteiro, T. I. R. C.; Porto, T. S.; Carneiro-Leão, A. M. A.; Silva, M. P. C.; Carneiro-Da-Cunha, M. G. Reversed Micellar Extraction of an Extracellular Protease from Nocardiopsis Sp. Fermentation Broth. *Biochem. Eng. J.* **2005**, *24* (1), 87–90. https://doi.org/10.1016/j.bej.2005.01.010.

(272) Doukyu, N.; Ogino, H. Organic Solvent-Tolerant Enzymes. *Biochem. Eng. J.* **2010**, *48* (3), 270–282. https://doi.org/10.1016/j.bej.2009.09.009.

(273) Vicente, M. S.; Gottifredi, J. C. Estimation of Solvent Activities in Polymers Solutions Using a Group-Contribution Method. *Sep. Purif. Technol.* **2001**, *22–23*, 671–679.

https://doi.org/10.1016/S1383-5866(00)00183-0.

(274) Wehtje, E.; Adlercreutz, P. Water Activity and Substrate Concentration Effects on Lipase Activity. *Biotechnol. Bioeng.* **1997**, *55* (5), 798–806. https://doi.org/10.1002/(SICI)1097-0290(19970905)55:5<798::AID-BIT10>3.0.CO;2-8.

(275) Song, J.; Kahveci, D.; Chen, M.; Guo, Z.; Xie, E.; Xu, X.; Besenbacher, F.; Dong, M. Enhanced Catalytic Activity of Lipase Encapsulated in PCL Nanofibers. *Langmuir* **2012**, *28* (14), 6157–6162. https://doi.org/10.1021/la300469s.

(276) Klibanov, A. M. Asymmetric Transformations Catalyzed by Enzymes in Organic Solvents. *Acc. Chem. Res.* **1990**, *23* (4), 114–120. https://doi.org/10.1021/ar00172a004.

(277) Petersson, A. E. V.; Adlercreutz, P.; Mattiasson, B. A Water Activity Control System for Enzymatic Reactions in Organic Media. *Biotechnol. Bioeng.* **2007**, *97* (2), 235–241. https://doi.org/10.1002/bit.21229.

(278) Subbiah, B.; Blank, U. K. M.; Morison, K. R. A Review, Analysis and Extension of Water Activity Data of Sugars and Model Honey Solutions. *Food Chem.* **2020**, *326* (February), 126981. https://doi.org/10.1016/j.foodchem.2020.126981.

(279) Adlercreutz, P. Comparison of Lipases and Glycoside Hydrolases as Catalysts in Synthesis Reactions. *Appl. Microbiol. Biotechnol.* **2017**, *101* (2), 513–519. https://doi.org/10.1007/s00253-016-8055-x.

(280) Hansson, T.; Adlercreutz, P. Enhanced Transglucosylation/Hydrolysis Ratio of Mutants of Pyrococcus Furiosus β-Glucosidase: Effects of Donor Concentration, Water Content, and Temperature on Activity and Selectivity in Hexanol. *Biotechnol. Bioeng.* **2001**, *75* (6), 656–665. https://doi.org/10.1002/bit.10043.

(281) Adlercreutz, P. Activation of Enzymes in Organic Media at Low Water Activity by Polyols and Saccharides. *Biochim. Biophys. Acta (BBA)/Protein Struct. Mol.* **1993**, *1163* (2), 144–148. https://doi.org/10.1016/0167-4838(93)90175-Q.

(282) Halling, P. J. Thermodynamic Predictions for Biocatalysis in Nonconventional Media: Theory, Tests, and Recommendations for Experimental Design and Analysis. *Enzyme Microb. Technol.* **1994**, *16* (3), 178–206. https://doi.org/10.1016/0141-0229(94)90043-4.

(283) Shipovskov, S.; Trofimova, D.; Saprykin, E.; Christenson, A.; Ruzgas, T.; Levashov, A. V.; Ferapontova, E. E. Spraying Enzymes in Microemulsions of AOT in Nonpolar Organic Solvents for Fabrication of Enzyme Electrodes. *Anal. Chem.* **2005**, *77* (21), 7074–7079. https://doi.org/10.1021/ac050505d.

(284) Biswas, R.; Pal, S. K. Caging Enzyme Function: α-Chymotrypsin in Reverse Micelle. *Chemical Physics Letters*. 2004, pp 221–226. https://doi.org/10.1016/j.cplett.2004.02.018.

(285) KHMELNITSKY, Y. L.; GLADILIN, A. K.; ROUBAILO, V. L.; MARTINEK, K.; LEVASHOV, A. V. Reversed Micelles of Polymeric Surfactants in Nonpolar Organic Solvents: A New Microheterogeneous Medium for Enzymatic Reactions. *Eur. J. Biochem.* **1992**, *206* (3), 737–745. https://doi.org/10.1111/j.1432-1033.1992.tb16980.x.

(286) Gazaryan, I. G.; Klyachko, N. L.; Dulkis, Y. K.; Ouporov, I. V.; Levashov, A. V. Formation and Properties of Dimeric Recombinant Horseradish Peroxidase in a System of Reversed Micelles. *Biochem. J.* **1997**, *328* (2), 643–647. https://doi.org/10.1042/bj3280643.

(287) Andrade, S. L. A.; Brondino, C. D.; Kamenskaya, E. O.; Levashov, A. V.; Moura, J. J. G. Kinetic Behavior of Desulfovibrio Gigas Aldehyde Oxidoreductase Encapsulated in

Reverse Micelles. *Biochem. Biophys. Res. Commun.* **2003**, *308* (1), 73–78. https://doi.org/10.1016/S0006-291X(03)01337-8.

(288) Ganesh, M.; Dave, R. N.; L'Amoreaux, W.; Gross, R. A. Embedded Enzymatic Biomaterial Degradation. *Macromolecules* **2009**, *42* (18), 6836–6839. https://doi.org/10.1021/ma901481h.

(289) Ganesh, M.; Gross, R. A. Embedded Enzymatic Biomaterial Degradation: Flow Conditions & Relative Humidity. *Polym. (United Kingdom)* **2012**, *53* (16), 3454–3461. https://doi.org/10.1016/j.polymer.2012.06.017.

(290) Ogino, H.; Ishikawa, H. Enzymes Which Are Stable in the Presence of Organic Solvents. *J. Biosci. Bioeng.* **2001**, *91* (2), 109–116. https://doi.org/10.1016/S1389-1723(01)80051-7.

(291) Schmid, R. D.; Verger, R. The Open Form . As with All Lipases Whose Lipases : Interfacial Enzymes with Attractive Applications. *Analysis* **1998**, *37* (12), 1608–1633.

(292) Van den Burg, B. Extremophiles as a Source for Novel Enzymes. *Curr. Opin. Microbiol.* **2003**, *6* (3), 213–218. https://doi.org/10.1016/S1369-5274(03)00060-2.

(293) Thumar, J. T.; Singh, S. P. Organic Solvent Tolerance of an Alkaline Protease from Salt-Tolerant Alkaliphilic Streptomyces Clavuligerus Strain Mit-1. *J. Ind. Microbiol. Biotechnol.* **2009**, *36* (2), 211–218. https://doi.org/10.1007/s10295-008-0487-6.

(294) Fukushima, T.; Mizuki, T.; Echigo, A.; Inoue, A.; Usami, R. Organic Solvent Tolerance of Halophilic α-Amylase from a Haloarchaeon, Haloarcula Sp. Strain S-1. *Extremophiles* **2005**, *9* (1), 85–89. https://doi.org/10.1007/s00792-004-0423-2.

(295) Gupta, A.; Roy, I.; Khare, S. K.; Gupta, M. N. Purification and Characterization of a Solvent Stable Protease from Pseudomonas Aeruginosa PseA. *J. Chromatogr. A* **2005**, *1069* (2),

155–161. https://doi.org/10.1016/j.chroma.2005.01.080.

(296) Gaur, R.; Gupta, A.; Khare, S. K. Purification and Characterization of Lipase from Solvent Tolerant Pseudomonas Aeruginosa PseA. *Process Biochem.* **2008**, *43* (10), 1040–1046. https://doi.org/10.1016/j.procbio.2008.05.007.

(297) Klibanov, A. M. What Is Remembered and Why? *Nature* **1995**, *374* (6523), 596. https://doi.org/10.1038/374596a0.

(298) Ke, T.; Klibanov, A. M. On Enzymatic Activity in Organic Solvents as a Function of Enzyme History. *Biotechnol. Bioeng.* **1998**, *57* (6), 746–750. https://doi.org/10.1002/(SICI)1097-0290(19980320)57:6<746::AID-BIT12>3.0.CO;2-5.

(299) Rich, J. O.; Dordick, J. S. Controlling Subtilisin Activity and Selectivity in Organic Media by Imprinting with Nucleophilic Substrates. *J. Am. Chem. Soc.* **1997**, *119* (14), 3245–3252. https://doi.org/10.1021/ja9637715.

(300) Cipolatti, E. P.; Valério, A.; Ninow, J. L.; de Oliveira, D.; Pessela, B. C. Stabilization of Lipase from Thermomyces Lanuginosus by Crosslinking in PEGylated Polyurethane Particles by Polymerization: Application on Fish Oil Ethanolysis. *Biochem. Eng. J.* **2016**, *112*, 54–60. https://doi.org/10.1016/j.bej.2016.04.006.

(301) Ishizuka, F.; Chapman, R.; Kuchel, R. P.; Coureault, M.; Zetterlund, P. B.; Stenzel, M. H. Polymeric Nanocapsules for Enzyme Stabilization in Organic Solvents. *Macromolecules* **2018**, *51* (2), 438–446. https://doi.org/10.1021/acs.macromol.7b02377.

(302) Ribeiro, E. S.; de Farias, B. S.; Sant'Anna Cadaval Junior, T. R.; de Almeida Pinto, L. A.; Diaz, P. S. Chitosan–Based Nanofibers for Enzyme Immobilization. *Int. J. Biol. Macromol.* **2021**, *183* (March), 1959–1970. https://doi.org/10.1016/j.ijbiomac.2021.05.214.

(303) Silva, C. J. S. M.; Zhang, Q.; Shen, J.; Cavaco-Paulo, A. Immobilization of Proteases with a Water Soluble-Insoluble Reversible Polymer for Treatment of Wool. *Enzyme Microb. Technol.* **2006**, *39* (4), 634–640. https://doi.org/10.1016/j.enzmictec.2005.11.016.

(304) Auriemma, F.; De Rosa, C.; Malafronte, A.; Di Girolamo, R.; Santillo, C.; Gerelli, Y.; Fragneto, G.; Barker, R.; Pavone, V.; Maglio, O.; Lombardi, A. Nano-in-Nano Approach for Enzyme Immobilization Based on Block Copolymers. *ACS Appl. Mater. Interfaces* **2017**, *9* (34), 29318–29327. https://doi.org/10.1021/acsami.7b08959.

(305) Haghju, S.; Bari, M. R.; Khaled-Abad, M. A. Affecting Parameters on Fabrication of β-D-Galactosidase Immobilized Chitosan/Poly (Vinyl Alcohol) Electrospun Nanofibers. *Carbohydr. Polym.* **2018**, *200*, 137–143. https://doi.org/10.1016/j.carbpol.2018.07.096.

(306) Uyar, T.; Besenbacher, F. Electrospinning of Uniform Polystyrene Fibers: The Effect of Solvent Conductivity. *Polymer (Guildf).* **2008**, *49* (24), 5336–5343. https://doi.org/10.1016/j.polymer.2008.09.025.

(307) Li, Y.; Gao, F.; Wei, W.; Qu, J. B.; Ma, G. H.; Zhou, W. Q. Pore Size of Macroporous Polystyrene Microspheres Affects Lipase Immobilization. *J. Mol. Catal. B Enzym.* **2010**, *66* (1–2), 182–189. https://doi.org/10.1016/j.molcatb.2010.05.007.

(308) Guerrand, D. *Economics of Food and Feed Enzymes: Status and Prospectives*; Elsevier Inc., 2018. https://doi.org/10.1016/B978-0-12-805419-2.00026-5.

(309) Massai, L.; Messori, L.; Micale, N.; Schirmeister, T.; Maes, L.; Fregona, D.; Cinellu, M. A.; Gabbiani, C. Gold Compounds as Cysteine Protease Inhibitors: Perspectives for Pharmaceutical Application as Antiparasitic Agents. *BioMetals* **2017**, *30* (2), 313–320. https://doi.org/10.1007/s10534-017-0007-0.

(310) Murthy, P. S.; Kusumoto, K. I. Acid Protease Production by Aspergillus Oryzae on Potato Pulp Powder with Emphasis on Glycine Releasing Activity: A Benefit to the Food Industry. *Food Bioprod. Process.* **2015**, *96*, 180–188. https://doi.org/10.1016/j.fbp.2015.07.013.

(311) Sinha, R.; Radha, C.; Prakash, J.; Kaul, P. Whey Protein Hydrolysate: Functional Properties, Nutritional Quality and Utilization in Beverage Formulation. *Food Chem.* **2007**, *101* (4), 1484–1491. https://doi.org/10.1016/j.foodchem.2006.04.021.

(312) Karn, S. K.; Kumar, A. Hydrolytic Enzyme Protease in Sludge: Recovery and Its Application. *Biotechnol. Bioprocess Eng.* **2015**, *20* (4), 652–661. https://doi.org/10.1007/s12257-015-0161-6.

(313) Zhou, C.; Qin, H.; Chen, X.; Zhang, Y.; Xue, Y.; Ma, Y. A Novel Alkaline Protease from Alkaliphilic Idiomarina Sp. C9-1 with Potential Application for Eco-Friendly Enzymatic Dehairing in the Leather Industry. *Sci. Rep.* **2018**, *8* (1), 1–18. https://doi.org/10.1038/s41598-018-34416-5.

(314) Ariaeenejad, S.; Kavousi, K.; Mamaghani, A. S. A.; Ghasemitabesh, R.; Hosseini Salekdeh, G. Simultaneous Hydrolysis of Various Protein-Rich Industrial Wastes by a Naturally Evolved Protease from Tannery Wastewater Microbiota. *Sci. Total Environ.* **2022**, *815*, 152796. https://doi.org/10.1016/j.scitotenv.2021.152796.

(315) Zhang, S.; Lei, H.; Gao, X.; Xiong, X.; Wu, W. D.; Wu, Z.; Chen, X. D. Fabrication of Uniform Enzyme-Immobilized Carbohydrate Microparticles with High Enzymatic Activity and Stability via Spray Drying and Spray Freeze Drying. *Powder Technol.* **2018**, *330*, 40–49. https://doi.org/10.1016/j.powtec.2018.02.020.

(316) Asaduzzaman, F.; Salmon, S. Enzyme Immobilization: Polymer–Solvent–Enzyme

Compatibility. *Mol. Syst. Des. Eng.* **2022**, *7* (11), 1385–1414. https://doi.org/10.1039/D2ME00140C.

(317) Kolbasov, A.; Sinha-Ray, S.; Joijode, A.; Hassan, M. A.; Brown, D.; Maze, B.; Pourdeyhimi, B.; Yarin, A. L. Industrial-Scale Solution Blowing of Soy Protein Nanofibers. *Ind. Eng. Chem. Res.* **2016**, *55* (1), 323–333. https://doi.org/10.1021/acs.iecr.5b04277.

(318) Sinha-Ray, S.; Sinha-Ray, S.; Yarin, A. L.; Pourdeyhimi, B. Theoretical and Experimental Investigation of Physical Mechanisms Responsible for Polymer Nanofiber Formation in Solution Blowing. *Polymer (Guildf).* **2015**, *56*, 452–463. https://doi.org/10.1016/j.polymer.2014.11.019.

(319) Choi, S.; Lee, H. M.; Kim, H. S. High Performance and Moisture Stable Humidity Sensors Based on Polyvinylidene Fluoride Nanofibers by Improving Electric Conductivity. *Polym. Eng. Sci.* **2019**, *59* (2), 304–310. https://doi.org/10.1002/pen.24905.

(320) Wang, Y.; Chao, G.; Li, X.; Dong, F.; Zhuang, X.; Shi, L.; Cheng, B.; Xu, X. Hierarchical Fibrous Microfiltration Membranes by Self-Assembling DBS Nanofibrils in Solution-Blown Nanofibers. *Soft Matter* **2018**, *14* (44), 8879–8882. https://doi.org/10.1039/c8sm01890a.

(321) Liu, R.; Xu, X.; Zhuang, X.; Cheng, B. Solution Blowing of Chitosan/PVA Hydrogel Nanofiber Mats. *Carbohydr. Polym.* **2014**, *101* (1), 1116–1121. https://doi.org/10.1016/j.carbpol.2013.10.056.

(322) Xu, X. lin; Zhou, G. qing; Li, X. jie; Zhuang, X. pin; Wang, W.; Cai, Z. jun; Li, M. qin; Li, H. jun. Solution Blowing of Chitosan/PLA/PEG Hydrogel Nanofibers for Wound Dressing. *Fibers Polym.* **2016**, *17* (2), 205–211. https://doi.org/10.1007/s12221-016-5800-9.

(323) Alwattar, A.; Haddad, A.; Zhou, Q.; Nascimento, T.; Greenhalgh, R.; Medeiros, E.; Blaker,

J.; Parry, A.; Quayle, P.; Yeates, S. Synthesis and Characterisation of Fluorescent Pyrene-End-Capped Polylactide Fibres. *Polym. Int.* **2019**, *68* (3), 360–368. https://doi.org/10.1002/pi.5712.

(324) Wang, H.; Zhuang, X.; Li, X.; Wang, W.; Wang, Y.; Cheng, B. Solution Blown Sulfonated Poly(Ether Sulfone)/Poly(Ether Sulfone) Nanofiber-Nafion Composite Membranes for Proton Exchange Membrane Fuel Cells. *J. Appl. Polym. Sci.* **2015**, *132* (38), n/a-n/a. https://doi.org/10.1002/app.42572.

(325) Xu, X.; Shao, Z.; Shi, L.; Cheng, B.; Yin, X.; Zhuang, X.; Di, Y. Enhancing Proton Conductivity of Proton Exchange Membrane with SPES Nanofibers Containing Porous Organic Cage. *Polym. Adv. Technol.* **2020**, No. February, 1–10. https://doi.org/10.1002/pat.4886.

(326) Zhang, J.; Kitayama, H.; Gotoh, Y. High Strength Ultrafine Cellulose Fibers Generated by Solution Blow Spinning. *Eur. Polym. J.* **2020**, *125* (January). https://doi.org/10.1016/j.eurpolymj.2020.109513.

(327) Liu, Y.; Wang, X.; Li, N.; Wang, X.; Shi, L.; Wu, E.; Wang, R.; Shan, M.; Zhuang, X. UV-Crosslinked Solution Blown PVDF Nanofiber Mats for Protective Applications. *Fibers Polym.* **2020**, *21* (3), 489–497. https://doi.org/10.1007/s12221-020-9666-5.

(328) Li, X.; Teng, S.; Xu, X.; Wang, H.; Dong, F.; Zhuang, X.; Cheng, B. Solution Blowing of Polyacrylonitrile Nanofiber Mats Containing Fluoropolymer for Protective Applications. *Fibers Polym.* **2018**, *19* (4), 775–781. https://doi.org/10.1007/s12221-018-7912-x.

(329) Rempel, S. P.; Engler, L. G.; Soares, M. R. F.; Catafesta, J.; Moura, S.; Bianchi, O. Nano/Microfibers of EVA Copolymer Obtained by Solution Blow Spinning: Processing, Solution Properties, and Pheromone Release Application. *J. Appl. Polym. Sci.* **2019**, *136*

(24), 47647. https://doi.org/10.1002/app.47647.

(330) Gombotz, W. R.; Wang, G. H.; Horbett, T. A.; Hoffman, A. S. Protein Adsorption to PEO Surfaces. *J. Biomed. Mater. Res.* **1991**, *25* (12), 1547–1562.

(331) Vereschagin, E. I.; Han, D. H.; Troitsky, A. W.; Grishin, O. V.; Petrov, S. E.; Gulyaeva, E. P.; Bogdanova, L. A.; Korobeinikov, M. V.; Auslender, V. L. Radiation Technology in the Preparation of Polyethylene Oxide Hydrophilic Gels and Immobilization of Proteases for Use in Medical Practice. *Arch. Pharm. Res.* **2001**, *24* (3), 229–233. https://doi.org/10.1007/BF02978263.

(332) Kappeler, S. R.; Van Den Brink, H. M.; Rahbek-Nielsen, H.; Farah, Z.; Puhan, Z.; Hansen, E. B.; Johansen, E. Characterization of Recombinant Camel Chymosin Reveals Superior Properties for the Coagulation of Bovine and Camel Milk. *Biochem. Biophys. Res. Commun.* **2006**, *342* (2), 647–654. https://doi.org/10.1016/j.bbrc.2006.02.014.

(333) Del Galdo, S.; Mancini, G.; Daidone, I.; Zanetti Polzi, L.; Amadei, A.; Barone, V. Tyrosine Absorption Spectroscopy: Backbone Protonation Effects on the Side Chain Electronic Properties. *J. Comput. Chem.* **2018**, *39* (22), 1747–1756. https://doi.org/10.1002/jcc.25351.

(334) LOWRY, O. H.; ROSEBROUGH, N. J.; FARR, A. L.; RANDALL, R. J. Protein Measurement with the Folin Phenol Reagent. *J. Biol. Chem.* **1951**, *193* (1), 265–275. https://doi.org/10.1016/s0021-9258(19)52451-6.

(335) Awad, G. E. A.; Ghanem, A. F.; Abdel Wahab, W. A.; Wahba, M. I. Functionalized κ-Carrageenan/Hyperbranched Poly(Amidoamine)for Protease Immobilization: Thermodynamics and Stability Studies. *Int. J. Biol. Macromol.* **2020**, *148*, 1140–1155.

https://doi.org/10.1016/j.ijbiomac.2020.01.122.

(336) Pucić, I.; Jurkin, T. FTIR Assessment of Poly(Ethylene Oxide) Irradiated in Solid State, Melt and Aqeuous Solution. *Radiat. Phys. Chem.* **2012**, *81* (9), 1426–1429. https://doi.org/10.1016/j.radphyschem.2011.12.005.

(337) Bergeron, C.; Perrier, E.; Potier, A.; Delmas, G. A Study of the Deformation, Network, and Aging of Polyethylene Oxide Films by Infrared Spectroscopy and Calorimetric Measurements. *Int. J. Spectrosc.* **2012**, *2012*, 1–13. https://doi.org/10.1155/2012/432046.

(338) Calabrò, E.; Magazù, S. Demicellization of Polyethylene Oxide in Water Solution under Static Magnetic Field Exposure Studied by FTIR Spectroscopy. *Adv. Phys. Chem.* **2013**, *2013*. https://doi.org/10.1155/2013/485865.

(339) Pelton, J. T.; McLean, L. R. Spectroscopic Methods for Analysis of Protein Secondary Structure. *Anal. Biochem.* **2000**, *277* (2), 167–176. https://doi.org/10.1006/abio.1999.4320.

(340) Yang, H.; Yang, S.; Kong, J.; Dong, A.; Yu, S. Obtaining Information about Protein Secondary Structures in Aqueous Solution Using Fourier Transform IR Spectroscopy. *Nat. Protoc.* **2015**, *10* (3), 382–396. https://doi.org/10.1038/nprot.2015.024.

(341) McKee, M.; Hunley, M.; Layman, J.; Macromolecules, T. L.-; 2006, undefined. Solution Rheological Behavior and Electrospinning of Cationic Polyelectrolytes. *ACS Publ.* **2006**, *39* (2), 575–583. https://doi.org/10.1021/ma051786u.

(342) Wang, Y.; Hsieh, Y. L. Immobilization of Lipase Enzyme in Polyvinyl Alcohol (PVA) Nanofibrous Membranes. *J. Memb. Sci.* **2008**, *309* (1–2), 73–81.

https://doi.org/10.1016/J.MEMSCI.2007.10.008.

(343) Nalam, P. C.; Clasohm, J. N.; Mashaghi, A.; Spencer, N. D. Macrotribological Studies of Poly(L-Lysine)-Graft-Poly(Ethylene Glycol) in Aqueous Glycerol Mixtures. *Tribol. Lett.* **2010**, *37* (3), 541–552. https://doi.org/10.1007/S11249-009-9549-9/FIGURES/9.

(344) Singh, A.; Walvekar, R.; Mohammad Khalid; Wong, W. Y.; Gupta, T. C. S. M. Thermophysical Properties of Glycerol and Polyethylene Glycol (PEG 600) Based DES. *J. Mol. Liq.* **2018**, *252*, 439–444. https://doi.org/10.1016/J.MOLLIQ.2017.10.030.

(345) Song, J.; Kahveci, D.; Chen, M.; Guo, Z.; Xie, E.; Xu, X.; Besenbacher, F.; Dong, M. Enhanced Catalytic Activity of Lipase Encapsulated in PCL Nanofibers. *Langmuir* **2012**, *28* (14), 6157–6162. https://doi.org/10.1021/la300469s.

(346) Joo, H. S.; Koo, Y. M.; Choi, J. W.; Chang, C. S. Stabilization Method of an Alkaline Protease from Inactivation by Heat, SDS and Hydrogen Peroxide. *Enzyme Microb. Technol.* **2005**, *36* (5–6), 766–772. https://doi.org/10.1016/J.ENZMICTEC.2005.01.002.

(347) Mellgren, R. L.; Mericle, M. T.; Lane, R. D. Proteolysis of the Calcium-Dependent Protease Inhibitor by Myocardial Calcium-Dependent Protease. *Arch. Biochem. Biophys.* **1986**, *246* (1), 233–239. https://doi.org/10.1016/0003-9861(86)90468-6.

(348) Stefansson, B.; Helgadóttir, L.; Olafsdottir, S.; Gudmundsdottir, Á.; Bjarnason, J. B. Characterization of Cold-Adapted Atlantic Cod (Gadus Morhua) Trypsin I - Kinetic Parameters, Autolysis and Thermal Stability. *Comp. Biochem. Physiol. - B Biochem. Mol. Biol.* **2010**, *155* (2), 186–194. https://doi.org/10.1016/j.cbpb.2009.11.004.

(349) Jabeen, N.; Majid, I.; Nayik, G. A. Bioplastics and Food Packaging: A Review. *http://www.editorialmanager.com/cogentagri* **2015**, *1* (1), 1117749.

https://doi.org/10.1080/23311932.2015.1117749.

(350) Siracusa, V.; Rocculi, P.; Romani, S.; Rosa, M. D. Biodegradable Polymers for Food Packaging: A Review. *Trends Food Sci. Technol.* **2008**, *19* (12), 634–643. https://doi.org/10.1016/J.TIFS.2008.07.003.

(351) Milovanovic, S.; Hollermann, G.; Errenst, C.; Pajnik, J.; Frerich, S.; Kroll, S.; Rezwan, K.; Ivanovic, J. Supercritical CO2 Impregnation of PLA/PCL Films with Natural Substances for Bacterial Growth Control in Food Packaging. *Food Res. Int.* **2018**, *107*, 486–495. https://doi.org/10.1016/J.FOODRES.2018.02.065.

(352) Tawakkal, I. S. M. A.; Cran, M. J.; Miltz, J.; Bigger, S. W. A Review of Poly(Lactic Acid)-Based Materials for Antimicrobial Packaging. *J. Food Sci.* **2014**, *79* (8), R1477–R1490. https://doi.org/10.1111/1750-3841.12534.

(353) Naser, A. Z.; Deiab, I.; Darras, B. M. Poly(Lactic Acid) (PLA) and Polyhydroxyalkanoates (PHAs), Green Alternatives to Petroleum-Based Plastics: A Review. *RSC Adv.* **2021**, *11* (28), 17151–17196. https://doi.org/10.1039/D1RA02390J.

(354) Yahiaoui, F.; Benhacine, F.; Ferfera-Harrar, H.; Habi, A.; Hadj-Hamou, A. S.; Grohens, Y. Development of Antimicrobial PCL/Nanoclay Nanocomposite Films with Enhanced Mechanical and Water Vapor Barrier Properties for Packaging Applications. *Polym. Bull.* **2015**, *72* (2), 235–254. https://doi.org/10.1007/S00289-014-1269-0/TABLES/4.

(355) Hadj-Hamou, A. S.; Metref, F.; Yahiaoui, F. Thermal Stability and Decomposition Kinetic Studies of Antimicrobial PCL/Nanoclay Packaging Films. *Polym. Bull.* **2017**, *74* (9), 3833–3853. https://doi.org/10.1007/S00289-017-1929-Y/TABLES/6.

(356) Khan, R. A.; Beck, S.; Dussault, D.; Salmieri, S.; Bouchard, J.; Lacroix, M. Mechanical and

Barrier Properties of Nanocrystalline Cellulose Reinforced Poly (Caprolactone) Composites: Effect of Gamma Radiation. *J Appl Polym Sci* **2013**, *110* (5), 3038–3046. https://doi.org/10.1002/app.38896.

(357) Cabedo, L.; Feijoo, J. L.; Villanueva, M. P.; Lagarón, J. M.; Giménez, E. Optimization of Biodegradable Nanocomposites Based on APLA/PCL Blends for Food Packaging Applications. *Macromol. Symp.* **2006**, *233* (1), 191–197. https://doi.org/10.1002/MASY.200690017.

(358) Grossen, P.; Witzigmann, D.; Sieber, S.; Huwyler, J. PEG-PCL-Based Nanomedicines: A Biodegradable Drug Delivery System and Its Application. *J. Control. Release* **2017**, *260*, 46–60. https://doi.org/10.1016/J.JCONREL.2017.05.028.

(359) Siddiqui, N.; Asawa, S.; Birru, B.; Baadhe, R.; Rao, S. PCL-Based Composite Scaffold Matrices for Tissue Engineering Applications. *Mol. Biotechnol. 2018 607* **2018**, *60* (7), 506–532. https://doi.org/10.1007/S12033-018-0084-5.

(360) Malikmammadov, E.; Tanir, T. E.; Kiziltay, A.; Hasirci, V.; Hasirci, N. PCL and PCL-Based Materials in Biomedical Applications. *https://doi.org/10.1080/09205063.2017.1394711* **2017**, *29* (7–9), 863–893. https://doi.org/10.1080/09205063.2017.1394711.

(361) Bosworth, L. A.; Downes, S. Physicochemical Characterisation of Degrading Polycaprolactone Scaffolds. *Polym. Degrad. Stab.* **2010**, *95* (12), 2269–2276. https://doi.org/10.1016/J.POLYMDEGRADSTAB.2010.09.007.

(362) Pitt, C. G.; Chasalow, F. I.; Hibionada, Y. M.; Klimas, D. M.; Schindler, A. Aliphatic Polyesters. I. The Degradation of Poly(ε-Caprolactone) in Vivo. *J Appl Polym Sci* **1981**, *26* (11), 3779–3787. https://doi.org/10.1002/app.1981.070261124.

(363) Murray, E.; Thompson, B. C.; Sayyar, S.; Wallace, G. G. Enzymatic Degradation of Graphene/Polycaprolactone Materials for Tissue Engineering. *Polym. Degrad. Stab.* **2015**, *111*, 71–77. https://doi.org/10.1016/J.POLYMDEGRADSTAB.2014.10.010.

(364) Li, F.; Yu, D.; Lin, X.; Liu, D.; Xia, H.; Chen, S. Biodegradation of Poly(ε-Caprolactone) (PCL) by a New Penicillium Oxalicum Strain DSYD05-1. *World J. Microbiol. Biotechnol.* **2012**, *28* (10), 2929–2935. https://doi.org/10.1007/S11274-012-1103-5/FIGURES/6.

(365) Shi, K.; Jing, J.; Song, L.; Su, T.; Wang, Z. Enzymatic Hydrolysis of Polyester: Degradation of Poly(ε-Caprolactone) by Candida Antarctica Lipase and Fusarium Solani Cutinase. *Int. J. Biol. Macromol.* **2020**, *144*, 183–189. https://doi.org/10.1016/j.ijbiomac.2019.12.105.

(366) Cao, Y.; Shen, C.; Yang, Z.; Cai, Z.; Deng, Z.; Wu, D. Polycaprolactone/Polyvinyl Pyrrolidone Nanofibers Developed by Solution Blow Spinning for Encapsulation of Chlorogenic Acid. *Food Qual. Saf.* **2022**, *6*. https://doi.org/10.1093/FQSAFE/FYAC014.

(367) Li, R.; Li, Z.; Yang, R.; Yin, X.; Lv, J.; Zhu, L.; Yang, R. Polycaprolactone/Poly(L-Lactic Acid) Composite Micro/Nanofibrous Membrane Prepared through Solution Blow Spinning for Oil Adsorption. *Mater. Chem. Phys.* **2020**, *241*, 122338. https://doi.org/10.1016/J.MATCHEMPHYS.2019.122338.

(368) Lorente, M. A.; Corral, A.; González-Benito, J. PCL/Collagen Blends Prepared by Solution Blow Spinning as Potential Materials for Skin Regeneration. *J. Appl. Polym. Sci.* **2021**, *138* (21), 50493. https://doi.org/10.1002/APP.50493.

(369) Lv, J.; Yin, X.; Li, R.; Chen, J.; Lin, Q.; Zhu, L. Superhydrophobic PCL/PS Composite Nanofibrous Membranes Prepared through Solution Blow Spinning with an Airbrush for Oil Adsorption. *Polym. Eng. Sci.* **2019**, *59*, E171–E181.

https://doi.org/10.1002/pen.24898.

(370) Tran, D. N.; Balkus, K. J. Enzyme Immobilization via Electrospinning. *Top. Catal.* **2012**, *55* (16–18), 1057–1069. https://doi.org/10.1007/S11244-012-9901-4/FIGURES/8.

(371) Festag, R.; Alexandratos, S. D.; Joy, D. C.; Wunderlich, B.; Annis, B.; Cook, K. D. Effects of Molecular Entanglements during Electrospray of High Molecular Weight Polymers. *J. Am. Soc. Mass Spectrom.* **1998**, *9* (4), 299–304. https://doi.org/10.1016/S1044-0305(98)00004-X.

(372) Annabi, N.; Fathi, A.; Mithieux, S. M.; Weiss, A. S.; Dehghani, F. Fabrication of Porous PCL/Elastin Composite Scaffolds for Tissue Engineering Applications. *J. Supercrit. Fluids* **2011**, *59*, 157–167. https://doi.org/10.1016/j.supflu.2011.06.010.

(373) Elzein, T.; Nasser-Eddine, M.; Delaite, C.; … S. B.-J. of colloid and; 2004, undefined. FTIR Study of Polycaprolactone Chain Organization at Interfaces. *Elsevier*.

(374) Ren, K.; Wang, Y.; Sun, T.; Yue, W.; Zhang, H. Electrospun PCL/Gelatin Composite Nanofiber Structures for Effective Guided Bone Regeneration Membranes. *Mater. Sci. Eng. C* **2017**, *78*, 324–332. https://doi.org/10.1016/j.msec.2017.04.084.

(375) Abdelrazek, E. M.; Hezma, A. M.; El-khodary, A.; Elzayat, A. M. Spectroscopic Studies and Thermal Properties of PCL/PMMA Biopolymer Blend. *Egypt. J. Basic Appl. Sci.* **2016**, *3* (1), 10–15. https://doi.org/10.1016/J.EJBAS.2015.06.001.

(376) Singh, A. K.; Mukhopadhyay, M. Overview of Fungal Lipase: A Review. *Appl. Biochem. Biotechnol. 2011 1662* **2011**, *166* (2), 486–520. https://doi.org/10.1007/S12010-011-9444-3.

(377) Gandhi, N. N. Applications of Lipase. *J. Am. Oil Chem. Soc.* **1997**, *74* (6), 621–634.

https://doi.org/10.1007/S11746-997-0194-X.

(378) Rajasekar, V. W.; Tambe, A.; Datla, A. Immobilization and Characterization of Recombinant Candida Antarctica Lipase B on Poly(Glycidyl Methacrylate-Ter-Divinyl Benzene-Ter-Ethylene Dimethacrylate) Beads, DILBEADS^{TM}TA. *Biocatal. Biotransformation* **2013**, *31* (2), 79–88. https://doi.org/10.3109/10242422.2013.775254.

(379) José, C.; Austic, G. B.; Bonetto, R. D.; Burton, R. M.; Briand, L. E. Investigation of the Stability of Novozym® 435 in the Production of Biodiesel. *Catal. Today* **2013**, *213*, 73–80. https://doi.org/10.1016/j.cattod.2013.02.013.

(380) Xin, J. Y.; Wang, Y.; Liu, T.; Lin, K.; Chang, L.; Xia, C. G. Biosysthesis of Corn Starch Palmitate by Lipase Novozym 435. *Int. J. Mol. Sci. 2012, Vol. 13, Pages 7226-7236* **2012**, *13* (6), 7226–7236. https://doi.org/10.3390/IJMS13067226.

(381) Khan, A.; Sharma, S. K.; Kumar, A.; Watterson, A. C.; Kumar, J.; Parmar, V. S. Novozym 435-Catalyzed Syntheses of Polyesters and Polyamides of Medicinal and Industrial Relevance. *ChemSusChem* **2014**, *7* (2), 379–390. https://doi.org/10.1002/CSSC.201300343.

(382) Mulinari, J.; Oliveira, J. V.; Hotza, D. Lipase Immobilization on Ceramic Supports: An Overview on Techniques and Materials. *Biotechnol. Adv.* **2020**, *42* (March), 107581. https://doi.org/10.1016/j.biotechadv.2020.107581.

(383) Yilmaz, E.; Can, K.; Sezgin, M.; Yilmaz, M. Immobilization of Candida Rugosa Lipase on Glass Beads for Enantioselective Hydrolysis of Racemic Naproxen Methyl Ester. *Bioresour. Technol.* **2011**, *102* (2), 499–506. https://doi.org/10.1016/J.BIORTECH.2010.08.083.

(384) Blanco, R. M.; Terreros, P.; Fernández-Pérez, M.; Otero, C.; Díaz-González, G. Functionalization of Mesoporous Silica for Lipase Immobilization: Characterization of the Support and the Catalysts. *J. Mol. Catal. B Enzym.* **2004**, *30* (2), 83–93. https://doi.org/10.1016/J.MOLCATB.2004.03.012.

(385) Ye, P.; Xu, Z. K.; Che, A. F.; Wu, J.; Seta, P. Chitosan-Tethered Poly(Acrylonitrile-Co-Maleic Acid) Hollow Fiber Membrane for Lipase Immobilization. *Biomaterials* **2005**, *26* (32), 6394–6403. https://doi.org/10.1016/j.biomaterials.2005.04.019.

(386) Reetz, M. T.; Zonta, A.; Simpelkamp, J. Efficient Immobilization of Lipases by Entrapment in Hydrophobic Sol-Gel Materials. https://doi.org/10.1002/(SICI)1097-0290(19960305)49:5.

(387) Huang, X. J.; Chen, P. C.; Huang, F.; Ou, Y.; Chen, M. R.; Xu, Z. K. Immobilization of Candida Rugosa Lipase on Electrospun Cellulose Nanofiber Membrane. *J. Mol. Catal. B Enzym.* **2011**, *70* (3–4), 95–100. https://doi.org/10.1016/J.MOLCATB.2011.02.010.

(388) Chen, B.; Miller, M. E.; Gross, R. A. Effects of Porous Polystyrene Resin Parameters on Candida Antarctica Lipase B Adsorption, Distribution, and Polyester Synthesis Activity. *Langmuir* **2007**, *23* (11), 6467–6474. https://doi.org/10.1021/la063515y.

(389) Peng, Y.; Zhu-Ping, H.; Yong-Juan, X.; Peng-Cheng, H.; Ji-Jun, T. Effect of Support Surface Chemistry on Lipase Adsorption and Activity. *J. Mol. Catal. B Enzym.* **2013**, *94*, 69–76. https://doi.org/10.1016/J.MOLCATB.2013.04.015.

(390) Zhang, X.; Lv, J.; Yin, X.; Li, Z.; Lin, Q.; Zhu, L. Nanofibrous Polystyrene Membranes Prepared through Solution Blow Spinning with an Airbrush and the Facile Application in Oil Recovery. *Appl. Phys. A Mater. Sci. Process.* **2018**, *124* (5), 1–10.

https://doi.org/10.1007/S00339-018-1769-0/FIGURES/9.

(391) Kasiri, A.; Domínguez, J. E.; González-Benito, J. Morphology Optimization of Solution Blow Spun Polystyrene to Obtain Superhydrophobic Materials with High Ability of Oil Absorption. *Polym. Test.* **2020**, *91*, 106859. https://doi.org/10.1016/J.POLYMERTESTING.2020.106859.

(392) Singhal, R.; Ishita, I.; Sow, P. K. Integrated Polymer Dissolution and Solution Blow Spinning Coupled with Solvent Recovery for Expanded Polystyrene Recycling. *J. Polym. Environ.* **2019**, *27* (6), 1240–1251. https://doi.org/10.1007/s10924-019-01427-w.

APPENDICES

A 2.1. ToF-SIMS high lateral resolution mass spectral maps of SBN-PEO and EFSBN-PEO webs

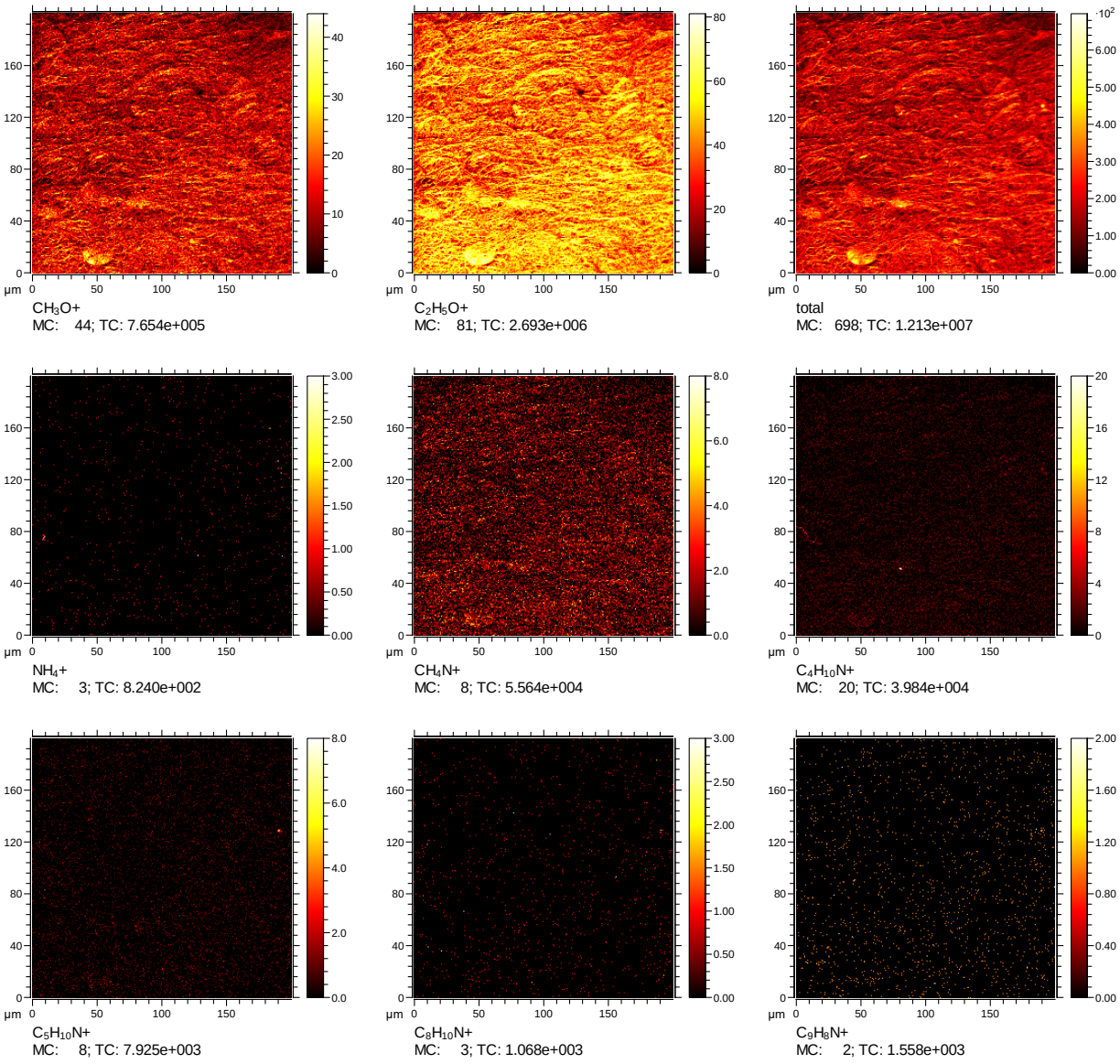

Figure A 2.1: ToF-SIMS distribution maps (analysis area 200x200 µm^2) (positive ions) of SBN-PEO webs.

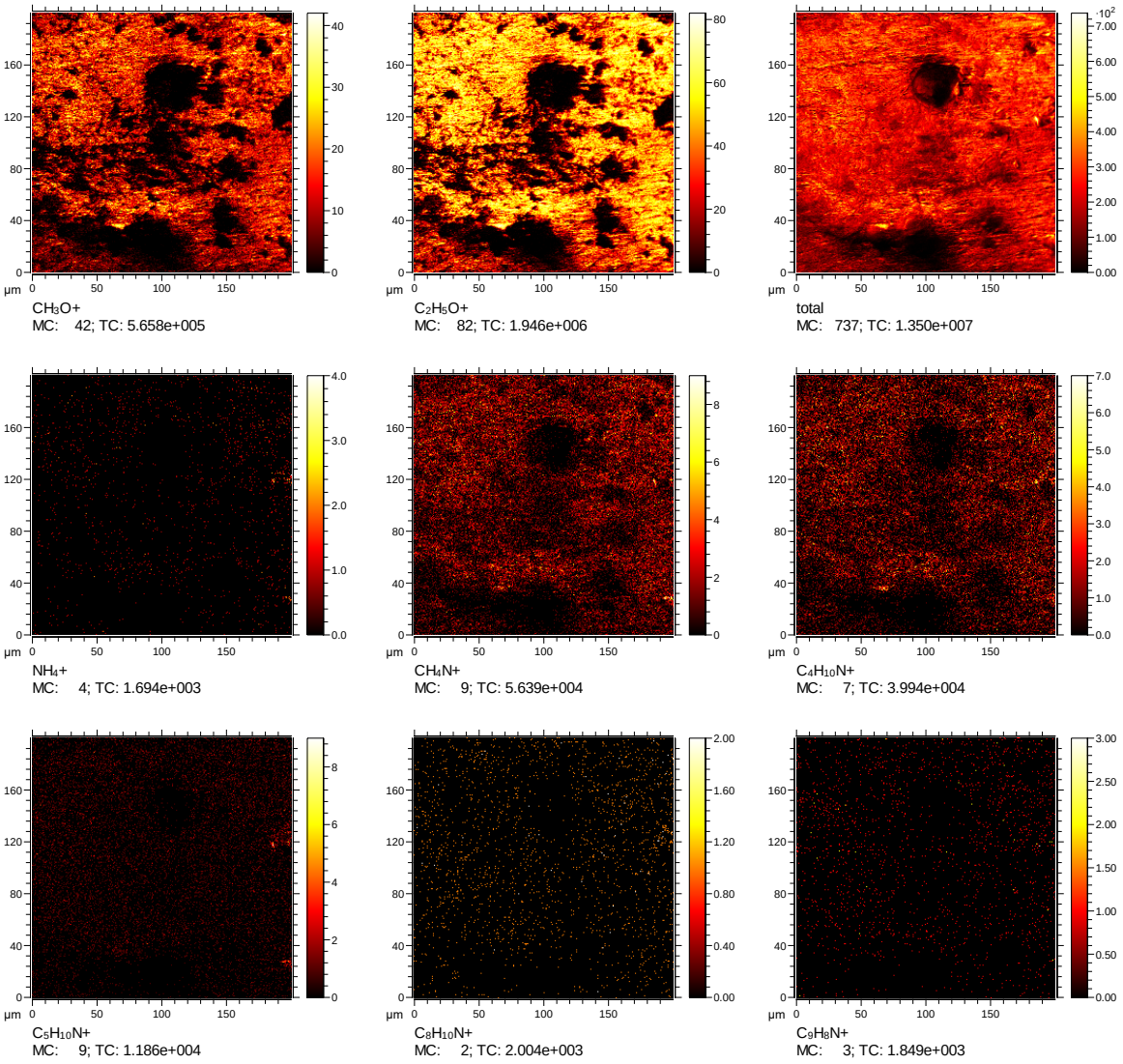

Figure A 2.2:ToF-SIMS distribution maps (analysis area 200x200 µm^2) (positive ions) of 1.3% (w/w) protease-EFSBN-PEO webs.

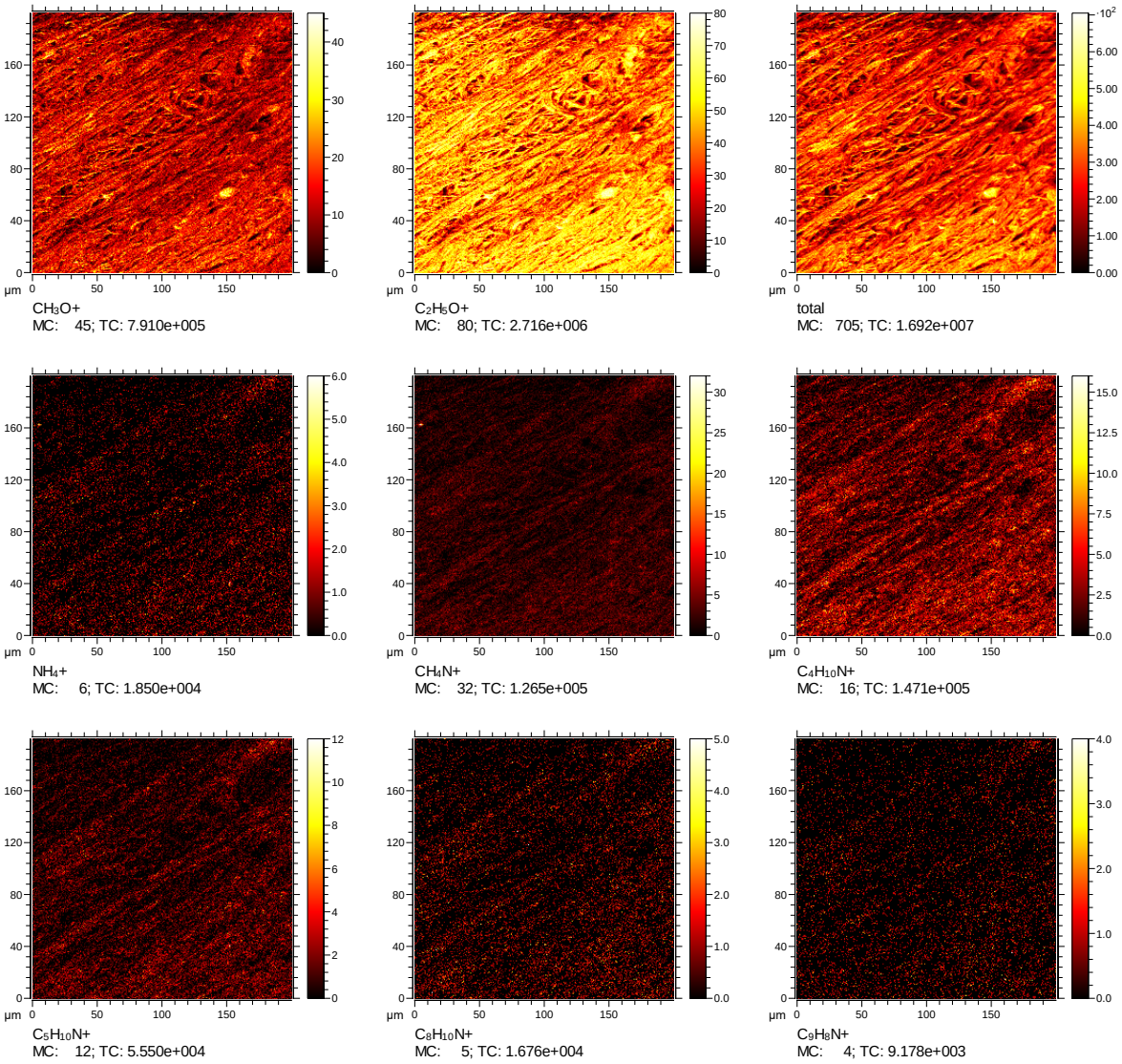

Figure A 2.3: ToF-SIMS distribution maps (analysis area 200x200 µm^2) (positive ions) of 7.4% (w/w) protease-EFSBN-PEO webs.

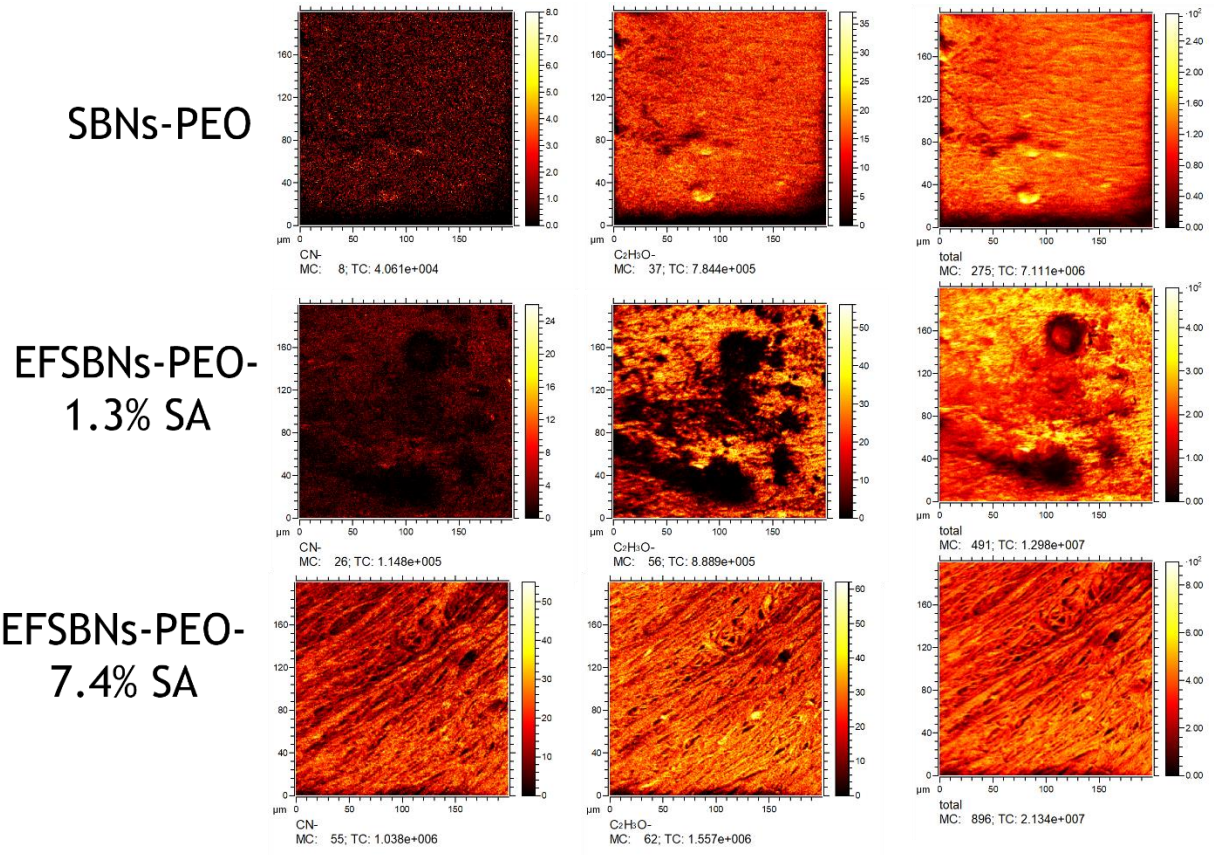

Figure A 2.4: ToF-SIMS distribution maps (analysis area 200x200 µm^2) (negative ions) of SBN-PEO and protease-EFSBN-PEO webs.

A 3.1. Lipase assay calculation of free CALB and redissolved CALB-EFSBN-PCL

Immobilized CALB stock solution in the buffer: 6.5 mg (exactly weighed) of 0.81 wt% CALB-EFSBN-PCL web was placed into a 1.5 ml microcentrifuge vial and incubated with 1.20 ml Tris HCl buffer (100 mM, pH 8.0) for 120 mins at 40 ℃ during which time EFSBN-PCL fibers were wholly dissolved to produce a stock solution.

Free CALB stock solution (0.1 µl CALB/ml buffer): The free CALB liquid enzyme sample was first diluted (100 times) to 10 µl CALB/ml buffer in 100 mM Tris buffer (pH 8.0) and then further diluted (total dilution) to 0.1 µl CALB/ml buffer in the same buffer.

p-nitrophenyl acetate substrate: The p-nitrophenyl acetate substrate was first dissolved in ethanol to prepare a 100 mM substrate stock solution and kept at -4 ℃ for further assay measurements. Before each set of an assay, 100 mM p-NPAc was diluted with deionized water to a final concentration of 8 mM.

Incubation: In the incubation step, 75 µl of EFSBN-PCL redissolved stock solution and 400 µl Tris HCl buffer (100 mM, pH 8.0) were mixed in a 1500 µl microcentrifuge tube and preheated for 5 mins. For free CALB activity, 475 µl of the dilution was added to a 1500 µl microcentrifuge tube and preheated for 5 mins at 45 ℃. Then, 25 µl 8 mM p-NPAc substrate solution was added to the free CALB and immobilized CALB solutions and mixed thoroughly by gentle manual mixing. The final solution (total volume 500 µl) was incubated for 30 minutes at 45 ℃. After incubation, the reaction was stopped by placing microcentrifuge tubes into ice water. Absorbance measurements of the assay solutions determine the concentration of p-nitrophenol (p-NP), the yellow-colored product of p-NPAc hydrolysis, with an absorbance maximum of 405 nm. Three replicates of each sample were measured. The blank control was made by maintaining the same procedure except adding an equivalent amount of SBN-PCL (neat PCL web) instead of EFSBN-PCL. Absorbance for One unit (U) of lipase activity is defined as the amount of enzyme that catalyzes the release of 1.0 µmole of p-NP per min from the p-NPAc substrate at 40 ℃ in the presence of

100 mM pH 8.0 Tris-HCl buffer. The micromoles of p-NP equivalents liberated were determined by using the standard curve.

p-nitrophenol standard curve: A p-NP standard curve was created by plotting absorbance versus known concentrations of p-NP (5-50 µg/ml).

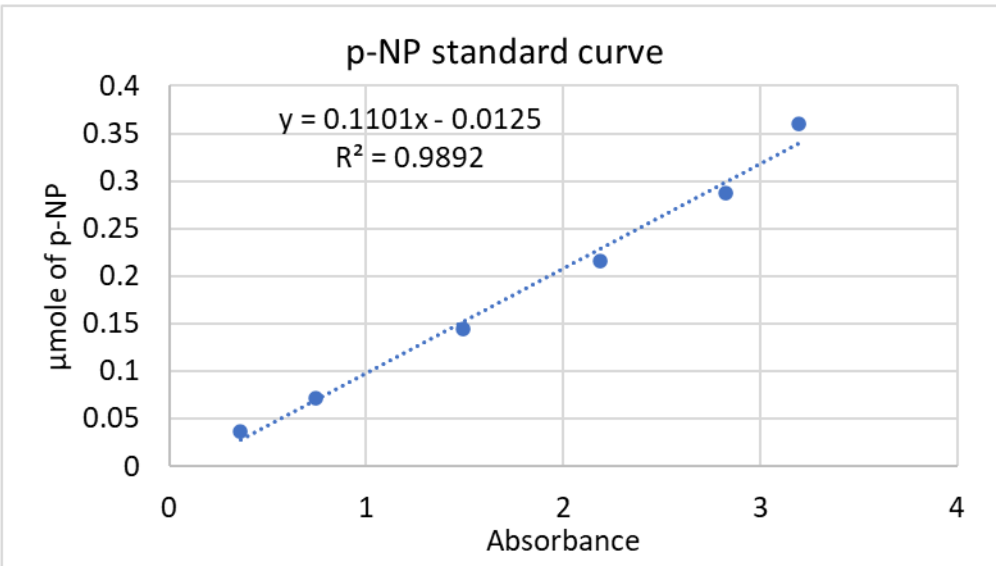

The lipase assay of the free liquid enzyme upon dilution was calculated based on the following equations:

$$\text{U/ml} = \frac{\mu\text{mole p}-\text{NP equivalent release} * \text{volume of total assay,ml}}{\text{Time}_{,\text{min}} * \text{volume of enzyme used,ml}} * \text{dilution} \ldots\ldots\ldots\ldots.\ldots\ldots\ldots\ldots\ldots\ldots.(3.3)$$

$$\text{U/mg}_{\text{protein}} = \frac{\text{U/ml}}{\text{mg of}\frac{\text{protein}}{\text{ml}}\text{of liquid CALB}} \ldots\ldots\ldots\ldots\ldots\ldots\ldots\ldots\ldots\ldots\ldots\ldots\ldots\ldots\ldots\ldots\ldots\ldots..\ldots\ldots\ldots\ldots\ldots.(3.4)$$

The lipase assay of immobilized CALB per mg of the EFSBN-PCL webs protein,

$$\text{U/mg}_{\text{ EFSBNs protein}} = \frac{\mu\text{mole of p}-\text{NP equivalent release} * \text{volume of total assay,ml}}{\text{Time,min} * \text{EFSBN protein used in assay,mg} * \text{volume of enzyme solution,ml}} \ldots\ldots.\ldots.(3.5)$$

The relative activity of immobilized CALB was calculated as the percentage of the free lipase activity and calculated as follows:

$$\text{Relative activity } (\%) = \frac{\text{Activity of immobilized lipase}}{\text{Activity of free lipase}} * 100 \quad \text{.....(3.6)}$$

Calculation:

Weight of 1.30 wt% CALB-EFSBN-PCL= 6.8 mg

The amount of protein in the webs = (6.8*1.30/100) = 0.0884 mg

The volume of tris buffer (100 mM, pH 8.0) used for web dissolution (stock solution 1) = 1200 µl

The volume (stock solution 1) used in lipase assay = 75 µl (make-up to 475 µl by adding buffer)

The amount of protein used in assay = (0.0884*75/1200) = 0.00552 mg = 5.52 µg

The conc. of free CALB in buffer (stock solution 2)= 0.1 µl CALB/ml buffer (10000 times dilution)

The volume of free CALB stock solution used in lipase assay = 475 µl

The substrate p-nitrophenyl acetate (8 mM) used in assay = 25 µl

So, the total volume of assay = 500 µl

Lipase activity of free CALB:

The absorbance of released p-NP by the free CALB = 1.964, 1.948, 1.818 = 1.91 (average)

The absorbance of the control samples = 1.270, 1.279, 1.320 = 1.290 (average)

The net absorbance of released p-NP by the free CALB = 1.91 – 1.290 = 0.62

Release of p-NP by the free CALB = (0.62*0.1101)-0.0125 = 0.0557 µmole

From equation (3.3), lipase activity of free CALB,

U/ml = U/ml = $\frac{0.0557 \text{ µmole} * 0.5 \text{ ml}}{30 \text{ min} * 0.475 \text{ ml}} * 10000$ = 19.56

And from equation (3.4), lipase activity of free CALB,

$U/mg_{protein} = \frac{27\ U/ml}{11.92\ mg/ml} = 1.64$

Lipase activity of CALB-EFSBN-PCL:

The absorbance of released p-NP by the dissolute EFSBN-PCL CALB = 2.739, 2.657, 2.623 = 2.673

The absorbance of the control sample = 1.274, 1.283, 1.277 = 1.278 (average)

The net absorbance of released p-NP by the dissolute EFSBN-PCL CALB = (2.673-1.278) = 1.395

Release of p-NP by the dissolved EFSBN-PCL CALB = (1.395*0.1101)-0.0125 = 0.141 µmole

From equation (3.5), the lipase activity,

$U/mg_{\text{ EFSBNs protein}} = \frac{0.141\ \mu\text{mole} * 0.5\ \text{ml}}{30\ min * 0.00552\ \text{mg} * 0.475\ \text{ml}} = 0.90$

Relative activity:

Applying equation (3.6),

Relative activity (%) = 0.90/1.64*100 =55%

A 4.1. SEM micrograph of SBN-PS at different solution blown spinning conditions.

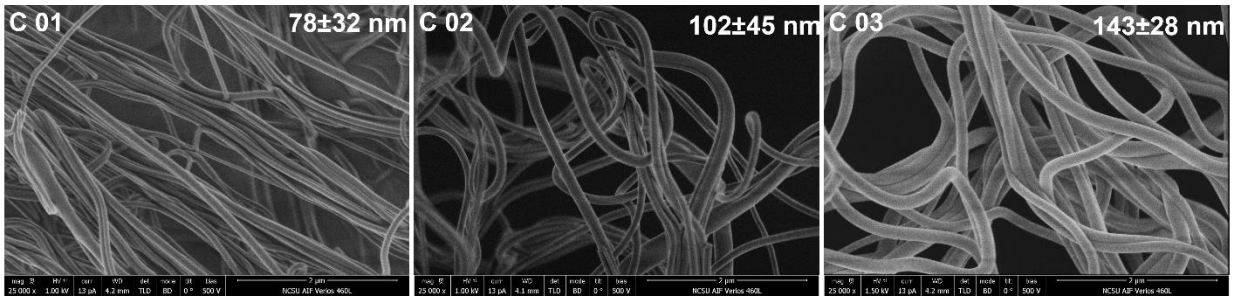

Figure A 4.1: SEM micrograph of SBN-PS webs at spinning parameters DCD distance 100 mm, air pressure 207 kPa, air temperature 40 ℃, solution throughput 0.5 ml/min with varying concentrations (C 01) 10 (w/v)% PS concentration, (C 02) 12.5 (w/v)% PS concentration, and (C 03) 15 (w/v) PS concentration.

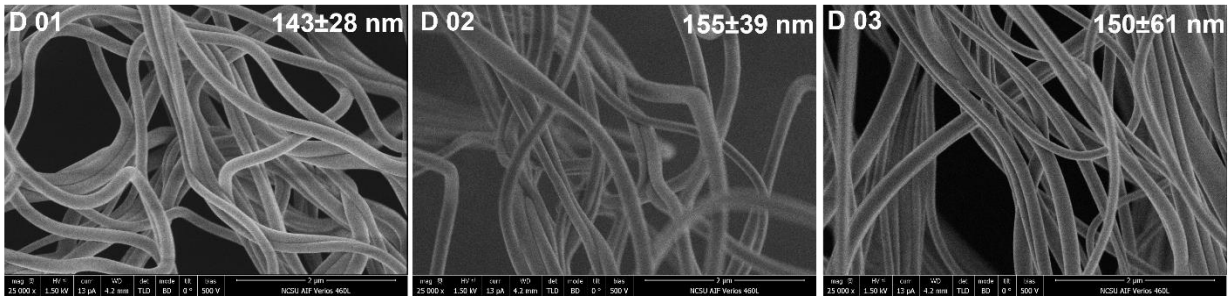

Figure A 4.2: SEM micrograph of SBN-PS webs at spinning parameters PS concentration 15 (w/v)%, air pressure 207 kPa, air temperature 40 ℃, solution throughput 0.5 ml/min with varying concentrations (D 01) 100 mm DCD distance, (C 02) 150 mm DCD distance, and (D 03) 200 mm DCD distance.

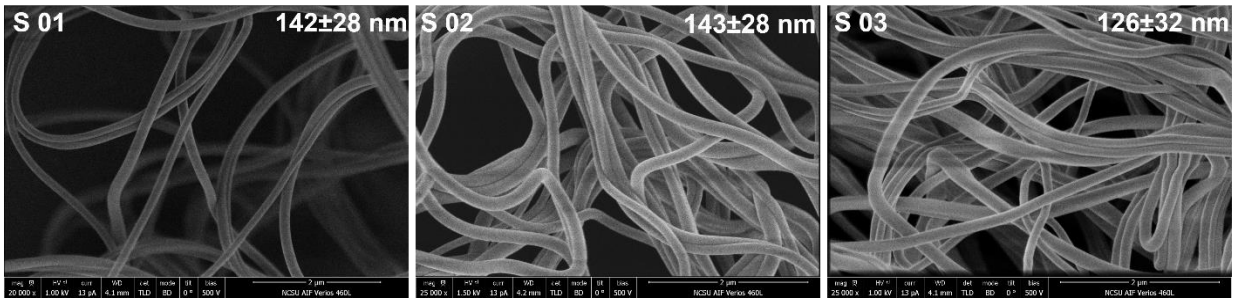

Figure A 4.3: SEM micrograph of SBN-PS webs at spinning parameters PS concentration 15 (w/v)%, 100 mm DCD distance, air temperature 40 ℃, solution throughput 0.5 ml/min with varying concentrations (S 01) air pressure 138 kPa, (S 02) air pressure 207 kPa, and (S 03) air pressure 276 kPa.

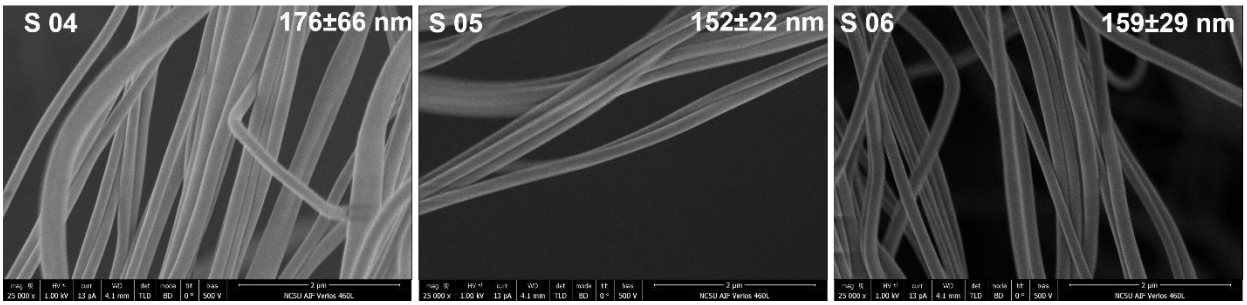

Figure A 4.4: SEM micrograph of SBN-PS webs at spinning parameters PS concentration 15 (w/v)%, 100 mm DCD distance, air temperature 40 ℃, solution throughput 1.0 ml/min with varying concentrations (S 04) air pressure 138 kPa, (S 05) air pressure 207 kPa, and (S 06) air pressure 276 kPa.

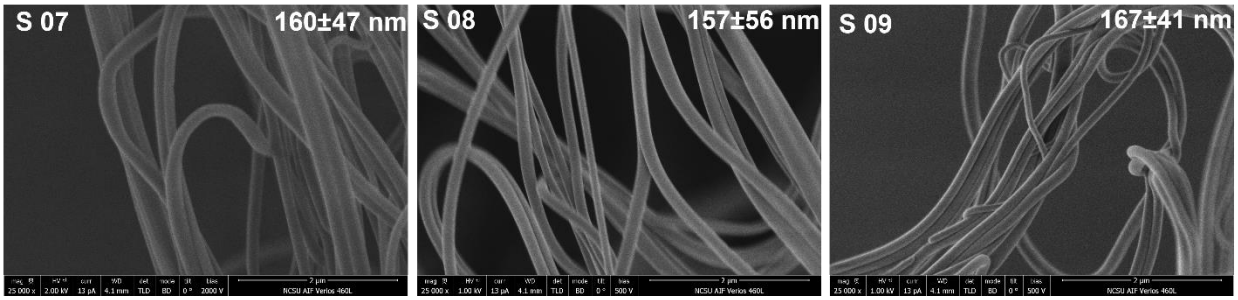

Figure A 4.5: SEM micrograph of SBN-PS webs at spinning parameters PS concentration 15 (w/v)%, 100 mm DCD distance, air temperature 40 ℃, solution throughput 1.5 ml/min with varying concentrations (S 07) air pressure 138 kPa, (S 08) air pressure 207 kPa, and (S 09) air pressure 276 kPa.